OXYTETRACYCLINE IN SOIL AND CONDITIONS THAT SELECT FOR ANTIBIOTIC RESISTANT BACTERIA

A Dissertation

by

MELISABEL DEL CARMEN MUÑOZ URRIOLA

Submitted to the Office of Graduate and Professional Studies of
Texas A&M University
in partial fulfillment of the requirements for the degree of

DOCTOR OF PHILOSOPHY

Chair of Committee,	Robin Autenrieth
Committee Members,	Ronald Kaiser
	Thomas McDonald
	Paul Schwab
Head of Department,	Ronald Kaiser

December 2017

Major Subject: Water Management and Hydrologic Science

ABSTRACT

The increased occurrence of antibiotic resistant bacteria (ARBs) in the environment is posing significant and increasing pressure on human health care in the U.S. and globally. The misuse, overuse and partial metabolism of antibiotics in humans and the animal-producing industry over the years has been accompanied by unintentional environmental antibiotic contamination. With the increased incidence of ARBs, attention has been paid to the environmental fate of antibiotics, including Oxytetracycline (OTC).

OTC is one of the most commonly administered antibiotics to livestock and has been categorized by the World Health Organization (WHO) as "critically important "because it is used as an alternative treatment of serious infections in humans and to treat diseases caused by bacteria that may be transmitted to humans from non-human sources. Even though OTC has a low potential for mobility due to its high sorption partition coefficient (Kd range between 115 to 269,097 L/Kg), OTC has been detected in surface and groundwater. OTC is strongly retained by soil component (alumninosilicates, organic matter, metal oxides) through multiple mechanisms, yet is still bioavailable to microorganisms suggesting a potential scenario for toxicity and/or emergence of antibiotic resistance.

This work presents an inventory of reported OTC concentrations distributed in aqueous and solid media and an evaluation of the fate of OTC in the environment. OTC concentrations were compared to threshold limits that delineate selective windows of resistance to assess the selective potential for resistant bacteria. A model to predict OTC partition coefficients based on soil properties was developed considering the importance of sorption on the fate, mobility and bioavailability of OTC, the variability of reported sorption and the complex interaction of OTC with soil components.

The fate and transport of OTC in soil was addressed by using a Two-site, One-rate

Non-equilibrium model. Simulation results were compared to antibiotic resistant selection regions to evaluate which scenarios resulted in the potential for antibiotic resistant harboring. The model predicted soil-bound OTC concentration levels that were within the antibiotic resistance selection ranges. Therefore, surface application of slurry and diluted slurry with manure-associated OTC concentrations on the order of 10^1 to 10^2 $\mu g/Kg$ could potentially select for antibiotic resistant bacteria (ARB), particularly in cases where no incorporation of manure is considered. Predicted concentrations resulted in potential selection of ARBs throughout the entire simulation period (120 days) for slurry application without incorporation and up to 50 days for slurry application with homogeneous incorporation of manure to a depth of 10 cm. For the cases of diluted slurry application without incorporation, predicted concentrations resulted in potential selection of ARBs throughout the entire simulation period (120 days) and up to 30 days for diluted slurry application with homogeneous incorporation of manure to a depth of 10 cm.

These results suggest that OTC concentrations in swine manure together with current waste management practices of land application of manure as fertilizer present the potential for selection of antibiotic resistance, in particular when no incorporation of manure is practiced. The incorporation of manure into soil effectively reduces OTC concentrations in soil and also in the aqueous phase to levels below antibiotic resistance selectivity. Incorporation of manure into soil and other manure management practices to reduce manure-associate OTC, such as stockpiling and composting, can be effective in minimizing the potential selection for antibiotic resistance. Additional research is needed to assess the microbial activity of soil-bound OTC to compare OTC concentration levels in soil with antibiotic selectivity ranges.

DEDICATION

To my loving husband, Francisco, my daugther Melisita, mom and dad.

"Life is not easy for any of us. But what of that? We must have perseverance and above all confidence in ourselves. We must believe that we are gifted for something and that thing must be attained. "

Marie Curie (1867-1934)

ACKNOWLEDGMENTS

It has been an honor and a privilege to work under the supervision of Dr. Robin Autenrieth. I will like to thank her for the time, patience, support and motivation. Dr. Autenrieth, thank you for the opportunity and guidance in this enriching experience.

Thanks to my committee member: Dr. Kaiser, Dr. McDonald and Dr. Schwab for their time and input.

I will like to thank the staff at the Zachry Department of Civil Engineering at Texas A&M University, very specially to Ms. Sarah Curylo and Mrs. Kay Choate for their support and help during my time at College Station.

To my mentors from Texas and Panama: Dr. Francisco Olivera, Dr. Dario Solis and Dr. Ramiro Vargas. Thank you for your advices and encouragement throughout this journey.

A special thanks to my family, Mr. Aurelio, Mrs. Teresa, Javi, Luchito, Almis and Juancho, for their visits, support and patience.

To my parents, Alma and Luis, thanks for your unconditional love and support. With your encouragement and prayers I have been able to achieve this goal. Your appreciation and dedication to education have largely influenced my life.

Finally, I would like to express my deepest affection and gratitude to my husband Francisco. Your endless support and sacrifice will not be forgotten. **Ph**inally **D**one! To my daughter Melisita, thanks for teaching me the beauty in the simple things of life. I Love you both. Thank you God for making this possible.

CONTRIBUTORS AND FUNDING SOURCES

Contributors

This work was supervised by a dissertation committee consisting of the following persons:

- Dr. Robin Autenrieth, P.E., A.P. and Florence Wiley Professor III, Zachry Department of Civil Engineering, Texas A&M University, College Station, Texas, USA [Chair]
- Dr. Ronald Kaiser , Professor, Department of Recreation, Park & Tourism Sciences, Texas A&M University, College Station, Texas, USA [Member]
- Dr. Thomas McDonald, Professor, Environmental and Occupational Health, Texas A&M University, College Station, Texas, USA [Member]
- Dr. Paul Schwab, Professor, Department of Soil and Crop Sciences, Texas A&M University, College Station, Texas, USA [Member]

All other work conducted for the dissertation was completed by the student independently.

Funding Sources

Graduate studies were supported through a five year Scholarship for Doctoral Studies sponsored the National Secretary of Science, Technology and Innovation (SENACYT) of the Republic of Panama.

Additional support has been provided by Dr. Robin Autenrieth, A.P. and Florence Wiley Professor III, Zachry Department of Civil Engineering, Texas A&M University.

TABLE OF CONTENTS

Page

LIST OF FIGURES

FIGURE Page

LIST OF TABLES

1. INTRODUCTION

The increased incidence of antibiotic resistant bacteria is posing a signicant human health concern in the U.S. and globally. The misuse and overuse of antibiotics has resulted in the release of antibiotics into the environment which has given rise to antibiotic resistant bacteria. The evolution of antibiotic resistance is enhanced by the presence of resistant genes on mobile genetic elements and by the use of antibiotics in concentrations that enable them to behave as selective agents (Witte, 1998). The use of antibiotics in animals has been associated with or suggested as a source of antibiotic resistant bacteria in humans (Levy et al., 1976; Spika et al., 1987; Hunter et al., 1994; Fey et al., 2000; Smith et al., 2002; Box et al., 2005; Mathew et al., 2007; Forsberg et al., 2012; Kilonzo-Nthenge et al., 2013). Although, the risk posed to humans by antibiotic resistant bacteria originating from agriculture has not been clearly established, there is a suspected indirect pathway of exposure.

Antibiotics are routinely administered prophylactically and for growth promotion in animals, and to control certain bacterial diseases in crops and animals. Oxytetraxycline (OTC), the antibiotic of interest in this work, is one of the most commonly administered antibiotics in animal husbandry. OTC is poorly absorbed by the animal gut. Thus, a fraction of OTC not metabolized is excreted through feces and/or urine some of which is collected and stored for use as fertilizer on farmland. Given the variability in the management of manure and agricultural practices, there is a wide range of OTC concentrations released to the environment through these practices. The extent to which there is the potential to develop antibiotic resistance in indigenous microbial populations that result from the exposure and selective pressure of antibiotics is not well understood.

The research reported in this dissertation was formulated to address three objectives.

The first objective was to identify a commonly used antibiotic whose occurrence in the environment has been documented and categorized concentration ranges in reported aqueous and solid media. An extensive literature review resulted in identifying OTC whose reported measurements in various types of aqueous and solid media is presented in chapter 2.

Key characteristics that led to identifying OTC include prevalence of use, frequency of residual concentrations found in soil, and strong sorption to soil components, such as aluminosilicates, organic matter and metal oxides, through multiple mechanisms. A second objective was to assess the fate and transport of OTC from land application of manure on agricultural soils. A third objective was to assess whether residual concentrations in the soil media have resulted in the potential to select for antibiotic resistance.

Partition coefficients (Kd) for OTC in soil samples range from 115 to 269,097 L/kg. Sorbed OTC had been reported to be bioavailable to microorganisms suggesting a potential scenario for toxicity and/or emergence of antibiotic resistance. Given the complex interaction of OTC and soil components, the variability of reported sorption and the importance of sorption on the fate, mobility and bioavailability of OTC, a model was developed to predict partition coefficients based on soil properties. The development of the model for K_d estimations is presented in chapter 3. Findings regarding the importance of the selected methodology for the quantification of K_d for OTC are also summarized in chapter 3.

To address the fate and transport, a two-site, one-rate, non-equilibrium model based on the classic advection-dispersion equation was selected to evaluate the mobility of OTC in agricultural soils. The conceptual framework of the mathematical model and assumptions considered for the implementations of the two-site, one rate, non-equilibrium model are described in chapter 4. The two-site, one rate, non-equilibrium model does not have an exact solution, therefore is approximated by means of the Finite Difference Method (FDM). A description of the FDM used for the discretization of the model and its numerical im-

plementation is presented in chapter 5.

Scenarios designed to evaluate the transport of OTC and simulation results are presented in chapter 6. Resulting aqueous and solid media concentrations are plotted against time and compared to minimal inhibitory concentrations to evaluate the potential of antibiotic resistance selection. Finally, a summary of results, conclusions and further studies are presented in chapter 7.

2. ENVIRONMENTAL OCCURRENCE OF OXYTETRACYCLINE AND THE POTENTIAL SELECTION OF ANTIBIOTIC RESISTANCE IN BACTERIA [1]

2.1 Introduction

Antibiotics in the environment can alter the composition and diversity of indigenous soil microbial communities, which can lead to inhibited decomposition of organic matter, altered nutrient cycling and changes in energy flow (Kennedy and Smith, 1995; Baquero et al., 2008; Martínez, 2009; Kong et al., 2012). Additional concerns for antibiotic presence in the environment are the effects from long-term environmental exposure to low concentrations of antibiotic, in the range of ng/L to $\mu g/L$.

Oxytetracycline (OTC), the subject antibiotic of this work, is commonly used to treat bacterial infections in human and is widely administered to farm animals to prevent (prophylactically) and treat (therapeutic) diseases, as well as increase productivity (growth promotion) due to its low toxicity profile, broad spectrum of activity and low cost (Chopra and Roberts, 2001; Miranda and Zemelman, 2002; Watanabe et al., 2010; Kong et al., 2012). In 2009, World Health Organization (WHO) categorized OTC as a "critically important"antibiotic because it is used as an alternative treatment of serious infections in humans and to treat diseases caused by bacteria that may be transmitted to humans from non-human sources. In the United States (US), OTC has been used as a feed additive since 1953 (Chopra and Roberts, 2001) for cattle, swine, poultry, turkeys, sheep, honey bees, pacific salmon, salmonids, cat fish, rainbow trout and lobster (CFR, 2017). OTC is also one of the most commonly used antibiotics on plants but, in a more modest degree relative to human and veterinary uses (McManus et al., 2002). OTC is partially absorbed in the digestive track: about 40-80% of the administered dose (Hirsch et al., 1999; Merck and

[1] adapted from Muñoz et al. (2017).

Co., 2002; de Liguoro et al., 2003; Sarmah et al., 2006; Boxall et al., 2006). With the increased incidence of antibiotic resistance detected and reported, increased attention has been paid to the environmental fate of OTC (Chopra and Roberts, 2001).

Even at low concentration levels, OTC and its transformation products have been shown to facilitate the development of antibiotic-resistant bacteria (ARB) and accelerate the evolution, mobilization and transfer of antibiotic resistant genes (ARG) to pathogens (Brown et al., 2006; Huang et al., 2012; Bengtsson-Palme and Larsson, 2015; Lundström et al., 2016). Several authors have highlighted water and soil environments as recipients, reservoirs and sources of ARGs to pathogens (Pruden et al., 2006; Martínez, 2008; Zhang et al., 2013). However, the scale at which the environmental presence of OTC contributes to the enrichment and prevalence of ARBs and ARGs is still unclear.

A general assumption in pharmacodynamics models is that selection of ARBs occurs on the range of a minimal inhibitory concentration (MIC) of the susceptible type (MIC_{susc}) and the MIC of resistant bacteria (MIC_{res}) as depicted in the orange shaded section in Figure 2.1 (Drlica, 2003; Drlica and Zhao, 2007; Gullberg et al., 2011). However, studies have shown that low concentration levels are relevant for the enhancement and prevalence of selected new mutants as well as pre-existing resistant mutants depicted by the yellow shaded section of Figure 2.1 (Gullberg et al., 2011; Liu et al., 2011; Quinlan et al., 2011; Lundström et al., 2016). This limit value is referred to as the minimal selective concentration (MSC), which can also be defined as the minimum concentration at which the resistant mutants can outgrow sensitive wild-type strains (Gullberg et al., 2011).

The objective of this section is to provide a through inventory of OTC concentrations reported in the many environmental compartments and an assessment for the potential development of ARBs. Understanding the occurrence of OTC in the different environmental compartments (surface water, runoff, sediment and soil) is being used to identify potential hot-spots for antibiotics resistance. Comparison of environmental concentrations

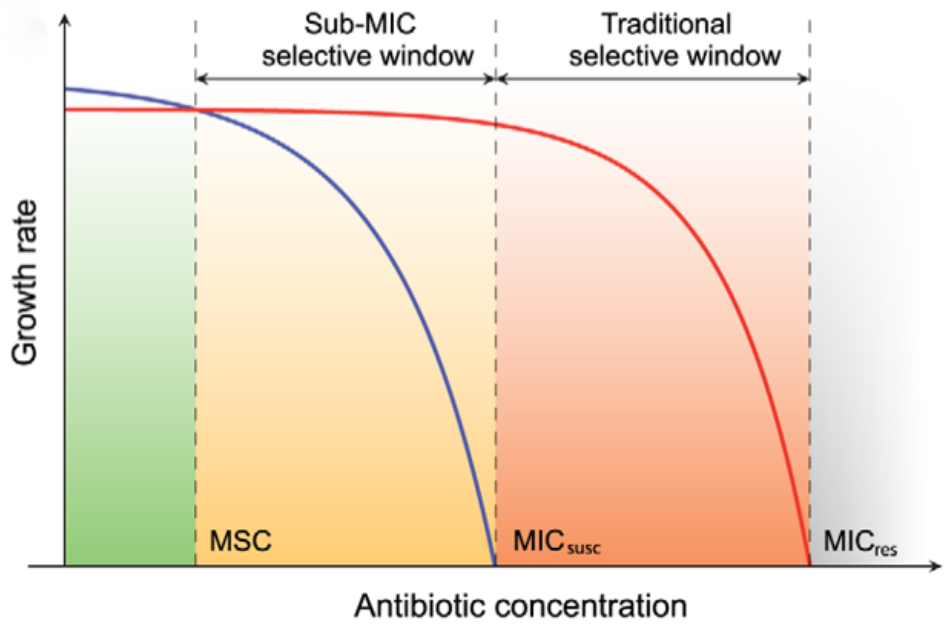

Figure 2.1: Schematic diagram of growth rates as a function of antibiotic concentration. The green region indicates the interval were sensitive strains (blue line) outcompete resistant strains (red line). The orange (sub-MIC selective window) and red (traditional selective window) regions indicate concentration intervals were resistant strains outcompete sensitive strains. MSC = minimal selective concentration; MIC_{susc} = minimal inhibitory concentration for the sensitive strain; MIC_{res} = minimal inhibitory concentration for the resistant strain. Figure reproduced from Gullberg et al. (2011)

of a specific medium with MSCs (thresholds for ARB development) is a potential means of identifying the selective pressure risk (Ashbolt et al., 2013). Such data could aid in developing guidelines and/or regulations for safe limits that take into account the risk of antibiotic resistance development (Lundström et al., 2016).

2.2 Methodology

OTC has been detected in several different media around the world by numerous investigations (around 45 journal papers). The data reported for OTC concentrations were initially categorized as either aqueous (Table A.1, Appendix A) or solid (Tables B.1 and

B.2, Appendix B). The aqueous media data were further delineated based on origin, either agricultural (Ag), urban (Urb) or Industrial (Ind). The data from each of these sources (Ag, Urb or Ind) were then sorted based on sample origin: surface water, groundwater, runoff, waste water treatment plant (WWTP) influent and effluent, waste water (WW) lagoon and anaerobic digester. OTC concentrations reported for solid media were also sorted based on sample origin: sediments (Ag, Urb, Ind or Fish farm), sludge (Urb, Ind, Cattle or Swine), fresh or aged manure (Cattle, Swine or Poultry), and soil.

Agricultural sediment is defined as those river sediments over areas influenced by agricultural activity, near manure composting facilities and concentrated animal feeding operations. Urban and industrial sediments are defined as river sediments over areas influenced by urban (domestic) and industrial (OTC production facilities) discharges, respectively. Fish farm sediment include river and marine sediment at (or near) fish farms lagoons. Urban and industrial sludge are defined as activated sludge samples from urban and OTC production WWTPs, respectively. Animal sludge is defined as samples taken from WW lagoons which collect surface runoff, wash water and manure generated at the agricultural facility. Fresh manure is defined as those samples taken directly in a house or barn, or from the influent of a waste treatment operation. Aged manure samples originated from some type of treatment such as: compost, storage tanks, digesters, manure heaps adjacent to the field.

To represent the OTC data by these categories, boxplots of aqueous and solid media were generated and are presented in Figure 2.2 and Figure 2.3, respectively. The number of observations is also identified on the figures. A total of 103 observations were reported for aqueous media and 429 were reported for solid media.

To assess if OTC presence in aqueous and soil media promotes development of resistance, concentrations were compared with threshold limits that delineate the sub-MIC selective window of resistance (Figure 2.1). For aqueous media, effective concentration of

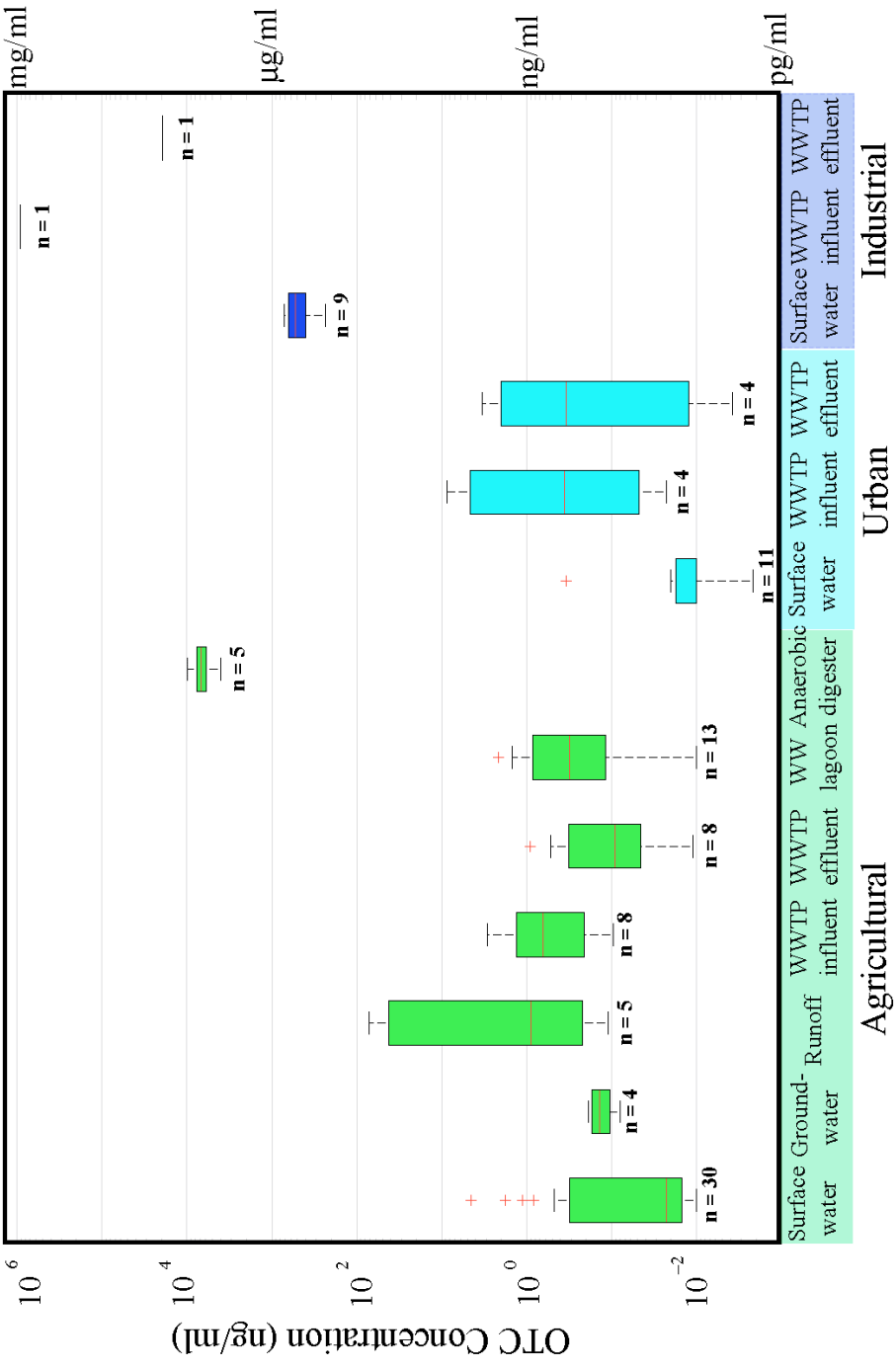

Figure 2.2: OTC concentration in aqueous media

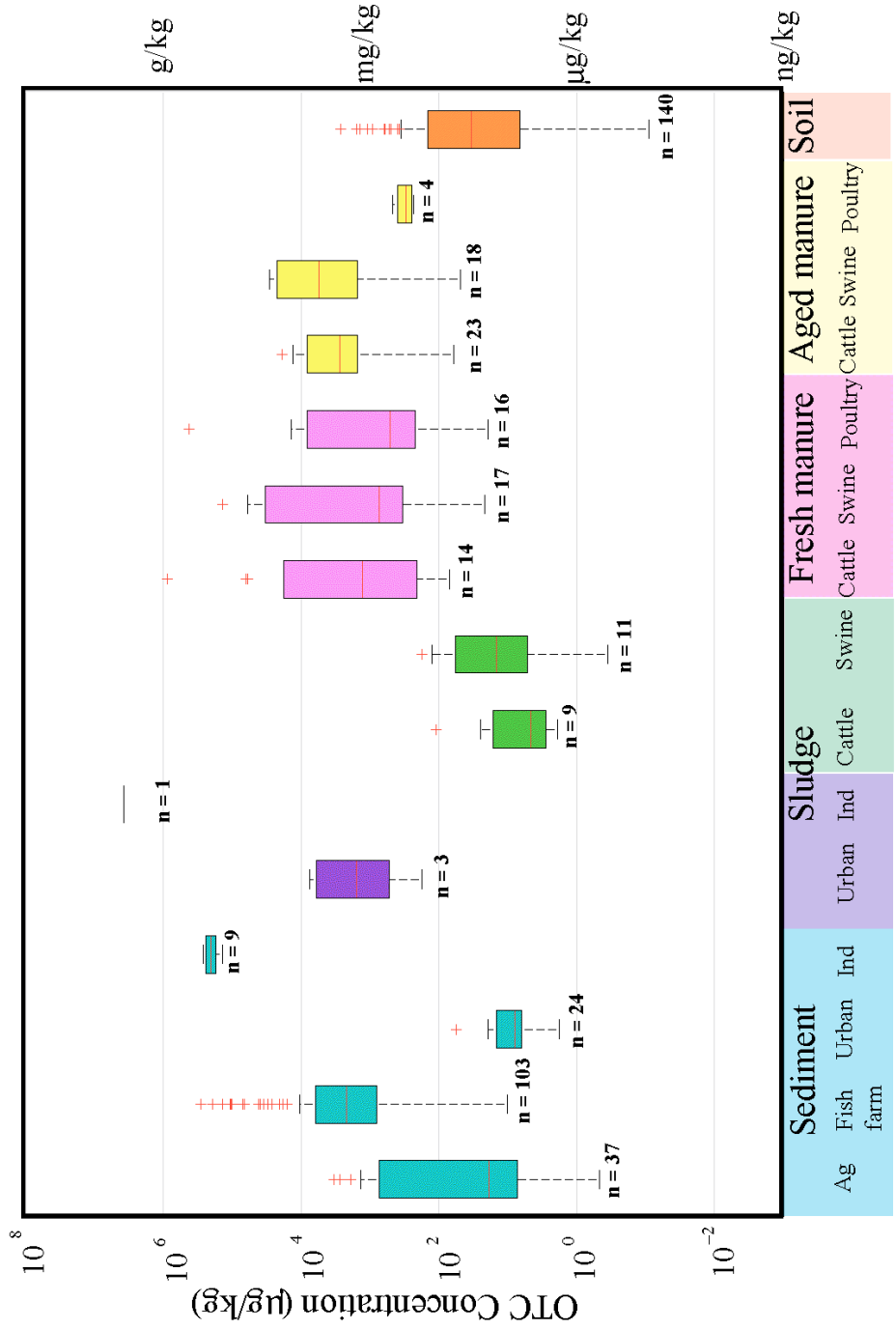

Figure 2.3: OTC concentration in solid media

10% activity inhibition (EC_{10}) and MIC on a pure sensitive strain (*E. coli* ATCC 25922) were assumed as MSC and MIC_{susc}, respectively (Peng et al., 2014). For soil media, 10% and 100% of decline in colony forming units (CFU) of *E. coli* ATCC 25922 in a silt loam soil were assumed as MSC and MIC_{susc}, respectively (Peng et al., 2014). EC_{10} and EC_{50} effect on substrate-induced respiration (SIR) from indigenous microbial population on a sandy loam soil were assumed as MSC and MIC_{susc}, respectively (Thiele-Bruhn and Beck, 2005). Values are presented in Table 2.1.

Table 2.1: Minimum Selective Concentration of OTC (ng/mL)

Bacteria strain	Limit	Value	Reference
Salmonella enterica sevorar typhimurium	MSC MIC_{susc} MIC_{res}	15 100 128000	Gullberg et al. (2011)
Salmonella sp[a]	MSC MIC_{susc}	53[b] 55000[b]	Chander et al. (2005)
E. coli ATCC 25922	MSC MIC_{susc}	4643[c] 200x10^{3}[c]	Peng et al. (2014)

[a] The power function % decline in CFU = $A(C_{soil})^B$ was used to estimate TC concentrations in soil to achieve 10 and 100 % decline in CFU on a loamy sand soil under manure incorporated conditions. 10% and 80% decline in CFU for *Salmonella* sp[s] were assumed as MIC_{susc} and MIC_{res}, respectively. [b] For *Salmonella*[s]: A = 16.96 and B = 0.18. [c] 10% and 100% decline in CFU for *E. coli* ATCC 25922 were assumed as MSC and MIC_{susc}, respectively.

2.2.1 Occurrence in aqueous media

A total of 73, 19 and 11 observations were reported for agricultural, urban and industrial areas, respectively, for aqueous media. Surface water presented the highest frequency of detection for the three sources. The rest of the categories reported a low detection frequency, below 10 observations, except for Ag WW lagoon with 13 (Figure 2.2).

OTC aqueous concentrations from agricultural areas range from 10^{-2} to 1 ng/mL, except for runoff and anaerobic digester (AD). Runoff concentrations range from approximately 10^{-1} to 10^{2} ng/mL. In this extensive review, only three authors reported OTC presence in runoff (Kay et al., 2005c; Blackwell et al., 2007; Popova et al., 2017) from overland flow experiments due to land application of manure contaminated with OTC. Kay et al. (2005c) and Blackwell et al. (2007) report that the slurry application rates were characteristic of standard agricultural practices in the UK (45,000 and 33,000 L/ha, respectively). In both cases, OTC was spiked into the slurry at concentrations of 18.85 and 26.2 mg/L, respectively. Popova et al. (2013) used a different approach in which the OTC contaminated manure (1 kg) was applied as a strip across the packed soil box. Manure was treated with OTC to achieve a concentration of 200 $\mu g/kg$.

Kay et al. (2005c) identified a peak concentration of OTC on the first rainfall event (24 hr after manure application) with 71.7 ng/mL and 32 ng/mL for tilled and no tilled plot soils, respectively. Blackwell et al. (2007) detected OTC only on the composite sample (0.9 ng/mL) collected 6 days after treatment. Popova et al. (2013) collected composite samples weekly over a 3 week period. An average total mass of 4.1 and 1.7 μg of OTC were detected over the three weeks from two silt loam soils representative of Northern California, USA. Reported mass losses in surface water runoff of initially applied OTC were estimated to be below 0.1% for the Kay et al. (2005c) study and 2.5% for Popova et al. (2013) study. These observations indicate that even compounds with high sorption coefficients for soil, such as OTC, can experience significant transport via surface runoff.

OTC concentrations in AD were in the range of 10^{3} ng/mL and are approximately three to four orders of magnitude higher than the highest OTC concentration reported for Ag WWTP influent (10^{0} ng/mL) and effluent (10^{-1} ng/mL), respectively. Reported OTC concentrations from urban sources ranged from 10^{-3} to 10^{0} ng/mL while industrial concentrations range from 10^{2} to 10^{5} ng/mL. Industrial sources are from OTC production

facilities (Li et al., 2008). For both sources groups, urban and industrial, surface water concentrations are lower than WWTP effluent (dilution effect), and WWTP effluent are lower than WWTP influent.

2.2.2 Occurrence in solid media

Among solid media, the most frequent reported detections were in sediments (173 observations) and soils (140 observations). Sludge, fresh and aged manure present 24, 47 and 45 observations, respectively. OTC concentrations in urban sediment range from 1 to 10^1 $\mu g/kg$; in agricultural and fish farm sediment range from 10^{-1} to 10^3 $\mu g/kg$ and 10^1 to 10^5 $\mu g/kg$, respectively, as depicted in Figure 2.3. Industrial sediment range at 10^5 $\mu g/kg$ and are much higher in comparison with Ag, Urb and fish farm sediment.

OTC is commonly used in the aquaculture industry which is reflected in a high detection frequency (103 observations). All urban sediment samples are from a study by Kim and Carlson (2007) along the Cache La Poudre River in northern Colorado. This watershed is a relatively complex system as it includes several municipal WWTP effluents, numerous tributaries and withdrawals along the river. Ag sediment observations include studies from Simon (2005), Boxall et al. (2006), Kim and Carlson (2007) and Awad et al. (2013).

OTC was detected in sludge from urban, industrial and agricultural sources. OTC concentrations in urban and industrial activated sludge range from 10^2 to 10^3 $\mu g/kg$ and at 10^6 $\mu g/kg$, respectively. OTC sludge concentrations from treatment lagoons for animal operations (cattle and swine) range from 10^{-1} to approximately 10^2 $\mu g/kg$. Treatment lagoons and storage ponds or pits are common structure used for management of waste in cattle and swine animal feeding operations to collect surface runoff, wash water and manure generated (Mackie et al., 2006; Watanabe et al., 2010; Zhang et al., 2013; Zhou et al., 2013). OTC concentration in fresh and aged manure (cattle, swine and poultry)

range from 10^1 to approximately 10^5 $\mu g/kg$ and 10^1 to 10^4 $\mu g/kg$, respectively.

OTC concentrations in soil include measurements from eight countries (China, Germany, Korea, Italy, Spain, UK, Turkey and USA) and range from approximately 10^{-1} $\mu g/kg$ to 10^3 $\mu g/kg$. Soil samples include measurements at various depths, times after treatment (time after land application of manure or slurry), and random sampling from agricultural areas (animal husbandry and crop fields).

2.3 Discussion

Aqueous phase OTC was detected in several wastewater treatment facilities, groundwater and surface water sources. Antibiotic removal by conventional wastewater treatment has been demonstrated to be incomplete (Kim et al., 2005; Jia et al., 2009; Shao et al., 2009). Traditional wastewater treatment processes are ineffective in completely eliminating aqueous phase OTC, as indicated by the presence of OTC in the effluent of urban and industrial discharges.

Despite OTCs high water solubility and low *n*-octanol/water partition potential based on its partition coefficient, OTC is known to be highly sorbed onto solids (manure, sediment and soil) (Tolls, 2001; Sassman and Lee, 2005; Kim et al., 2005; Figueroa, 2012; Huang et al., 2012). Consequently, sorption can be a significant removal mechanism for OTC from WWTPs (Kim et al., 2005; Huang et al., 2012), as OTC sorbs to biomass in the activated sludge (Kim et al., 2005). However, great attention has to be given when sludge is recycled for agricultural purposes (de Cazes et al., 2014). Ozonation has been reported as effective in reducing OTC concentrations levels from industrial WWTP facilities (Zheng and Bennett, 2002a).

OTC occurrence in shallow groundwater has been associated with seepage from treatment lagoons (Mackie et al., 2006). OTC occurrence in surface water influenced by agricultural activities suggests that its sorption to solid medium is not an irreversible process

and that certain conditions could facilitate their mobility in the environment (Kim et al., 2005; Watkinson et al., 2007).

OTC is commonly used in the fish farming industry to protect against bacterial diseases which are a frequent problem. The occurrence and persistence of OTC in sediments from fish farm lagoons has been investigated by several authors (Jacobsen and Berglind, 1988; Björklund et al., 1990; Samuelsen et al., 1992; Capone et al., 1996; Kerry et al., 1996) and include measurements from Finland, Ireland, Norway and the US. OTC persistence in sediment may be significantly affected by the physical and chemical characteristics of sediment, temperature, pH (Björklund et al., 1990). Half-life values for marine sediments originating from fish farming operations range from 32 to 419 days (Samuelsen, 1989; Björklund et al., 1990).

Even substances with high sorptive capacity are not necessarily immobile. The presence of OTC-contaminated river sediment in areas influenced by agricultural activities could be explained by transport from overland flow. Overland flow from manure treated farmlands has been previously identified by Kay et al. (2004) as a pathway by which OTC enters surface waters and can be transported either solubilized or associated with suspended sediments.

OTC occurrence in soil has been extensively documented in crop fields and animal production farms (de Liguoro et al., 2003; Kay et al., 2004; Aga et al., 2005; Brambilla et al., 2007; Andreu et al., 2009; Karci and Balcioǵlu, 2009; Zhou et al., 2013; Huang et al., 2013). Its presence in soil has usually been associated with land application of OTC-contaminated manure. To a lesser extent relative to veterinary and human use, OTC is used on several fruit crops (pears, peaches, nectarines and apples) to control bacterial diseases (McManus et al., 2002).

Potential selection of resistant bacteria in aqueous media was assessed by comparing aqueous OTC concentrations with MSC and MIC_{susc} values for *E. coli* (Table 2.1). As

depicted in Figure 2.4, all aqueous sources were found to be below the sub-MIC selective window except samples taken from industrial sources and Ag anaerobic digester. This comparison illustrates that OTC surface water receiving WWTP discharges from OTC production facilities have the potential to select for resistant strains of *E. coli* ATCC 25922 under the sub-MIC selective window concept.

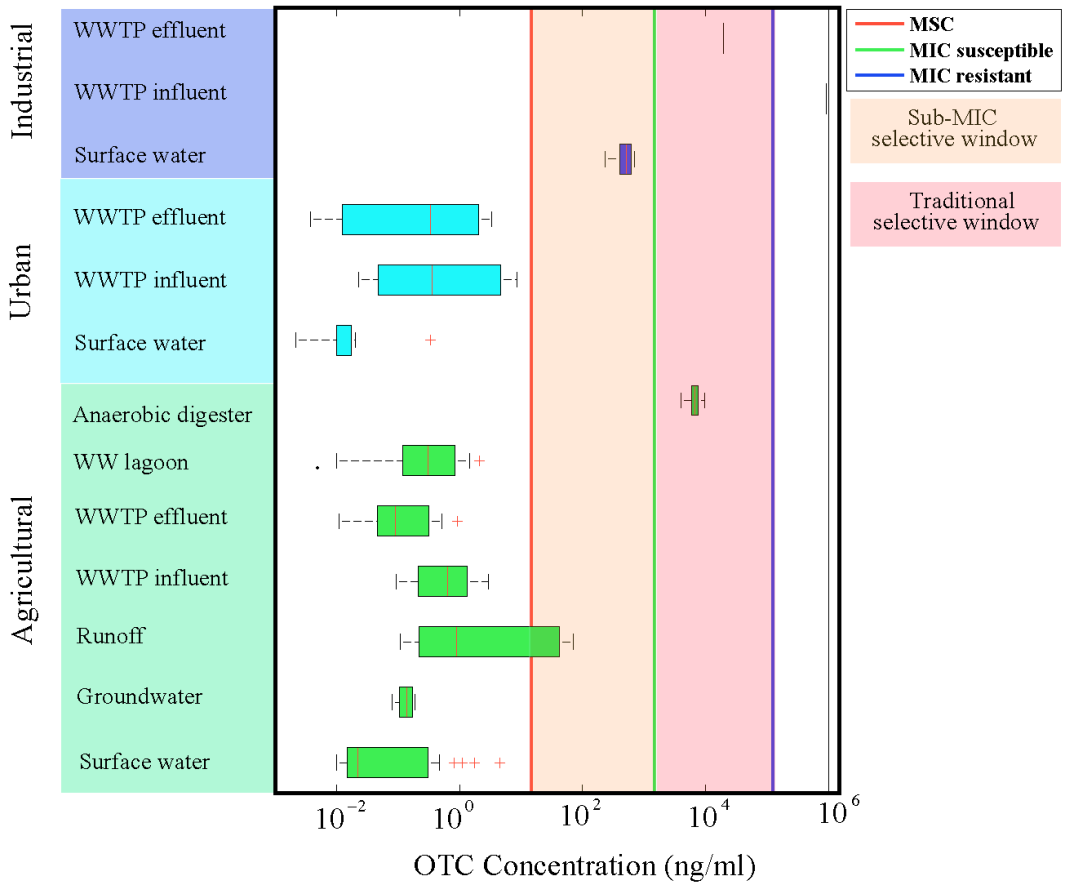

Figure 2.4: Comparison of OTC concentration in aqueous media with sub-MIC and traditional selective window for *Salmonella typhimurium*

Potential selection of resistant bacteria in soil was assessed by comparing soil OTC concentrations with MSC and MIC_{susc} for *E. coli* and indigenous microbial population in

loamy sand and sandy loam, respectively. As depicted in Figure 2.5, no OTC concentration measurements are inside the sub-MIC selective window for an *E. coli* sensitive strain (Figure 2.5a), while several OTC concentration are within the sub-MIC selective window for the indigenous microbial population in a sandy loam soil sample (Figure 2.5b). These comparisons suggest that residual OTC concentrations in soil induce a selective pressure for resistance in soil microorganisms, however, the real extent of the sub-MIC selective window is unknown since EC_{50} is being used as the upper end of the resistance selective range. Results from Figure 2.5 illustrate that the potential selective pressure of a particular bacterial strain, cannot be extrapolated to bacterial populations in soil where bacterial diversity can harbor a variety of antibiotic resistant genes that can be exchanged potentially.

2.4 Summary

The inventory of OTC presence in aqueous and solid media revealed multiple sources and a range of concentrations. Surface water receiving industrial WWTP effluent was identified as a potential source of OTC concentrations that might select for OTC resistance of *E. coli* in aqueous media. Strategies aimed at reducing WWTP effluent concentrations of OTC should be implemented to minimize the potential selection of resistant bacteria once discharged.

Soil was identified as a reservoir for OTC concentrations with the potential to select for resistance among indigenous soil microorganism. Comparison of OTC concentrations with resistant selective zone ranges demonstrate that the presence of OTC can result in the selection of resistant bacterial strains in soil. However, is important to highlight that MICs of a given antibiotic differ from organism to organism and within species as depicted in Figure 2.5a and 2.5b.

Several MIC assays of tetracycline have been reported for single bacterial strains and complex bacterial communities in aquatic environments. However, no reported MSC and

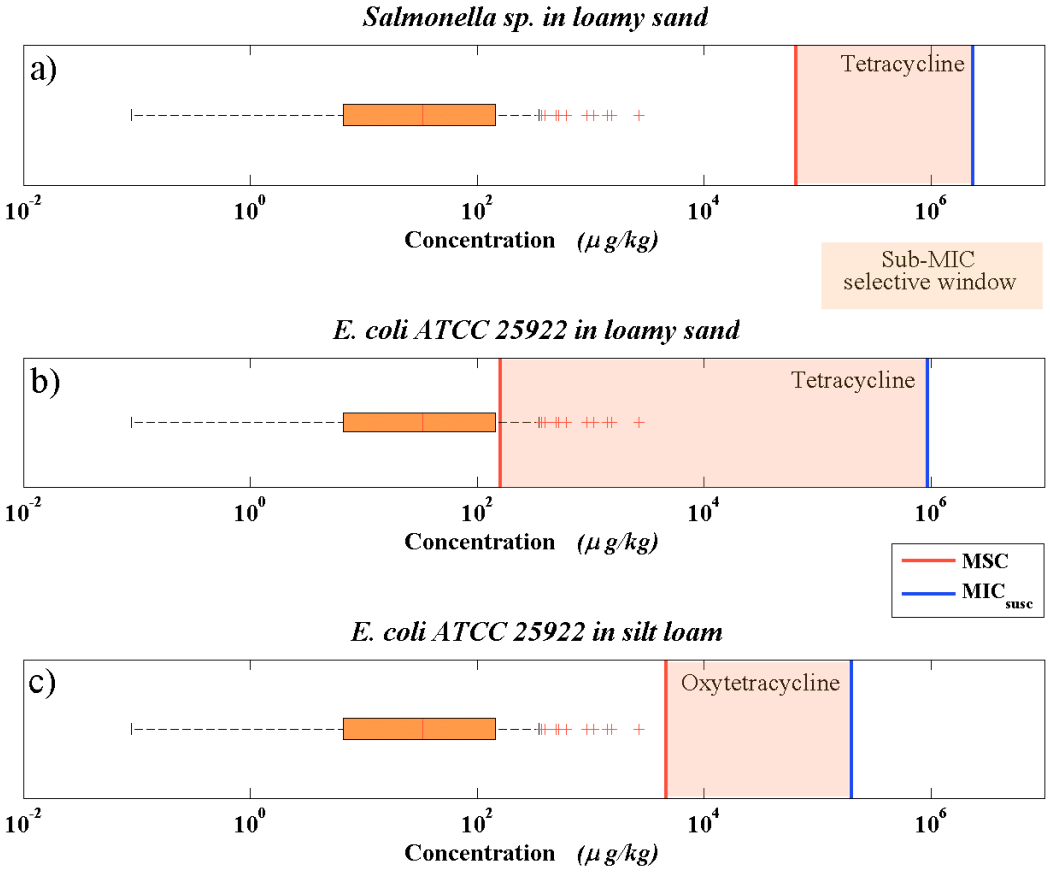

Figure 2.5: Comparison of OTC concentration in soil with sub-MIC selective window for a. *Salmonella* sp and b. *E. coli* ATCC 25922

MIC_{susc} range was found for OTC. Further studies are required to identify OTC concentration ranges for resistance selection in aqueous and solid media considering the biodiversity of indigenous microbial populations. Such data can provide a basis to develop guidelines and/or regulations for usage of antibiotics and their subsequent release to the environment.

3. SORPTION BEHAVIOR OF OXYTETRACYCLINE IN SOIL MEDIA

Land application of animal waste is a common agricultural practice worldwide due to its value as a nutrient supplier and low cost disposal method (Aga et al., 2003; Kumar et al., 2005; Chee-Sanford et al., 2009; Chen et al., 2012). Land application has been shown to be also a large areal scale means of antibiotics and genetic resistant determinants (Chee-Sanford et al., 2009) introduction to the environment and has been identified as a source of resistant genes to pathogens (D'Costa et al., 2006; Martínez, 2008; Wright, 2010; Pruden et al., 2013; Finley et al., 2013).

OTC can be strongly retained by certain components of soils, such as aluminosilicates, organic matter and metal oxides, through multiple mechanisms. Yet, OTC is still bioavailable to microorganisms suggesting a potential scenario for toxicity and/or emergence of antibiotic resistance (Thiele-Bruhn and Beck, 2005; Kong et al., 2012; Peng et al., 2014). Sorption, the distribution between the aqueous and solid phase, is one of the most important environmental processes responsible for the retention of OTC and other antibiotics in the soil environment. Sorption controls not only the fate, mobility and bioavailability of OTC, but also the potencial for transformation reactions and biological effects (Figueroa, 2012; Jechalke et al., 2014). A common practice of estimating a soil partition coefficient (K_d), is based on the octanol-water and organic carbon partition coefficients (K_{ow} and K_{oc}, respectively). However, this technique does not necessarily provide an accurate means of predicting the sorption behavior of OTC and other antibiotics to soil particles (Tolls, 2001; Loke et al., 2002; MacKay and Canterbury, 2005). Complex interactions between soil and OTC beyond hydrophobicity contribute to partitioning.

Accurate determination of K_d is critical for environmental fate predictions of antibiotics. Several authors have reported soil-water distribution coefficient (K_d) models based

on soil physico-chemical properties (Figueroa et al., 2004; Jones et al., 2005; ter Laak et al., 2006b; Gong et al., 2012; Kong et al., 2012; Teixido et al., 2012). Most of the existing models demonstrated the importance of texture, cation exchange capacity (CEC), organic matter (OM) and crystalline oxide content in predicting the distribution of antibiotics in soils. However, equilibrium sorption experiments that do not account for potential complexation reactions, such as with Calcium, result in decreased K_d values. Consequently, the use of K_d to predict the fate of OTC has not proven to be adequate.

3.1 OTC characteristics and properties

OTC was one of the first tetracycline antibiotics discovered in 1948. OTC is a broad spectrum bacteriostatic antibiotic (inhibits growth while not necessarily killing bacteria) with high activity against a wide variety of disease-producing bacteria including: *Bacillus substilis, Echerichia coli, Mycrobacterium, Salmonella schottmulleri, and Staphlociccus aureus* (Sithole and Guy, 1987b). In the US, OTC has been used as a feed additive since 1953 (Chopra and Roberts, 2001) for cattle, swine, poultry, turkeys, sheep, honey bees, pacific salmon, salmonids, catfish, rainbow trout and lobster (CFR, 2017) and plants (in a smaller scale) (McManus et al., 2002). OTC is poorly absorbed in the digestive track, resulting in the excretion of about 20-60% of the administered dose (Hirsch et al., 1999; de Liguoro et al., 2003; Merck and Co., 2002; Sarmah et al., 2006).

Oxytetracycline (OTC) is a large amphoteric polyfunctional ionogenic molecule (Figure 3.1a) (Sassman and Lee, 2005; MacKay and Vasudevan, 2012; Kong et al., 2012) that can interact with multiple sorption sites on environmental solids though multiple sorption mechanisms. OTC is positively charged (OTC^{00+}) under strong acidic conditions when the dimethyl amine group is protonated (Kulshrestha et al., 2004). The zwitterion species (OTC^{-0+}) results from the loss of a proton from the tricarbonyl-methane system and is dominant over the pH range of approximately 3.6 to 7.5. OTC is negatively

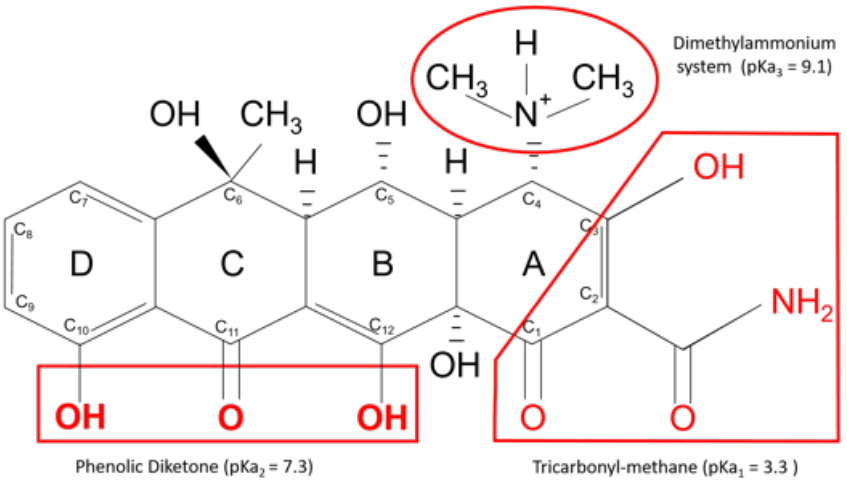

Functional Group	pH			
	< 3.3 Cation (0 0 +)	3.3 to 7.3 Zwitterion (- 0 +)	7.3 to 9.1 Anion (- - +)	> 9.1 Anion (- - 0)
C3-OH	0	-	-	-
C12-OH	0	0	-	-
C4-$NH^{+}(CH_3)_2$	+	+	+	0

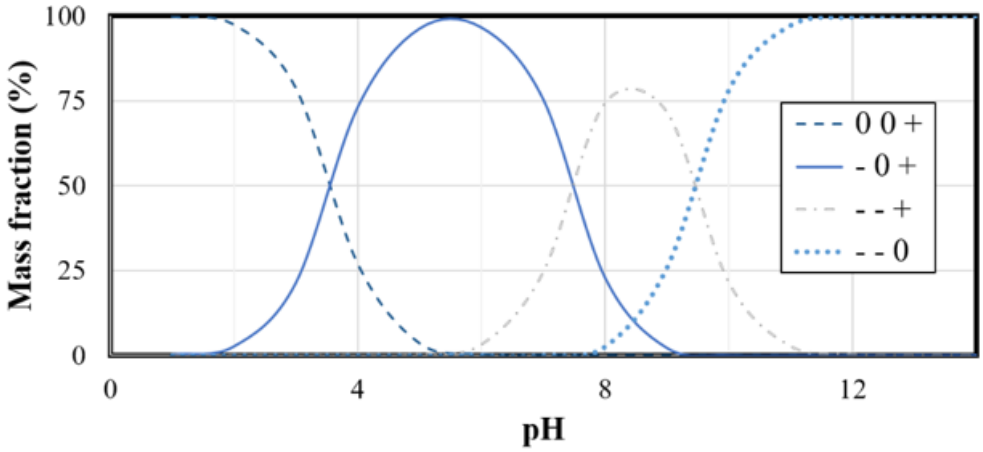

Figure 3.1: OTC structure molecule, corresponding acid/base dissociation constants (pKa), charge of ionizable groups and speciation diagram. OTC structure modified from Sassman and Lee (2005) and Figueroa and MacKay (2005).

charged (OTC^{--+} and OTC^{--0}) under alkaline conditions when the phenolic diketone and dymethylammonium system loose protons (Figure 3.1b), respectively (Sassman and Lee, 2005; Pils and Laird, 2005).

OTC^{00+} is the dominant species up to pH $\approx$ 3.5, but is present up to pH $\approx$ 5.5. OTC^{-0+} is present from pH $\approx$ 5.5 and becomes the dominant species at pH $\approx$ 7.5. OTC is considered highly soluble in water (1 to 300 g/mL) (Kay et al., 2004; Sanderson et al., 2005; Chu, 2011). Octanol/water partitioning coefficients (K_{ow}) change considerably with pH. Log K_{ow} values from -2.45 to -1.06 have been reported (Collaizzi and Klink, 1969; Kulshrestha et al., 2004). OTC is susceptible to abiotic transformation by processes including hydrolysis, photolysis and oxidation reactions (Halling-Sørensen et al., 2002; Rose and Pedersen, 2005).

3.2 Interaction with pure clays

Structural characteristics of the soil mineral composition together with favorable chemical speciation affect the sorption behavior and retention process of OTC in soil medium (Figueroa et al., 2004; Aristilde et al., 2010). Figueroa et al. (2004) reported more favorable sorption of a fully protonated OTC to montmorillonite (K_d = 44108 L/kg) than to kaolinite (K_d = 222 L/kg). In a study by Kong et al. (2012), illite and kaolinite content showed a negative and positive correlation, respectively with sorption capacity K_d. Aristilde et al. (2010) demonstrated the presence of OTC in montmorillonite interlayer spaces under acidic pH. At alkaline pH, sorption was explained by complexation of external sites.

Although, OTC sorption decreases as solution pH is raised (Figueroa et al., 2004; Aristilde et al., 2010; Figueroa et al., 2010), the sorption coefficient decreases gradually (from pH 6 to 8) instead of showing the expected characteristic “edge” behavior due to the absence of cationic OTC species competing for negatively charge sites (Figueroa et al., 2004). These results demonstrate the importance of the zwitterionic species (OTC^{-0+}) at

environmentally relevant pH ranges. Even though the net charge of a zwitterion is neutral, the partial positive and negative charges are spatially distant and react individually on charge exchange sites (Sassman and Lee, 2005).

Ionic strength of the soil suspension can also affect the sorption to the clay particles. Assessment of OTC adsorption on pure clays at low ionic strength suggests cation exchange and surface complexation as the most important sorption mechanisms for the cationic (OTC^{00+}) and zwitterionic (OTC^{-0+}) species, respectively (Figueroa et al., 2004). Figueroa et al. (2004) reported reduced adsorption on clay as ionic strength increases. These results indicate the importance of considering solution speciation and presence of competitor ions in soil pore water in modeling the sorption of OTC.

Sorption of OTC onto clay surfaces is also affected by the type of cation(s) present due to competition at the sites. OTC replaces cations in sodium (Na^{+}) saturated clays more efficiently than in calcium (Ca^{+2}) saturated clays under acidic conditions. At low pH where OTC^{00+} and OTC^{-0+} are the dominant species (competing for negative charge sites on clays), higher sorption occurred in the presence of Na^{+}. In contrast, under alkaline conditions (OTC^{--+} and OTC^{--0} as dominant species), calcium based clays exhibited higher sorption than sodium based clays. Sorption occurs through cation exchange and cation bridging at low and high pH, respectively (Figueroa et al., 2004; Figueroa, 2012). OTC and other Tetracycline antibiotics are known to form complexes with several divalent and trivalent metal ions (Martin, 1979; Kulshrestha et al., 2004; ter Laak et al., 2006a). Batch equilibrium sorption experiments are typically performed using 10 mM $CaCl_2$. Consequently, a significant amount of OTC is expected to be complexed with calcium in these batch equilibrium sorption experiments resulting in the overall sorption coefficient being underestimated due to possible dissolved Ca-OTC complexation (ter Laak et al., 2006b; Figueroa and MacKay, 2005).

3.3 Interaction with organic matter and metal oxides

Organic matter is also an important component that influences the sorption of OTC to soils. Mineral particles are generally coated with organic matter, becoming a first-line surface to which sorption can occur (Figure 3.2) (Figueroa, 2012). OTC is typically released into the environment through land application of liquid slurry or manure (biosolids). Organic matter contains acidic functional groups which may have pH-dependent ionization and interact with a ionized OTC species. (Sithole and Guy, 1987a; Figueroa, 2012)

Biosolids are rich in organic matter, however the amount of acidic functional groups is expected to be lower in comparison with natural soil organic matter (Riffaldi et al., 1983; Figueroa, 2012). Riffaldi et al. evaluated the chemical composition of different organic wastes and concluded that immature humic substances have more complex molecular structures, lower degree of carbonization and acidic groups in comparison with natural soil organic matter. Thus, sorption of OTC to mature soil organic matter is expected to be greater than to fresh solid waste. Experimental results from Figueroa (2012) confirmed this trend in behavior for OTC interaction with fresh and aged manure. K_d values of 72 and 1020 L/Kg were reported for fresh and aged solid manure, respectively, at similar pH (5.5 and 5, respectively). Cation exchange has been suggested as the primary sorption mechanism with humic substance, as a result sorption is directly affected by the quantity of acidic functional groups in organic matter and not only the amount of organic matter per se (OM$\%$). Other mechanisms involved are cation bridging and hydrogen bonding (Figueroa, 2012).

Studies on the interaction of OTC with metal oxides show increased sorption with increase of pH to an apparent maximum at pH $\sim$ 8 (Figueroa and MacKay, 2005). Results from the same study suggest the formation of surface complexes as the prevalent sorption mechanism. A Langmuir isotherm was fitted to geothite and hematite batch sorption

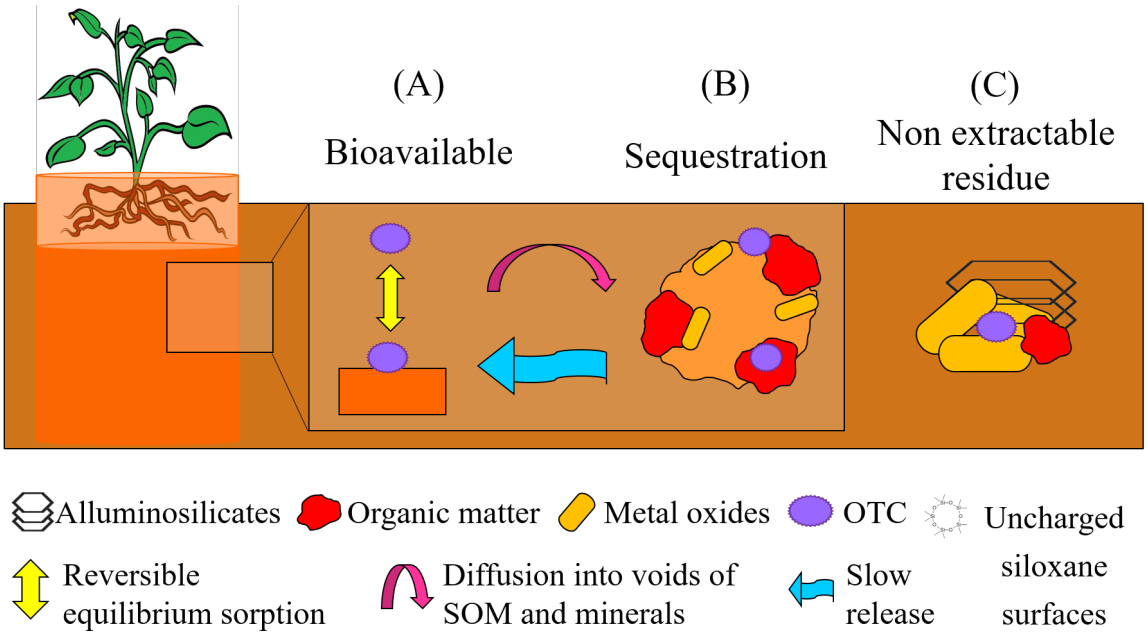

Key / Soil component — Receptor site					Corresponding Sorption mechanism
Non-polar	x			x	Hydrophobic partitioning
Polar	x	x	x		Electron donor acceptor
Positive charge		x	x		Anion exchange
Surface bound Al and Fe		x	x		Surface complexation
Negative charge	x	x	x		Cation exchange
Negative charge with sorbed cation	x	x	x		Cation bridging

Figure 3.2: OTC interactions with soil components (alluminosilicates, organic matter, metal oxides. There is a fraction that is immediately bioavailable (A). The sequestered fraction (B) can be slowly be release back into a solution or as easily extractable forms. Besides the reversible equilibrium sorption (A) and sequestration process (B) there is a fraction that may form non-extractable residues (C). Modified from Jechalke et al. (2014) and MacKay and Vasudevan (2012).

experiments over the concentration range tested at pH conditions of 5.5 .

3.4 Interaction with soils

Soils are complex systems which host a variety of physical, chemical and biological processes. Soils typically are considered to include three components relevant to chemical activity: alluminosilicates, organic matter and metal oxides and hydroxides. OTC interaction with soil components has one or more key receptor sites (e.g. positive charge, negative charge, polar domain, non-polar domain and surface bound Fe and Al) with a corresponding sorption mechanism (Figure 3.2) (MacKay and Vasudevan, 2012).

Organic matter, alluminosilicates and metal oxides have been individually reported as important contributors to OTC sorption. Several authors investigated the sorption of OTC to soils and have contributed to the understanding of this phenomenon (Jones et al., 2005; ter Laak et al., 2006b; Chu, 2011; Kong et al., 2012; Teixido et al., 2012; Gong et al., 2012; Figueroa, 2012).

Multi-linear regression K_d models whose derivation is based on the physical and chemical soil properties have been reported and are summarized in Table 3.1. The Jones et al. (2005) model highlighted effective cation exchange capacity (ECEC) and free or crystalline Fe (DCB Fe) as probable predictor variables of K_d. Other authors reported cation exchange capacity (CEC), organic carbon (OC), pH, texture (clay content) and free or crystalline Al (DCB Al) also as probable predictor variables of K_d (ter Laak et al., 2006b; Gong et al., 2012; Teixido et al., 2012). The models were reported with satisfactory estimations ($R^2 > 0.7$), except for Jones et al. (2005) ($R^2 = 0.24$). Jones et al.'s (2005) model uses ECEC which was measured at the natural soil pH, whereas batch sorption experiments were conducted at pH 5.5. Thus, the prediction capability of the K_d model from Jones et al. (2005) does not reflect the CEC of the soil samples at the experimental sorption pH because CEC is pH dependent. In addition, it is noteworthy to highlight that batch

sorption experiments corresponding to the models summarized in Table 3.1, except that by Jones et al. (2005), were conducted with electrolyte solutions of 10 mM $CaCl_2$ (Table 3.2) according to the standard protocol from Organization of Economic Co-operation and Development (OECD) guideline 106 for batch equilibrium sorption measurements (OECD, 2000).

Calcium presence in a soil solution can interfere with OTC sorption by competition with OTC for cationic exchange sites or formation of OTC-Ca^{2+} complexes resulting in a reduced sorption (Martin, 1979; Kulshrestha et al., 2004; ter Laak et al., 2006a; Essington et al., 2010). The resulting degree of complexation at the experimental salt concentration prescribed (10 mM $CaCl_2$) is significantly higher than what would be found in pore water of neutral soils (Rees et al., 1995; Orem et al., 1997; Sposito, 2008; Essington, 2015). ter Laak et al. (2006a) observed approximately 60% and 54% degree of complexation at 10 mM $CaCl_2$ for a loam and sandy loam soil, respectively, whereas, 24% and 18% were observed for 1 mM $CaCl_2$ and decreased sorption with increasing ionic strength (ter Laak et al., 2006a; Figueroa and MacKay, 2005).

Organic matter presence in soil can increase and decrease OTC sorption. Batch sorption experiments with manure amended soils have shown significant enhanced sorption of OTC to soils compared unamended controls (Li et al., 2010; Figueroa, 2012). For example, increased organic carbon (OC) content in soil (16 g/kg, 32 g/kg and 50 g/kg) resulted in increased sorption (Li et al., 2010). In contrast, dissolved organic matter (DOM) present in soil increased and decreased OTC sorption, depending on the pH and amount of DOM (Kulshrestha et al., 2004). High concentrations of DOM (10 mg/L) were reported to decrease sorption on clay, while low concentrations (1 mg/L) increased sorption. As DOM concentration increases, the availability of receptor sites on the clay sorbent decreases resulting in freely dissolved humic acids which may desorb OTC from clay-associated humic acids to form OTC-DOM complexes (Kulshrestha et al., 2004; Essington et al., 2010;

Table 3.1: Model Parameters summary

Predictor	Model	R^2	References	Stock solution	pH
K_d =	19.56 (ECEC) + 4.16 (DCB Fe)	0.24	Jones et al. (2005)	MES	5.5[a]
log K_d =	3.67 - 1.39 $\times$ 10^1 (pH) + 1.32 $\times$ 10^2 (Clay) + 7.07 $\times$ 10^{-4} (DCB Fe) + 5.91 $\times$ 10^{-3} (DCB Al) + 2.84 $\times$ 10^{-2} (Al) + 1.37 $\times$ 10^{-2} (Ca)	0.87	Gong et al. (2012)	$CaCl_2$	4.7 - 7.8[b]
log K_d =	4.008 + 1.138(α) + 0.752 (log OC) + 0.160(log Clay) + 0.186(log CEC) - 0.089 (log FeOx) + 0.001(log AlOx)	0.69	ter Laak et al. (2006b)	$CaCl_2$	3.4 - 7.4[b]
log K_d =	3.630 - 0.131(pH) + 0.023(OC) - 0.016(Clay) - 0.181(K_2O) + 0.028 (Al_2O_3)	0.92	Teixido et al. (2012)	$CaCl_2$	3.9 - 8.2[c]

[a] pH titrated with NaOH; [b] batch experiments at natural soil pH; [c] pH measured after equilibration with 10mM of $CaCl_2$.

Table 3.2: Experimental conditions of batch sorption experimets conducted on clay, organic matter, iron oxides and soil sorbents

Stock solution	Sorbent	$[OTC]_{sol}$ (mM)	Sorbent loading (g/L)	$[OTC]_{soil}$ $\left(\frac{mg_{OTC}}{kg_{sorbent}}\right)$	K_d (L/kg)	Measurement Technique	Reference
$NaHCO_3$	Clay[c]	0.083	0.4	95540	44108	HPLC-UV/vis spectroscopy	Figueroa et al. (2004)
$NaHCO_3$	Clay[d]	0.083	4.8	8025	222		Figueroa et al. (2004)
$CaCl_2^{+PIPES}$	OM fresh	0.13	58	1034	72		Figueroa (2012)
$CaCl_2^{+PIPES}$	OM aged	0.13	2.5	23942	1020		Figueroa (2012)
PIPES[b]	Iron oxides	0.04 to 0.24	10	1841 to 11050	Langmuir		Figueroa and MacKay (2005)
MES[a]	Soil	0.01	5	920	486 to 12,047	HPLC/diode array (λ = 360 nm)	Jones et al. (2005)
PIPES[b]	Soil	0.005 to 0.03	5	460 to 2762	327 to 2737	HPLC with Lichrospher RP-18 endcapped column (λ = 360 nm)	Figueroa and MacKay (2005)
PIPES[b]	Soil	0.13	2.5	23943	140 to 7600	HPLC with Lichrospher RP-18 endcapped column (λ = 360 nm)	Figueroa et al. (2010)
$CaCl_2$	Soil	1.25 to 25 mg/L	125	10 to 200	417 to 1026	LC with fluorescence detection (λ = 390 nm)	(Rabølle and Spliid, 2000)

Table 3.2: Continued

Stock solution	Sorbent	$[OTC]_{sol}$ (mM)	Sorbent loading (g/L)	$[OTC]_{soil}$ $\left(\frac{mg_{OTC}}{kg_{sorbent}}\right)$	K_d (L/kg)	Measurement Technique	Reference
$CaCl_2$	Soil	0.0004 to 0.065	17	11 to 1746	1229 to 269,097	HPLC with UV and fluorescence detector,C-18 guard column,and a Supelcosil LC-18 reverse-phase column (λ = 370 nm)	Sassman and Lee (2005)
$CaCl_2$	Soil	7.5 to 15 mg/L	1,0000	7.5 to 15	946 to 7199	HPLC with YMC C-18 column (λ = 360 nm)	ter Laak et al. (2006b)
$CaCl_2$[e]	Soil	0.005 to 0.5	200	11.5 to 1151	295 to 2209	HPLC with UV detector (λ = 360 nm)	Chu (2011)
$CaCl_2$	Soil	0.5 to 10 mg/L	20	0.75 to 1.5	115 to 2399	HPLC with diode array detector (λ = 360 nm)	Teixido et al. (2012)
$CaCl_2$	Soil	N/A	N/A	N/A	380 to 15848	HPLC with UV and fluorescence detector and a C-18 reverse phase column (λ = 360 nm)	Gong et al. (2012)
KNO_3	Soil	0.005	5	460	650 to 2191	HPLC with photodiode array detector and C-18 reversed-phase column (λ = 355 nm)	Kong et al. (2012)
KNO_3	Soil	0.008 to 0.258	5	737 to 23758	K_f		Kong et al. (2012)

[a] 2-(4-Morpholino) ethaneusulfonic acid; [b] 1,4-piperazinebis (ethanesulfonic acid); [c] Montmorillonite; [d] Kaolinite [e] Ionic strenght of electrolite solution = 5 mM

Chen et al., 2015). This phenomenon suggests that high levels of DOM, as those found in animal manure, may decrease OTC sorption to soil, hence increasing the mobility of OTC (Kulshrestha et al., 2004).

Once spread on soil, OTC interacts with soil and is susceptible to transformations. OTC is transformed due to photodegradation (Halling-Sørensen et al., 2002; Rose and Pedersen, 2005) however poor light penetration in soil limits this degradation pathway (Jechalke et al., 2014). Like other organic compounds, the sorption of OTC to soil is primarily governed by a reversible equilibrium reaction (Figure 3.2A) and following a kinetic sorption/desorption with a slow release rate (Figure 3.2B) which results in sorption hysteresis (Jechalke et al., 2014; Lee et al., 2014). It follows that bioavailability is reduced with increasing contact time by secondary sorption reactions and mobilization into micro and nanopores. This phenomenon of sequestration, could reduce acute toxicity but increase residence time of OTC in soil. Variability of concentrations (Aga et al., 2005) and increases in concentration of Tetracyclines (Hamscher et al., 2002) without additional antibiotic input have been reported suggesting persistence of TCs in soil over time (Aga et al., 2005).

In addition to the reversible equilibrium sorption and sequestration, a fraction of OTC may form non-extractable residues (Figure 3.2C) (Jechalke et al., 2014). Studies on removal of extractable OTC showed high availability of non-extractable residues (0.1 mol/L Na_2EDTA-McIlvaine as extractant) (Bao and Zhou, 2015). Changes in the composition of the soil (organic material, microbial population, pH or redox potential) (Hamscher et al., 2002; Aga et al., 2005) may result in the release of OTC from soil over time.

3.5 Methodology

A multiple stepwise regression (MSR) to evaluate the relationship between sorption coefficients (K_d - dependent variable) and the group of soil properties as potential pre-

dictors (independent variables) was performed using JMP® PRO. A backward stepwise regression method was used to compare several regression models. Predicted values with the highest p-value were removed one at a time. The stopping criteria for the removal of provable predictors used for the model was that where all predictors had a strong statistical significance in making predictions on K_d (p-value ≤ 0.01).

The K_ds and soil properties used to generate the MSR model are those from Figueroa et al. (2010) where the buffer solution PIPES was used as the electrolyte solution for the batch sorption experiments to minimize potential complex formations. Another reason to select the data reported by Figueroa et al. (2010) to generate the MSR model is that the CEC was measured at the pH at which the sorption experiment was conducted. It is important to highlight that CEC was measured using a direct method by saturating the soil samples with $MgCl_2$ and thereafter Mg^{2+} was displaced with $BaNO_3$ (Figueroa et al., 2010). Summation of exchangeable base cations is a common indirect method used for estimating CEC. However, CEC estimates are lower in comparison with those obtain using direct methods.

Predicted values were plotted against measured values together with the confidence interval for the model. Pearson product-moment correlation analysis between soil properties and sorption coefficient were conducted with two-tailed significance test using JMP. The predictive ability of the resulting multi-linear regression model was tested with sorption experimental data developed from equilibrium experiments using PIPES buffer solutions and $CaCl_2$ as the electrolyte solution.

3.6 Results and discussion

The influence of physical-chemical soil properties on OTC sorption was evaluated using the Peason correlation analysis method (Table 3.3). Results indicate that OM and dithionite citrate bicarbonate (DCB) (Fe+Al) have a strong positive correlation with the

sorption coefficient (K_d). CEC exhibits a moderate positive correlation whereas clay content and pH exhibit weakly negative correlation values. MSR identified a three term model (Equation 3.1) with the input of Clay (%), OM(%), CEC ($cmol_c$/kg), pH and DCB (Al+Fe) (mmol/kg) as provable predictors of K_d. CEC, OM% and DCB (Al+Fe) explain 95% of the variation in K_d (Figure 3.3) and are in line with available understanding of soil solid components, sorbent receptor sites and interaction mechanisms that influence sorption behavior of OTC in soil. Equation 3.1 was generated from K_ds of batch sorption experiments and soil properties of seven soil samples at three pH values (5.0, 7.0 and 8.5) (Figueroa et al., 2010). The buffer solution (PIPES) selected for the batch sorption experiment provided the conditions to prevent interference in OTC sorption. The absence of Ca^{2+} prevents competition for cationic exchange sites and reduces OTC complex formation. Additionally, the CEC was measured at the pH of the sorption experiment. CEC was measured using a direct method by saturating the soil samples with $MgCl_2$ and thereafter Mg^{2+} was displaced with $BaNO_3$ (Figueroa et al., 2010).

Table 3.3: Correlation between soil properties and soprtion coefficient (K_d)

	Clay	OM	CEC	pH	Al+Fe	Kd
Clay	1.00	-0.03	0.49*	-0.06	-0.08	-0.16
OM		1.00	0.60*	0.19	0.34*	0.60**
CEC			1.00	0.49*	0.40	0.43*
pH				1.00	0.05	0.03
Al+Fe					1.00	0.93**

* Significant at $\alpha \leq 0.05$ ** Significant at $\alpha \leq 0.01$

$$K_d = -626.8 - 28.0 \text{ CEC} + 277.7 \text{ OM} + 3.9 \text{ DCB (Fe+Al)} \tag{3.1}$$

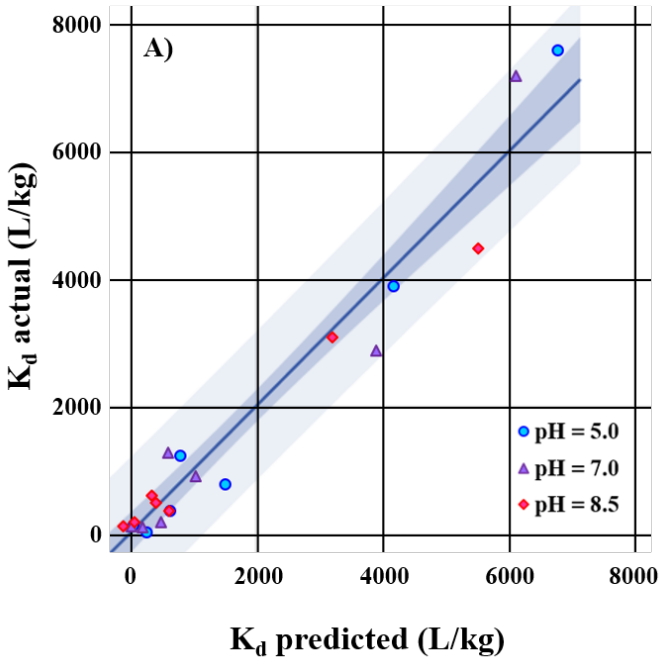

Figure 3.3: A) Estimation of OTC sorption coefficients using Equation 3.1. Solid line: 1:1 relationship; dark shaded area: confidence interval of the expected value; light shaded areas: prediction interval of the expected value. Measured and reported values from Figueroa et al. (2010) at pH $\approx$ 5.0 (●, blue), 7.0 (◇, violet) and 8.5 (▲, magenta).

The range of soil properties values covered by the model are presented in Figure 3.4 as box plots. Efforts to evaluate the applicability of the model (Equation 3.1) with other soil data are currently limited due to the terms included as predictors in equation 3.1 or the conditions at which the model is valid. For example, soil oxide content (DCB Fe and Al) is not a soil property typically reported in sorption studies (Figueroa et al., 2010); CEC corresponds to cation exchange capacity measured at the experimental condition pH; the model was generated with data from batch sorption experiments conducted with the PIPES buffer solution to minimize OTC-Ca^{2+} complex formation. Most K_ds reported in the literature are a result of equilibrium batch sorption experiments that use $CaCl_2$ as electrolyte solution (Table 3.2). Therefore, is expected that the K_d values reported from these studies were affected by complexation with Ca^{2+}.

Efforts to evaluate the applicability of Equation 3.1 are presented in Figure 3.5. The only available data of batch sorption experiments to test the applicability of equation 3.1 where a PIPES buffer solution was used (other than the ones used to generate the model) were two soil samples (Orangeburg and Georgeville) from Figueroa and MacKay (2005). Estimated sorption coefficients for both soils (Georgeville and Orangeburg) are within the prediction interval. Despite CEC being reported at the natural soil pH (5.3 and 6.0, respectively) and K_ds being obtained from batch sorption experiments conducted at pH 5.5, the difference in pH and speciation distribution is not significant.

Another OTC sorption coefficient data set available with extensive characterization of soil properties reported is that from Jones et al. (2005) (30 soils). Data from Jones et al. (2005) could not be used to verify the predictability of equation 3.1 due to reported CEC values at conditions other than that of the experiment. Jones et al. (2005) measured CEC at natural soil pH (pH_w) which ranged from 3.2 to 7.5 by using an indirect method

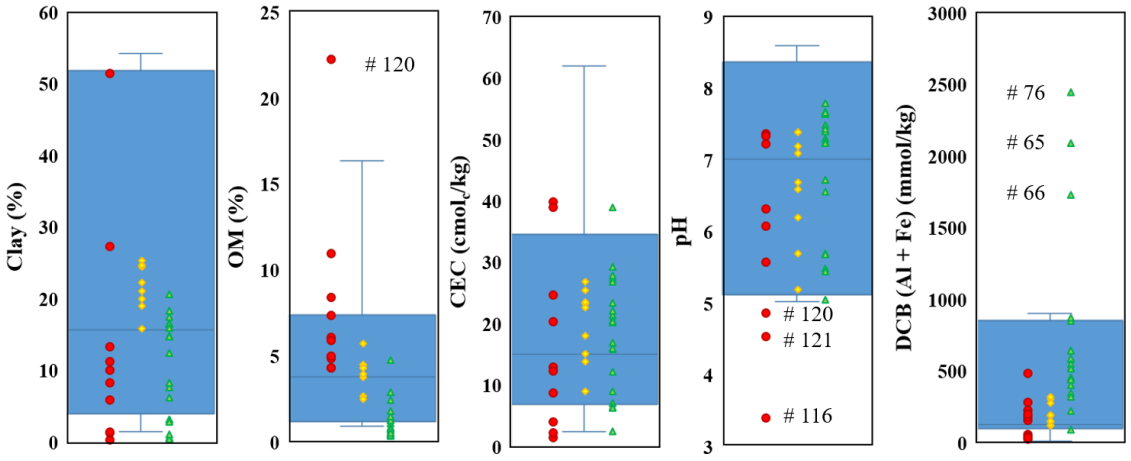

Figure 3.4: Range of soil properties reported for soil samples used to generate Equation 3.1 (Box plot) and compared to soil properties from ter Laak et al. (red ●), Chu (yellow ◇) and Gong et al. (green ▲). Soil properties of soil samples #65, #66, #76, #116, #120 and #121 are considered outliers because pH or Al+Fe values are significantly outside the range of soil properties used to generate the model.

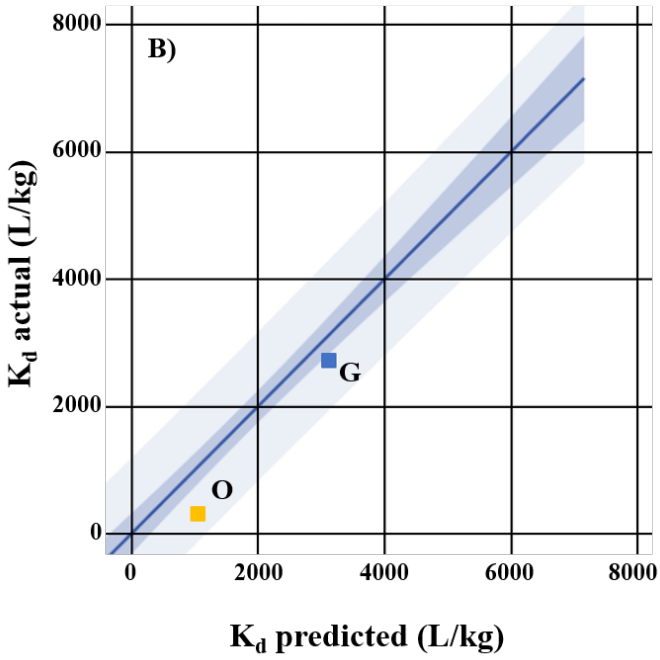

Figure 3.5: Actual and Predicted sorption coefficients for soil samples Orangeburg (O) and Georgeville (G) from Figueroa and MacKay (2005). Solid line: 1:1 relationship; light shaded area: prediction interval of the expected value using Equation 3.1.

(summation of exchangeable cation), whereas batch sorption experiments were conducted at pH 5.5 with MES buffer solution. Differences in experimental pH conditions and those at which CEC was measured may result in either under- and over-estimation of CEC. For example, experimental conditions with pH>pH$_w$ can result in an under-estimation of CEC, while experimental conditions with pH<pH$_w$ can result in an over-estimation of CEC.

The soil samples that Figueroa et al. (2010) used for batch sorption experiments are a subset of soil samples used by Jones et al. (2005). Comparison of the same soil K_ds at pH 5.0 (Figueroa and MacKay, 2005) and 5.5 (Jones et al., 2005) are presented in Figure 3.6. Buffer solutions used were PIPES and MES, respectively. Even though experimental conditions are similar (pH range and use of buffer solution), there are significant differences in the K_ds reported. The K_d values generated by Jones et al. (2005) are between

2 to 18 times higher (Heide and Goldsboro, respectively) than the K_d values reported by Figueroa et al. (2010), except for the Adams soil which is lower. The difference in these results highlight the importance or sensitivity of the K_d determination process associated with the experimental conditions. In a similar way, the experimental conditions and ranges of parameters introduced in equation 3.1 should be kept within those covered by the data used to develop equation 3.1.

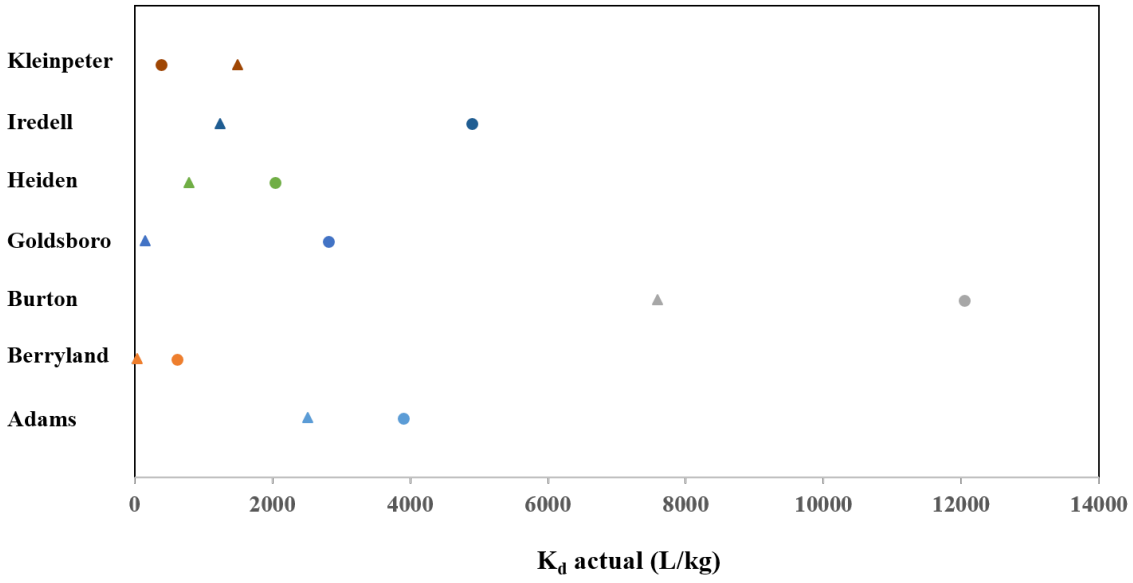

Figure 3.6: Comparison of measured sorption coefficients on the same 7 soil samples under similar experimental conditions. K_ds from Figueroa et al. (2010) (●) and Jones et al. (2005) (▲).

Additional efforts to assess the applicability of equation 3.1 for studies that used $CaCl_2$ are presented in Figure 3.7. K_d estimates with soils properties reported by ter Laak et al. (2006b), Chu (2011) and Gong et al. (2012) were plotted against measured K_ds from batch sorption experiments conducted with $CaCl_2$ as electrolyte solution. Experimental conditions and quantification techniques of the studies are summarized in Table 3.2. About

60% of the predicted sorption coefficients are within the prediction interval. The other 40% of the predicted sorption coefficients are above the 1:1 relationship line suggesting under-prediction values. Given the electrolyte solution used in these experiments, calcium complexation is expected to occur, therefore lower K_d values. In addition, soil samples from Chu (2011) and Gong et al. (2012) were analyzed with HPLC-UV. OTC quatification with HPLC-UV has been reported to be impacted by complex formations with metals of varying valency (Buckley, 1985; Figueroa and MacKay, 2005). These results suggest the importance of the analytical methods used for the quantification of OTC sorption coefficients (Wegst-Uhrich et al., 2014) and resulting estimated model parameters.

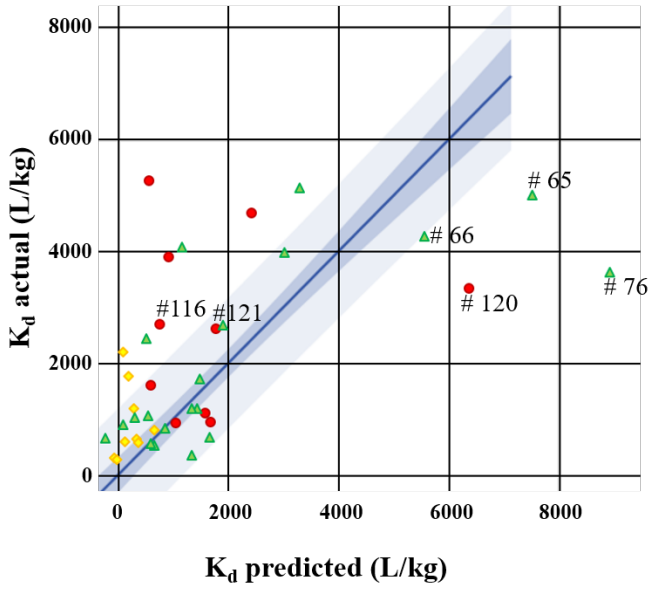

Figure 3.7: Actual and estimated K_d for data from ter Laak et al. (2006b) (red •), Chu (2011) (yellow ⋄) and Gong et al. (2012) (green ▲). Soil properties of soil samples #65, #66, #76, #116, #120 and #121 are considered outliers because pH or Al+Fe values are significantly outside the range of soil properties used to generate the model as shown in Figure 3.4.

3.7 Summary

OTC sorbs strongly to the components of soils (aluminosilicates, metal oxides and OM) through multiple interaction mechanisms. The determination of K_d values from batch sorption experiment is highly influenced by several features, such as such as the electrolyte solution and the analytical method for quantification of sorbed mass.

A model to predict K_d values was developed based on physical and chemical soil properties. Out of five soil properties considered, OM%, CEC and DCB (Al+Fe) were highly correlated with K_d and were identified as provable predictors of K_d in the MSR analysis and explained about 95% of the variation.

The model (equation 3.1) is valid for the ranges of the predictor variables presented in Figure 3.4. Also, no complexation effect is considered in the model, as the data to develop equation 3.1 is from batch sorption experiments that used PIPES buffer solution. The presence of multivalent cations interfere with true K_d estimations due to competition of sorption sites and complexation. Therefore, using the model to estimate sorption under such conditions (multivalent cation presence), underestimation of K_ds is expected.

Currently, limited data of K_ds and soil properties are available under the conditions above described. More data is needed for further testing the applicability of the developed model.

4. FUNDAMENTALS OF TRANSPORT AND SORPTION MODELING IN POROUS MEDIA

During the past century, thousands of anthropogenic substances of human origin have been found to be environmental contaminants, either by intentional application (applied to land during agricultural practices) or unintentionally released (leakage from industrial or municipal waste sites). Some of these chemicals pose a significant risk to human health when the food chain and/or surface and subsurface water supplies are compromised (Šimůnek and van Genuchten, 2007).

Modern agriculture utilizes an unprecedented number of chemicals for plant and animal production, such as, fertilizers, pesticides, hormones and antibiotics. These chemicals can undergo physical, chemical and biological transformations that directly impact and control their fate in the environment and alter natural processes in soil, surface water and groundwater. Sorption is believed to be the main mechanism that influences the environmental fate of organic chemicals into the groundwater and soil matrix (Altfelder et al., 2001; Magga et al., 2012). For example, some organic contaminants are degraded in the soil within a certain time. In contrast, others degrade slowly or are strongly sorbed onto and within the soil particles and are generally considered not bioavailable. However, several studies report an "apparent availability" in which desorption is not a prerequisite for biodegradation of the soil-sorbed organic contaminant (Park et al., 2003)..

Persistence of contaminants in soils increases the potential for environmental consequences. To assess the potential impact of natural and/or human induced stresses, understanding and predicting contaminant transport processes is essential. Thus, contaminant transport simulations support the development of best management practices (BMPs) to minimize of amend the environmental impact on ground, surface and groundwater of nu-

trients and pesticides from agricultural practices. Most BMPs attempt to optimize the handling, timing and land surface application of fertilizers in order to optimize the crop, nutrient uptake efficiency and reduce leaching of nutrients which all turns into economic benefits and contributes to human well being.

Since the 1960's several models have been developed to quantitatively describe the movement or transport of inorganic and organic contaminants through porous media. The Advection-Dispersion Equation (ADE) is the most used approach to describe solute transport in porous media and was developed on the basis of solute transport experiments in soil columns inside a laboratory (Bronswijk et al., 1995). This solute transport model is based on assumptions of homogeneous porous medium, inter-phase mass transfer process (e.g. sorption, liquid-liquid partitioning or volatilization) and transformation reactions that are linear and essentially instantaneous. Solute transport that follows these behaviors is considered to be ideal (Figure 4.1) (Brusseau, 1998; Konikow, 2011). Unfortunately, at the field scale, it is not realistic to expect such ideal behavior and controlled conditions (Feyen et al., 1998; Zhou, 2002; Šimůnek, 2005). The reasons for this include spatial variability of the soil properties and preferential flow at the field scale, among others (Bronswijk et al., 1995). Figure 4.1 shows a comparison of the classic ADE (ideal transport, dashed lines) and the nonequilibrium models (nonideal transport, solid lines) for nonreactive (blue lines, no sorption) and reactive (red lines, sorption) solutes.

Water flow and solute transport in heterogeneous porous media can present physical heterogeneity, caused by the various shapes and particle size distribution and chemical heterogeneity caused by the nonuniform composition of the soil matrix (Ma and Selim, 1998). These nonuniformities cause nonequilibrium processes on the soil which are difficult to quantify (Leij and Toride, 1998) and can be grouped into two general categories: transport related (physical nonequilibrium) and sorption related (chemical nonequilibrium) (Brusseau et al., 1989).

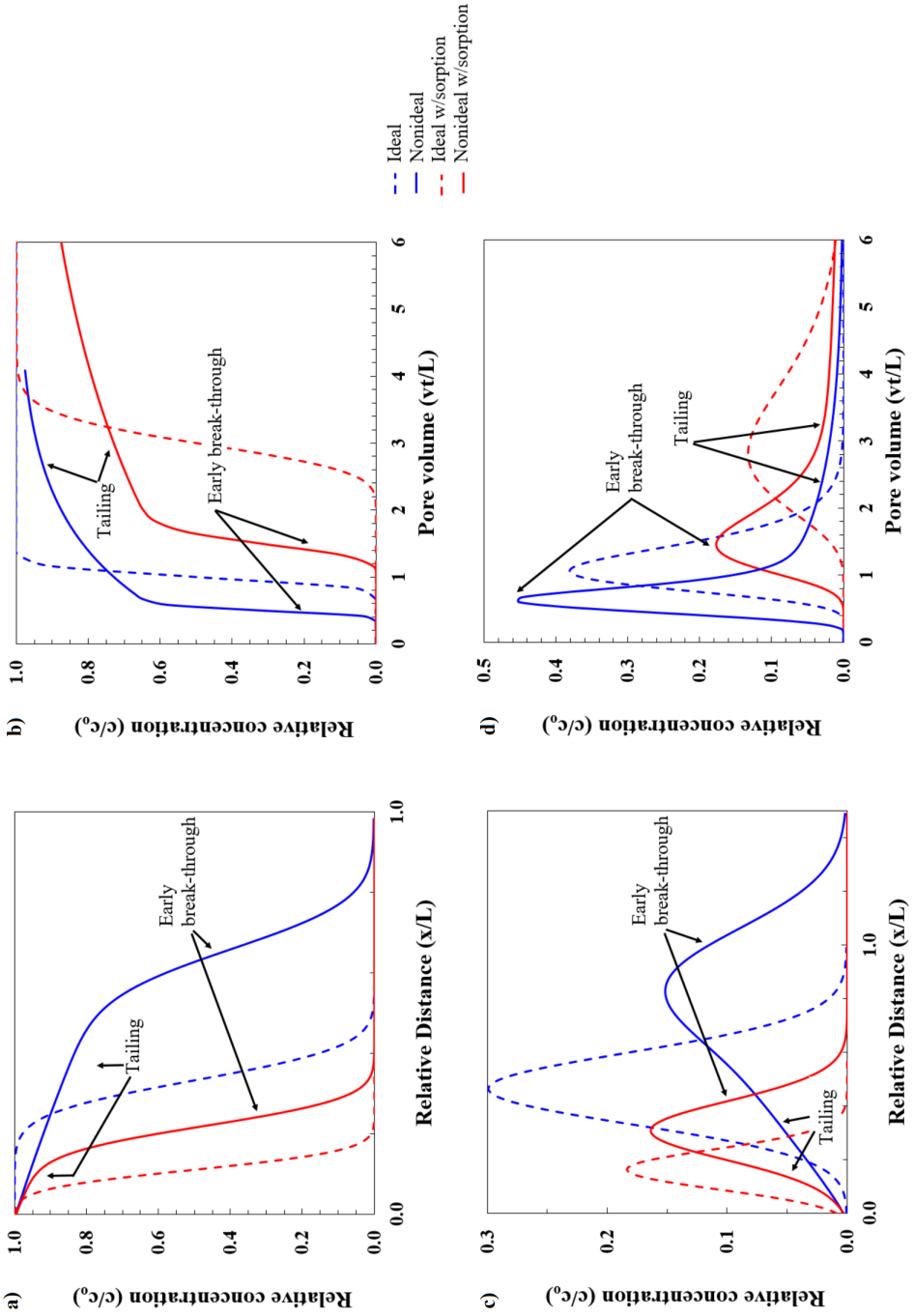

Figure 4.1: Break-through curves for ideal and non ideal transport. Figures a) and b) shows the effluent curve for a step input and c) and d) for a Pulse. Modified from (Brusseau, 1998)

Physical nonequilibrium models are based on the assumption of a mobile and an immobile region in the soil matrix. Chemical nonequilibrium models are based on two or more types of sorption sites where each site is subject to a different mass-rate transfer. For many transport simulations, the physical and chemical transport parameters are commonly assumed constant along the soil profile to facilitate the derivation of an analytical solution (Leij and van Genuchten, 1995). For this same reason, mass transfer processes are assumed to be linear. While analytical solutions are available for relatively simple problems, one must rely on numerical methods to compute an approximate solution when the problem are complicated by factors such as, irregular geometry of the problem, heterogeneous soil properties and nonlinear equations (Bear and Verruijt, 1987; Logan, 2001).

Two of the earliest models that account for some degree of heterogeneity in the soil matrix are the dual-porosity model developed by Coats and Smith (1964) and the two-site surface adsorption model developed by Selim et al. (1976). Selim et al. (1977) and Barry and Parker (1987) proposed chemical and physical nonequilibrium models for multilayered soils, respectively. The prediction of solute transport was significantly improved by the inclusion of the nonequilibrium concept in the transport equation (accounting for heterogeneities) (Selim and Ma, 1998; Zhou, 2002; Stagnitti et al., 2003) even when the physical and chemical transport parameters are considered constant. An illustration of the applicability of the nonequilibrium models is shown in Figure 4.2. The examples consider the movement of a tracer (^3H_2O) and a herbicide (2,4,5-T) through a Glendale clay loam at low and high flow velocities. Both, the ADE and the Nonequilibrium models (NE) models were fitted to data presented by van Genuchten et al. (1977a,b). Figure 4.2 shows the fit of the data for all the examples which improves significantly using the non-equilibrium models in contrast to the classic ADE.

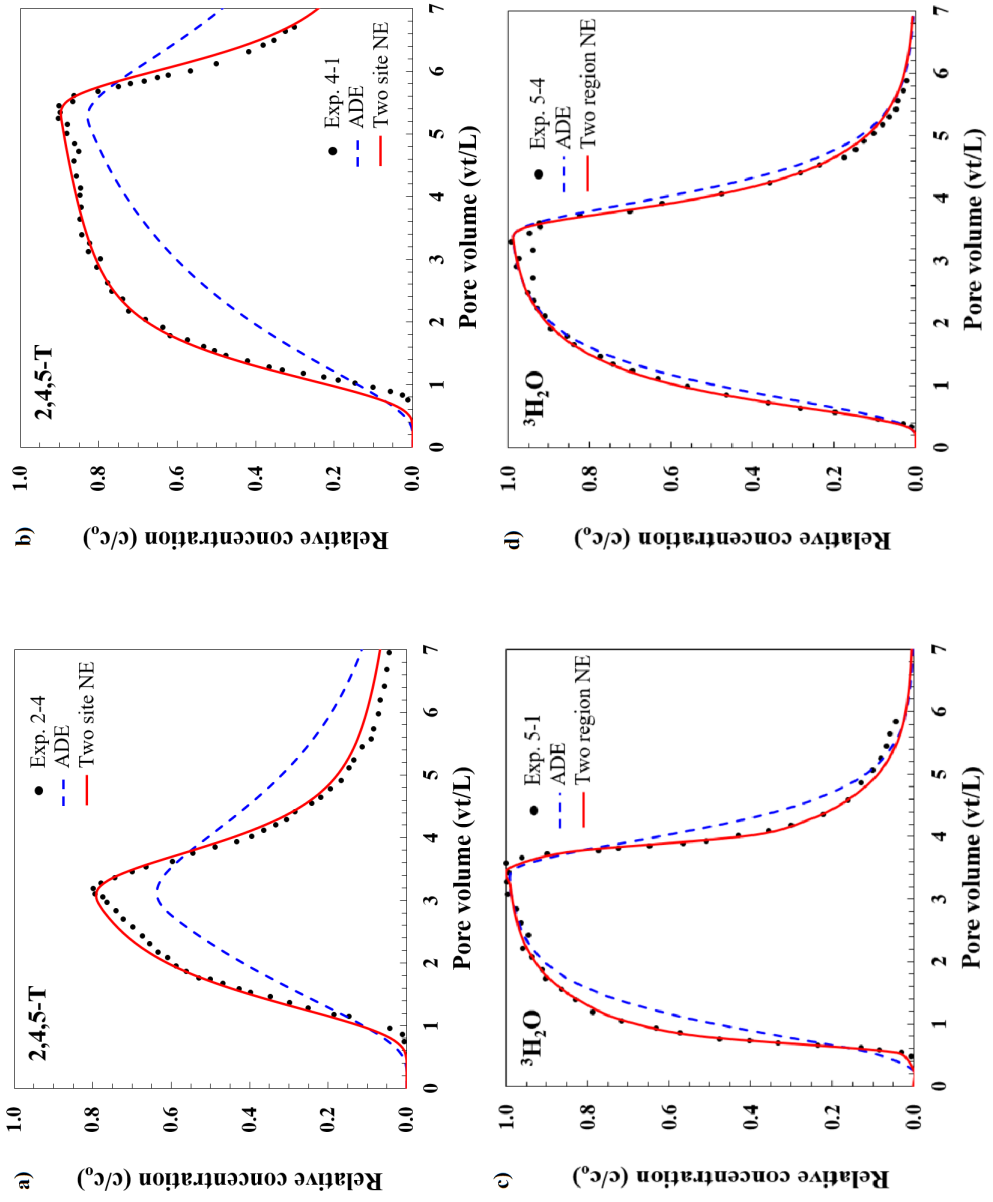

Figure 4.2: Measured and fitted BTC for a tracer (^3H_2O) and a herbicide (2,4,5-T). The dashed blue lines represents the best fit of the ADE in all figures. Figures a) and b) were fitted with the Two-site Nonequilibrium model (solid red lines) and figures c) and d) were fitted with the Two-region Nonequilibrium model (solid red line). Figures a) and d) represent columns with low flow velocity, 4.59 cm/day and 5.54 cm/day, respectively. Figures b) and c) represent columns with high flow velocity, 16.8 cm/day and 33.9 cm/day, respectively. Data for figures a) and b) was presented by van Genuchten et al. (1977b), experiments 2-4 and 4-1, respectively. Data for figures c) and d) was presented by van Genuchten et al. (1977a), experiments 5-1 and 5-4, respectively.

Even though the physical and chemical transport parameters are considered constant, the prediction of water flow and solute transport can be significantly improved by the inclusion of the nonequilibrium concept in the transport equation (to account for heterogeneities) (Selim and Ma, 1998; Zhou, 2002; Stagnitti et al., 2003).

4.1 Transport of non-reactive solutes

In nature, transport takes place through the combination of dispersion and advection. The concentration distribution behavior of the solute transport in porous media is described by the partial differential equation (PDE) known as the advection-dispersion equation (ADE) (equation 4.1). The one-dimensional ADE for solute transport into a homogeneous porous medium for nonreactive solutes is derived on the principle of mass conservation as follows (Huang et al., 1995; Leij and van Genuchten, 2000; Zhou, 2002):

$$\frac{\partial \theta c}{\partial t} = \frac{\partial}{\partial x}\left(\theta D \frac{\partial c}{\partial x}\right) - q\frac{\partial c}{\partial x} \tag{4.1}$$

where

c = solute concentration expressed as mass-per-solvent volume (mg/L)

θ = volumetric water content (cm^3/cm^3)

D = dispersion coefficient (cm^2/hr)

t = time (hr)

q = θv = volumetric flow (cm/hr)

v = average pore-water velocity (cm/hr)

x = distance (cm)

The term on the left-hand side $\left(\frac{\partial \theta c}{\partial t}\right)$ represents the rate of change (net gain or loss of mass) per unit volume and time (Kuzmin, 2010). The first term on the right-hand side $\left(\frac{\partial}{\partial x}\left(\theta D \frac{\partial c}{\partial x}\right)\right)$ of equation 4.1 represents the dispersive transport (which includes both molecular diffusion and mechanical dispersion (Konikow, 2011)) and the second term

$\left(q\frac{\partial c}{\partial x}\right)$ represents the advective transport. A usual assumption to simplify analysis, is to consider the volumetric water content (θ), the volumetric flux (q) and the dispersion coefficient (D) as constants in time and space. Thus, the ADE may be simplified to (van Genuchten and Alves, 1982; Leij and van Genuchten, 2000):

$$\frac{\partial c}{\partial t} = D\frac{\partial^2 c}{\partial x^2} - v\frac{\partial c}{\partial x} \tag{4.2}$$

When the soil water system is changing over time, equation 4.1 must be solved simultaneously with the Richards equation in its mixed-form (Huang et al., 1998) (equation 4.2) for water flow in a varibly-saturated porous medium (Jury et al., 1991; Jury and Flühler, 1992; Huang et al., 1998)

$$\frac{\partial \theta}{\partial t} = \frac{\partial}{\partial x}\left[K(h)\left(\frac{\partial h}{\partial x} - 1\right)\right] \tag{4.3a}$$

$$= \frac{\partial}{\partial x}K(h)\frac{\partial h}{\partial x} - \frac{\partial K(h)}{\partial x} \tag{4.3b}$$

where

h = pressure head or matric potential (cm)

$K(h)$ = unsaturated hydraulic conductivity (cm/hr)

The Richards equation describes the movement of water in unsaturated soil. Equation 4.3 is a nonlinear PDE and does not have a closed-form analytical solution except for a limited number of cases involving homogeneous soils (Šimůnek, 2005). The term inside the square brackets on the right-hand side of equation 4.3a $\left(K(h)\left(\frac{\partial h}{\partial x} + 1\right)\right)$ represents the Darcian fluid flux density. Mathematically, equation 4.3b has the characteristics of the ADE (equation 4.1). Comparing both equations shows a dispersive term associated with

hydraulic conduction and an advective term associated with gravitational flow (Huang et al., 1998).

4.2 Transport of reactive solutes

The ADE (equation 4.1) has been relatively successful in describing the transport of nonreactive chemicals as a function of depth in a homogeneous soil profile which produces a nearly symmetrical concentration distribution (Coats and Smith, 1964; van Genuchten and Wierenga, 1976; Jury and Flühler, 1992; Singh et al., 1996). However, it has been less accurate in describing the transport process of reactive solutes (Singh et al., 1996), particularly organic chemicals, which tend to a strong asymmetrical distribution (van Genuchten and Wierenga, 1976), and a tailing effect.

To improve the mobility prediction of organic solutes, the ADE has been subject to several modifications, such as, inclusion of linear (Figure 4.3) (Davidson and Chang, 1972; Davidson and McDougal, 1973) and nonlinear (Swanson and Dutt, 1973; van Genuchten et al., 1974) adsorption isotherms and first-order type non-equilibrium rate expressions (Singh et al., 1996).

Figure 4.3 shows the results of the ADE considering a linear adsorption isotherm. By analyzing figure 4.3a we see that the solute concentration distribution at a particular time is delayed and reduced as the value of the retardation factor (R, see section 4.6) increases. Figure 4.3b shows that the solute concentration distribution takes longer time to reach a particular depth of the soil column as R increases and also the total concentration in the solute has decreased because a fraction of it has been sorbed.

Several models have attributed this asymmetry and tailing effect of the break-through curves to either physical or chemical nonequilibrium processes (Gamerdinger et al., 1990) such as, the Two-Region and Two-Site Nonequilibrium models which are discussed later on sections 4.7.1.1 and 4.7.2.1, respectively. The cause of the long tailing effect still

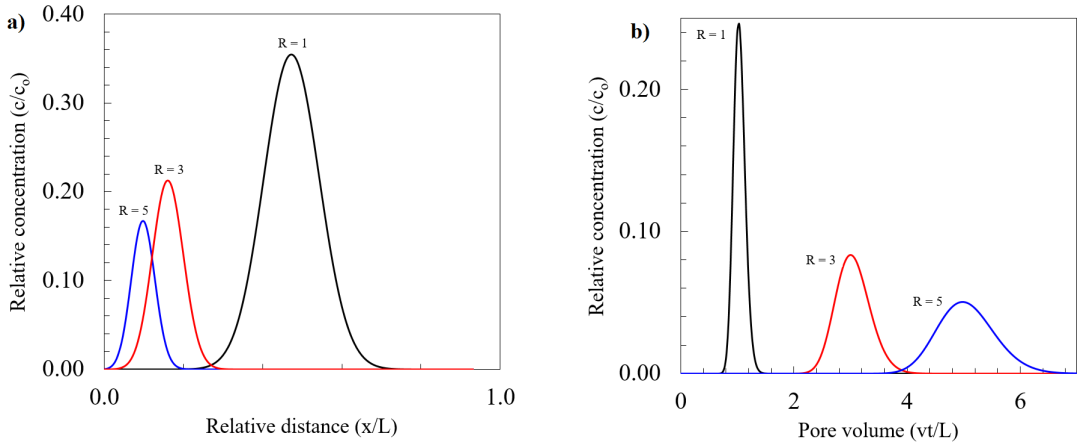

Figure 4.3: Effluent curves of the classic ADE considering linear sorption $\left(R = 1 + \frac{\rho_b K_d}{\theta}\right)$. Figure a) shows concentration distributions vs relative depth (x/L) evaluated at a same time. Comparing the three effluent curves at the same depth, shorter distance is traveled as R increases. Figure b) shows concentration distributions vs pore volume (vt/L) evaluated at the same depth or distance. As R increases, it takes longer time for the effluent curve to travel the same distance or depth. Also, the solute concentration in the liquid phase is reduced because a fraction of it has been sorbed onto the soil particles.

remains an area of active research (Li, 2004; Field and Leij, 2014).

To describe the transport of reactive solute in a porous medium, an additional term must be added to the left-hand side of the general ADE (equation 4.2) to account for the interaction between the reactive solute and the medium ($\frac{\partial s}{\partial t}$) (van Genuchten and Wierenga, 1976; Ladha, 1999). The added term ($\frac{\partial s}{\partial t}$) represents the mass exchange between the portion of the transport volume where water is flowing and other portions where mass may be stored (Jury and Flühler, 1992). The influence of sorption on reactive solute transport is of particular importance because it may slow the transport process thereby allowing greater time for microbial interaction and chemical transformations (Huang et al., 1998). The ADE can be modified to considering sorption is given by:

$$\frac{\partial \theta c}{\partial t} + \rho_b \frac{\partial s}{\partial t} = \frac{\partial}{\partial x}\left(\theta D \frac{\partial c}{\partial x}\right) - q\frac{\partial c}{\partial x} \tag{4.4}$$

where

s = sorbed concentration expressed as sorbed mass-per-soil mass (mg/Kg)

ρ_b = bulk density (g/cm^3 or Kg/L)

Equation 4.4 presents two dependent variables: the solute concentration (c) and the adsorbed concentration (s). Therefore, the solution of equation 4.4 requires an expression which relates both variables (van Genuchten and Wierenga, 1976; Huang et al., 1998). A general expression to describe the adsorption isotherm is given by:

$$s = f(c) \tag{4.5}$$

where $f(c)$ is an arbitrary function (Huang et al., 1998), such as a linear, nonlinear, first-order isotherm. The selection of the appropriate isotherm to describe $f(c)$ and the determination of the coefficients that define the isotherm should be based on the thermodynamics of the components interacting with a particular soil under consideration (Bear and Verruijt, 1987).

4.3 Equilibrium sorption models - solute retention mechanism

A plot of the concentration in the liquid phase versus the sorbed concentration from an experiment, is known as an adsorption isotherm (Jury and Flühler, 1992; Zheng and Bennett, 2002b). When equilibrium between the adsorbed and solution concentration is assumed to be reached in the experiment, the slope ($\frac{ds}{dc}$) of the plot is determined. The Linear and Freundlich isotherms are the two most common mathematical expressions for equation 4.5 that relate adsorption isotherm and are considered in this study. The temporal change in sorbed concentration ($\frac{\partial s}{\partial t}$) seen in equation 4.4 can be represented in terms of the solute concentration ($\frac{\partial c}{\partial t}$) by using the chain of rule (Goode and Konikow, 1989) as presented in equations 4.6a and 4.6b:

$$\frac{\partial s}{\partial t} = \frac{ds}{dc} \cdot \frac{\partial c}{\partial t} \tag{4.6a}$$

$$\frac{\partial s}{\partial t} = \frac{df(c)}{dc} \cdot \frac{\partial c}{\partial t} = \frac{\partial f(c)}{\partial t} \tag{4.6b}$$

4.3.1 Linear isotherm

The simplest and most widely used sorption isotherm is the linear equation, given by:

$$s = K_d \cdot c \tag{4.7}$$

where

K_d = distribution coefficient (cm^3/g or L/Kg)

According to equation 4.7, the linear sorption isotherm considers that the sorbed concentration is directly proportional to the solute concentration in the pore fluid. Thus, the slope ($\frac{\partial s}{\partial c}$) is simply the equilibrium distribution coefficients K_d. This process is assumed to be instantaneous and reversible (Goode and Konikow, 1989). To estimate the temporal change in sorbed concentration shown in equation 4.4 one can differentiate equation 4.7 and apply the chain of rule (equation 4.6) which produces the following expression; based on previously defined variables:

$$\frac{\partial s}{\partial t} = \frac{\partial s}{\partial c} \cdot \frac{\partial c}{\partial t} = K_d \frac{\partial c}{\partial t} \tag{4.8}$$

4.3.2 Freundlich isotherm

Another widely used equation to describe the relationship between the concentration of a solute in the adsorbed and dissolved phase is the Freundlich isotherm and can be

described by a relationship of the form :

$$s = K_f \cdot c^N \tag{4.9}$$

where

K_f = Freundlich distribution coefficient ($mg\ L^N/Kg\ mg^N$)

N = dimensionless coefficient

The variable K_f and the Freundlich exponent N are constant values which need to be determined in laboratory experiments for each contaminant in each porous medium. K_f is an indicator of the adsorption capacity. The Freundlich exponent N is a measure of the intensity of the adsorption and is generally less than unity (Jury and Flühler, 1992). The Freundlich isotherm is used when the adsorption isotherm behavior deviates from linearity (Jury and Flühler, 1992).

Note that when the Freundlich exponent equals unity ($N = 1$), the Freundlich equation becomes linear, and the paramenter K_f reduces to the solid-liquid phase partitioning coefficient K_d (Huang et al., 1997). Thus, the linear isotherm is a special case of the Freundlich isothem. One consequence of the nonlinear sorption ($N \neq 1$) is that the solute transport process in the soil matrix becomes dependent on the concentration and so the shape of the effluent concentration curve is strongly influenced by the variation of the effective solute velocity (v/R) with concentration (Spurlock et al., 1995; Serrano, 2001), where R is the retardation factor.

The effect from the nonlinear behavior of the Freundlich isotherm (equation 4.9) over the transport process in comparison to the linear isotherm (equation 4.7) are: (1) it makes the travel time of the pulse concentration dependent and (2) it reshapes the symmetry of the effluent concentration distribution (Jury and Flühler, 1992).

To estimate the temporal change in sorbed concentration shown in equation 4.4 one

can differentiate equation 4.9 and apply the chain of rule (equation 4.6) which gives the following equation:

$$\frac{\partial s}{\partial t} = \frac{ds}{dc} \cdot \frac{\partial c}{\partial t} = K_f N c^{N-1} \frac{\partial c}{\partial t} \tag{4.10}$$

4.4 Nonequilibrium sorption models

The use of equilibrium adsorption models is based on the assumption that equilibrium between the soil matrix and the reactive solute is so rapid that it is considered practically instantaneous. However, for some chemicals this is not the case. The use of a rate-limited (kinetic) model seems to be more appropriate to describe the sorption-desorption relationship (Travis, 1978). The rationale of this assumption is that the rate of sorption is slow compared to the rate at which the solute moves through the soil matrix (van Genuchten and Wierenga, 1976). A first order kinetic model considering linear (equation 4.11a) and nonlinear (equation 4.11b) isotherm may be written as:

$$\frac{\partial s}{\partial t} = \alpha[K_d c - s] \tag{4.11a}$$

$$\frac{\partial s}{\partial t} = \alpha[K_f c^N - s] \tag{4.11b}$$

where

α = first order mass transfer coefficient governing the rate of solute exchange between the sorbed and liquid regions; first order kinetic adsorption rate coefficient $(1/hr)$

This first order reaction rate was first incorporated into the ADE by Lapidus and Amundson (1952). Figure 4.1 shows the results of the classic ADE considering equilibrium and nonequilibrium processes. Comparing the plots on figures 4.1a and 4.1b for a step input and 4.1c and 4.1d for a pulse type input an early, high peak and an increased tail can be observed, which are characteristic features often attributed to nonequilibrium mass exchange between regions (Leij and Toride, 1998; Kamra et al., 2001).

4.5 Equilibrium transport

The sorption equilibrium relationship ($\frac{\partial s}{\partial t}$, equation 4.6b) can be substituted into the governing equation 4.4 allowing the transport equation to be expressed in term of one dependent variable, the solute concentration (c) (van Genuchten et al., 1974; Goode and Konikow, 1989) which results in:

$$\frac{\partial \theta c}{\partial t} + \rho_b \frac{\partial f(c)}{\partial t} = \frac{\partial}{\partial x}\left(\theta D \frac{\partial c}{\partial x}\right) - q\frac{\partial c}{\partial x} \tag{4.12}$$

The second term on the left hand side $\left(\rho_b \frac{\partial f(c)}{\partial t}\right)$ represents the adsorbed concentration of a generic form where $f(c)$ can take the form of any isotherm. This equation is valid regardless of how the sorption process is assumed, for example, as an equilibrium or kinetic process (Spurlock et al., 1995). Factoring out the term $(1 + \frac{\rho_b}{\theta}\frac{df(c)}{dc})$ gives:

$$\frac{\partial \theta R c}{\partial t} = \frac{\partial}{\partial x}\left(\theta D \frac{\partial c}{\partial x}\right) - q\frac{\partial c}{\partial x} \tag{4.13}$$

where R is retardation factor and is defined by:

$$R = 1 + \frac{\rho_b}{\theta}\frac{df(c)}{dc} \tag{4.14}$$

The resulting expression (equation 4.13) is solved for the solute concentration (c) and the sorbed concentration is computed by using the equilibrium relationship (equation 4.7

or 4.9) (Goode and Konikow, 1989).

4.6 Retardation factor

The retardation factor (R) was first defined by Hashimoto et al. (1964). Utilizing the traditional linear equilibrium sorption isotherm (equation 4.7), the general form of R (equation 4.14) is given by:

$$R = 1 + \frac{\rho_b}{\theta} K_d \tag{4.15}$$

The use of the Freundlich isotherm does not yield an equivalent retardation factor as presented in equation 4.15 (Selim, 2015). Thus, utilizing the nonlinear equilibrium controlled-sorption isotherm (equation 4.9), the nonlinear form of the retardation factor is given by:

$$R = 1 + \frac{\rho_b}{\theta} N K_f c^{N-1} \tag{4.16}$$

4.7 Non-equilibrium transport

4.7.1 Physical nonequilibrium

Regarding physical nonequilibrium, water flow and solute transport are significantly influenced by the ocurrence of micro-heterogeneity (macropores and structured elements) or/and macro-heterogeneity (spatial variability of soil properties). Micro- and macro-heterogeneities have distinct effects on the water flow and solute transport precess (Feyen et al., 1998).

Preferential flow, which happens mainly by advection (Leij and Toride, 1998), often occurs due to the presence of macropores and accelerates the passage of solute, contaminants, nutrients and microbes through soil (Stagnitti et al., 2003). On the other hand, there are micropores with little or no flow in which solute movement occurs mainly by

diffusion (Leij and Toride, 1998). Thus, in heterogeneous soil, the transport of solutes are expected to go faster and deeper compared to homogeneous soils (Sposito and Reginato, 1992; Zhou, 2002) however, will be retarded by the nonequilibrium exchange between macro (mobile) and micro (immobile) pores (Leij and Toride, 1998; Parlange et al., 1999). The solute break-through for such heterogeneous soil will show an early, high peak and a long tail (Leij and Toride, 1998).

Several transport models have been proposed that assume the presence of two distinct soil water regions: mobile and immobile. Differences between the models are based on assumptions about the location and form of the immobile water region. However, due to the uncertainty on its heterogeneity (e.g. the composition of the soil regarding size and shape), a more practical approach has been to assume a solute transfer process between the mobile (flowing) and immobile (stagnant) water regions (Nkedi-Kizza, 1983). The transport process in the mobile region is described by the ADE and the solute transfer between the mobile and immobile regions is described as a simple first-order rate process (Nkedi-Kizza, 1983; Leij and Bradford, 2009).

4.7.1.1 Two-Region Nonequilibrium Linear Transport Model

The Two-Region Transport Model is a physical nonequilibrium model formulated to describe the movement of a chemical through an unsaturated, sorbing porous medium (van Genuchten and Wierenga, 1976). The Two-region Model assumes: (1) the solute transport in the mobile solute phase occurs by advection and disperion, (2) solute exchange between the mobile and immobile liquid region occurs by first-order diffusion (always from the region of higher concentration to the region of lower concentration) (Bear and Verruijt, 1987), (3) the solid phase region can be partitioned into a fraction f_r that equilibrates instantaneously with the mobile liquid region and a fraction $(1 - f_r)$ that equilibrates with the immobile liquid region (Coats and Smith, 1964; van Genuchten and Wierenga,

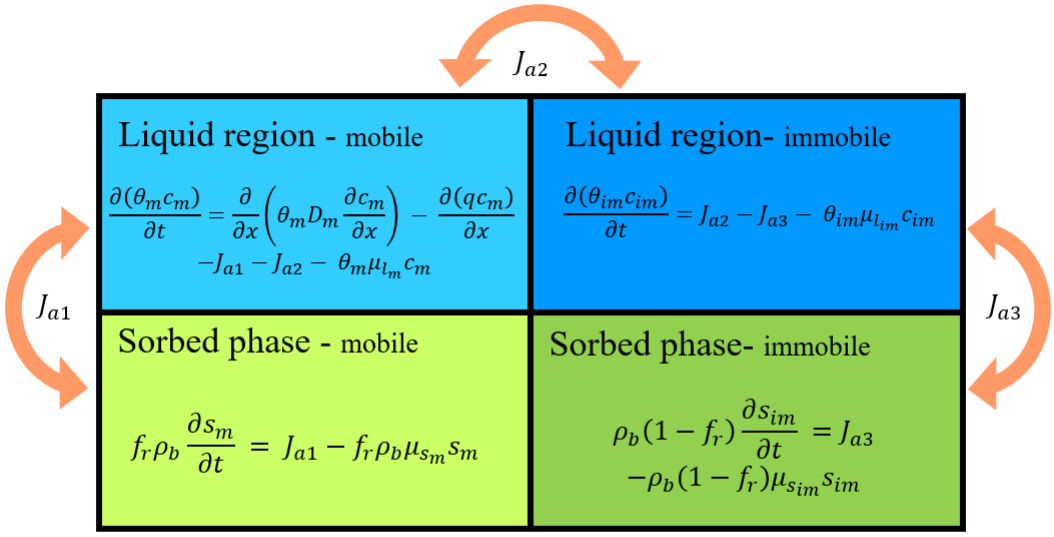

Figure 4.4: Schematic diagram of the Two-region Transport Model with degradation. The mobile liquid region is associated with the larger conducting pore and the immobile liquid region does not contribute to water flow. Similarly, the solid partitioned in two, a fraction f_r and another fraction $(1 - f_r)$ which equilibrate instantaneously with the mobile and immobile liquid region, respectively. Figure modified from van Genuchten and Wagenet (1989).

1976; Leij and Toride, 1998). Figure 4.4 presents a schematic diagram of the Two-Region Transport Model considering degradation in both regions (mobile and immobile) of the liquid and sorbed phase. This is because the decay rates inside and on the edge of the soil particles can be considerably different due to varying oxygen and/or microbial activity.

The mass balance for the mobile liquid region (c_m), denoted by the subscript m, considering degradation may be stated as follows:

$$\frac{\partial \theta_m c_m}{\partial t} = \frac{\partial}{\partial x}\left(\theta_m D_m \frac{\partial c_m}{\partial x} - q c_m\right) - J_{a1} - J_{a2} - \theta_m \mu_{L_m} c_m \tag{4.17}$$

where

q = volumetric flow (cm/hr) $(v_m\theta_m)$

J_{a1} = transfer rate from liquid to solid of the mobile region $(mg/L\ hr)$

J_{a2} = transfer rate from mobile to immobile liquid region $(mg/L\ hr)$

μ_{L_m} = mobile liquid phase degradation coefficient $(1/hr)$

The mass balance for the mobile sorbed concentration (s_m) may be stated as follows:

$$f_r\rho_b\frac{\partial s_m}{\partial t} = J_{a1} - f_r\rho_b\mu_{s_m}s_m \tag{4.18}$$

where

f_r = fraction of the solid phase that equilibrates instantaneously with the mobile liquid

μ_{s_m} = mobile sorbed phase degradation coefficient $(1/hr)$

The transport equation for the mobile region as a whole can be obtained by adding equations 4.17 and 4.18, which gives the following expression:

$$\frac{\partial\theta_m c_m}{\partial t} + f_r\rho_b\frac{\partial s_m}{\partial t} = \frac{\partial}{\partial x}\left(\theta_m D_m\frac{\partial c_m}{\partial x} - qc_m\right) - f_r\rho_b\mu_{s_m}s_m - J_{a2} - \theta_m\mu_{Lm}c_m \tag{4.19}$$

Similarly, the mass balance for the immobile liquid region (without the convection-dispersion terms) and the immobile solid region is represented, respectively, by the expressions:

$$\frac{\partial\theta_{im}c_{im}}{\partial t} = J_{a2} - J_{a3} - \theta_{im}\mu_{Lim}c_{im} \tag{4.20}$$

$$(1-f_r)\rho_b\frac{\partial s_{im}}{\partial t} = J_{a3} - (1-f_r)\rho_b\mu_{s_{im}}s_{im} \tag{4.21}$$

where

$(1 - f_r)$ = fraction of the solid phase that equilibrates instantaneously with the immobile liquid

μ_{Lim} = immobile liquid phase degradation coefficient $(1/hr)$

μ_{Sim} = immobile sorbed phase degradation coefficient $(1/hr)$

The transport equation for the immobile region as a whole can be obtained by adding equations 4.20 and 4.21, which gives the following expression:

$$\frac{\partial \theta_{im} c_{im}}{\partial t} + (1 - f_r)\rho_b \frac{\partial s_{im}}{\partial t} = J_{a2} - \theta_{im}\mu_{L_{im}} c_{im} - (1 - f_r)\rho_b \mu_{s_{im}} s_{im} \tag{4.22}$$

The subscripts m and im refer to the mobile and immobile liquid phase, respectively. The parameter f_r characterizes the fraction of sorption sites which are in direct contact with the mobile fluid (equilibrates instantaneously with the mobile fluid). The other fraction, $(1 - f_r)$, can be defined as the fraction of sorption sites in contact with the immobile fluid which equilibrates instantaneously with the immobile fluid (van Genuchten and Wierenga, 1976; van Genuchten, 1981; van Genuchten and Wagenet, 1989). The mass transfer process between the two liquid regions is governed by diffusion. Adsorption is assumed to take place from the immobile liquid region to the immobile solid region of the porous media.

By using the first-order kinetic exchange between the mobile and immobile liquid regions, analogous to equation 4.11, J_{a2} can be approximated by:

$$J_{a2} = \alpha(c_m - c_{im}) \tag{4.23}$$

where

α = first order mass transfer coefficient governing the rate of solute exchange between the mobile and immobile liquid regions; first order mass transfer rate coefficient $(1/hr)$

Sorption inside and at the edge areas of the aggregate can be described with a linear isotherm (equation 4.7), respectively:

$$s_m = K_d c_m \tag{4.24}$$

$$s_{im} = K_d c_{im} \tag{4.25}$$

By substituing equations 4.23, 4.24 and 4.25 in equations 4.19 and 4.22 the expressions for the Two-Region Nonequilibrium Linear Model with degradation are given by:

$$\begin{aligned} \frac{\partial \theta_m c_m}{\partial t} + f_r \rho_b K_d \frac{\partial c_m}{\partial t} &= \frac{\partial}{\partial x}\left(\theta_m D_m \frac{\partial c_m}{\partial x} - q c_m\right) - \alpha(c_m - c_{im}) \\ &\quad -\theta_m \mu_{L_m} c_m - f_r \rho_b K_d \mu_{s_m} c_m \end{aligned} \tag{4.26}$$

$$\begin{aligned} \frac{\partial \theta_{im} c_{im}}{\partial t} + (1 - f_r) \rho_b K_d \frac{\partial c_{im}}{\partial t} &= \alpha(c_m - c_{im}) \\ &\quad -\theta_{im} \mu_{L_{im}} c_{im} - (1 - f_r) \rho_b K_d \mu_{s_{im}} c_{im} \end{aligned} \tag{4.27}$$

And can be simplified into:

$$\frac{\partial(\theta_m + f_r\rho_b K_d)c_m}{\partial t} = \frac{\partial}{\partial x}\left(\theta_m D_m \frac{\partial c_m}{\partial x} - q c_m\right) - \alpha(c_m - c_{im}) - (\theta_m \mu_{L_m} + f_r \rho_b K_d \mu_{s_m}) c_m \quad (4.28)$$

$$\frac{\partial(\theta_{im} + (1-f_r)\rho_b K_d)c_{im}}{\partial t} = \alpha(c_m - c_{im}) - (\theta_{im} \mu_{L_{im}} + (1-f_r) \rho_b K_d \mu_{s_{im}}) c_{im} \quad (4.29)$$

Assuming a steady-state flow in a uniform soil ($D, \theta_m, \theta_{im}, f_r, \rho_b$ and q are constants), equations 4.28 and 4.29 simplify to:

$$\left(1 + \frac{f_r \rho_b K_d}{\theta_m}\right)\frac{\partial c_m}{\partial t} = D_m \frac{\partial^2 c_m}{\partial x^2} - v_m \frac{\partial c_m}{\partial x} - \frac{\alpha}{\theta_m}(c_m - c_{im}) - \left(\mu_{L_m} + \frac{f_r \rho_b K_d \mu_{s_m}}{\theta_m}\right) c_m \quad (4.30)$$

$$\left(1 + \frac{(1-f_r)\rho_b K_d}{\theta_{im}}\right)\frac{\partial c_{im}}{\partial t} = \frac{\alpha}{\theta_{im}}(c_m - c_{im}) - \left(\mu_{L_{im}} + \frac{(1-f_r)\rho_b K_d \mu_{s_{im}}}{\theta_{im}}\right) c_{im} \quad (4.31)$$

4.7.1.2 Two-Region Nonequilibrium Nonlinear transport model

The Two-region Nonequilibrium Model modified to consider the nonlinear Freundlich isotherm (equation 4.9) to describe the solute retention mechanism can be derived in a similar manner as the linear model presented in section 4.7.1.1 (Spurlock et al., 1995).

Sorption inside and at the edge areas of the aggregate can be described with a nonlinear

isotherm (equation 4.7), respectively:

$$s_m = K_f c_m^N \tag{4.32}$$

$$s_{im} = K_f c_{im}^N \tag{4.33}$$

By substituing equations 4.23, 4.32 and 4.33 in equations 4.19 and 4.22 the expressions for the modified Two-Region Nonequilibrium Nonlinear Model with degradation are given by:

$$\begin{aligned} \frac{\partial \theta_m c_m}{\partial t} + f_r \rho_b \frac{\partial K_f c_m^N}{\partial t} &= \frac{\partial}{\partial x}\left(\theta_m D_m \frac{\partial c_m}{\partial x} - q c_m\right) - f_r \rho_b \mu_{s_m} K_f c_m^N \\ &- \alpha(c_m - c_{im}) - \theta_m \mu_{Lm} c_m \end{aligned} \tag{4.34}$$

$$\begin{aligned} \frac{\partial \theta_{im} c_{im}}{\partial t} + (1 - f_r) \rho_b \frac{\partial K_f c_{im}^N}{\partial t} &= \alpha(c_m - c_{im}) - \theta_{im} \mu_{L_{im}} c_{im} \\ &- (1 - f_r) \rho_b \mu_{s_{im}} K_f c_{im}^N \end{aligned} \tag{4.35}$$

Assuming a steady-state flow in a uniform soil ($D, \theta_m, \theta_{im}, f, \rho_b$ and q are constants), equations 4.34 and 4.35 simplify to:

$$\begin{aligned} \left(1 + \frac{f_r \rho_b K_f c_m^{N-1}}{\theta_m}\right) \frac{\partial c_m}{\partial t} &= D_m \frac{\partial^2 c_m}{\partial x^2} - v_m \frac{\partial c_m}{\partial x} - \frac{f_r \rho_b K_f \mu_{s_m}}{\theta_m} c_m^N \\ &- \frac{\alpha}{\theta_m}(c_m - c_{im}) - \mu_{Lm} c_m \end{aligned} \tag{4.36}$$

$$\left(1+\frac{(1-f_r)\rho_b K_f c_{im}^{N-1}}{\theta_{im}}\right)\frac{\partial c_{im}}{\partial t} = \frac{\alpha}{\theta_{im}}(c_m - c_{im}) - \mu_{L_{im}} c_{im} - \left(\frac{(1-f_r)\rho_b K_f \mu_{s_{im}}}{\theta_{im}}\right) c_{im}^N \quad (4.37)$$

4.7.2 Chemical nonequilibrium

Chemical nonequilibrium usually results when the sorption of mass transfer rates between the solute and the specific sorption sites of the sorbent are different. The sorption sites are commonly referred to as Type-1 and Type-2 sorption, distinguished by the solute mass exchange either instantaneous (equilibrium) or time dependent (kinetic), respectively (Brusseau et al., 1989; Toride et al., 1993; Leij and Toride, 1998) .

4.7.2.1 Two-Site Nonequilibrium Linear Transport Model

The Two-Site Transport Model is a chemical nonequilibrium formulated to describe the differences in exchange sites with equilibrium and nonequilibrium (kinetic) sorption (Leij and Toride, 1998). The basic idea for the Two-Site Model is that the different solid phases of the soil (constitued by soil minerals, organic matter, aluminum and iron oxides) react at different rates and different intensities with the chemical (van Genuchten, 1981). The Two-Site Model assumes that the sorption sites can be divided into two fractions: 1) exchange sites that are at equilibrium (Type-1) 2) exchange sites that are time dependent (kinetic). Figure 4.5 presents a schematic diagram of the Two-Site Transport Model considering degradation in all phases, the liquid (μ_L) region and the phases of the soil with instantaneous (μ_{s_1}) and kinetic (μ_{s_2}) sorption.

The mass balance for the liquid region (c) may be stated as follows:

$$\frac{\partial \theta c}{\partial t} = \frac{\partial}{\partial x}\left(\theta D \frac{\partial c}{\partial x} - qc\right) - J_a - \theta \mu_L c \quad (4.38)$$

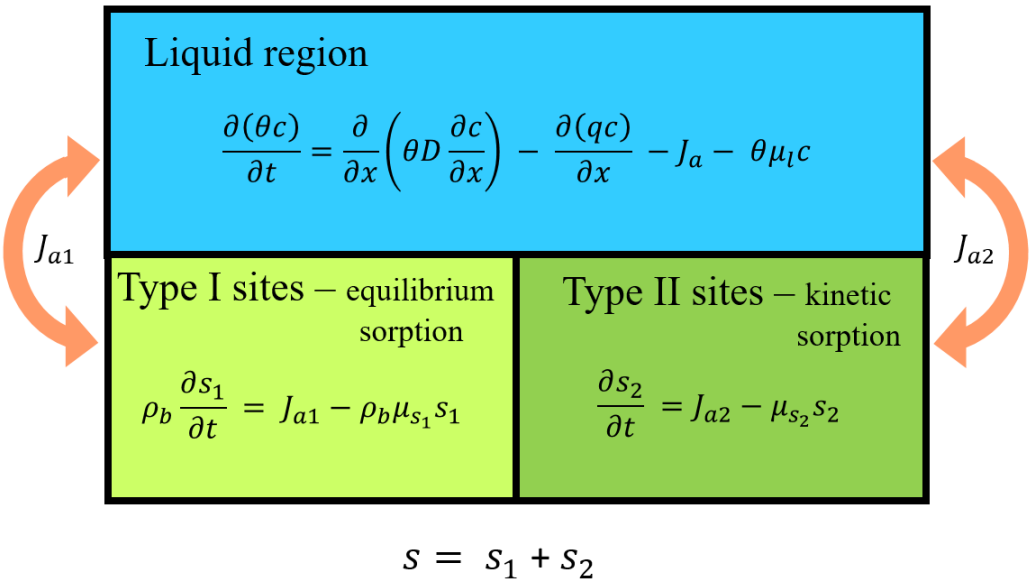

Figure 4.5: Schematic diagram of the Two-site Transport Model with degradation (modified from van Genuchten and Wagenet (1989)).

where

J_a = transfer rate from solution to sorbed phase due to sorption ($mg/L\ hr$)

J_{a1} = transfer rate from solution to Type-1 exchange sites ($mg/L\ hr$)

J_{a2} = transfer rate from solution to Type-2 exchange sites ($mg/L\ hr$)

μ_L = decay rate in the liquid region ($1/hr$)

The subscripts 1 and 2 denote the Type-1 and Type-2 exchange sites, respectively.

The mass balance for the instantaneous (Type-1, equation 4.39) and kinetic (Type-2, equation 4.40) exchange sites may be stated as follows, respectively:

$$\rho_b \frac{\partial s_1}{\partial t} = J_{a1} - \mu_{s_1} \rho_b s_1 \tag{4.39}$$

$$\rho_b \frac{\partial s_2}{\partial t} = J_{a2} - \mu_{s_2} \rho_b s_2 \tag{4.40}$$

where

μ_{S_1} = decay rate in the Type-1 exchange sites $(1/hr)$

μ_{S_2} = decay rate in the Type-2 exchange sites $(1/hr)$

The mass transport equation for the whole system follows by adding equations 4.39, 4.40 and 4.38 and noting that $J_a = J_{a1} + J_{a2}$:

$$\frac{\partial \theta c}{\partial t} + \rho_b \frac{\partial s_1}{\partial t} + \rho_b \frac{\partial s_2}{\partial t} = \frac{\partial}{\partial x}\left(\theta D \frac{\partial C}{\partial x} - qc\right) - \theta \mu_L c - \rho_b \mu_{s_1} s_1 - \rho_b \mu_{s_2} s_2 \tag{4.41}$$

At equilibrium, the sorption process for the Type-1 (s_1) and Type-2 (s_2) exchange sites can be described as, respectively:

$$s_1 = f_r K_d c \tag{4.42}$$

$$s_2 = (1 - f_r) K_d c \tag{4.43}$$

where

f_r = exchange sites considered to be at equilibrium

The total adsorption (s) at equilibrium is simply given by:

$$s = s_1 + s_2 \tag{4.44}$$

Because Type-1 sorption sites are always at equilibrium, the mass balance is given by:

$$\frac{\partial s_1}{\partial t} = f_r K_d \frac{\partial c}{\partial t} \tag{4.45}$$

On the other hand, the concentration of Type-2 sorption sites are time dependent so, can be described by using a first order kinetic sorption rate, analogous to 4.11a. Sorption onto these sites becomes:

$$\frac{\partial s_2}{\partial t} = \alpha[(1 - f_r)K_d c - s_2] - \mu_{s_2} s_2 \tag{4.46}$$

where

α = first order mass transfer coefficient governing the rate of solute exchange between the sorbed and liquid regions;
first order kinetic adsorption rate coefficient $(1/hr)$

By substituting equations 4.45 and 4.46 into equation 4.41 the transport equation for the Two-Site Model is given by:

$$\begin{aligned} \frac{\partial \theta c}{\partial t} + \rho_b f_r K_d \frac{\partial c}{\partial t} &= \frac{\partial}{\partial x}\left(\theta D \frac{\partial c}{\partial x} - qc\right) - \theta \mu_L c \\ &\quad - f_r \rho_b K_d \mu_{s_1} c - \alpha \rho_b [(1 - f_r)K_d c - s_2] \end{aligned} \tag{4.47}$$

and can be simplified to:

$$\begin{aligned} \frac{\partial(\theta + f_r \rho_b K_d)c}{\partial t} &= \frac{\partial}{\partial x}\left(\theta D \frac{\partial c}{\partial x} - qc\right) - \theta \mu_L c - f_r \rho_b K_d \mu_{s_1} c \\ &\quad - \alpha(1 - f_r)\rho_b K_d \left(c + \frac{s_2}{(1 - f_r)K_d}\right) \end{aligned} \tag{4.48}$$

Assuming a steady-state flow in a uniform soil (D, θ, f_r, ρ_b and q are constants), equation 4.48 simplify to:

$$\left(1+\frac{f_r\rho_b K_d}{\theta}\right)\frac{\partial c}{\partial t} = D\frac{\partial^2 c}{\partial x^2} - v\frac{\partial c}{\partial x} - \mu_L c - \frac{f_r\rho_b K_d}{\theta}\mu_{s_1} c - \frac{\alpha(1-f_r)\rho_b K_d}{\theta}\left[c - \frac{s_2}{(1-f_r)K_d}\right] \quad (4.49)$$

Hence, the complete model is given by equations 4.49 and 4.46.

4.7.2.2 Two-Site Nonequilibrium Nonlinear Transport Model

The Two-site Nonequilibrium Model considering the nonlinear Freundlich isotherm (equation 4.9) to describe the solute retention mechanism is an alternative model and can be derived in similar manner as the linear model. The temporal change in sorbed concentration for the Type-1 and Type-2 exchange sites can be described as, respectively:

$$\frac{\partial s_1}{\partial t} = f_r K_f N c^{N-1} \quad (4.50)$$

$$\frac{\partial s_2}{\partial t} = \alpha[(1-f_r)K_f c^N - s_2] - \mu_{s_2} s_2 \quad (4.51)$$

By substituting equation 4.50 into equation 4.41, the governing transport equation is given by:

$$\frac{\partial \theta c}{\partial t} + \rho_b\frac{\partial f_r K_f c^N}{\partial t} = \frac{\partial}{\partial x}\left(\theta D\frac{\partial C}{\partial x} - qc\right) - \theta\mu_L c - \rho_b\mu_{s_1} f_r K_f c^N - \rho_b\left(\alpha[(1-f_r)K_f c^N - s_2] - \mu_{s_2} s_2\right) - \rho_b\mu_{s_2} s_2 \quad (4.52)$$

and can be simplified to:

$$\frac{\partial \theta c}{\partial t} + \rho_b \frac{\partial f_r K_f c^N}{\partial t} = \frac{\partial}{\partial x}\left(\theta D \frac{\partial c}{\partial x} - qc\right) - \theta \mu_L c - \rho_b \mu_{s_1} f_r K_f c^N - \rho_b \alpha [(1 - f_r) K_f c^N - s_2] \quad (4.53)$$

Therefore, the complete model is given by equations 4.53 and 4.51 (Magga et al., 2012; Zou and Zheng, 2013). Assuming a steady-state flow in a uniform soil (D, θ, f_r, ρ_b and q are constants), equation 4.53 simplifies to:

$$\left(1 + \frac{\rho_b f_r K_f c^{N-1}}{\theta}\right) \frac{\partial c}{\partial t} = D \frac{\partial^2 c}{\partial x^2} - v \frac{\partial c}{\partial x} - \mu_L c - \frac{f_r \rho_b K_f}{\theta} \mu_{s_1} c^N - \frac{\rho_b \alpha}{\theta} [(1 - f_r) K_f c^N - s_2] \quad (4.54)$$

Hence, the complete model is given by equations 4.51 and 4.54.

4.8 Initial and boundary conditions

To apply any of these models to a specific case, appropriate auxiliary conditions are needed to complete the mathematical description of solute transport through a semi-infinite ($0 \leq x \leq \infty$) or a finite ($0 \leq x \leq L$) porous medium profile. Proper selection of boundary conditions to simulate solute transport in porous media has received considerable attention in the literature (van Genuchten et al., 2013). Incorrect use of boundary conditions for laboratory experiments can lead to serious errors when scaling results to field conditions (van Genuchten and Wierenga, 1986).

4.8.1 Initial condition

Since the governing equation contains a time derivative, it must be supplemented by an initial condition that defines the distribution of mass at $t = 0$. The general initial condition

is:

$$c(x, t = 0) = f(x) \tag{4.55}$$

where $f(x)$ can take the form of a constant value with distance, an exponential function with x or a steady state type distribution for production and decay (van Genuchten and Alves, 1982).

4.8.2 Boundary conditions

Two types of boundary conditions are typically used to initiate calculations for a continuous, step input or a pulse input at the soil surface. The first-type (Dirichlet) or continuous concentration-type of boundary condition is of the form:

$$c(x = 0, t) = g(t) \tag{4.56}$$

and the third-type (Robin) or continuous flux-type of boundary condition is of the form:

$$-D\frac{\partial c}{\partial x} + vc = vg(t) \tag{4.57}$$

and for a third-type (Robin) B.C. pulse input we have:

$$-D\frac{\partial c}{\partial x} + vc = vg(t) \qquad g(t) = \begin{cases} 0 & t < t_p \\ 1 & t \geq t_p \end{cases} \tag{4.58}$$

where $g(t)$ can also take several distributions such as, a constant value, a pulse-type distribution or an exponential functions with time (van Genuchten et al., 2013).

The first-type of boundary condition (equation 4.56) describes a tracer solution applied at a specified rate from a well mixed reservoir at the surface of the soil profile in which the concentration itself can be specified at the inlet boundary. However, this is not usually possible in practice (Selim, 2015). The third-type of boundary condition (equation 4.58)

accounts for advection and dispersion across the interface of solute that is applied at a specific rate from a well mixed reservoir at the surface of the soil profile (Selim, 2015).

The exit boundary condition can be defined in terms of a zero gradient at a finite and infinite distance from the inlet and is given by:

$$\frac{\partial c}{\partial x}(x = \infty, t) = 0 \tag{4.59a}$$

$$\frac{\partial c}{\partial x}(x = L, t) = 0 \tag{4.59b}$$

which is a second-type (Neumann) of boundary condition used for solute effluent (Selim, 2015).

4.9 Summary

The fate and transport in porous media of many inorganic and organic chemicals was typically modeled using the ADE. However, the BTCs for many of these chemicals were not adequately represented by the classical ADE. The classical ADE is based on assumptions of homogeneous porous medium, inter-phase mass transfer process, such as sorption, and transformation reactions that are linear and essentially instantaneous, which are not expected to occur at the field scale. Field scale conditions include physical and chemical heterogeneities which are difficult to quantity. BTCs for these non-uniform conditions cause non-equilibrium processes and are characterized by early peaks and long tails. Particularly chemical non-equilibrium indicates the simultaneous occurrence instantaneous and time-dependent sorption-desorption processes.

The use of nonequilibrium models significantly improve the modeling of organic chemicals. More complex models have been developed which improve even further transport modeling. However, many of these models include parameters that are difficult to quantify

or there are no available methods to be measure and are often fitted to experimental data.

Fitted values are usually found through optimization algorithms where the result is a combination of values that gives the smallest approximation error. However, with higher amount of parameter to be fitted, greater is the amount of possible combinations that could adequately fit a particular problem.

The Two-site Nonequilibrium Nonlinear Transport model was selected for modeling mobility of OTC. Many studies (Selim et al., 1976; Brusseau et al., 1992; Mao and Ren, 2004) have reported this model improves the prediction of mobility approximations for a range of pesticides in soil compared to the classical ADE. This model offers a higher degree of complexity that could represent more realistic field properties without compromising the level of uncertainty of the parameters included in the model.

5. NUMERICAL IMPLEMENTATION

5.1 Introduction

The transport of many solutes through the natural environment has been described by some version of the classical Advection-Dispersion Equation (ADE) (Hogarth et al., 1990; Li et al., 1992). The PDE that describes the groundwater flow and solute transport in porous media can be solved mathematically using analytical solutions (when possible to apply one) or numerical solutions. An advantage of an analytical solution is that it provides an exact solution of the governing equation. However, this requires idealized properties and boundary conditions of the particular problem sometimes to an unrealistic level (Konikow et al., 2007; Leij and Bradford, 2009; Konikow, 2011). Thus, for most field scale problems, the benefits of having an exact solution are outweighed by the level of error introduced from the simplification of the assumptions (Konikow, 2011).

For many cases, numerical methods are needed to approximate a solution, particularly when simplified analytical models cannot describe the physics of the particular conditions (e.g. heterogeneous system, complicated boundary conditions, governing equation is non-linear) (Logan, 2001; Konikow et al., 2007; van der Zee and Leijnse, 2013; Selim, 2015).

A general group of the many different numerical methods used to solve the ADE can be classified as Eulerian, Lagrangian or mixed Eulerian-Lagrangian approaches (Zheng and Bennett, 2002c). Lagrangian approaches require tracking a detailed history of each fluid particle (flow properties which may change in time) whereas the Eulerian approach records the evolution of the flow properties at every point in space and time (Zheng and Bennett, 2002c; Yue, 2011). And as can be expected, the mixed Eulerian-Lagrangian method is the combination of both.

Eulerian approaches (mainly used in fluid mechanics (Yue, 2011)) such as, finite dif-

ference and finite elements, are mathematically simpler to apply, yet more abstract conceptually. Eulerian methods are commonly affected by numerical dispersion and artificial oscillation errors (under and over shooting), but can be addressed by reducing the temporal and spatial grid (or mesh) step. Lagrangian approaches such as the random walk method, are less abstract, more accurate and efficient by effectively eliminating numerical dispersion. Hoever, these solutions are affected by numerical instabilities and computational difficulties from the lack of a fixed grid or mesh (Zheng and Bennett, 2002c). Mixed Eulerian-Lagrangian approaches combine the strength of both methods. However, they are not as computationally efficient as the other two (Zheng and Bennett, 2002c).

The numerical solution of the solute transport equation has been an area of active research for many years and reflects the difficult task that it is to solve the ADE numerically (Zheng and Bennett, 2002c). The root cause is the variation of mathematical properties that the transport equation can describe whether advection-dominanted or diffusion-dominanted in a particular situation (Ingebritsen and Sanford, 1998; Konikow et al., 2007). Advection and diffusion are simultaneous processes that promote mass transport differently (Zheng and Bennett, 2002c).

The solute transport equation is a mixed type (Parabolic-Hyperbolic) PDE depending upon the magnitude of the parameters (Ingebritsen and Sanford, 1998). Mathematically, this means that the numerical method needs to handle simultaneously hyperbolic and parabolic terms associated with advection and dispersion, respectively. This is a problem that no numerical method has fully overcome (Zheng and Bennett, 2002c). When the PDE is dominated by advection (as is common in many field problems), the governing equation approximates a hyperbolic type equation (Ingebritsen and Sanford, 1998; Konikow, 2011). Whereas the governing equation approximates a parabolic-type PDE when the diffusive components dominate (similar to the groundwater flow equation) (Ingebritsen and Sanford, 1998; Konikow, 2011). The degree of dominance of the advection or dispersion

component is typically measured by the Peclet number ($Pe = \frac{vL}{D}$). Pe values tends to infinity for purely advective problems (Zheng and Bennett, 2002c).

The solute transport equation, particularly if it is advection dominated (hyperbolic-type PDE), is more difficult to solve than the groundwater flow equation (parabolic-type PDE) (Thomas, 1995a; Konikow et al., 2007). For example, solute transport for unsaturated conditions requires an accurate description of the flow field for the specific target area. In other words, because the solute transport model is linked to the flow model, both flow and transport process have to be evaluated. The groundwater flow model is independent of solute transport (Konikow, 2011), therefore solutions to the PDE are more easily found.

Eulerian approaches are commonly used for fluid flows. Two of the most widely used and accepted Eulerian methods to approximate the groundwater flow and ADE are the finite difference method (FDM) and finite element method (FEM) (Zheng and Bennett, 2002d; Konikow et al., 2007), each of which have advantages and disadvantages (Ingebritsen and Sanford, 1998). An advantage of FDM is conceptual and mathematical simplicity and ease to program (Konikow et al., 2007). While FEM offer great flexibility in the geometry discretization (see Figure 5.1) of a space, it is at the expense of greater numerical complexity and computational effort (Zheng and Bennett, 2002d; Konikow et al., 2007). Both methods are subject to numerical difficulties, such as, numerical dispersion and artificial oscillation errors. FEMs use higher order approximation which commonly generates more accurate solutions than the standard FDM. However, higher order approximations can also be accommodated in FDMs at the expense of loss of the simplicity and the efficiency of the method (Zheng and Bennett, 2002c).

In brief, it is difficult to generalize which numerical method, FDM or FEM, is preferable to approximate the groundwater flow and ADE. Each method has its own advantages and disadvantages, but there are very few groundwater problems for which either is clearly superior. The accuracy of the numerical solution is dictated by the selection of the numer-

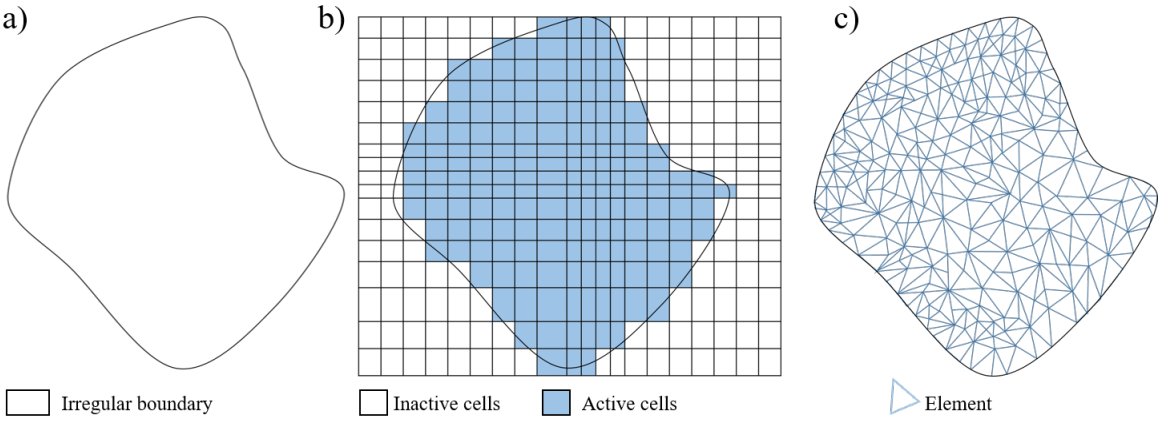

Figure 5.1: Showing a hypothetical problem with (a) irregular boundaries, discretized using (b) a finite difference grid and (c) a finite elements mesh. (Figure modified from Konikow et al. (2007))

ical approach. But the quality of the numerical solution is dictated by the selection of the mathematical model (Kuzmin, 2010). Numerical errors can be reduced with increased computational effort and therefore computational time. Hence, a tradeoff between accuracy and efficiency, features significantly influenced by the selected numerical methods, must always be assessed (Konikow, 2011).

The numerical method of choice, FDM or FEM, is usually based on the ability or familiarity of the individual with a particular method (Zheng and Bennett, 2002c; Konikow et al., 2007). The Finite Difference (FD) numerical method to approximate the ADE subject to sorption and reaction processes. Thus, the primary objective of this chapter is to describe the FD numerical approach considered to solve the ADE assuming chemical non-equilibrium and nonlinear sorption processes, as described in chapter 4.

5.2 Finite Difference Method - basic concept

The FDM is a numerical approximation technique to solve PDEs within a spatial region subject to initial conditions (in case of time dependecy, e.g. non-steady state) and

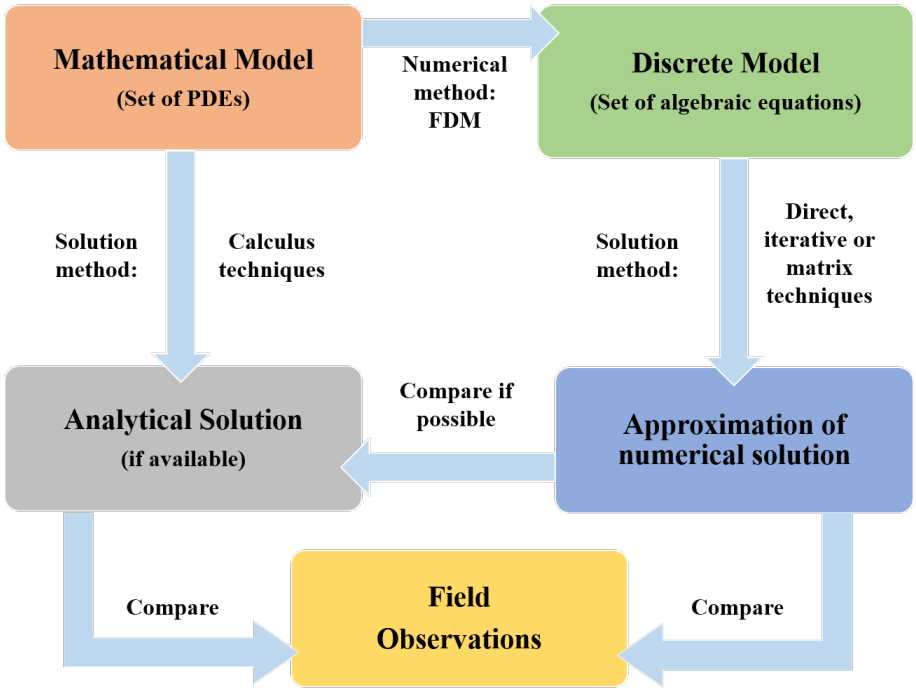

Figure 5.2: Relation between continuous and discrete problems. Figure modified from Recktenwald (2011) and Igboekwe and Amos-Uhegbu (2011)

boundary conditions. The basic approach of FDM is to divide the continuous space and time dimension into discrete segments to create an equivalent representation of the relevant system (Figure 5.2) (Grzybowski, 2009). Thus, the continuous differential equation is replaced by a finite number of algebraic equations (generally solved using matrix techniques) that define the solute concentration at specific points in the groundwater or porous system (Konikow et al., 2007).

To understand the FDM techniques it is important first to consider the nomenclature and fundamental concepts encountered in this form of numerical approximation (Lapidus and Pinder, 1999). Consider the continuous function with a single independent variable $f(x)$ (Figure 5.3). The domain x is discretized into a set of nodes such that the arbitrary node i and its adjacent nodes $i+2$, $i+1$, $i-1$ and $i-2$ may be specified at any nodal

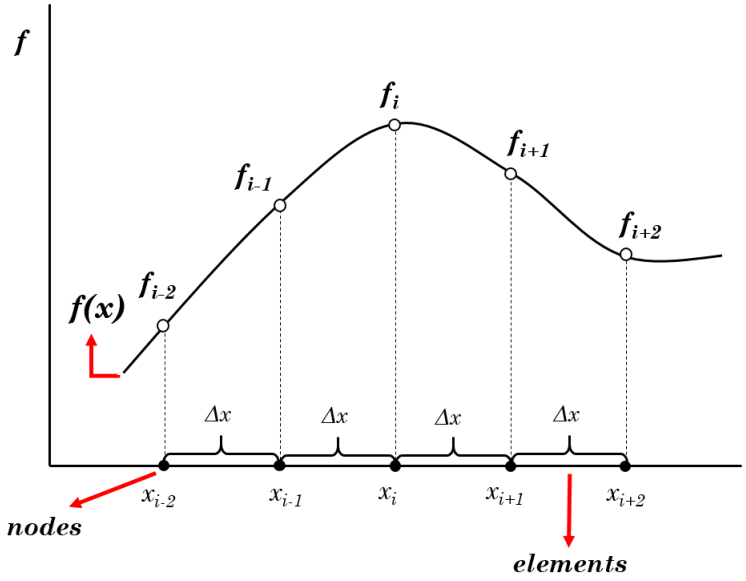

Figure 5.3: Finite Difference discretization of $f = f(x)$ using a constant grid spacing Δx.

location as:

$$f(x_i) \equiv f(i \cdot \Delta x) \equiv f_i \tag{5.1a}$$

$$f(x_{i+1}) \equiv f(i + 1 \cdot \Delta x) \equiv f_{i+1} \tag{5.1b}$$

$$f(x_{i-1}) \equiv f(i - 1 \cdot \Delta x) \equiv f_{i-1} \tag{5.1c}$$

$$f(x_{i+2}) \equiv f(i + 2 \cdot \Delta x) \equiv f_{i+2} \tag{5.1d}$$

$$f(x_{i-2}) \equiv f(i - 2 \cdot \Delta x) \equiv f_{i-2} \tag{5.1e}$$

Taylor series expansions are used in the formulation and classification of FD schemes (Lapidus and Pinder, 1999). The Taylor series expansion of a function $f(x)$ about a point $x = x_i$ is written as follows:

$$f(x) = f(x_i) + (x - x_i)\frac{\partial f}{\partial x}\bigg|_{x_i} + \frac{(x - x_i)^2}{2!}\frac{\partial^2 f}{\partial x^2}\bigg|_{x_i} + \frac{(x - x_i)^3}{3!}\frac{\partial^3 f}{\partial x^3}\bigg|_{x_i} + ... \qquad (5.2)$$

The derivative of the function $f(x_i)$ can be approximated as $\frac{\Delta f}{\Delta x}$, where Δx is the discrete change in the function f over the interval Δx (Figure 5.4). Denoting $\Delta x = x - x_i$ and $-\Delta x = x - x_i$, equation 5.2 can be written as, respectively:

$$f(x_i + \Delta x) = f(x_i) + \Delta x\frac{\partial f}{\partial x}\bigg|_{x_i} + \frac{\Delta x^2}{2!}\frac{\partial^2 f}{\partial x^2}\bigg|_{x_i} + \frac{\Delta x^3}{3!}\frac{\partial^3 f}{\partial x^3}\bigg|_{x_i} + ... \qquad (5.3a)$$

$$f(x_i - \Delta x) = f(x_i) - \Delta x\frac{\partial f}{\partial x}\bigg|_{x_i} + \frac{\Delta x^2}{2!}\frac{\partial^2 f}{\partial x^2}\bigg|_{x_i} - \frac{\Delta x^3}{3!}\frac{\partial^3 f}{\partial x^3}\bigg|_{x_i} + ... \qquad (5.3b)$$

where Δx is finite and small but not necessarily infinitesimally small. By using equation 5.3, the derivative of f at x_i $\left(\frac{\partial f}{\partial x}\big|_{x_i} = \frac{\partial f}{\partial x}\big|_i\right)$ in the continuum can be approximated in the discrete case using the concept of a truncated and rearranged Taylor series expansion as presented in equations 5.4a (forward difference) and 5.4b (backward difference) (Rao, 2002a).

$$\frac{\partial f}{\partial x}\bigg|_{x_i} = \frac{f(x_{i+1}) - f(x_i)}{\Delta x} - \underbrace{\left[\frac{\partial^2 f}{\partial x^2}\bigg|_{x_i}\frac{\Delta x}{2!} + \frac{\partial^3 f}{\partial x^3}\bigg|_{x_i}\frac{\Delta x^2}{3!} + ...\right]}_{\text{Truncation error}} \qquad (5.4a)$$

$$\frac{\partial f}{\partial x}\bigg|_{x_i} = \frac{f(x_i) - f(x_{i-1})}{\Delta x} + \underbrace{\left[\frac{\partial^2 f}{\partial x^2}\bigg|_{x_i}\frac{\Delta x}{2!} - \frac{\partial^3 f}{\partial x^3}\bigg|_{x_i}\frac{\Delta x^2}{3!} + ...\right]}_{\text{Truncation error}} \qquad (5.4b)$$

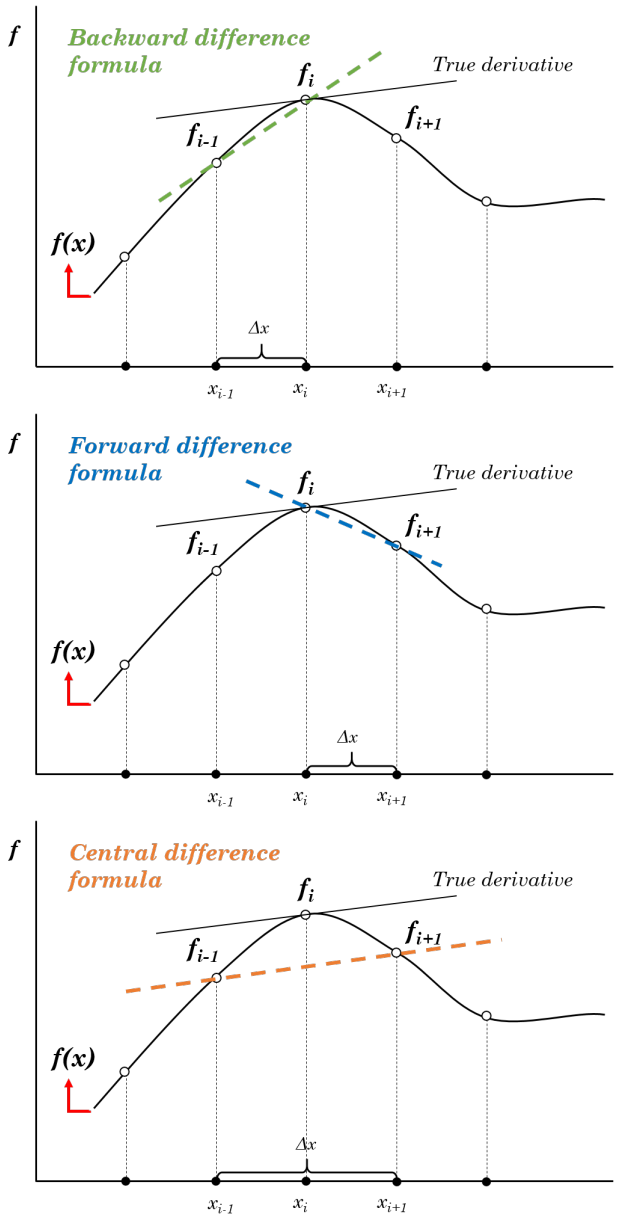

Figure 5.4: Finite Difference discretization of $f = f(x)$ using a constant grid spacing Δx. Example of backward-space (BS) (green), forward-space (FS) and central-space (CS) (orange) approximation to the derivative at the point x_i (modified form Rao (2002a)).

Additionally, subtracting equation 5.3b from 5.3a yields equation 5.4c (central difference).

$$\left.\frac{\partial f}{\partial x}\right|_{x_i} = \frac{f(x_{i+1}) - f(x_{i-1})}{2\Delta x} - \underbrace{\left[\left.\frac{\partial^3 f}{\partial x^3}\right|_{x_i} \frac{\Delta x^2}{3!} + ...\right]}_{\text{Truncation error}} \tag{5.4c}$$

The term in the square brackets is the error associated with truncating the Taylor series after the second term and will be identified as $O(\Delta x_i)$ from now on. Thus, the discrete changes in f and x can be found using the Taylor series in three different ways:

$$\left.\frac{\partial f}{\partial x}\right|_{x_i} = \frac{f(x_{i+1}) - f(x_i)}{\Delta x} + O(\Delta x) \tag{5.5a}$$

$$\left.\frac{\partial f}{\partial x}\right|_{x_i} = \frac{f(x_i) - f(x_{i-1})}{\Delta x} + O(\Delta x) \tag{5.5b}$$

$$\left.\frac{\partial f}{\partial x}\right|_{x_i} = \frac{f(x_{i+1}) - f(x_{i-1})}{2\Delta x} + O(\Delta x^2) \tag{5.5c}$$

where the expressions 5.5a, 5.5b and 5.5c are the forward, backward and central difference approximation for $\frac{\partial f}{\partial x}\big|_i$ (Figure 5.4), respectively. Note that the error of the forward and backward difference approximation is proportional to (Δx) while the error of the central difference approximation is proportional to (Δx^2). The three approximations use information at only two points but the central difference delivers twice the order of error in contrast with the other two methods. As Δx decreases, the error in the central difference approximation reduces more rapidly due to the square power (i.e. if the grid spacing is reduced by half, the truncation error reduced by a factor of 2^2). Hence, the central difference approximation is more accurate than the forward and backward (Rao, 2002a). This property will hold in general whenever the grid spacing (Δx) is constant.

To approximate an expression for the second derivative we follow a similar procedure

as was presented above for the first derivative. For this, we consider the Taylor's series expansion for $f_{i+2} = f(x_{i+2})$ and $f_{i-2} = f(x_{i-2})$ (Figure. 5.3) using equation 5.2 considering $x - x_i = x_{i+2} - x_i = 2\Delta x$ and $x - x_i = x_{i-2} - x_i = -2\Delta x$, respectively.

$$f(x_i + 2\Delta x) = f(x_i) + \left.\frac{\partial f}{\partial x}\right|_{x_i} (2\Delta x) + \left.\frac{\partial^2 f}{\partial x^2}\right|_{x_i} \frac{(2\Delta x)^2}{2!} + \left.\frac{\partial^3 f}{\partial x^3}\right|_{x_i} \frac{(2\Delta x)^3}{3!} + ... \quad (5.6a)$$

$$f(x_i - 2\Delta x) = f(x_i) - \left.\frac{\partial f}{\partial x}\right|_{x_i} (2\Delta x) + \left.\frac{\partial^2 f}{\partial x^2}\right|_{x_i} \frac{(2\Delta x)^2}{2!} - \left.\frac{\partial^3 f}{\partial x^3}\right|_{x_i} \frac{(2\Delta x)^3}{3!} + ... \quad (5.6b)$$

Multiplying equation 5.3a by 2 and subtracting from equation 5.6a; multiplying equation 5.3b by 2 and subtracting from equation 5.6b; and finally, the addition of 5.3a and 5.3b yields the following

$$f(x_i + 2\Delta x) - 2f(x_i + \Delta x) = -f(x_i) + \left.\frac{\partial^2 f}{\partial x^2}\right|_{x_i} \Delta x^2 + \left.\frac{\partial^3 f}{\partial x^3}\right|_{x_i} \Delta x^3 + ... \quad (5.7a)$$

$$f(x_i - 2\Delta x) - 2f(x_i - \Delta x) = -f(x_i) + \left.\frac{\partial^2 f}{\partial x^2}\right|_{x_i} \Delta x^2 - \left.\frac{\partial^3 f}{\partial x^3}\right|_{x_i} \Delta x^3 + ... \quad (5.7b)$$

$$f(x_i + \Delta x) + f(x_i - \Delta x) = 2f(x_i) + \left.\frac{\partial^2 f}{\partial x^2}\right|_{x_i} \Delta x^2 + \left.\frac{\partial^4 f}{\partial x^4}\right|_{x_i} \frac{\Delta x^4}{12} + ... \quad (5.7c)$$

from which the second derivative can be expressed as:

$$\left.\frac{\partial^2 f}{\partial x^2}\right|_{x_i} = \frac{f(x_i + 2\Delta x) - 2f(x_i + \Delta x) + f(x_i)}{\Delta x^2} - \underbrace{\left.\frac{\partial^3 f}{\partial x^3}\right|_{x_i} \frac{\Delta x}{3!} + ...}_{\text{Truncation error}} \quad (5.8a)$$

$$\left.\frac{\partial^2 f}{\partial x^2}\right|_{x_i} = \frac{f(x_i - 2\Delta x) - 2f(x_i - \Delta x) + f(x_i)}{\Delta x^2} - \underbrace{\left.\frac{\partial^3 f}{\partial x^3}\right|_{x_i} \frac{\Delta x}{3!} + ...}_{\text{Truncation error}} \quad (5.8b)$$

$$\left.\frac{\partial^2 f}{\partial x^2}\right|_{x_i} = \frac{f(x_i+\Delta x) - 2f(x_i) + f(x_i-\Delta x)}{\Delta x^2} - \underbrace{\left.\frac{\partial^4 f}{\partial x^4}\right|_{x_i} \frac{\Delta x^2}{12} + ...}_{\text{Truncation error}} \tag{5.8c}$$

or

$$\left.\frac{\partial^2 f}{\partial x^2}\right|_{x_i} = \frac{f(x_i+2\Delta x) - 2f(x_i+\Delta x) + f(x_i)}{\Delta x^2} + O(\Delta x) \tag{5.9a}$$

$$\left.\frac{\partial^2 f}{\partial x^2}\right|_{x_i} = \frac{f(x_i-2\Delta x) - 2f(x_i-\Delta x) + f(x_i)}{\Delta x^2} + O(\Delta x) \tag{5.9b}$$

$$\left.\frac{\partial^2 f}{\partial x^2}\right|_{x_i} = \frac{f(x_i+\Delta x) - 2f(x_i) + f(x_i-\Delta x)}{\Delta x^2} + O(\Delta x^2) \tag{5.9c}$$

Equation 5.9a, 5.9b and 5.9c denotes the forward, backward and central difference approximation for $\left.\frac{\partial^2 f}{\partial x^2}\right|_{x_i}$ (Rao, 2002a). A summary of the FD approximations for first and second derivative is presented in Table 5.1.

Table 5.1: Finite Difference approximation and error order (modified from Lapidus and Pinder (1999))

Derivative	**Finite Difference Approximation**	**Formula**	**Truncation error**
$\frac{\partial f}{\partial x}$	Forward-space (FS)	$\frac{f(x_{i+1})-f(x_i)}{\Delta x_i}$	$O(\Delta x)$
	Backward-space (BS)	$\frac{f(x_i)-f(x_{i-1})}{\Delta x_i}$	$O(\Delta x)$
	Central-space (CS)	$\frac{f(x_{i+1})-f(x_{i-1})}{2\Delta x_i}$	$O(\Delta x^2)$
$\frac{\partial^2 f}{\partial x^2}$	Forward-space (FS)	$\frac{f(x_{i-2})-2f(x_{i+1})+f(x_i)}{\Delta x_i^2}$	$O(\Delta x)$
	Backward-space (BS)	$\frac{f(x_{i-2})-2f(x_{i-1})+f(x_i)}{\Delta x_i^2}$	$O(\Delta x)$
	Central-space(CS)	$\frac{f(x_{i-1})-2f(x_i)+f(x_{i+1})}{\Delta x_i^2}$	$O(\Delta x^2)$

5.3 Solute transport equation

The PDE describing the groundwater flow (equation 4.3) and solute transport (equation 4.1) include terms representing a derivative of continuous variables. Using FDM to approximate these derivatives (slope or curves) by discrete linear changes over small discrete intervals of space (Δx) and time (Δt), if Δx is sufficiently small, then all the linear increments will represent a good approximation of the curvilinear surface $f(x)$ (Konikow et al., 2007).

To apply the FDM to equation 4.3, the problem domain is divided into a rectangular finite difference grid or mesh (series of cells or blocks) (Zheng and Bennett, 2002c; Konikow et al., 2007). Two possible types of grid are illustrated in one dimension in Figure 5.5 to subdivide the domain region in the spatial and temporal plane (Konikow et al., 2007). Figure 5.5a shows the calculating points (nodes) at the center of each block formed by the grid lines (Block centered grid) and Figure 5.5b the nodes are considered to be located in the intersections of the grid lines (Node centered grid) (Zheng and Bennett, 2002c; Konikow et al., 2007). Under the block centered grid, the region of simulation may be visualized as a block surrounding each node. Although there is no particular advantage on one type of grid over the other, there will be some operational differences for the handling of the boundary conditions (Konikow et al., 2007).

5.3.1 Spatial discretization

The spatial discretization of the **dispersion** term (second derivative $\frac{\partial^2 c}{\partial x^2}$) from equation 4.1 is given by the central weighting scheme (equation 5.10) analogous to equation 5.9c.

$$\left.\frac{\partial^2 c}{\partial x^2}\right|_{x_i} = \frac{c_{i+1} - 2c_i + c_{i-1}}{\Delta x^2} \tag{5.10}$$

The spatial discretization of the **advection** term (first derivative $\frac{\partial c}{\partial x}$) from equation 4.1

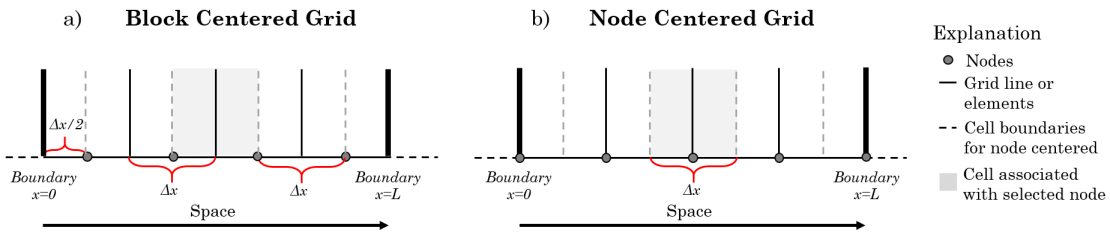

Figure 5.5: Two possible types of finite difference grid: block centered grid and node centered grid (modified from Konikow et al. (2007)). a) Block centered grid: cells have a width Δx and the data is associated to the node in the center of the cell. Note that the data will start $\Delta x/2$ inside the boundary. b) Node centered grid: the data is associated with the node spaced Δx apart. Note that there can be a nodes exactly on the boundary.

is given by the central weighting scheme (equation 5.11) analogous to equation 5.5c.

$$\left.\frac{\partial c}{\partial x}\right|_{x_i} = \frac{c_{i+1} - c_{i-1}}{2\Delta x^2} \tag{5.11}$$

Since the error terms are proportional to the square of the grid width (Δx^2), the central weighting approximations are said to be accurate to the second order with respect to the spatial discretization.

Physical dispersion occurs in proportion to the second derivative term $\left(\frac{\partial^2 c}{\partial x^2}\right)$, thus, numerical dispersion error will occur if the term $\frac{\partial^2 c}{\partial x^2}$ showed up in the expressions of the truncation error. However, the second derivative term $\left(\frac{\partial^2 c}{\partial x^2}\right)$ is canceled out for the approximation of the advection term (equation 5.4c) and is isolated to the left side on the approximation of the dispersion term (equation 5.8c). This implies that the central weighting scheme is free of numerical dispersion error associated with spatial discretization (Zheng and Bennett, 2002c).

The central in space weighting approximation tends to create artificial oscillation, especially for advection dominated problems. However, artificial oscillation can be reduced by utilizing the forward differentiation scheme (equation 5.5a), also known as the upstream

or upwind weighting scheme. The upwind weighting scheme provides a first order error accuracy and introduces again the numerical dispersion error (due to the presence of $\frac{\partial^2 c}{\partial x^2}$ in the truncation error, see equation 5.4a). A problem that was overcome with the use of the central in space weighting scheme (Zheng and Bennett, 2002c). Another solution to reduce artificial oscillation is to use a higher resolution spatial grid, with a choice based on the Peclet number, as discussed subsequently.

5.3.2 Temporal discretization

In an analogous fashion one can obtain the finite difference approximation for the **temporal** derivative, which may be viewed as another dimension and hence represented with another index (n) (Konikow et al., 2007). The time derivative term on the left hand side of equation 4.1 can be approximated by:

$$\left.\frac{\partial c}{\partial t}\right|_{t^n} = \frac{c_i^{n+1} - c_i^n}{\Delta t} \tag{5.12}$$

where the index n and $n+1$ represent the present and future time level, respectively. Some of the well known FD numerical schemes to approximate the ADE are the forward-time (FT) or explicit , backward-time (BT) or implicit and central-time (CT) or Crank-Nicolson schemes (Huang et al., 1997).

First, lets consider the forward in time or **explicit method**. If only the old time level (c^n) is used in approximating the dispersion and advection terms of the ADE, the temporal discretization at a grid point (i, n) is said to be forward or explicit (Figure. 5.6a) as shown on equation 5.13.

$$\frac{c_i^{n+1} - c_i^n}{\Delta t} = D\frac{c_{i-1}^n - 2c_i^n + c_{i+1}^n}{\Delta x^2} - v\frac{c_{i+1}^n - c_{i-1}^n}{2\Delta x} \tag{5.13}$$

where c^{n+1} and c^n are the unknown and known terms, respectively. The known values

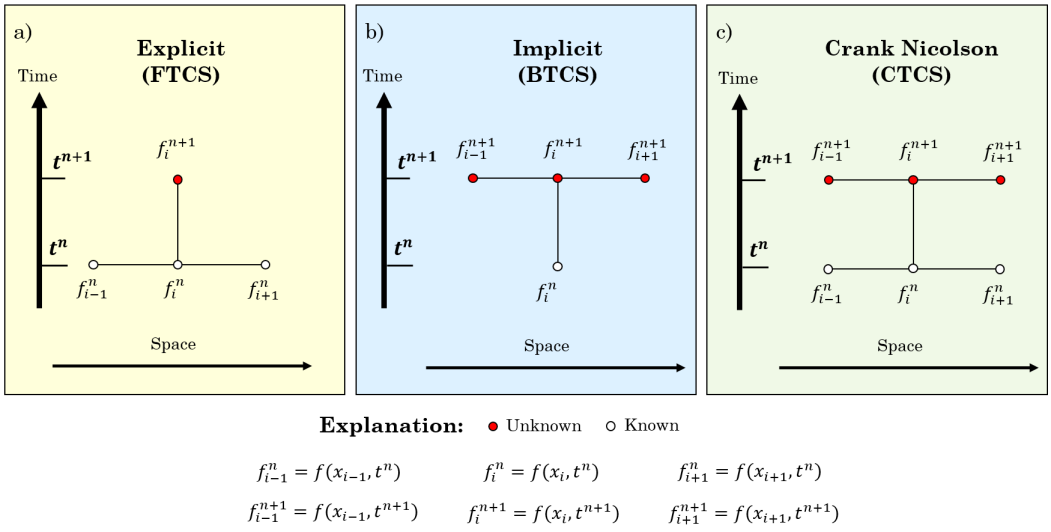

Figure 5.6: Grid stencil showing discretization of time at node (i) in a 1D finite difference grid: (a) explicit (FTCS: forward-time central-space) difference formulation, (b) implicit (BTCS: backward-time central-space) difference formulation (c) Crank-Nicolson (CTCS: central-time central-space) difference formulation. Index i denotes space and n denotes time.

come from initial conditions specified for the first time step or from the solutions of the previous time step (Konikow et al., 2007). Three terms are associated with the old time level (n) while only one is associated with the new time level ($n+1$) (Figure 5.6a). Thus, every node of the grid will have an equation with one unknown c_i^{n+1} term. Then, the concentration at the new time level $n+1$ can be computed directly from concentrations at the previous time level n when equation 5.13 is rearranged as follows:

$$c_i^{n+1} = \left(\frac{D\Delta t}{\Delta x^2} + \frac{v\Delta t}{2\Delta x}\right) c_{i-1}^n + \left(1 - \frac{2D\Delta t}{\Delta x^2}\right) c_i^n + \left(\frac{D\Delta t}{\Delta x^2} - \frac{v\Delta t}{2\Delta x}\right) c_{i+1}^n \qquad (5.14)$$

Next, consider the backward in time or **fully implicit method**, in which only the new time level (c^{n+1}) is used in approximating the dispersion and advection terms of the ADE

for the temporal discretization at a grid point (i, n) (Figure. 5.6b) as shown in equation 5.15 (Zheng and Bennett, 2002c).

$$\frac{c_i^{n+1} - c_i^n}{\Delta t} = D\frac{c_{i-1}^{n+1} - 2c_i^{n+1} + c_{i+1}^{n+1}}{\Delta x^2} - v\frac{c_{i+1}^{n+1} - c_{i-1}^{n+1}}{2\Delta x} \tag{5.15}$$

as before, c^{n+1} and c^n are the unknown and known terms, respectively. The known values come from initial conditions specified for the first time step or from the solutions of the previous time step (Konikow et al., 2007). It is seen here that for every grid node only one term is associated with the old time level (n) while three terms are associated with the new time level $(n + 1)$ (equation 5.16) (Figure. 5.6b), which cannot be solved directly, in contrast with the explicit scheme. This scheme requires the system of algebraic equations (equation 5.17) to be solved simultaneously for all the grid nodes in the entire domain for each time step (Rao, 2002b) together with specified boundary conditions (Konikow et al., 2007) using an iterative solution method or a direct matrix solution technique (i.e. Thomas Algorithm) (Zheng and Bennett, 2002c).

$$\left(-\frac{D\Delta t}{(\Delta x)^2} - \frac{v\Delta t}{2\Delta x}\right) c_{i-1}^{n+1} + \left(1 + \frac{2D\Delta t}{(\Delta x)^2}\right) c_i^{n+1} + \left(-\frac{D\Delta t}{(\Delta x)^2} + \frac{v\Delta t}{2\Delta x}\right) c_{i+1}^{n+1} = c_i^n \tag{5.16}$$

equation 5.16 can be written in the form:

$$a_{i,i-1}\, c_{i-1}^{n+1} + a_{i,i}\, c_i^{n+1} + a_{i,i+1}\, c_{i+1}^{n+1} = RHS_i \tag{5.17}$$

where the coefficients $a_{i,i-1}$, $a_{i,i}$ and $a_{i,i+1}$ and the right hand side (RHS_i) term are given by:

$$a_{i,i-1} = -\frac{D\Delta t}{\Delta x^2} - \frac{v\Delta t}{2\Delta x} \tag{5.18a}$$

$$a_{i,i} = 1 + \frac{2D\Delta t}{\Delta x^2} \tag{5.18b}$$

$$a_{i,i+1} = -\frac{D\Delta t}{\Delta x^2} + \frac{v\Delta t}{2\Delta x} \tag{5.18c}$$

$$RHS_i = c_i^n \tag{5.18d}$$

Equation 5.17 in matrix form is:

$$[A]\, c^{n+1} = RHS \tag{5.19}$$

where the coefficient matrix $[A]$ is the tridiagonal or Jacobi matrix (Rao, 2002c) due to the three nonzeno diagonal elements centered about the main diagonal (Figure. 5.7)

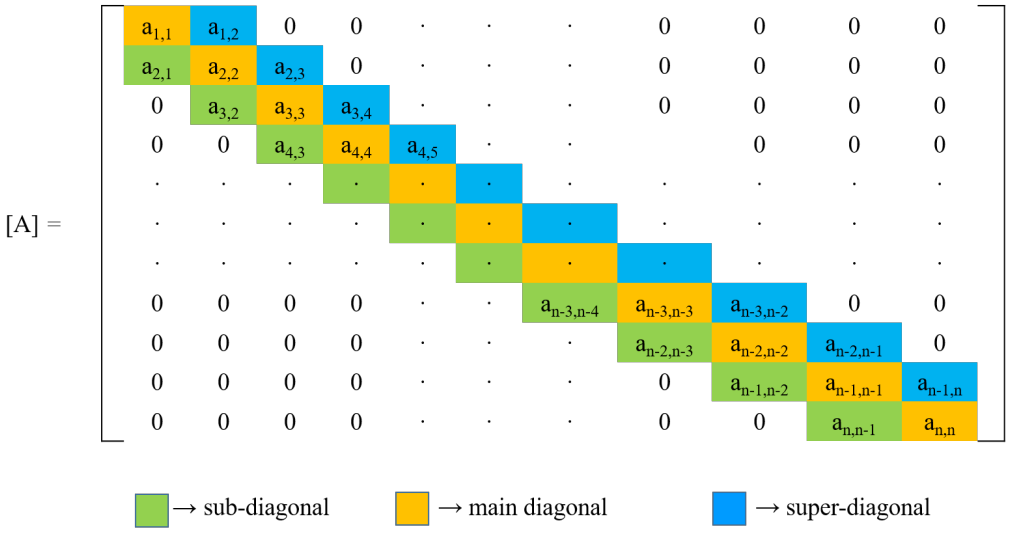

Figure 5.7: Tridiagonal matrix or Jacobi matrix

$$[A] = \text{ tridiagonal } \{a_{i,i-1}, a_{i,i}, a_{i,i+1}\}$$

and the vector of unknowns c^{n+1} and the right hand side RHS (depends on known concentration values at the time level n) are given by:

$$c^{n+1} = \begin{bmatrix} c_1^{n+1} \\ c_2^{n+1} \\ c_3^{n+1} \\ \vdots \\ c_{N-1}^{n+1} \\ c_N^{n+1} \end{bmatrix} \qquad RHS = \begin{bmatrix} RHS_1 \\ RHS_2 \\ RHS_3 \\ \vdots \\ RHS_{N-1} \\ RHS_N \end{bmatrix}$$

To solve for the unknowns c^{n+1} one can use the Thomas algorithm which is an efficient and simple way to solve the tridiagonal system (equation 5.19) (Lapidus and Pinder, 1999) (see Appendix C). The Thomas algorithm is a simplified variation of the Gaussian elimination that can be used to solve the tridiagonal systems of equations.

The temporal approximation at the node i of the ADE can be expressed as:

$$\begin{aligned} \frac{c_i^{n+1} - c_i^n}{\Delta t} &= (w_1)\left[D\frac{c_{i-1}^{n+1} - 2c_i^{n+1} + c_{i+1}^{n+1}}{\Delta x^2} - v\frac{c_{i+1}^{n+1} - c_{i-1}^{n+1}}{2\Delta x}\right] \\ &+ (1 - w_1)\left[D\frac{c_{i-1}^{n} - 2c_i^{n} + c_{i+1}^{n}}{\Delta x^2} - v\frac{c_{i+1}^{n} - c_{i-1}^{n}}{2\Delta x}\right] \end{aligned} \tag{5.20}$$

where w_1 is a temporal weight factor that ranges from 0 to 1. Thus, the explicit ($w_1 = 0$) and implicit ($w_1 = 1$) schemes can be considered as special cases of more general temporal discretization scheme which uses a weighted concentration at the new ($n + 1$) and old (n)

time levels to approximate the dispersion and advection terms of the ADE (Lapidus and Pinder, 1999; Zheng and Bennett, 2002c):

Rearranging all the unknown values to the left and the known values to the right side of the equal sign yield the following:

$$\begin{aligned}
\left(-w_1\frac{D\Delta t}{\Delta x^2}-w_1\frac{v\Delta t}{2\Delta x}\right)c_{i-1}^{n+1} & \\
+\left(1+w_1\frac{2D\Delta t}{\Delta x^2}\right)c_i^{n+1} & \\
+\left(-w_1\frac{D\Delta t}{\Delta x^2}+w_1\frac{v\Delta t}{2\Delta x}\right)c_{i+1}^{n+1} & \\
= \left((1-w_1)\tfrac{D\Delta t}{\Delta x^2}+(1-w_1)\tfrac{v\Delta t}{2\Delta x}\right)c_{i-1}^{n} & \\
+\left(1-(1-w_1)\tfrac{2D\Delta t}{\Delta x^2}\right)c_i^{n} & \\
+\left((1-w_1)\tfrac{D\Delta t}{\Delta x^2}-(1-w_1)\tfrac{v\Delta t}{2\Delta x}\right)c_{i+1}^{n} & \qquad (5.21)
\end{aligned}$$

In a similar way, equation 5.21 can be written in the form of equation 5.17 where the coefficients $a_{i,i-1}$, $a_{i,i}$ and $a_{i,i+1}$ and the right hand side (RHS_i) term are given by:

$$a_{i,i-1} = -\frac{D\Delta t}{\Delta x^2}-\frac{v\Delta t}{2\Delta x} \qquad (5.22a)$$

$$a_{i,i} = 1+\frac{2D\Delta t}{\Delta x^2} \qquad (5.22b)$$

$$a_{i,i+1} = -\frac{D\Delta t}{\Delta x^2}+\frac{v\Delta t}{2\Delta x} \qquad (5.22c)$$

$$\begin{aligned}
RHS_i = & \left((1-w_1)\frac{D\Delta t}{\Delta x^2}+(1-w_1)\frac{v\Delta t}{2\Delta x}\right)c_{i-1}^{n} \\
& +\left(1-(1-w_1)\frac{2D\Delta t}{\Delta x^2}\right)c_i^{n} \\
& +\left((1-w_1)\frac{D\Delta t}{\Delta x^2}-(1-w_1)\frac{v\Delta t}{2\Delta x}\right)c_{i+1}^{n} \qquad (5.22d)
\end{aligned}$$

An alternative approximation scheme is obtained by setting $w_1 = \frac{1}{2}$ and is referred to

as the central in time approximation or Crank Nicolson scheme (which is the average of the explicit and the implicit scheme) (Zheng and Bennett, 2002c). The Crank Nicolson scheme can be solved by writing the matrix form (equation 5.19) and using the Thomas algorithm.

There are four fundamental properties of FD approximation for every PDE that must be considered before selecting a specific approach or scheme which are: consistency, order, stability and convergence (Hoffman, 2001).

A finite difference scheme is said to be consistent with a PDE if the truncation error (difference between the finite difference equation and the partial differential equation) vanishes as the grid size goes to zero (Δt, $\Delta x \rightarrow 0$). The order of the finite difference approximation refers to the rate at which the global or total error (round-off error + truncation error) is reduced as the grid size approaches zero. A numerical approximation scheme of a PDE is considered stable if the errors are not magnified in the calculations causing large deviations from the exact solution. Finally, a finite difference approximation is said to be convergent if it approaches the real solution of the underlying PDE as the grid size reduces to zero.

Stability of the numerical scheme implies that a solution will be obtained, although not necessarily that the solution will be accurate. Similarly, consistency is a necessary condition but not sufficient for convergence. Thus, the numerical approximation needs both properties (consistency and stability) in order to be convergent (consistency $+$ stability $\Leftrightarrow$ convergence).

Explicit schemes are extremely simple and straightforward to implement in a simulation and are efficient with respect to memory usage (Zheng and Bennett, 2002c), but may have stability problems (is conditionally stable). To ensure the stability of the explicit solution, the condition of $0 < \frac{D\Delta t}{\Delta x^2} \leq 0.5$ has to be met. This requirement imposes a restriction on the temporal and spatial step size (i.e Δt must be very small since $\Delta t \leq \frac{\Delta x^2}{2D}$)

which might require more computational work over large values of time (Rao, 2002b).

Even though the implicit schemes (fully implicit and Crank Nicolson) are more complicated to solve, they have the advantage of generally being unconditionally stable because there is no time step requirement (Konikow et al., 2007; Zheng and Bennett, 2002c). Implicit methods are quite competitive with standard explicit methods in use and performance due to the unconditional stability, the tridiagonal system of the coefficient matrix and the Thomas algorithm for solving the algebraic equation which is very efficient and simple to implement (Lapidus and Pinder, 1999).

Both the explicit (forward-time) and fully implicit (backward-time) finite difference approximation schemes provide a first order error accuracy in time $O(\Delta t)$, similar to the forward and backward approximation in space (see equations 5.5a and 5.5b, respectively). On the other hand, the Crank Nicolson (center-time) finite difference approximation ($w_1 = \frac{1}{2}$) provides a second order accuracy error ($O(\Delta t^2)$) (similar to equation 5.5c). Thus, the forward-time central-space (FTCS) FD approximation presented in equation 5.13 and the backward-time central-space (BTCS) FD approximation presented in equation 5.15 are first order accurate in time and second order accurate in space ($O(\Delta t, \Delta x^2)$). The central-time central-space presented in equation 5.20 is similar to the BTCS implicit scheme but with improved local truncation error: second order accurate in time and space ($O(\Delta t^2, \Delta x^2)$) (Thomas, 1995b; Zheng and Bennett, 2002c).

5.3.3 Discretization constraints: Peclet and Courant number

As briefly mentioned above, the numerical approximation of the solute transport equation can be limited by spatial and temporal discretization constrains which are required for accuracy and stability of the numerical scheme. The two constrains considered here, Peclet and Courant number, are best expressed in terms of grid-based dimensionless variables (Craig, 2004).

The Peclet number (Pe, sometimes referred to as the Reynolds cell number) is given by equation 5.23 and represents the ratio of the grid size to the dispersivity (D/v) (Ingebritsen and Sanford, 1998; Zheng and Bennett, 2002c; Zhou, 2002; Craig, 2004). Solute transport problems are considered dispersion dominated for Pe values much lower than one ($Pe \ll 1$), whereas advection dominated problems are considered for Pe values much greater than one ($Pe \gg 1$) (Craig, 2004). The concentration distribution will spread out faster than it moves down the soil column for diffusion dominated conditions. In contrast, the concentration distribution will move faster down the soil column than it spreads out for advection dominated problems (Socolofsky and Jirka, 2005). The larger the Peclet number ($Pe \rightarrow \infty$) the more dominant is the advection term and thus, the more significant the artificial oscillation error (Zheng and Bennett, 2002c).

$$Pe = \frac{vL}{D} \tag{5.23}$$

where v is the velocity, D is the dispersion coefficient, and L is the length scale. For numerical simulations, the length scale can be defined as the local representative grid size (Δx) to evaluate the "grid Peclet number "(Pe_{grid}). As mentioned previously, the central-space weighting scheme leads to artificial oscillation which can be reduced by using a finer spatial grid size based on Pe. Huyakorn and Pinder (1983) recommend that the spacing size (Δx) be designed so that the $Pe_{grid} \leq 2$ to avoid or reduce oscillation of the numerical solution (Zheng and Bennett, 2002c; Craig, 2004).

The Courant number (Cr), given by equation 5.24, is an indicator of the advection speed relative to the cell size of the grid ($\Delta t/\Delta x$) (Craig, 2004). Cr can be interpreted as the number or fraction of cells that a solute particle will cross by advection in one time step. Therefore, the Courant number is used to determine the appropriate temporal spacing (Δt) by setting the requirement that the solute particle will move no more than one cell

size within the duration of the time step (Zheng and Bennett, 2002c; Craig, 2004).

$$Cr = \frac{v\Delta t}{\Delta x} \tag{5.24}$$

Even though the Crank Nicolson (and fully implicit) approximation to the temporal derivative have no stability constrain (unconditionally stable, no Δt size requirement) to achieve a stable solution, a maximum Courant number of one ($Cr \leq 1$) is generally recommended to achieve a sufficiently accurate solution (Zheng and Bennett, 2002c; Craig, 2004).

5.3.4 Auxiliary condition discretization

Just as the governing equation was discretized, so must the auxiliary conditions to specify the solution of the PDE. Three types of boundary conditions (BCs) are utilized in this work: Dirichlet, Neumann and, Robin.

The Dirichlet (first-type) condition represent a value, constant or known function, specified at the boundary. The discretized form of equation 4.55 is given by:

$$C_i^{n=1} = f(i\Delta x), \qquad i = 0, \cdots, M \tag{5.25}$$

The Neumann (second-type) condition represents a fixed flux at the boundary. This mean that the value at the boundary is variable with time and the system requires an additional auxiliary equation to be able to be solved. Recall that the chosen approximation scheme for the governing equation (central in time and central in space) is second order accurate in time and space ($\Delta t^2, \Delta x^2$). Thus, the auxiliary conditions are approximated with a central-space scheme to be consistent with the order error accuracy in space (Δx^2). In order to maintain the second order error, a ghost node needs to be used as shown in Figure 5.8 and the Neumann condition is given by:

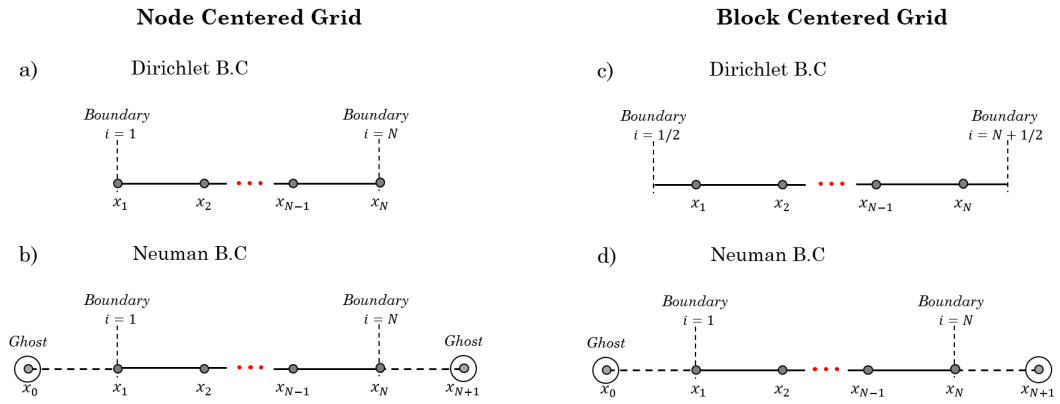

Figure 5.8: Illustration of a node centered grid and block centered grid for a Neumann boundary condition

$$\frac{C_{i+1}^n - C_{i-1}^n}{2\Delta x} = g_1(n\Delta t), \qquad n = 1, \cdots \tag{5.26}$$

The Robin (third-type) conditions are a linear combination of Dirichlet and Neumann and represent a mass flux into the domain proportional to the difference in concentration at the boundary and the surrounding medium.

$$vC_i^n - D\frac{C_{i+1}^n - C_{i-1}^n}{2\Delta x} = vh_1(n\Delta t), \qquad n = 1, \cdots \tag{5.27}$$

5.3.5 Modified Picard iteration scheme

The solute transport equation, considering the Freundlich isotherm for the sorption process, is highly nonlinear (Zarba, 1988; Huang et al., 1998), and as a result requires a different approach to solve it. Typically, nonlinearities are solve with iterative methods based on successive linearizations (Celia et al., 1990). Usual iterative linearization methods include: lag nonlinear term method, linearization about the previous time step method, Newton method, standard Picard method, and modified Picard method (Celia et al., 1990;

Thomas, 1995c).

A common problem for nonlinear water flow and solute transport problems are the mass balance errors (MBEs) generated in the numerical simulation given the nonlinear nature of the equations. These MBEs are in addition to the numerical errors generated by the numerical methods for the linear approximations. Small time steps are usually required to minimize the MBEs produced during the numerical simulation which can cause the solution to be "very time consuming" (Huang et al., 1998).

The Newton iterative scheme has been used to solve the nonlinear flow and solute transport equation (Huang et al., 1998). However, depending on how the method is implemented, the coefficient matrix can be non-symmetric which demands more computational effort to be solve in contrast with a symmetric coefficient matrix (Mehl, 2006).

Another approach is to use an operator splitting technique (OPS) in which the complete solute transport equation is separated into a system of linear PDEs (involving the advection and dispersion term) and nonlinear ordinary differential equations (ODEs) involving the reaction term. However, the approach may cause mass balance errors for continuous mass flux boundary conditions (Huang et al., 1998).

A more convenient alternative for nonlinear problems of the water flow and solute transport equation is using the “modified Picard iteration”method proposed by Celia et al. (1990). The modified Picard iteration scheme is a mass conservative numerical scheme originally developed and applied to solve the mixed form Richards equation. Later, it was generalized for the solute transport equation by Huang et al. (1998) given the similarity between the ADE and the flow equation which can be seen by comparing the components of both equation as presented in Table 5.2 (Huang et al., 1998). Celia et al. (1990) claimed that the mass conservative property of the modified Picard methods holds for all types of boundary conditions and all numerical approximations as long as spatial symmetry is maintained (Huang et al., 1998).

Table 5.2: Similarity between the water flow and solute transport equation (modified from Huang et al. (1998))

Flow equation		**Transport equation**	
Pressure head	h	Concentration	c
Water content	$\theta(h)$	Solute content	$M(c)$
Gravitational flow		Convectional transport	v
Hydraulic conduction	$K(h)$	Hydrodynamic disperiosn	D
Sink and source terms		Decay and production terms	
Specific water capacity	$\frac{\partial\theta}{\partial h}$	Specific solute capacity	$\frac{\partial M}{\partial c}$

The numerical performance of the modified Picard iteration method was tested for the flow equation (using finite elements) by Huang et al. (1996) and included scenarios with highly nonlinear soil hydraulic properties, very dry soil conditions and layered soil. Its implementation, reduced the mass balance error in all the tests to almost zero ($< |10^{-8}|\%$) (Huang et al., 1998).

To explain the implementation of the "modified Picard iteration" method a simple case of local equilibrium sorption will be presented. Substituting the general form of the adsorption isotherm (equation 4.5) into equation 4.4 leads to:

$$\frac{\partial\theta c}{\partial t} + \rho_b \frac{\partial f(c)}{\partial t} = \frac{\partial}{\partial x}\left(\theta D \frac{\partial c}{\partial x}\right) - q\frac{\partial c}{\partial x} \tag{5.28}$$

$$\frac{\partial\theta\left(1 + \frac{\rho_b}{\theta}\frac{f(c)}{c}\right)c}{\partial t} = \frac{\partial}{\partial x}\left(\theta D \frac{\partial c}{\partial x}\right) - q\frac{\partial c}{\partial x} \tag{5.29}$$

$$\frac{\partial\theta R c}{\partial t} = \frac{\partial}{\partial x}\left(\theta D \frac{\partial c}{\partial x}\right) - q\frac{\partial c}{\partial x} \tag{5.30}$$

where R is the retardation factor (see section 4.6) defined as:

$$R = 1 + \frac{\rho_b}{\theta}\frac{f(c)}{c} \tag{5.31}$$

Note that the retardation factor defined in equation 5.31 is related to $\frac{f(c)}{c}$ instead of the usual definition of the isotherm slope $\left(\frac{\partial f(c)}{\partial c}\right)$ (see equation 4.14) (Huang et al., 1997, 1998). Next, the ADE is written in a "mixed-form" formulation and is given by:

$$\frac{\partial M(c)}{\partial t} = \frac{\partial}{\partial x}\left(\theta D\frac{\partial c}{\partial x}\right) - q\frac{\partial c}{\partial x} \tag{5.32}$$

where $M(c)$ is the solute content (total concentration of solute per unit volume of soil) and is defined as:

$$M(c) = \theta c + \rho_b f(c) = \theta R c \tag{5.33}$$

The temporal derivative term $\frac{\partial M}{\partial t}$ is differentiated in the same way as equation 5.12 with an iterative superscript and is given by:

$$\frac{\partial M}{\partial t} = \frac{M_i^{n+1,p+1} - M_i^n}{\Delta t} \tag{5.34}$$

Thus, the nonlinear ADE approximated with central-space and Crank-Nicolson in time differentiation scheme is given below:

$$\begin{aligned}
\frac{M_i^{n+1,p+1} - M_i^n}{\Delta t} &= w_1 \left[\frac{(\theta D)_{i+\frac{1}{2}}^{n+\frac{1}{2}} \left(\frac{c_{i+1}^{n+1,p+1} - c_i^{n+1,p+1}}{\Delta x} \right) - (\theta D)_{i-\frac{1}{2}}^{n+\frac{1}{2}} \left(\frac{c_i^{n+1,p+1} - c_{i-1}^{n+1,p+1}}{\Delta x} \right)}{\Delta x} \right. \\
&\quad \left. -(\theta v)_i^{n+\frac{1}{2}} \frac{c_{i+1}^{n+1,p+1} - c_{i-1}^{n+1,p+1}}{\Delta x} \right] \\
&+ (1 - w_1) \left[\frac{(\theta D)_{i+\frac{1}{2}}^{n+\frac{1}{2}} \left(\frac{c_{i+1}^n - c_i^n}{\Delta x} \right) - (\theta D)_{i-\frac{1}{2}}^{n+\frac{1}{2}} \left(\frac{c_i^n - c_{i-1}^n}{\Delta x} \right)}{\Delta x} \right.
\end{aligned}$$

$$-(\theta v)_i^{n+\frac{1}{2}} \frac{c_{i+1}^n - c_{i-1}^n}{\Delta x}\Bigg] \tag{5.35}$$

where n denote the time level and p denotes the iteration level. To solve equation 5.35, the solute content at the new time and iteration level $M_i^{n+1,p+1}$ is replaced with a truncated Taylor expansion with respect to the solution concentration (c) about the expansion point $c^{n+1,p}$ (Huang et al., 1996, 1998), i.e.

$$M_i^{n+1,p+1} = M_i^{n+1,p} + \left(\frac{dM}{dc}\right)_i^{n+1,p} \left(c_i^{n+1,p+1} - c_i^{n+1,p}\right) + O(\Delta p)^2 \tag{5.36}$$

Substituting equation 5.36 into equation 5.35 gives:

$$\begin{aligned}
&\frac{M_i^{n+1,p} - M_i^n}{\Delta t} + \frac{B_i^{n+1,p}}{\Delta t}\left(c_i^{n+1,p+1} - c_i^{n+1,p}\right) \\
= \quad & w_1 \Bigg[\frac{(\theta D)_{i+\frac{1}{2}}^{n+\frac{1}{2}} \left(\frac{c_{i+1}^{n+1,p+1} - c_i^{n+1,p+1}}{\Delta x}\right) - (\theta D)_{i-\frac{1}{2}}^{n+\frac{1}{2}} \left(\frac{c_i^{n+1,p+1} - c_{i-1}^{n+1,p+1}}{\Delta x}\right)}{\Delta x} \\
& \quad -(\theta v)_i^{n+\frac{1}{2}} \frac{c_{i+1}^{n+1,p+1} - c_{i-1}^{n+1,p+1}}{\Delta x}\Bigg] \\
+ \quad & (1 - w_1) \Bigg[\frac{(\theta D)_{i+\frac{1}{2}}^{n+\frac{1}{2}} \left(\frac{c_{i+1}^{n} - c_i^{n}}{\Delta x}\right) - (\theta D)_{i-\frac{1}{2}}^{n+\frac{1}{2}} \left(\frac{c_i^{n} - c_{i-1}^{n}}{\Delta x}\right)}{\Delta x} \\
& \quad -(\theta v)_i^{n+\frac{1}{2}} \frac{c_{i+1}^n - c_{i-1}^n}{\Delta x}\Bigg]
\end{aligned} \tag{5.37}$$

After the similar terms are grouped, and the known ($c^{n+1,p+1}$) and unknown (c^n) terms are organized on the left and right hand side of the equation, respectively, the equation has the following form:

$$
\begin{aligned}
&\left[-w_1\left(\frac{\theta D\Delta t}{\Delta x^2}\right)^{n+\frac{1}{2}}_{i-\frac{1}{2}} - w_1\left(\frac{\theta v\Delta t}{\Delta x}\right)^{n+\frac{1}{2}}_{i}\right]\left(c_{i-1}^{n+1,p+1}\right)\\
&+\left[w_1\left(\frac{\theta D\Delta t}{\Delta x^2}\right)^{n+\frac{1}{2}}_{i+\frac{1}{2}} + w_1\left(\frac{\theta D\Delta t}{\Delta x^2}\right)^{n+\frac{1}{2}}_{i-\frac{1}{2}}\right]\left(c_{i}^{n+1,p+1}\right)\\
&+\left[-w_1\left(\frac{\theta D\Delta t}{\Delta x^2}\right)^{n+\frac{1}{2}}_{i+\frac{1}{2}} + w_1\left(\frac{\theta v\Delta t}{\Delta x}\right)^{n+\frac{1}{2}}_{i}\right]\left(c_{i+1}^{n+1,p+1}\right)\\
&+B_i^{n+1,p}\left(c_i^{n+1,p+1}-c_i^{n+1,p}\right)\\
=\;& M_i^n - M_i^{n+1,p}\\
&+\left[(1-w_1)\left(\frac{\theta D\Delta t}{\Delta x^2}\right)^{n+\frac{1}{2}}_{i-\frac{1}{2}} + (1-w_1)\left(\frac{\theta v\Delta t}{\Delta x}\right)^{n+\frac{1}{2}}_{i}\right]\left(c_{i-1}^{n}\right)\\
&+\left[-(1-w_1)\left(\frac{\theta D\Delta t}{\Delta x^2}\right)^{n+\frac{1}{2}}_{i+\frac{1}{2}} - (1-w_1)\left(\frac{\theta D\Delta t}{\Delta x^2}\right)^{n+\frac{1}{2}}_{i-\frac{1}{2}}\right]\left(c_{i}^{n}\right)\\
&+\left[(1-w_1)\left(\frac{\theta D\Delta t}{\Delta x^2}\right)^{n+\frac{1}{2}}_{i+\frac{1}{2}} - (1-w_1)\left(\frac{\theta v\Delta t}{\Delta x}\right)^{n+\frac{1}{2}}_{i}\right]\left(c_{i+1}^{n}\right) \qquad (5.38)
\end{aligned}
$$

From each $c^{n+1,p+1}$, we may subtract $c^{n+1,p}$, and also subtract the same term from the right hand side to maintain algebraic equivalence (Zarba, 1988). Now the equation being solved remains the same and displays the following algebraic form:

$$
\begin{aligned}
& \left[-w_1\left(\frac{\theta D\Delta t}{\Delta x^2}\right)^{n+\frac{1}{2}}_{i-\frac{1}{2}} - w_1\left(\frac{\theta v\Delta t}{\Delta x}\right)^{n+\frac{1}{2}}_{i}\right]\left(c^{n+1,p+1}_{i-1} - c^{n+1,p}_{i-1}\right) \\
& + \left[w_1\left(\frac{\theta D\Delta t}{\Delta x^2}\right)^{n+\frac{1}{2}}_{i+\frac{1}{2}} + w_1\left(\frac{\theta D\Delta t}{\Delta x^2}\right)^{n+\frac{1}{2}}_{i-\frac{1}{2}}\right]\left(c^{n+1,p+1}_{i} - c^{n+1,p}_{i}\right) \\
& + \left[-w_1\left(\frac{\theta D\Delta t}{\Delta x^2}\right)^{n+\frac{1}{2}}_{i+\frac{1}{2}} + w_1\left(\frac{\theta v\Delta t}{\Delta x}\right)^{n+\frac{1}{2}}_{i}\right]\left(c^{n+1,p+1}_{i+1} - c^{n+1,p}_{i+1}\right) \\
& + B^{n+1,p}_i\left(c^{n+1,p+1}_i - c^{n+1,p}_i\right) \\
= \; & M^n_i - M^{n+1,p}_i \\
& + \left[(1-w_1)\left(\frac{\theta D\Delta t}{\Delta x^2}\right)^{n+\frac{1}{2}}_{i-\frac{1}{2}} + (1-w_1)\left(\frac{\theta v\Delta t}{\Delta x}\right)^{n+\frac{1}{2}}_{i}\right]\left(c^{n}_{i-1}\right) \\
& + \left[-(1-w_1)\left(\frac{\theta D\Delta t}{\Delta x^2}\right)^{n+\frac{1}{2}}_{i+\frac{1}{2}} - (1-w_1)\left(\frac{\theta D\Delta t}{\Delta x^2}\right)^{n+\frac{1}{2}}_{i-\frac{1}{2}}\right]\left(c^{n}_{i}\right) \\
& + \left[(1-w_1)\left(\frac{\theta D\Delta t}{\Delta x^2}\right)^{n+\frac{1}{2}}_{i+\frac{1}{2}} - (1-w_1)\left(\frac{\theta v\Delta t}{\Delta x}\right)^{n+\frac{1}{2}}_{i}\right]\left(c^{n}_{i+1}\right) \\
& - \left[-w_1\left(\frac{\theta D\Delta t}{\Delta x^2}\right)^{n+\frac{1}{2}}_{i-\frac{1}{2}} - w_1\left(\frac{\theta v\Delta t}{\Delta x}\right)^{n+\frac{1}{2}}_{i}\right]\left(c^{n+1,p}_{i-1}\right) \\
& - \left[w_1\left(\frac{\theta D\Delta t}{\Delta x^2}\right)^{n+\frac{1}{2}}_{i+\frac{1}{2}} + w_1\left(\frac{\theta D\Delta t}{\Delta x^2}\right)^{n+\frac{1}{2}}_{i-\frac{1}{2}}\right]\left(c^{n+1,p}_{i}\right) \\
& - \left[-w_1\left(\frac{\theta D\Delta t}{\Delta x^2}\right)^{n+\frac{1}{2}}_{i+\frac{1}{2}} + w_1\left(\frac{\theta v\Delta t}{\Delta x}\right)^{n+\frac{1}{2}}_{i}\right]\left(c^{n+1,p}_{i+1}\right)
\end{aligned}
\tag{5.39}
$$

$$
\begin{aligned}
& \left[-w_1\left(\frac{\theta D\Delta t}{\Delta x^2}\right)^{n+\frac{1}{2}}_{i-\frac{1}{2}} - w_1\left(\frac{\theta v\Delta t}{\Delta x}\right)^{n+\frac{1}{2}}_{i}\right]\left(\delta^{n+1,p}_{c_{i-1}}\right) \\
+ & \left[w_1\left(\frac{\theta D\Delta t}{\Delta x^2}\right)^{n+\frac{1}{2}}_{i+\frac{1}{2}} + w_1\left(\frac{\theta D\Delta t}{\Delta x^2}\right)^{n+\frac{1}{2}}_{i-\frac{1}{2}} + B^{n+1,p}_{i}\right]\left(\delta^{n+1,p}_{c_i}\right) \\
+ & \left[-w_1\left(\frac{\theta D\Delta t}{\Delta x^2}\right)^{n+\frac{1}{2}}_{i+\frac{1}{2}} + w_1\left(\frac{\theta v\Delta t}{\Delta x}\right)^{n+\frac{1}{2}}_{i}\right]\left(\delta^{n+1,p}_{c_{i+1}}\right) \\
= & \; M^n_i - M^{n+1,p}_i \\
& + \left[(1-w_1)\left(\frac{\theta D\Delta t}{\Delta x^2}\right)^{n+\frac{1}{2}}_{i-\frac{1}{2}} + (1-w_1)\left(\frac{\theta v\Delta t}{\Delta x}\right)^{n+\frac{1}{2}}_{i}\right]\left(c^n_{i-1}\right) \\
& + \left[-(1-w_1)\left(\frac{\theta D\Delta t}{\Delta x^2}\right)^{n+\frac{1}{2}}_{i+\frac{1}{2}} - (1-w_1)\left(\frac{\theta D\Delta t}{\Delta x^2}\right)^{n+\frac{1}{2}}_{i-\frac{1}{2}}\right]\left(c^n_i\right) \\
& + \left[(1-w_1)\left(\frac{\theta D\Delta t}{\Delta x^2}\right)^{n+\frac{1}{2}}_{i+\frac{1}{2}} - (1-w_1)\left(\frac{\theta v\Delta t}{\Delta x}\right)^{n+\frac{1}{2}}_{i}\right]\left(c^n_{i+1}\right) \\
& - \left[-w_1\left(\frac{\theta D\Delta t}{\Delta x^2}\right)^{n+\frac{1}{2}}_{i-\frac{1}{2}} - w_1\left(\frac{\theta v\Delta t}{\Delta x}\right)^{n+\frac{1}{2}}_{i}\right]\left(c^{n+1,p}_{i-1}\right) \\
& - \left[w_1\left(\frac{\theta D\Delta t}{\Delta x^2}\right)^{n+\frac{1}{2}}_{i+\frac{1}{2}} + w_1\left(\frac{\theta D\Delta t}{\Delta x^2}\right)^{n+\frac{1}{2}}_{i-\frac{1}{2}}\right]\left(c^{n+1,p}_{i}\right) \\
& - \left[-w_1\left(\frac{\theta D\Delta t}{\Delta x^2}\right)^{n+\frac{1}{2}}_{i+\frac{1}{2}} + w_1\left(\frac{\theta v\Delta t}{\Delta x}\right)^{n+\frac{1}{2}}_{i}\right]\left(c^{n+1,p}_{i+1}\right)
\end{aligned}
\tag{5.40}
$$

where

$$
\delta^{n+1,p}_{c_i} = c^{n+1,p+1}_i - c^{n+1,p}_i \tag{5.41}
$$

Equation 5.40 can be written in matrix form, similar to equation 5.19, as follows:

$$
[A]\,\delta^{n+1,p}_c = RHS \tag{5.42}
$$

where $[A]$ is the tridiagonal matrix, and RHS is the finite difference approximation at

the present time n and iteration level p. RHS can be considered as a residual because it provides a measure of the failure of the p^{th} iteration on solving the finite difference equation (Zarba, 1988). It should be noted that $\delta_c^{n+1,p}$ is now the unknown variable instead of $c^{n+1,p+1}$. After solving equation 5.40 using the Thomas algorithm, the desired solution for the solute concentration in the liquid phase $c^{n+1,p+1}$ can be obtained from equation 5.41 (Huang et al., 1996).

5.3.5.1 Convergence criterion

An iterative process starts with an initial guess of the unknown variable. Estimates continue to be improved through successive numerical adjustments until the solution converges (in practice, neither a necessary nor a wise option (Kuzmin, 2010)), satisfies a convergence criteria or reaches a pre-established maximum number of iterations (Zheng and Bennett, 2002c; Reddy, 2015). Otherwise, the iterative process will continue into a loop of indefinite number of iterations in the case that convergence is not achieved (Reddy, 2015). In addition, terminating the iterative process too early or too late, might result in large iteration error or waste of computational time, respectively (Kuzmin, 2010).

Thus, an important aspect of any iterative process is to determine a suitable or rational stopping criteria in order to monitor convergence. The selection of a convergence criterion not only influences the accuracy of the solution, but the computational efficiency as well, which is a an aspect of significant concern in numerical methods (Huang et al., 1996; Zheng and Bennett, 2002c). Huang et al. (1996) evaluated two general aspects of a standard, a mixed and a nonlinear convergence criterion for the particular case of the flow equation. The two general categories evaluated included solution quality (solution accuracy and MBE) and computational efficiency (total number of iterations and computer simulation time). Huang et al. (1996) reported that the three criteria provide an accurate solution of the mixed-form Richards equation, implemented with the modified Picard iter-

ation method for simulating variably saturated water flow in soils. However, the nonlinear convergence criterion performed better than the standard and mixed criteria in terms of computational efficiency. Given the similarity of the mixed-form Richard equation (equation 4.3) for water flow in variably saturated porous media and the mixed form transport equation (equation 5.32) presented in table 5.2, the nonlinear convergence criterion proposed by Huang et al. (1996) can be generalized for the mixed-form transport equation as follows

$$B^{n+1,p}|\delta_c^{n+1,p}| = |M^{n+1,p+1} - M^{n+1,p}| \leq \delta_M \tag{5.43}$$

The nonlinear convergence criterion for the equation 5.32 considers the Taylor expansion on equation 5.36 as the center of the modified Picard iteration method. Usual value for δ_M is 0.0001 (Huang et al., 1996). Additionally, as a rule, the convergence criterion to monitor the difference between two successive iterations and/or the residual is measured in a suitable chosen norm (Kuzmin, 2010). This implies that equation 5.43 is estimated by:

$$\sqrt{\frac{\sum_{i=1}^{I} |M_i^{p+1} - M_i^p|^2}{\sum_{i=1}^{I} |M_i^{p+1}|^2}} \leq \delta_M \tag{5.44}$$

5.4 Finite Difference Method - models discretization

The general form of the FDM for equations equations 4.51 and 4.54 is given by equation 5.17. The coefficients for the general form of equation 5.17 are presented in Tables 5.3, 5.4 and 5.5. Step by step details on how was the FDM applied to equations 4.51 and 4.54 are presented in Appendix D.

Table 5.3: Coefficients for terms $a_{i,i-1}$, $a_{i,i}$, $a_{i,i+1}$ and the right hand side (RHS_i) for the Two-site Nonequilibrium Model with Non-Linear Sorption

$a_{i,i-1}$ =	$-w_1\theta r - w_2\theta\frac{Cr}{2}$
$a_{i,i}$ =	$2w_1\theta r + w_4\theta\mu_L\Delta t + B_i^{n+1,m} + F_i^{n+1,m} - I_i^{n+1,m}$
$a_{i,i}$ =	$-w_1\theta r + w_2\theta\frac{Cr}{2}$
RHS_i =	$M_i^n - M_i^{n+1,m} - E_i^{n+1,m} - E_i^n + H_i^{n+1,m} + H_i^n$
	+ $\left[(1-w_1)\theta r + (1-w_2)\theta\frac{Cr}{2}\right] c_{i-1}^n$
	+ $\left[-2(1-w_1)\theta r - (1-w_4)\theta\mu_l\Delta t\right] c_i^n$
	+ $\left[(1-w_1)\theta r - (1-w_2)\theta\frac{Cr}{2}\right] c_{i+1}^n$
	- $\left[(1-w_4)\Delta t\rho_b\mu_{s2}\right] s_{2_i}^n$
	- $\left[\left(\rho_b + w_4\Delta t\rho_b\mu_{s2}\right)\frac{(1-\Delta t(1-w_3)(\alpha+\mu_{s2}))}{(1+\Delta t w_3(\alpha+\mu_{s2}))}\right] s_{2_i}^n + \left[\rho_b\right] s_{2_i}^n$
	- $\left[-w_1\theta r - w_2\theta\frac{Cr}{2}\right] c_{i-1}^{n+1,m}$
	- $\left[2w_1\theta r + w_4\theta\mu_l\Delta t\right] c_i^{n+1,m}$
	- $\left[-w_1\theta r + w_2\theta\frac{Cr}{2}\right] c_{i+1}^{n+1,m}$

Note: For defitions for the the following terms see Appendix D. Cr (Eq. D.44); r (Eq. D.43); $B_i^{n+1,m}$ (Eq. D.29); $F_i^{n+1,m}$ (Eq. D.34); $I_i^{n+1,m}$ (Eq. D.39)

Table 5.4: Coefficients for terms $a_{i,i}$ and $a_{i,i+1}$ and the right hand side (RHS_i) assuming a Pulse boundary condition (Equation 4.58) at the top for the Two-site Nonequilibrium Model with Non-Linear Sorption

$a_{i,i}$=	$2w_1\theta r + w_4\theta\mu_L\Delta t + B_i^{n+1,m} + F_i^{n+1,m} - I_i^{n+1,m}$ $-\left(-w_1\theta r - w_2\theta\frac{Cr}{2}\right)\left(\frac{2\Delta xv}{D}\right)$
$a_{i,i}$=	$-w_1\theta r + w_2\theta\frac{Cr}{2} - w_1\theta r - w_2\theta\frac{Cr}{2}$
RHS_i =	$M_i^n - M_i^{n+1,m} - E_i^{n+1,m} - E_i^n + H_i^{n+1,m} + H_i^n$
	+ $\left[(1-w_1)\theta r + (1-w_2)\theta\frac{Cr}{2}\right]\left(c_{i+1}^n - \frac{2\Delta xv}{D}c_i^n + \frac{2\Delta xv}{D}g\right)$
	+ $\left[-2(1-w_1)\theta r - (1-w_4)\theta\mu_l\Delta t\right]c_i^n$
	+ $\left[(1-w_1)\theta r - (1-w_2)\theta\frac{Cr}{2}\right]c_{i+1}^n$
	- $\left[(1-w_4)\Delta t\rho_b\mu_{s2}\right]s_{2_i}^n$
	- $\left[\left(\rho_b + w_4\Delta t\rho_b\mu_{s2}\right)\frac{(1-\Delta t(1-w_3)(\alpha+\mu_{s2}))}{(1+\Delta tw_3(\alpha+\mu_{s2}))}\right]s_{2_i}^n + \left[\rho_b\right]s_{2_i}^n$
	- $\left[-w_1\theta r - w_2\theta\frac{Cr}{2}\right]\left(c_{i+1}^{n+1,m} - \frac{2\Delta xv}{D}c_i^{n+1,m} + \frac{2\Delta xv}{D}g\right)$
	- $\left[2w_1\theta r + w_4\theta\mu_l\Delta t\right]c_i^{n+1,m}$
	- $\left[-w_1\theta r + w_2\theta\frac{Cr}{2}\right]c_{i+1}^{n+1,m}$

Note: For defitions for the the following terms see Appendix D. Cr (Eq. D.44); r (Eq. D.43); $B_i^{n+1,m}$ (Eq. D.29); $F_i^{n+1,m}$ (Eq. D.34); $I_i^{n+1,m}$ (Eq. D.39); $g = 1$ for the duration of the pulse, otherwise $g = 0$.

Table 5.5: Coefficients for terms $a_{i,i-1}$, $a_{i,i}$ and the right hand side (RHS_i) assuming a second-type of boundary condition (Eq. 4.59) for the Two-site Nonequilibrium Model with Non-Linear Sorption

$a_{i,i-1}$ =	$-w_1\theta r - w_2\theta\frac{Cr}{2} - w_1\theta r + w_2\theta\frac{Cr}{2}$
$a_{i,i}$ =	$2w_1\theta r + w_4\theta\mu_L\Delta t + B_i^{n+1,m} + F_i^{n+1,m} - I_i^{n+1,m}$
RHS_i =	$M_i^n - M_i^{n+1,m} - E_i^{n+1,m} - E_i^n + H_i^{n+1,m} + H_i^n$
	+ $\left[(1-w_1)\theta r + (1-w_2)\theta\frac{Cr}{2}\right] c_{i-1}^n$
	+ $\left[-2(1-w_1)\theta r - (1-w_4)\theta\mu_l\Delta t\right] c_i^n$
	+ $\left[(1-w_1)\theta r - (1-w_2)\theta\frac{Cr}{2}\right] c_{i-1}^n$
	- $\left[(1-w_4)\Delta t\rho_b\mu_{s2}\right] s_{2_i}^n$
	- $\left[\left(\rho_b + w_4\Delta t\rho_b\mu_{s2}\right)\frac{(1-\Delta t(1-w_3)(\alpha+\mu_{s2}))}{(1+\Delta tw_3(\alpha+\mu_{s2}))}\right] s_{2_i}^n + \left[\rho_b\right] s_{2_i}^n$
	- $\left[-w_1\theta r - w_2\theta\frac{Cr}{2}\right] c_{i-1}^{n+1,m}$
	- $\left[2w_1\theta r + w_4\theta\mu_l\Delta t\right] c_i^{n+1,m}$
	- $\left[-w_1\theta r + w_2\theta\frac{Cr}{2}\right] c_{i-1}^{n+1,m}$

Note: For defitions for the the following terms see Appendix D. Cr (Eq. D.44); r (Eq. D.43); $B_i^{n+1,m}$ (Eq. D.29); $F_i^{n+1,m}$ (Eq. D.34); $I_i^{n+1,m}$ (Eq. D.39)

6. SOIL MOBILITY OF OXYTETRACYCLINE AND SELECTION OF RESISTANT BACTERIA

6.1 Introduction

Oxytetraycline (OTC) is one of several antibiotics widely used in animal husbandry to treat and prevent disease and increase growth. Up to 80% of the administered dose is excreted as the active parent compound (Hirsch et al., 1999; de Liguoro et al., 2003; Merck and Co., 2002; Sarmah et al., 2006) and as active metabolites (Brambilla et al., 2007). OTC excreted in manure reaches the soil media from direct droppings by grazing animals and/or land application of manure as fertilizer on agricultural soils. OTC has been characterized as an immobile (ter Laak et al., 2006a; Chee-Sanford et al., 2009) and persistent (Aga et al., 2005; Kulshrestha, 2007; Blackwell et al., 2007; Wang and Yates, 2008) compound because it sorbs strongly onto soils and does not rapidly degrade after application (Hamscher et al., 2002, 2005; Aga et al., 2005). Solute transport studies have presented no evidence of OTC leaching into deeper soil compartments or groundwater (Rabølle and Spliid, 2000; Hamscher et al., 2005; Kay et al., 2005b,a; Kim et al., 2010). Kim et al. (2010) reported no colloid-facilitated transport effect for OTC in soil.

OTC concentrations in fresh and aged manure range from 10^1 to 10^6 $\mu g/kg$ and 10^1 to 10^4 $\mu g/kg$, respectively, while concentrations in soil media range between 10^{-1} to 10^3 $\mu g/kg$. OTC half life in manure, soil, and manure amended soil has been reported on the order of 8.1 (Wang and Yates, 2008), 12.8 (Chen et al., 2014) and 33 days (Wang and Yates, 2008), respectively. Although, OTC is photosensitive (Halling Sørensen et al., 2003), light penetration in soil is limited to the first millimeter of topsoil (Hamscher et al., 2002; Jechalke et al., 2014). OTC can undergo biological degradation (Yang et al., 2009; Kim et al., 2010), and chemical transformation (Yang et al., 2009). Temperature and pH

strongly affect OTC degradation while ionic strength does not (Loftin et al., 2008). Transformation pathways have been proposed for photo- and biodegradation. Transformation products have been reported with potential biological activity (Palmer et al., 2010; Hamscher et al., 2005).

The fate of many pesticides has been reported and the fate of OTC is comparable (Wehrhan, 2006), as well as for other antibiotics. Mobility is typically predicted using the advection-dispersion equation (ADE):

$$\frac{\partial C_t}{\partial t} = \frac{\partial}{\partial z}\left(\theta D \frac{\partial C}{\partial z} - qC\right) - \mu C_t \tag{6.1}$$

where C_t is the total mass of solute per unit volume of soil $[mg/L]$, C is the solute concentration in the aqueous phase $[mg/L]$, θ is the volumetric water content $[cm^3/cm^3]$, D is the hydrodynamic dispersion coefficient $[cm^2/hr]$, q is the flow velocity $[cm/hr]$, μ is the first order decay coefficient for degradation $[1/hr]$, t is time $[hr]$ and z is depth $[cm]$.

Under the assumption of constant water content and steady-state flow conditions in soil, equation 6.1 simplifies to:

$$\frac{\partial C_t}{\partial t} = \theta D \frac{\partial^2 C}{\partial z^2} - q\frac{\partial C}{\partial z} - \mu C_t \tag{6.2}$$

No volatilization is considered, therefore the total mass per unit volume of soil (C_t) is given by:

$$C_t = \theta C + \rho_b S \tag{6.3}$$

where S is the solute concentration sorbed onto solids $[mg/Kg]$ and ρ_b is the soil bulk density $[Kg/L$ or $g/cm^3]$. Mathematical sorption models are typically coupled with the advection-dispersion transport equation (Magga et al., 2012) and several sorption models

are available to characterize the interaction between chemicals in solution and the solid phase. Assumptions in sorption models may differ with respect to: a) the type of sorption isotherm (S_1, linear or non-linear), b) time dependency (S_1, instantaneous - equilibrium or S_2, rate-limited - kinetic) and c) process reversibility (S_3, reversible or irreversible) (Wehrhan, 2006).

Equilibrium sorption produces symmetrical breakthrough curves (BTC) with no tailing (Brusseau et al., 1992). However, asymmetric BTCs and tailing have widely been reported for a variety of organic chemicals leached through porous media (Gamerdinger et al., 1990). Early peaks on the BTC and increased tailing indicate the presence of non-equilibrium (rate-limited) and non-linear sorption processes (Brusseau et al., 1992). Non-equilibrium processes involved can be of physical (transport related) and/or chemical (sorption-related) nature (Brusseau et al., 1992; Mao and Ren, 2004). While physical non-equilibrium transport influences reactive and non-reactive tracers, chemical non-equilibrium influences only the behavior of reactive tracers. Chemical non-equilibrium is produced by differences in sorption processes between the chemical in the aqueous phase and particular sorption sites (instantaneous and kinetic) of the solid phase (Brusseau et al., 1992).

The total sorbed concentration is the sum of all sorption sites given by:

$$S = S_1 + S_2 + S_3 \tag{6.4}$$

where S_1, S_2 and S_3 represent reversible-equilibrium, reversible-kinetic and irreversible sorption processes. Equilibrium and kinetic sorption characteristics are described by equations 6.5 and 6.6, respectively. Kinetic sorption is usually represented as a first-order rate process. Irriversible sorption is often represented as a first-order kinetic sink of the dissolved chemical in the aqueous phase (equation 6.7).

Equilibrium

$$\frac{\partial S_1}{\partial t} = f K_f \frac{\partial C^N}{\partial t} \tag{6.5}$$

Kinetic

$$\frac{\partial S_2}{\partial t} = \alpha((1-f) K_f C^N - S_2) - \mu_{s_2} S_2 \tag{6.6}$$

Irreversible

$$\frac{\partial S_3}{\partial t} = \frac{\theta}{\rho_b} \beta C \tag{6.7}$$

Sorption of organic compounds is typically characterized by the nonlinear Freundlich isotherm, $S = K_f C^N$, where K_f is the Freundlich distribution coefficient [$mg\ L^N/Kg\ mg^N$] and N is the dimensionless Freundlich exponent. Linear sorption is a special case of the Freundlich isotherm when $N = 1$. f is the fraction of exchange sites that are at equilibrium and range from 0 to 1. β is the irreversible sorption rate coefficient [$1/hr$].

A schematic representation of the cross combination on the aforementioned sorption assumptions is presented in Figure 6.1. Sorption with equilibrium Figures 6.1a and kinetic 6.1b sorption processes are considered reversible. Figure 6.1c considers two reversible types of sorption sites: equilibrium and kinetics. Figures 6.1d and 6.1e also consider two types of sorption sites where one of them is a reversible-equilibrium or reversible-kinetic sorption processes and the second one is irreversible, respectively. Figure 6.1f presents

three types of sorption sites: reversible-equilibrium, reversible-kinetic and irreversible.

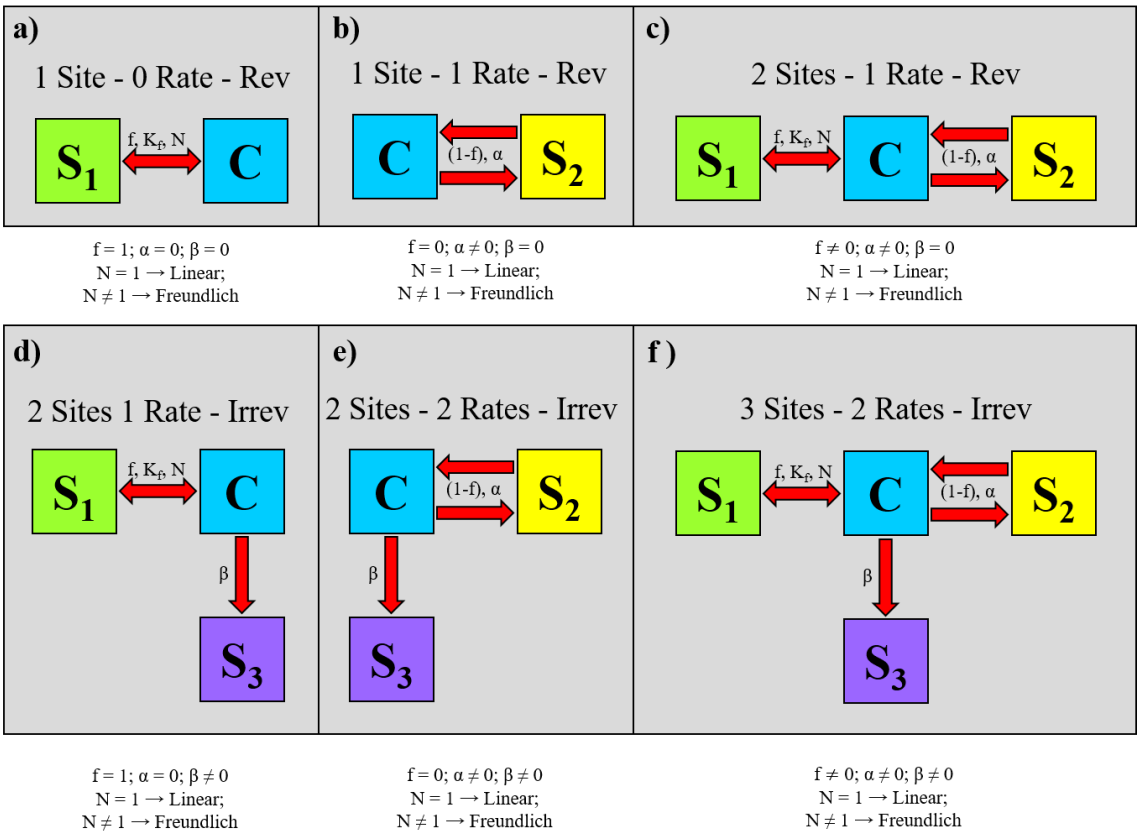

Figure 6.1: Schematic representation of solute-soil distribution models where C represents the concentration in the aqueous phase and S represents the concentration in the solid phase. S_1, S_2 and S_3 represent reversible-equilibrium, reversible-kinetic and irreversible, respectively. K_f is the Freundlich sorption partition coefficient, N is the dimensionless Freundlich exponent, f is the fraction of exchange site that are at equilibrium, β is the irreversible sorption rate coefficient.

The objectives of this work were to assess the fate and transport of OTC in agricultural soils, compare concentration levels in aqueous and solid phases to that concentrations that select for antibiotic resistance, and identify the time range of antibiotic resistance selectivity. To the author's knowledge, there have been no other reports of modeling the fate and

transport of OTC in manure-amended soils that also include assessment of potential antibiotic resistance selectivity. A two-site, one rate, non-equilibrium model (Figure 6.1c) was chosen as the appropriate model to assess the fate and transport of OTC on an agricultural soil. The two-site one-rate model provides an increased degree of complexity considering the non-equilibrium condition as compared to the ADE (Figure 6.1a). At the same time, the two-site one rate model minimizes the number optimization parameters that would have to be adjusted.

Transport parameters (v and D) are commonly determined from BTCs of non reactive tracers. Partition coefficients (K_d = S/C or C_s/C_w) are typically obtained from batch sorption experiments. Loss rates through transformation (μ) may be estimated from mass balance analysis of the experimental chemical, from independent experiments, or by inverse fitting (Brusseau et al., 1992). Sorption related parameters (e.g. f, α, β) except K_d, are difficult to measure. A common practice for estimating such parameters is by means of inverse modeling techniques. Currently, limited data for OTC transport is available and values for some parameters (f, α, β) have not been characterized specifically for OTC in any soil type. Column transport experiments with Chlortetracycline (CTC) (Lee et al., 2014) and Sulfadiazine (SDZ) (Wehrhan, 2006) used numerical inverse modeling techniques to fit the Two-Sites, One Rate, Reversible model (Figure 6.1c) to experimental data of BTCs and determined values for the parameters f and α. In the absence of values for the parameters f and α for OTC transport, values characterized for CTC and SDZ were used as surrogates.

6.2 Approach

Given the variability in the management of manure and agricultural practices, realistic worst case conditions were considered for simulations. Nitrogen is often the most limiting plant nutrient for yield efficiency and financially advantageous crop production

(Mikkelsen and Hartz, 2008). Corn was chosen as the target crop for manure application estimates based on nitrogen demand. Corn has a high nitrogen demand due to its high yield potential and is the most widely produced crop in the U.S. Also, manure application for corn production is a common practice. Thus, the assessment is appropriate in the Midwest part of the U.S. which has the largest corn production (Figure 6.2a), commonly known as the "Corn Belt". Coarse to medium textured soils (well drained soils), such as sandy loams and loam are best suited for corn production (Tacker et al., 2008; Lamb et al., 2015). However, a wide range of soil types have produced corn successfully (Tacker et al., 2008). A sandy loam textured soil was selected for simulation scenarios as it allows higher water infiltration rates (EPA, 2012). Land application of liquid manure and surface spreading of semi-solid manure with and without incorporation were considered as manure management practices. Immediate incorporation minimizes nitrogen loss through volatilization.

Swine manure is considered for this study as the source of manure due to the hog production concentration in the Midwest of the U.S. (Figure 6.2b) (Mackie et al., 2006) which accounts for two thirds of national production (Key et al., 2011). North Carolina also has a high density of hog production operations (Key et al., 2011; Pornsukarom and Thakur, 2016), however North Carolina was not considered in this study. Typically, swine production operations have been located near areas of copious corn production which provide a low cost feed supply (Key et al., 2011). In a cyclic fashion, swine manure is used as fertilizer on crop fields. Swine manure is typically managed in lagoons and pit or tanks storage structures (Key et al., 2011). Lagoons are large earthen containment basins that collect manure and flushed wastewater. Manure pits are typically located underneath swine production facilities collecting direct manure drops through slatted decks. Lagoons and pits maintain a liquid and slurry consistency, respectively. Key et al. (2011) and Pornsukarom and Thakur (2016) reported the use of pits as the dominant swine manure management

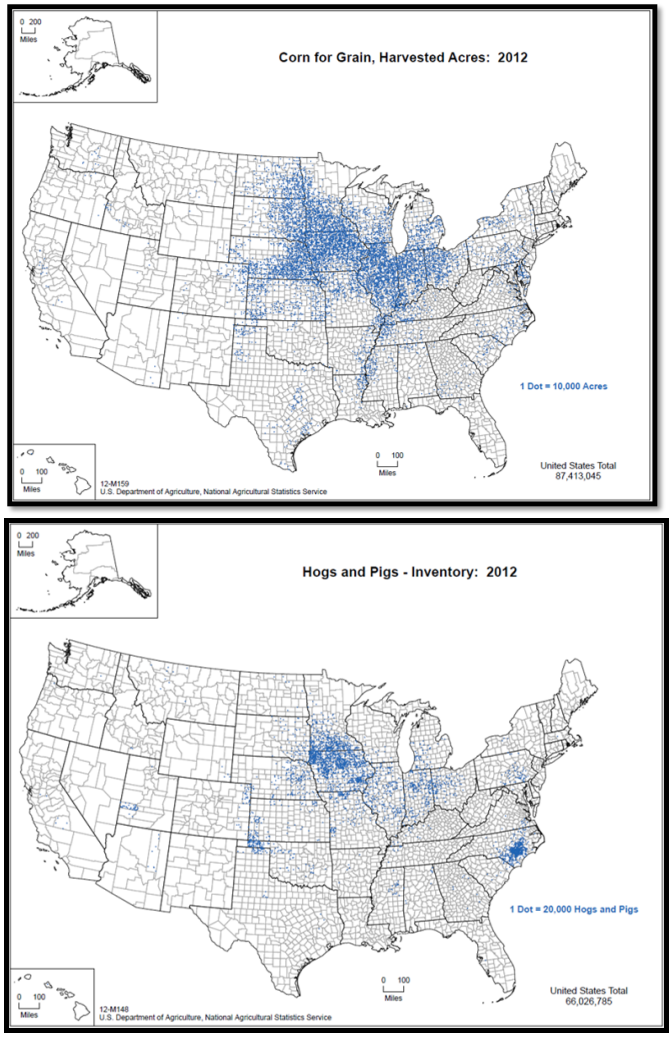

Figure 6.2: Map of corn crop harvested for grain purposes (top) and swine production (bottom) in the U.S. according to the USDA 2012 census of agriculture.

systems in the Midwest of the U.S. while lagoons are the preferred method in North Carolina. Changes in manure management practices between 1998 and 2009 are partially attributed to increases in the cost of chemical fertilizers. Pit management systems provide a higher nutrient conservation efficiency than lagoon systems (Key et al., 2011). Waste for pit or tanks systems is commonly land applied as slurry or liquid and liquid waste from lagoon systems is typically applied with irrigation technology (Key et al., 2011).

Slurry and diluted slurry application rates were determined based on nitrogen recommendation rates of 240 lb N/acre-yr assuming a corn goal of 150 bushel/acre (Stichler and McFarland, 1997) and an average nitrogen content of 6 lb/ton manure following procedures from the Agricultural Waste Management Field Handbook (USDA, 2009b). Swine manure, as excreted, is considered a slurry with 10 % of total solids (Figure 6.3) (USDA, 2009b). The slurry is diluted for liquid waste application scenarios assuming 15 gallons of water added per cubic foot of slurry to reduce the percentage of solid from 10% to 3%. Liquid waste application rates were selected based on soil texture to avoid ponding and runoff (USDA, 2009b). Slurry and dilute slurry application rate estimates are presented in Appendix E. Slurry and dilute slurry, both containing OTC, are assumed to be homogeneously mix into the incorporation zone. Thus, the mass of OTC is considered to be homogeneously distributed along the soil depth.

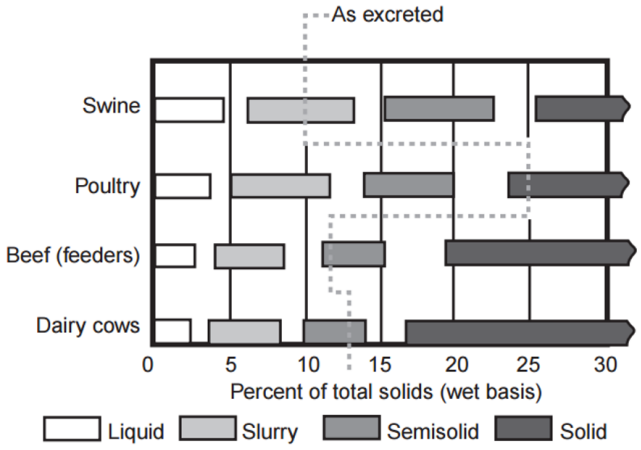

Figure 6.3: Typical total solid content in different types of manure (USDA, 2009a)

Fate and transport scenarios were evaluated using the parameters and conditions selected to reflect the aforementioned conditions: high nitrogen demand crop, average ni-

trogen content in manure, well drained soil for corn production and related physical soil properties (Table 6.1). A sensitivity analysis was performed to assess which parameters would affected the most simulation results. The sensitivity analysis was performed at OTC concentration of 48 $\mu g_{OTC}/Kg_{manure}$ reported from swine manure storage tanks (Jacobsen and Halling-Sørensen, 2006) and an average incorporation depth of 10 cm. Aqueous, equilibrium sorption sites (type 1) and kinetic sorption sites (type 2) concentration results were plotted versus time and grouped in the same figure for each individual parameter assessment. For example, aqueous, equilibrium sorption sites and kinetic sorption sites concentrations are presented in Figures F.2A-C, respectively.

The sensitivity of a model with respect to an input parameter is typically defined as the change in concentration caused by the change in the parameter and is expressed as (Zheng and Bennett, 2002e; Mao and Ren, 2004):

$$X_{i,k} = \frac{\partial C_i}{\partial a_k} \tag{6.8}$$

where $X_{i,k}$ is the sensitivity coefficient of the model parameter k_{th} evaluated at the i_{th} observation point. Equation 6.8 can be normalized in order to express all sensitivity coefficients in the same units and is defined as (Zheng and Bennett, 2002e; Mao and Ren, 2004):

$$X'_{i,k} = \frac{\partial C_i}{\partial a_k / a_k} \tag{6.9}$$

Sensitivity of the model with respect to a particular parameter can be determine by using a finite difference approximation given by:

$$X_{i,k} \approx \frac{\partial C_i}{\partial a_k} = \frac{C_i(a_k + \Delta a_k) - C_i(a_k)}{\Delta a_k} \tag{6.10}$$

Table 6.1: Summary of values utilized for simulations

Parameter	Description	Value	Units
	Crop	Corn	
	Crop yield	150	bushel/acre
	Length of growing season	120	days
	Crop nitrogen (N) demand	240	lb N/acre
	Manure source	Swine manure	
	Manure composition	Solid (aged)	
		Liquid	
	Manure N content [a]	6 [d]	lb N/ ton$_{manure}$
	Manure N content (liquid)	0.9	lb N/1000 gal$_{manure}$
	Manure density (as excreted)	0.99 [e]	Kg/L
	OTC in manure	48 [m] & 29000 [n]	μg$_{OTC}$/kg$_{manure}$
	Incorporation depth	10 & 25	cm
	Soil type	Sandy Loam	
ρ_b	Bulk density	1.4 [f]	g/cm^3 or Kg/L
θ	Volumetric water content	0.2	cm^3/cm^3
v	Pore water velocity	2.1 [g,h]	cm/hr
D	Dispersion	3.1 [g]	cm^2/hr
λ	Dispersivity	1.5	cm
K_f	Partition Coefficient	665 [i]	mg L^N/Kg mg^N
N	Exponent	0.75	
f	Fraction of equibrium sorption sites	0.05 [j] & 0.20 [k]	
α	First order kinetic rate coefficient	0.003 [k] & 0.12 [j]	1/hr
DT$_{50_l}$	Half life in aqueous phase	33 [l]	days
μ_l	First order decay rate for aqueous phase	0.0009[b]	1/hr
DT$_{50_{s_1,s_2}}$	Half life in solid phase	33 & 8.25 [c]	days
μ_{s_1}, μ_{s_2}	First order decay rate for solid phase	0.0009[c] & 0.0035[b]	1/hr

[a] Storage pit beneath slotted floors (USDA, 2009b). [b] Decay rate was estimated by $\alpha = \frac{ln(2)}{t_{1/2}}$, where $t_{1/2}$ is the manure-amended soil half-life (Wang and Yates, 2008).
[c] μ_s assumed 25% of half-life in aqueous phase. [d](USDA, 2009b) [e](Lorimor et al., 2004) [f](NRCS, 2008) [g](Singh et al., 1996) [h](Fedler and Borreli, 2001) [i](ter Laak et al., 2006a) [j](Lee et al., 2014) [k](Wehrhan, 2006) [l](Wang and Yates, 2008) [m](Jacobsen and Halling-Sørensen, 2006) [n](Brambilla et al., 2007)

where Δa_k is a small change in the perturbed parameter. Equation 6.10 expressed in normalized form is given by:

$$X_{i,k} \approx \frac{\partial C_i}{\partial a_k} = \frac{C_i(a_k + \Delta a_k) - C_i(a_k)}{\Delta a_k / a_k} \tag{6.11}$$

The two-site, one-rate, non-equilibrium model was run with three different values of the assessed parameter while keeping the remaining variables constant. For example, each run used values for the soil bulk density (ρ_b) of 1.2, 1.4 and 1.6 g/cm^3, representing $a_k - \Delta a_k$, a_k, and $a_k + \Delta a_k$, respectively. The values for the remaining variables are listed in Table 6.1. Aqueous, equilibrium sorption site (type 1) and kinetic sorption site (type 2) concentrations at 2.94 days and a depth of 10 cm are summarized in Table F.1. Concentrations at 2.94 days were chosen as the i_{th} observation point for the sensitivity analysis because resulted in the maximum value for the time dependent concentration curves of the base case (a_k). Sensitivity coefficients estimated using equation 6.11 are presented in Figure 6.4 and Table F.2.

The assessment highlighted different parameters as most sensitive for each type of concentration. For the aqueous concentration, the parameters that resulted with the highest normalized sensitivity coefficients are: the soil bulk density (ρ_b), the partition coefficient (K_d), the Freundlich isotherm exponent (N) and the OTC concentration in manure (Figure 6.4A). For equilibrium site concentrations, the highest normalized sensitivity coefficients are: the soil bulk density (ρ_b), the available fraction of sorption sites at equilibrium (f), the OTC concentration in manure and the Freundlich isotherm exponent (N) (Figure 6.4B). For kinetic site concentrations, the highest normalized sensitivity coefficients are: the soil bulk density (ρ_b) and OTC concentration in manure (Figure 6.4C). The available fraction of sorption sites at equilibrium (f), the first order kinetic rate coefficient (α), and the degradation rate coefficient in the solid media also appear as sensitive for the kinetic sites

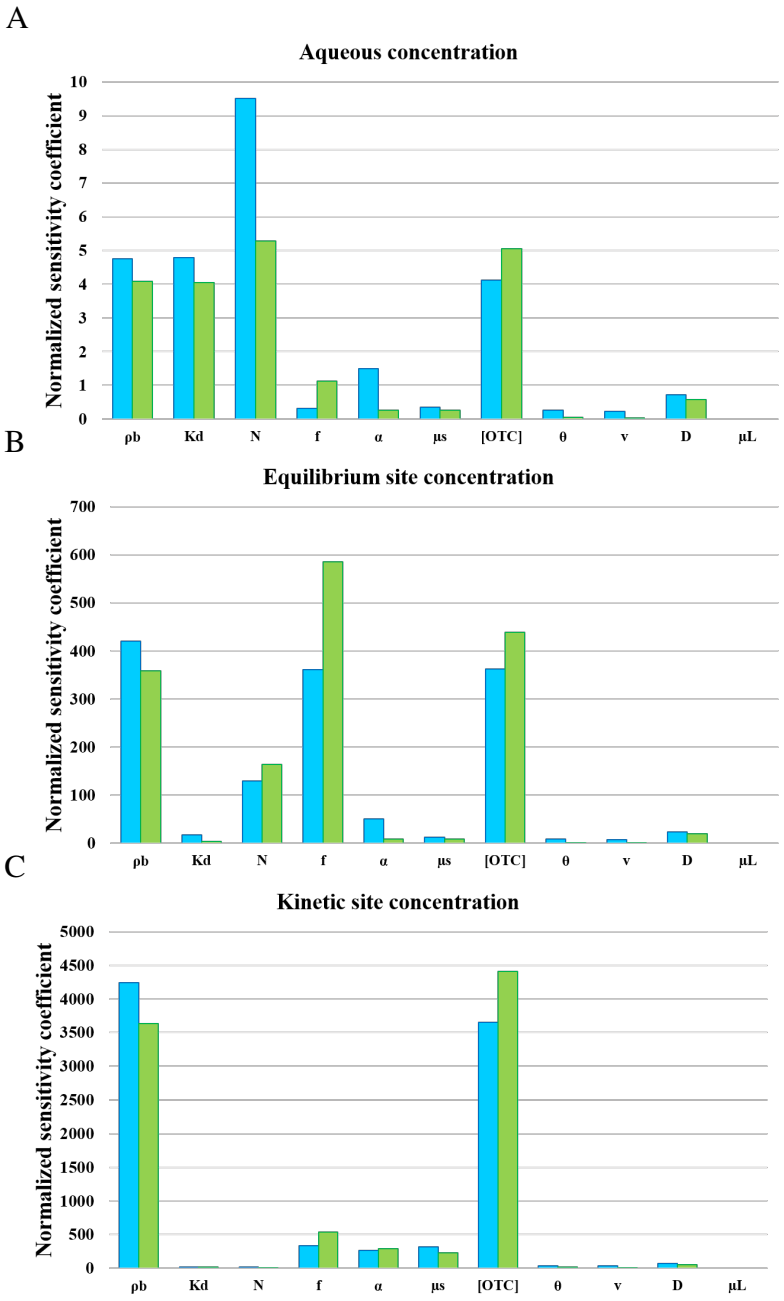

Figure 6.4: Normalized sensitivity coefficients for each parameter for the Aqueous (A) and solid concentrations (at equilibrium (B) and time dependent (C) sorption sites). Blue bars designate normalized sensitivity coefficients for backward simulation run ($a_k - \Delta a_k$). Green bars designate normalized sensitivity coefficients for forward simulation run ($a_k + \Delta a_k$).

concentrations, however, on a much lower scale.

Overall, the assessment revealed the following seven (7) parameters as the most sensitive: 1) fraction of exchange sites to be at equilibrium (Type 1 sites) (f, Figure F.1); 2) soil bulk density (ρ_b, Figure F.2); 3) Freundlich isotherm exponent (N, Figure F.3); 4) first order kinetic rate coefficient (α, Figure F.4); 5) first order decay coefficient for the adsorbed phase (μ_s, Figure F.5); 6) partition coefficient (K_d, Figure F.6); and 7) the concentration of OTC in manure (Figure F.7). The parameters θ (Figure F.8), v (Figure F.9), D (Figure F.10) and μ_L (Figure F.11) did not present significant differences in compared simulations for aqueous, equilibrium site and kinetic site concentrations (Table F.1 and F.2).

Given that ρ_b is dependent in part on soil texture, a fixed value was chosen in agreement with the soil type (sandy loam) for all simulated cases (Table 6.1). Scenarios were modeled with two alternative values for each of the remaining sensitive parameters (e.g. f = 0.05 and 0.20; α = 0.003 and 0.12 1/hr; DT_{50s} = 33 and 8.3 days). Minimum and maximum values of OTC concentrations in aged manure that have been reported by Jacobsen and Halling-Sørensen (2006) and Brambilla et al. (2007) from waste storage tanks at swine production farms were used for simulations. Initial and boundary condition calculation procedures are detailed in Appendix E for surface and liquid application of manure.

Estimated slurry application rates (L/m^2), presented in Table 6.2, are similar among application rates reported in U.S. studies but approximately three times higher than studies from the UK (Table 6.3). OTC loading rates into soil ($\mu g/m^2$) reported for the experimental studies in Table 6.3, which had a range of objectives including runoff, transport, persistence and ARB selection assessment, are within the range used for modeled scenarios in this works which are presented in Table 6.2. Simulations evaluated low and high OTC loading for the wide range of concentrations reported in experimental studies. Minimum and maximum OTC concentrations in swine manure were selected, rather than average or mode concentrations, due to the wide variability of manure application rates and agri-

Table 6.2: Comparison of application rates and OTC concentrations used in the fate and transport modeling scenarios

Manure source	Application method	Manure or Slurry application rate $\left(\frac{L}{m^2}\right)$	[OTC] in manure $\left(\frac{\mu g}{Kg}\right)$	OTC loading into soil $\left(\frac{\mu g}{m^2}\right)$	ED* -Nominal [OTC] in soil $\left(\frac{\mu g}{Kg}\right)$
Swine	Surface application without incorporation	13.2	48	629	90
			2900	380305	54330
	Surface application with 10 cm incorporation	13.2	48	629	4.5
			2900	380305	2717
	Surface application with 25 cm incorporation	13.2	48	629	1.8
			2900	380305	1087
	Liquid spreading without incorporation	39.7	16	629	49
			9587	380305	29410
	Liquid spreading with 10 cm incorporation	39.7	16	629	2.4
			9587	380305	1470

Note: Swine slurry density = 0.99 Kg/L (Lorimor et al., 2004). * ED = Effective Dose

cultural management practices, instead of the manure application rate. Thus, simulation results represent a lower and upper boundary of experimental studies and field conditions currently happening.

6.3 Results

Resultant concentrations from simulated scenarios were plotted versus time and at various depths (Figures 6.5 to 6.36). Each figure denotes a scenario and represents one of the possible combinations of parameter values presented in Table 6.1. Simulations with minimum OTC concentration in manure (48 $\mu g/Kg$) are not shown since all simulations were below the sublethal-minimum inhibitory concentrations (sub-MIC) selectivity region. Also, simulations with maximum OTC concentration in manure (29 mg/Kg) mixed to a depth of 25 cm resulted in aqueous, type 1 sorption site and type 2 sorption site concentrations below potential selectivity levels.

Each of the figures presented has three graphs labeled *A, B* and *C* which represent time dependent concentration for aqueous, equilibrium sorption (Type 1) sites and kinetic sorption (Type 2) sites, respectively. In addition, sub-MIC and traditional resistant selective regions (Table 6.4) are superimposed on each graph (*A,B* and *C*) in order to visually compare simulation results with antibiotic selective ranges.

6.3.1 Surface application of manure

For surface application of manure **without incorporation** , all aqueous phase concentrations with a slow first order kinetic rate coefficient (α = 0.003) are below the sub-MIC selective region (Figures 6.5A, 6.7A, 6.9A and 6.11A). Using a faster first order kinetic rate coefficient (α = 0.12) resulted in concentrations in the top soil layer (z < 1.0 cm) to be within the selective window for less than five days (Figures 6.6A, 6.8A, 6.10A and 6.12A). Concentrations of type 1 (equilibrium) sorption sites on the top layer are inside the sub-MIC selective region for all the cases (Figures 6.5B to 6.12B). Concentration of type

Table 6.3: Application rates and OTC concentrations used in other transport studies

Manure source	Application method	Manure or Slurry application rate	[OTC] in manure $\left(\frac{\mu g}{Kg}\right)$	OTC loading into soil $\left(\frac{\mu g}{m^2}\right)$	Objective	Location	Reference
Swine	Slurry spreading with pre-tilled soil (10 cm)	4.5 $\frac{L}{m^2}$	18850	84825	Runoff	UK	Kay et al. (2004)
Swine	Slurry spreading with pre-tilled soil (10 cm)	4.5 $\frac{L}{m^2}$	18850	84825	Leaching column	UK	Kay et al. (2005a)
Swine	Slurry spreading with and without incorporation (25 cm)	4.5 $\frac{L}{m^2}$	18850	84825	Lysimeter column	UK	Kay et al. (2005b)
Swine	Slurry spreading without incorporation	3.3 $\frac{L}{m^2}$	26200	86460	Leaching and runoff	UK	Blackwell et al. (2007)
Cattle	Surface application with 45 cm incorporation	9.46 $\frac{Kg}{m^2}$	820	7757	Soil amendment	Italy	de Liguoro et al. (2003)

Table 6.3: Continued

Manure source	Application method	Manure or Slurry application rate	[OTC] in manure $\left(\frac{\mu g}{Kg}\right)$	OTC loading into soil $\left(\frac{\mu g}{m^2}\right)$	Objective	Location	Reference
Cattle	Application in soil pots of corn	9 $\frac{Kg}{m^2}$	11300	101324	Crop growth effect	USA	Patten et al. (1980)
Swine	Liquid spreading without incorporation	1.4 to 1.8[a] $\frac{L}{m^2}$	N/A [b]	16240 to 20880 [b]	Soil microbial community impact	USA	Stone et al. (2011)
Hogs and Cattle	Liquid spreading without incorporation	N/A [a]	N/A [b]	35000 [b]	Runoff	USA	Davis et al. (2006)
Swine	Liquid spreading without incorporation	6.2 to 55.8	N/A [b]	6746 to 60711 [b]	Antibiotic resistance selection in soil	USA	Popova et al. (2017)
Swine	Slurry spreading with 30 cm incorporation	3 to 4 $\frac{L}{m^2}$	3200 to 4000 [b]	11088 to 13860 [b]	TC and CTC persistence in soil	Germany	Hamscher et al. (2002)
Dairy cows	Solid spreading and slurry injection with 15 cm incorporation / injection	9 to 13 $\frac{Kg}{m^2}$	N/A	N/A	Nitrogen transport	Canada	Hengnirun et al. (1999)

[a] Antibiotic in solution was directly sprayed to soil plots (Davis et al., 2006).
[b] Chlortetracycline (CTC) was used in the study, not OTC.

Table 6.4: Sublethal and traditional minimum inhibitory concentration ranges for Oxytetracycline in aqueous and solid media

Type of media	Selective region	Lower boundary	Upper boundary	Reference
Aqueous (ng/mL)	Sub-MIC	78.5	1000	Thiele-Bruhn and Beck (2005)
	Traditional	1000	2000	Thiele-Bruhn (2005)
Solid ($\mu g/kg$)	Sub-MIC	930	31,200	Thiele-Bruhn and Beck (2005)
	Traditional	31,200	200,000	Peng et al. (2014)

2 (kinetic) sorption sites are within the traditional and sub-MIC selective region (Figures 6.5C to 6.12C).

Under the assumption of **10 cm incorporation**, all aqueous concentration are below the sub-MIC selective window at all depths (Figures 6.13A to 6.20A). All type 1 sorption site concentrations are below the sub-MIC selective region (Figures 6.13B to 6.20B). Although, when the available equilibrium sorption sites are increased to $f = 0.20$, the sorbed concentration also increased (Figures 6.17B to 6.20B), but is still below the selection zone. Type 2 sorption site concentrations are inside the selective region for all cases throughout the entire mixing zone for up to 40 days. Low ($\mu_s = 0.00088$) and high ($\mu_s = 0.0035$) decay values reduce concentrations to levels below selectivity after approximately 40 days (Figures 6.13C, 6.14C, 6.17C and 6.18C) and 10 days (Figures 6.15C, 6.16C, 6.19C and 6.20C), respectively .

6.3.2 Liquid application of manure

Aqueous concentrations for the scenarios of liquid manure application and **no incorporation** resulted in levels below the sub-MIC selective region for all cases (e.g. $f = 0.05$ and 0.20; $\alpha = 0.003$ and 0.12; $\mu_s = 0.00088$ and 0.0035) (Figures 6.21A to 6.28A). Type 1 (Figures 6.21B to 6.28B) and Type 2 (Figures 6.21C to 6.28C) sorption site concentrations are within the sub-MIC selective region throughout the entire simulation (120 days) for all the cases of f, α, and μ_s.

Simulations of liquid manure application assuming **10 cm of incorporation** and maximum OTC resulted in only type 2 sorption site concentrations inside the sub-MIC selective region for up to 30 days (Figures 6.29C, 6.30C, 6.33C and 6.34C) and 15 days (Figures 6.31C, 6.32C, 6.35C and 6.36C) for cases of low decay ($\mu_s = 0.00088$) and high decay($\mu_s = 0.0035$), respectively. Aqueous (Figures 6.29A to 6.32A and 6.33A to 6.36A) and type 1 site (Figures 6.29B to 6.32B and 6.33B to 6.36B) concentrations were below the potential selectivity region.

6.4 Discussion

Our simulation results consider worst case scenarios with a high nitrogen requirement in combination with minimum and maximum OTC concentrations reported in aged swine slurry. The effects of OTC complexation with divalent cations (ter Laak et al., 2006a) and dissolved organic matter (DOM) (Chen et al., 2015) known to potentially interfere with soil sorption were not considered. Overall, modeling results show persistence and potential accumulation following additional slurry applications. Simulations with minimum OTC in manure (48 $\mu g/Kg$) resulted in concentrations in aqueous and solid media below the sub-MIC selection region.

A summary of the concentration levels at the end of the corn growing season (approximately 120 days) is presented in Tables 6.5 and 6.6. Overall, by the end of the simulation

time, scenarios which assumed slurry application (Table 6.5) and incorporation depth of 10 cm resulted in concentration levels in the solid media below the sub-MIC selection region (930 to 31,200 $\mu g/kg$). However, potential selection of antibiotic resistant bacteria was present from 5 to 50 days. Scenarios assuming slurry application (Table 6.5) and no incorporation depth resulted in concentration levels in the solid media within the sub-MIC selection region throughout the entire simulation. These results suggest that, under the conditions established in Tables 6.1 and 6.2, concentrations of OTC in manure in the order of 29 mg/kg have the potential to select for antibiotic resistant bacteria, specially if no incorporation of manure is done.

Scenarios assuming liquid application of manure (Table 6.6) and no incorporation resulted in potential selectivity through the simulation period (120 days). In contrast, homogeneous incorporation to a depth of 10 cm resulted in potential selectivity to up to 30 days. By the end of the growing season, concentration levels for scenarios assuming liquid application of manure (Table 6.6) were significantly lower than their equivalent scenarios of (undiluted) slurry application (Table 6.5). These results highlight the effect of dilution.

It is important to emphasize that the OTC concentrations in manure used for the simulations, 48 $\mu g/Kg$ (minimum) and 29 mg/Kg (maximum), correspond to the lowest and highest reported concentrations for aged swine manure (see Figure 2.3), respectively. Concentrations for fresh swine and cattle manure have been reported up to 136 mg/Kg (swine) (Winckler et al., 2004) and 871.7 mg/Kg (cattle) (de Liguoro et al., 2003). These concentrations are approximately more than 4.5 and 30 times higher than the maximum OTC concentration in aged swine manure used for the simulations in this work, respectively. Land application of fresh manure with OTC concentrations on the order of 10^3 mg/Kg could reach concentrations in the solid media within and above the traditional selective window (31,200 to 200,000 $\mu g/kg$).

Concentrations above the traditional selective window are expected to cause a mortal-

Table 6.5: Summary of OTC concentration levels in the solid media by the end of the corn growing season for scenarios assuming slurry application of manure

f	μ_s	Depth (cm)	OTC in solid media by the end of simulations ($\mu g/kg$)	Selectivity range by the end of simulations	*Time inside the selection region (days)
5%	8.8x10^{-4}	0	$>$ 2500	Sub-MIC	120
		10	$>$ 200	*No selection	50
	3.5x10^{-3}	0	$>$ 2500	Sub-MIC	120
		10	$>$ 150	No selection	15
20%	8.8x10^{-4}	0	$>$11000	Sub-MIC	120
		10	$>$ 600	No selection	35
	3.5x10^{-3}	0	$>$11000	Sub-MIC	120
		10	$>$ 500	No selection	5

*No selection indicates that concentration is below the sub-MIC selective region

ity effect among the soil microbial population and could potentially cause adverse effect in soil fauna and plants development. Effects of no mortality have been reported for *Eisinia foetida* S. at OTC concentrations of 100x10^3 $\mu g/kg$ (Boleas et al., 2005). Lowest observed effect concentration (LOEC) values greater than 5,000x10^3 $\mu g/kg$ have been reported for soil fauna including: *F. fimetaria*, *E. crypticus* and *A. caliginosa* (Baguer et al., 2000). Effect on plant development have been observed on plants (*Triticum aestivum* L. and pinto beans) at concentrations of 160x10^3 $\mu g/kg$.

Our results are in agreement with observations made by Kay et al. (2005a) and Blackwell et al. (2007) who reported that OTC largely remained in the top soil layer. These results demonstrated reduced mobility of OTC. In other words, OTC remained within the incorporated mixing zone. Soil concentrations were reported to be 526 $\mu g/kg$ after 64 days after incorporation to 10 cm (Kay et al., 2005a) and 1000 $\mu g/kg$ after 127 days after surface application with no incorporation (Blackwell et al., 2007). Modeled scenarios in our work assumed similar incorporation practices. Simulations resulted in soil concentra-

Table 6.6: Summary of OTC concentration levels in the solid media by the end of the corn growing season for scenarios assuming liquid application of manure with maximum OTC

f	μ_s	Depth (cm)	OTC in solid media by the end of simulations ($\mu g/kg$)	Selectivity range by the end of simulations	*Time inside the selection region (days)
5%	8.8x10^{-4}	0	$>$ 1500	Sub-MIC	120
		10	$>$ 100	No selection	30
	3.5x10^{-3}	0	$>$ 1500	Sub-MIC	120
		10	$>$ 100	No selection	10
20%	8.8x10^{-4}	0	$>$5000	Sub-MIC	120
		10	$>$ 300	No selection	30
	3.5x10^{-3}	0	$>$5000	Sub-MIC	120
		10	$>$ 300	No selection	10

*No selection indicates that concentration is below the sub-MIC selective region

tion ranges, expressed as the sum of equilibrium and kinetic site concentrations, in the order of 10^3 $\mu g/kg$ (Figures 6.13, 6.14, 6.17 and 6.18).Transport parameters for Kay et al.'s (2005a) and Blackwell et al.'s (2007) experimental studies were not explicitly measured. Therefore, the predictive capability of the Two-Site, One-Rate, Reversible model cannot be tested with these studies. However, reported concentrations could be compared for the mass of OTC applied to the soil and incorporation depth. OTC loading into soil used in both experiments were 84,825 $\mu g/m^2$ (Kay et al., 2005a) and 86,460 $\mu g/m^2$ (Blackwell et al., 2007) which are within the range simulated in our work (Table 6.2).

Sorption is a dominant process affecting the fate and transport of pesticides, antibiotics and other organic compounds in soil (Magga et al., 2012). Particularly in this work, the availability of equilibrium sorption sites (f) and the amount of OTC in the manure are two determinant parameters affecting OTC concentration levels in soil, followed by soil density (ρ_b), partitioning (K_d), decay in the solid medium (μ_s), and the sorption kinetic rate (α). As time passes, changes of microbial population, organic matter, redox poten-

tial and pH in the soil are expected to result in the release of OTC-bound residues in soil under natural conditions (Hamscher et al., 2002). This time dependent release behavior has been previously reported for the Tetracycline class of antibiotics. A study by Liu et al. (2015) reported soil-bound antibiotic release behavior with increasing time. The short term experiment, approximately 20 days, showed increased extractable amounts of OTC with different aging times in the presence of horsebeans (Liu et al., 2015). In a monitoring study performed with Tetracycline (TC) and Chlortetracycline (CTC), sandy agricultural soils were fertilized with swine liquid manure on April 2000 and 2001 and sampled on May and November of 2000 and May 2001 (Hamscher et al., 2002). Hamscher et al. (2002) reported an increase in soil TC concentration from 40 $\mu g/kg$ (November 2000) to 110 $\mu g/kg$ (May 2001) which was greater than expected based on the corresponding liquid manure application (21 $\mu g/kg$). The observation of greater concentration than expected was attributed to possible TC release from the previous fertilizer application and suggest TC sorption as a reversible process and possible non-equilibrium sorption. These observed processes of reversibility and non-equilibrium suggest that the two-site, one rate, non-equilibrium model used for simulations in this work is adequate for OTC transport assessment in soil media.

Land application of manure from conventional concentrated animal feeding operations (CAFOs) that practice prophylactic and growth promotion use of antibiotics can introduce to soil the following constituents: nutrients for plant growth; ARBs carrying resistant genes which might be transferred to other bacteria (Davison et al., 2000); and bioactive antibiotic and antibiotic metabolites which can potentially select for antibiotic resistance (Heuer et al., 2009; Zwonitzer et al., 2016). The occurrence of antibiotics, ARBs and ARGs in soil, water and sediment have been widely reported in several studies performed in various countries (Sengeløv et al., 2003; Schmitt et al., 2006; Mackie et al., 2006; Ghosh and LaPara, 2007; Peak et al., 2007; Knapp et al., 2008; Heuer et al., 2011; Shentu et al.,

2015; Popowska et al., 2010; Pornsukarom and Thakur, 2016). While the presence of antibiotic, ARBs and ARGs has a synergic effect in the selection, prevalence and spread of antibiotic resistance, our work focuses on the assessment of residual OTC concentrations in soil media and its potential pressure for antibiotic resistance selectivity.

The selective ability of an antibiotic for bacterial resistance can be assessed by different methodologies. Phenotypic (growth patterns), genotypic (presence of genes) or taxonomic (community composition) assays can disclose distinct endpoints (Davison et al., 2000) as was reported by Lundström et al. (2016) for tetracycline in complex bacterial communities. A phenotypic resistance assay may evaluate the ability of bacteria to tolerate antibiotic concentrations, based on colony forming units (CFU) count or MIC ranges from an exposure-response experiment in which resistance is developed either by mutation, gene acquisition or both Davies (1997). A genotypic resistance assay can evaluate the selective ability of novel resistant genes which may be mobilized and cause horizontal transference (movement of genetic material). A taxonomic resistance assay can evaluate changes in microbial activity or indices such as, diversity, richness or evenness relative to basal levels (Lundström et al., 2016).

Relative to phenotypic resistance, several laboratory studies have reported the enrichment of antibiotic resistance at concentrations that are several orders of magnitude below the minimal inhibitory concentration (MIC) of susceptible strains (Kohanski et al., 2010; Gullberg et al., 2011; Liu et al., 2011; Quinlan et al., 2011; Lundström et al., 2016). However, the sub-MIC thresholds reported (where antibiotic resistant bacteria starts to outnumber susceptible strains) are for aqueous media, and data are limited for the solid media. Peng et al. (2014) reported inhibitory concentrations of soil-bound OTC in the range of 100 to 200 mg/kg (reduction in CFU of *E.coli* ATCC25922 by 50 and 90%, respectively). The potential for ARB generation has been verified by testing for the presence of specific resistant genes in manure and soil media.

OTC concentrations applied into soil in our work (Table 6.2) are comparable to those from Shentu et al. (2015) which ranged from 16 to 570 $\mu g/kg$. Shentu et al. (2015) reported a strong positive correlation for *tet*(M) and *tet*(Q) resistance genes with residual OTC concentrations in soil. The same study found an increased abundance of *tet*(A), *tet*(L), *tet*(M) and *tet*(Q) genes in soil following the application OTC-spiked swine manure. Swine manure was collected from a farm with no history of antibiotic use in feed. Manure was spiked with OTC to concentration ranges of 500 to 17500 $\mu g/kg$ and applied to soil on 10 occasions every two weeks, simulating high frequency of waste disposal and low OTC loading into soil. Schwaiger et al. (2009) demonstrated that tetracycline levels in swine manure lead to higher doxycycline minimum inhibitory concentrations (MICs) in *E. faecalis*, genetically based on co-occurrence of tet(M) and tet(L). Strains carrying *tet*(M), *tet*(L), both or neither genes were isolated from manure samples containing mean antibiotic concentrations of 510, 1180, 4080 and 350 $\mu g/kg$, respectively. These observations are in agreement with simulated results from maximum OTC and no incorporation scenarios where OTC-soil bound concentrations are within the sub-MIC selective region potentially selective for antibiotic resistance. Thus, frequent disposal of waste with OTC content in the range of 10^3 to 10^5 $\mu g/Kg$ can select and increase the abundance of antibiotic resistant genes, such as *tet*(M) and *tet*(Q).

In contrast, another study concluded that high levels of OTC in manure were not relevant for the antibiotic resistant genes persistence in soil (Kyselková et al., 2013). The study reported the presence of tetracycline resistant genes in cattle manure regardless of antibiotic intake. Kyselková et al. (2013) reported no significant differences in the abundance nor total number of tetracycline resistant genes detected in soil that repeatedly received either treatments (OTC-contaminated and OTC-free manure). However, the behavior of individual genes was significantly different.These results demonstrate that the fate of *tet* genes in manure-amended soils depends on the mobile genetic elements and the host bac-

teria carrying the resistant gene (Kyselková et al., 2013; Chessa et al., 2016). Even though this results are contradictory to our assessment, it can be argued that the objetive of the study was to assess the persistence in soils of antibiotic resistant genes present in manure. Thus, soil sample were assessed only for the presence or absence of those specific genes previously detected in manure. In other words, the approach followed for the microcosm study may have underestimated the potential selection for antibiotic resistance because of the limited scope of gene been monitored in soil.

Regarding a taxonomic resistance endpoint, our work simulated OTC loading into soil comparable to those from Thiele-Bruhn and Beck (2005) which reported reduced substrate-induced respiration and Fe(III) reduction at relevant agricultural OTC loadings in a sandy loam soil. OTC loading of 930 and 31200 $\mu g/kg$ might be comparable to scenarios of surface application considering maximum OTC with 25 cm of incorporation depth and liquid application of manure considering maximum OTC without incorporation (Table 6.2), respectively. Thus, a selective pressure on soil microbial populations is expected in cases with OTC loading in the order of 10^4 $\mu g_{OTC}/Kg_{soil}$ based on results from the simulated scenarios.

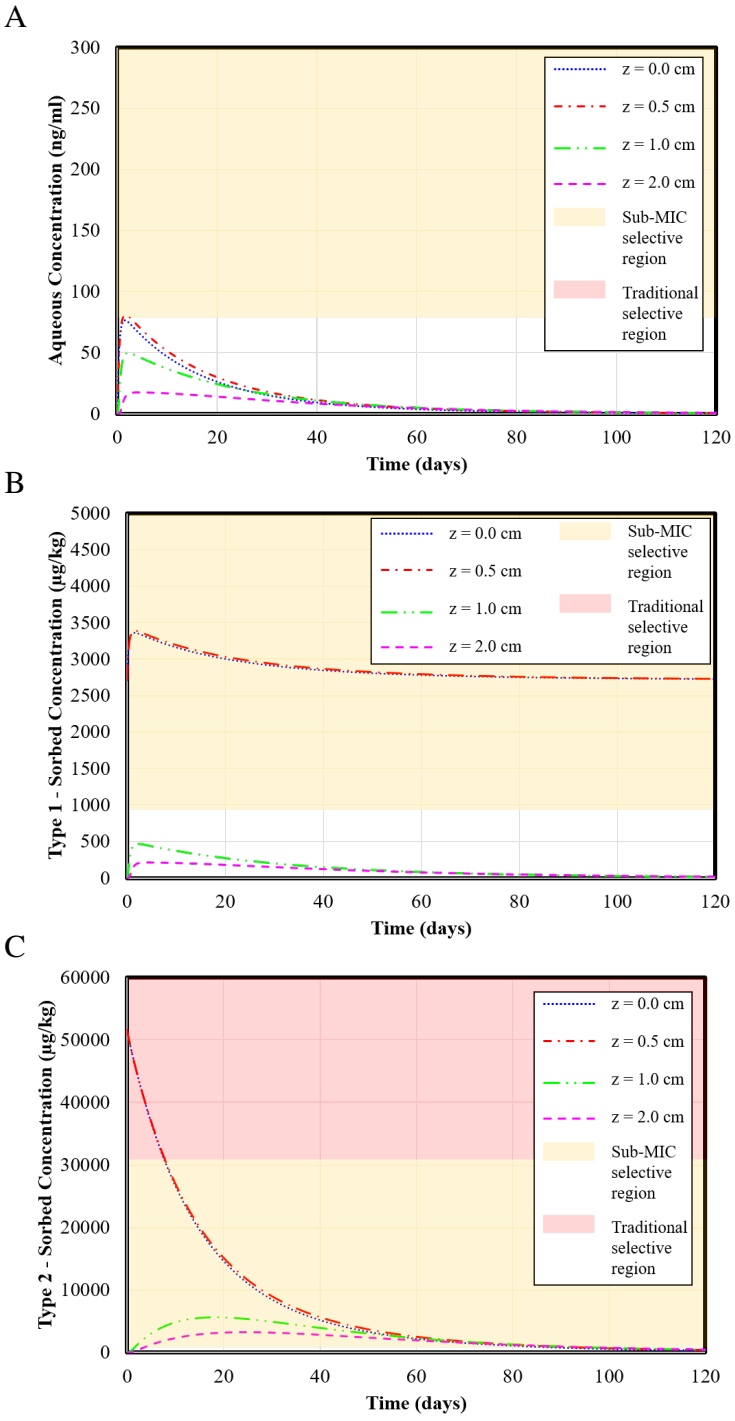

Figure 6.5: Predicted time dependent aqueous concentration (A), equilibrium sorption site (Type 1) concentration (B), and kinetic sorption site (Type 2) (C) concentration of OTC assuming surface application of manure without incorporation, maximum OTC, f = 0.05, α = 0.003 1/hr, and $\mu_{s_1} = \mu_{s_2} = 0.00088$

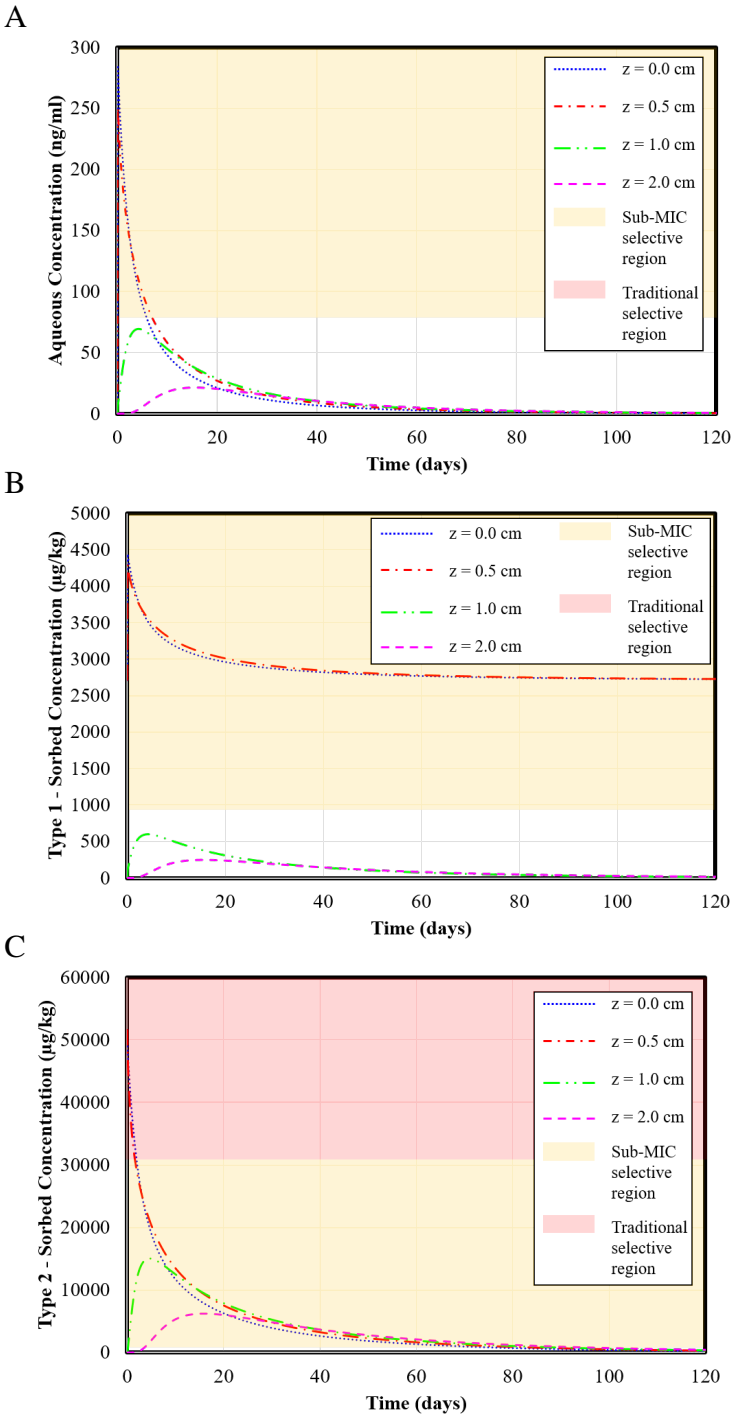

Figure 6.6: Predicted time dependent aqueous concentration (A), equilibrium sorption site (Type 1) concentration (B), and kinetic sorption site (Type 2) (C) concentration of OTC assuming surface application of manure without incorporation, maximum OTC, f = 0.05, α = 0.12 1/hr, and $\mu_{s_1} = \mu_{s_2}$ = 0.00088

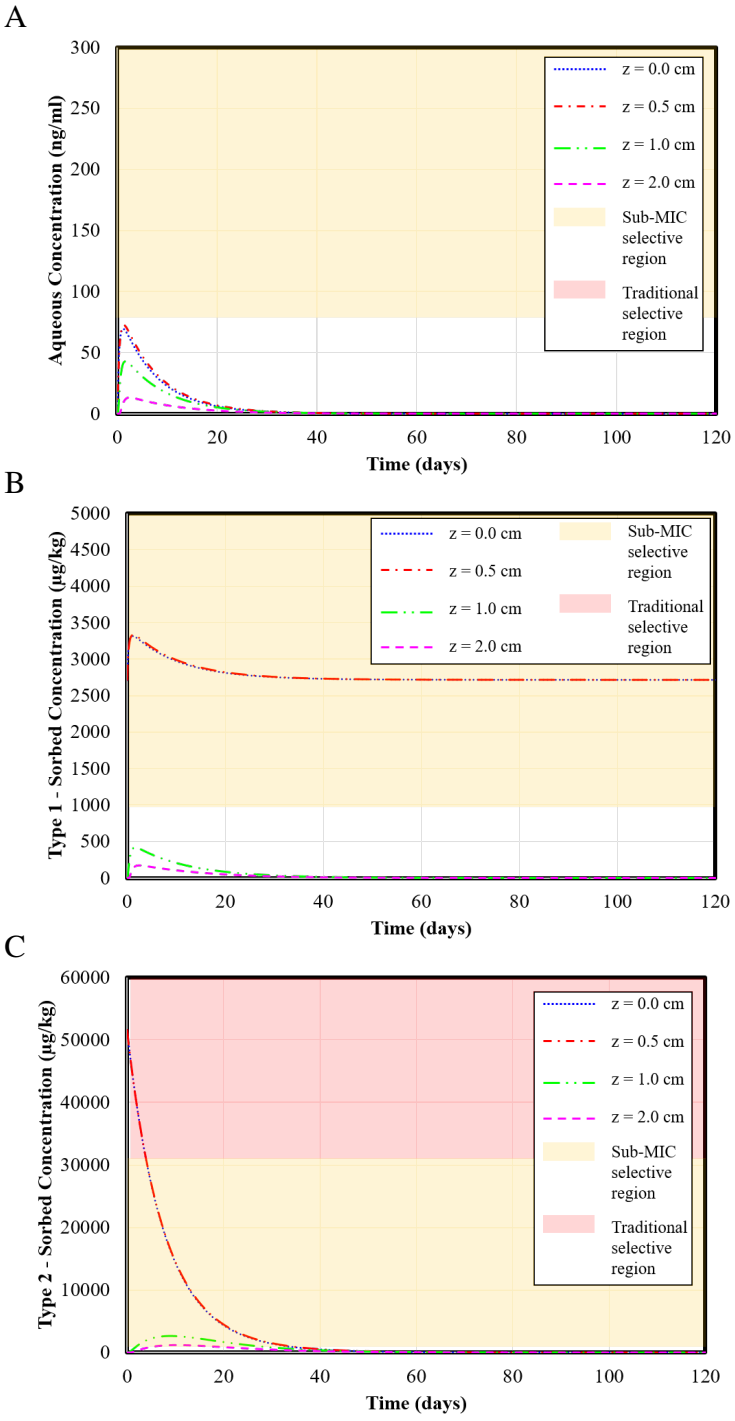

Figure 6.7: Predicted time dependent aqueous concentration (A), equilibrium sorption site (Type 1) concentration (B), and kinetic sorption site (Type 2) (C) concentration of OTC assuming surface application of manure without incorporation, maximum OTC, f = 0.05, α = 0.003 1/hr, and $\mu_{s_1} = \mu_{s_2} = 0.0035$

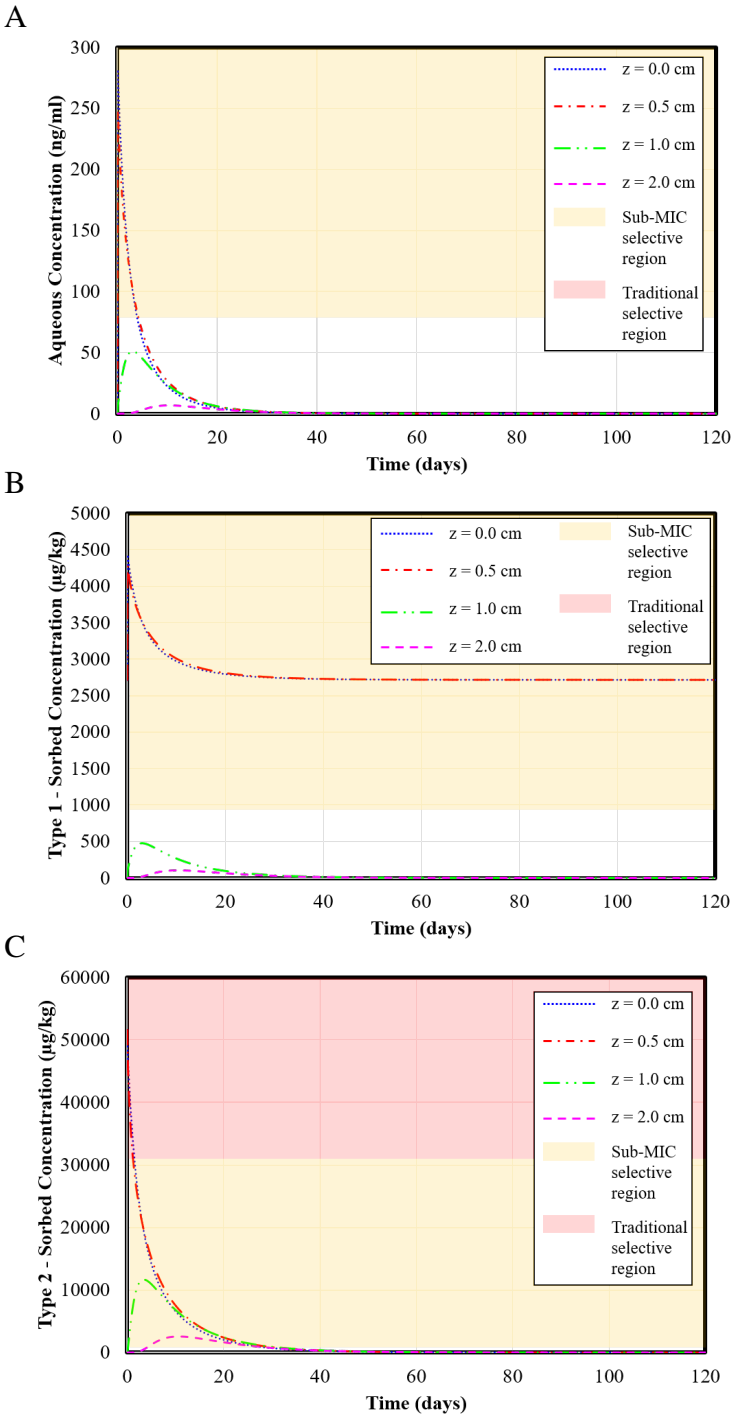

Figure 6.8: Predicted time dependent aqueous concentration (A), equilibrium sorption site (Type 1) concentration (B), and kinetic sorption site (Type 2) (C) concentration of OTC assuming surface application of manure without incorporation, maximum OTC, f = 0.05, α = 0.12 1/hr, and $\mu_{s_1} = \mu_{s_2} = 0.0035$

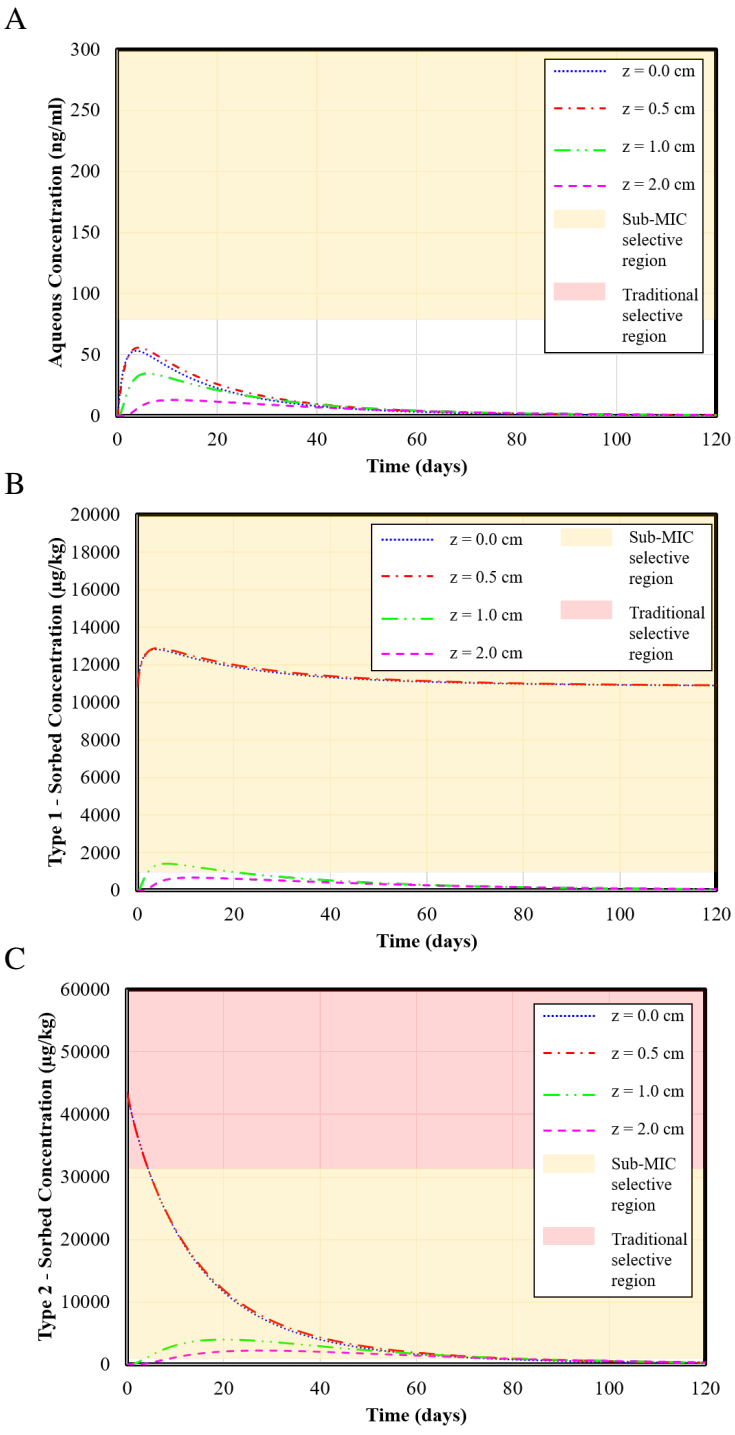

Figure 6.9: Predicted time dependent aqueous concentration (A), equilibrium sorption site (Type 1) concentration (B), and kinetic sorption site (Type 2) (C) concentration of OTC assuming surface application of manure without incorporation, maximum OTC, f = 0.2, α = 0.003 1/hr, and $\mu_{s_1} = \mu_{s_2}$ = 0.00088

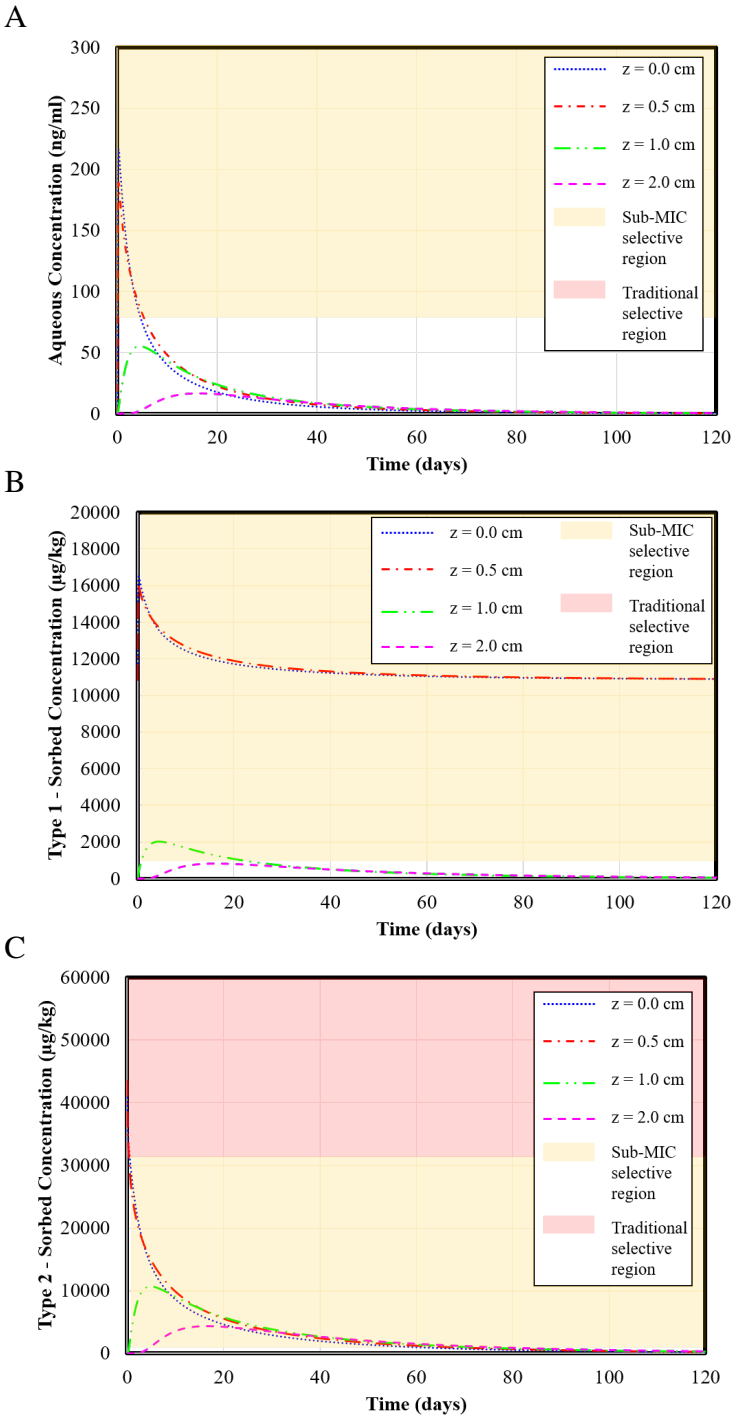

Figure 6.10: Predicted time dependent aqueous concentration (A), equilibrium sorption site (Type 1) concentration (B), and kinetic sorption site (Type 2) (C) concentration of OTC assuming surface application of manure without incorporation, maximum OTC, f = 0.2, α = 0.12 1/hr, and $\mu_{s_1} = \mu_{s_2}$ = 0.00088

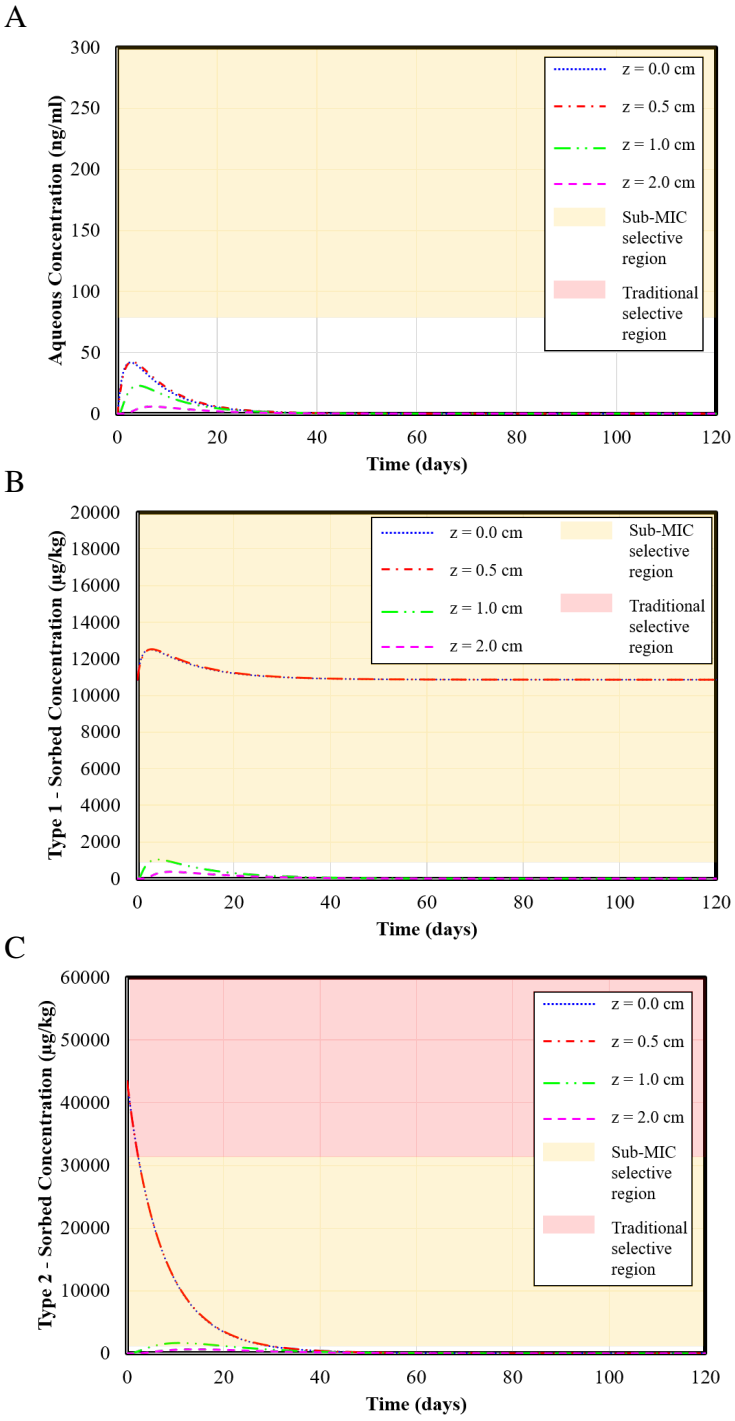

Figure 6.11: Predicted time dependent aqueous concentration (A), equilibrium sorption site (Type 1) concentration (B), and kinetic sorption site (Type 2) (C) concentration of OTC assuming surface application of manure without incorporation, maximum OTC, f = 0.2, α = 0.003 1/hr, and $\mu_{s_1} = \mu_{s_2}$ = 0.0035

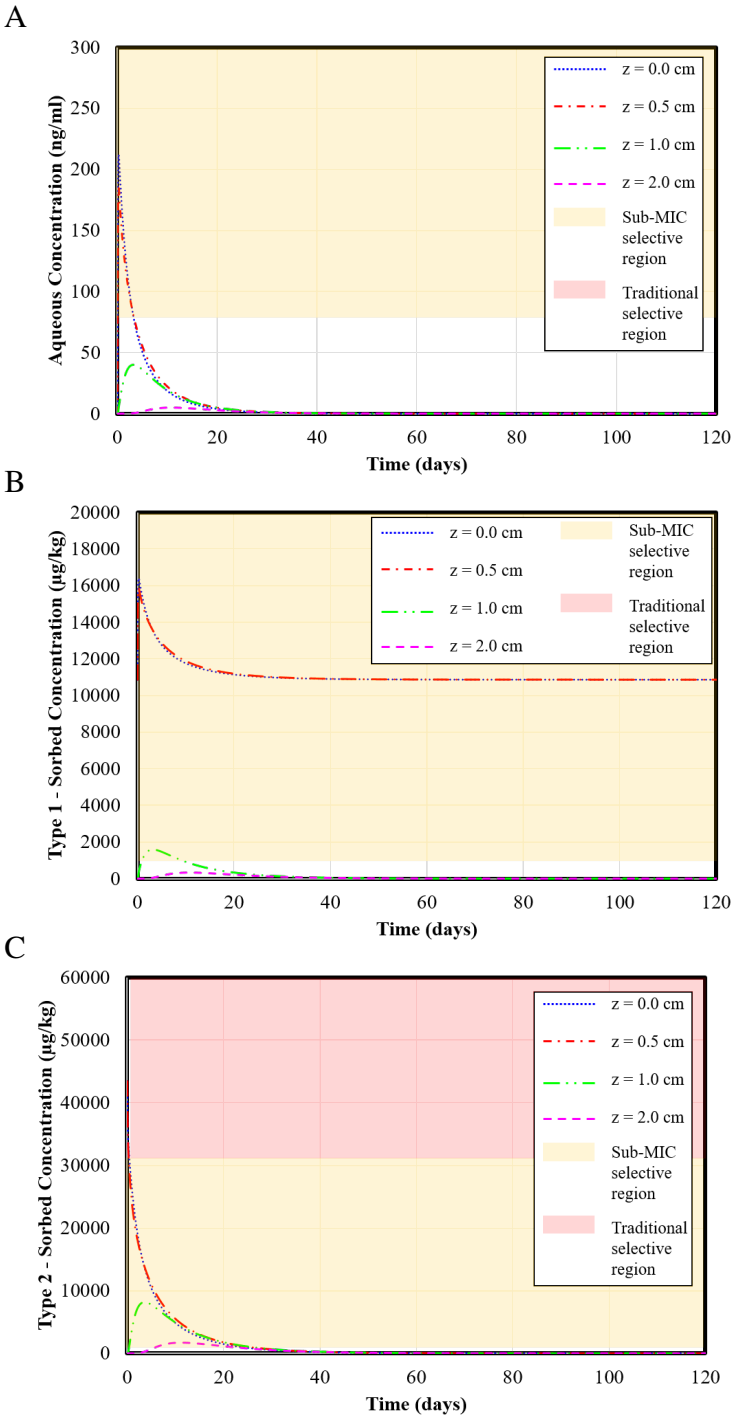

Figure 6.12: Predicted time dependent aqueous concentration (A), equilibrium sorption site (Type 1) concentration (B), and kinetic sorption site (Type 2) (C) concentration of OTC assuming surface application of manure without incorporation, maximum OTC, f = 0.2, α = 0.12 1/hr, and $\mu_{s_1} = \mu_{s_2}$ = 0.0035

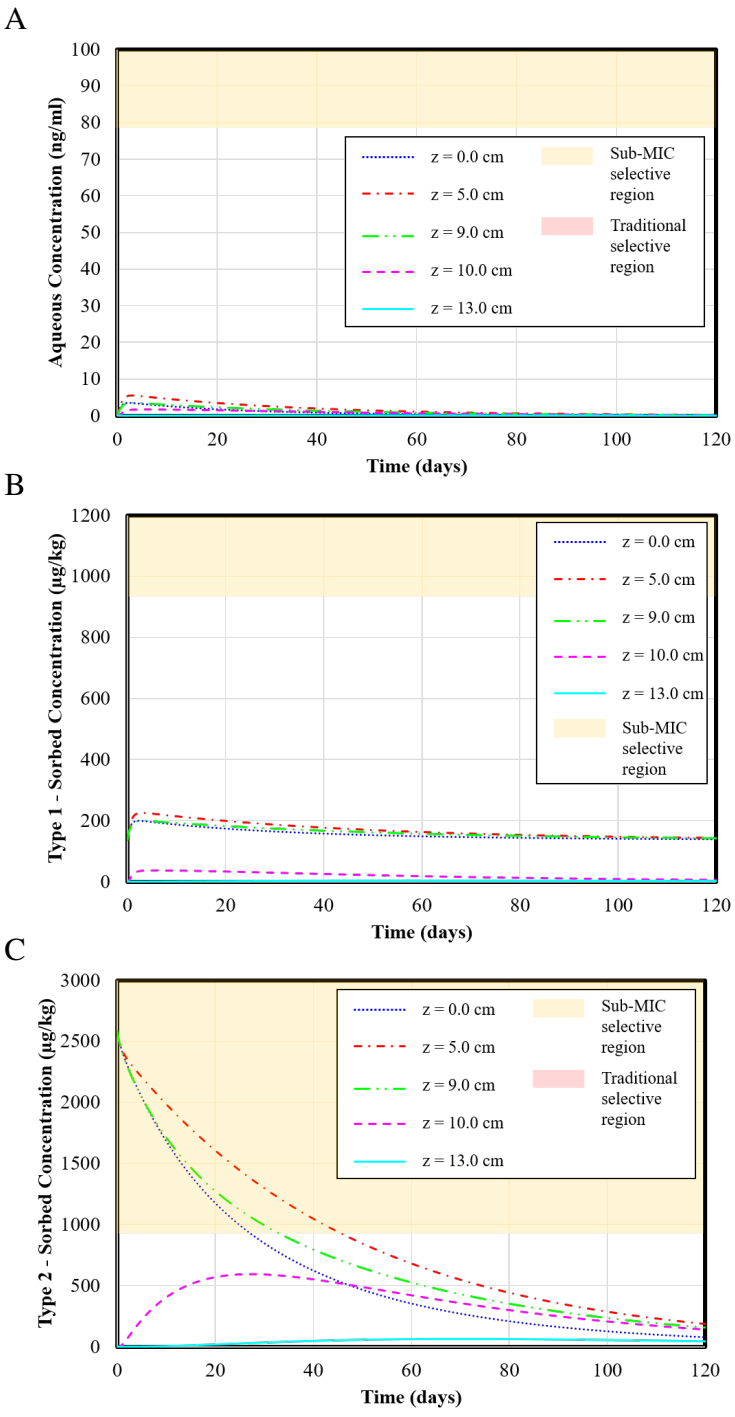

Figure 6.13: Predicted time dependent aqueous concentration (A), equilibrium sorption site (Type 1) concentration (B), and kinetic sorption site (Type 2) (C) concentration of OTC assuming surface application of manure with 10 cm incorporation, maximum OTC, f = 0.05, α = 0.003 1/hr, and $\mu_{s_1} = \mu_{s_2} = 0.00088$

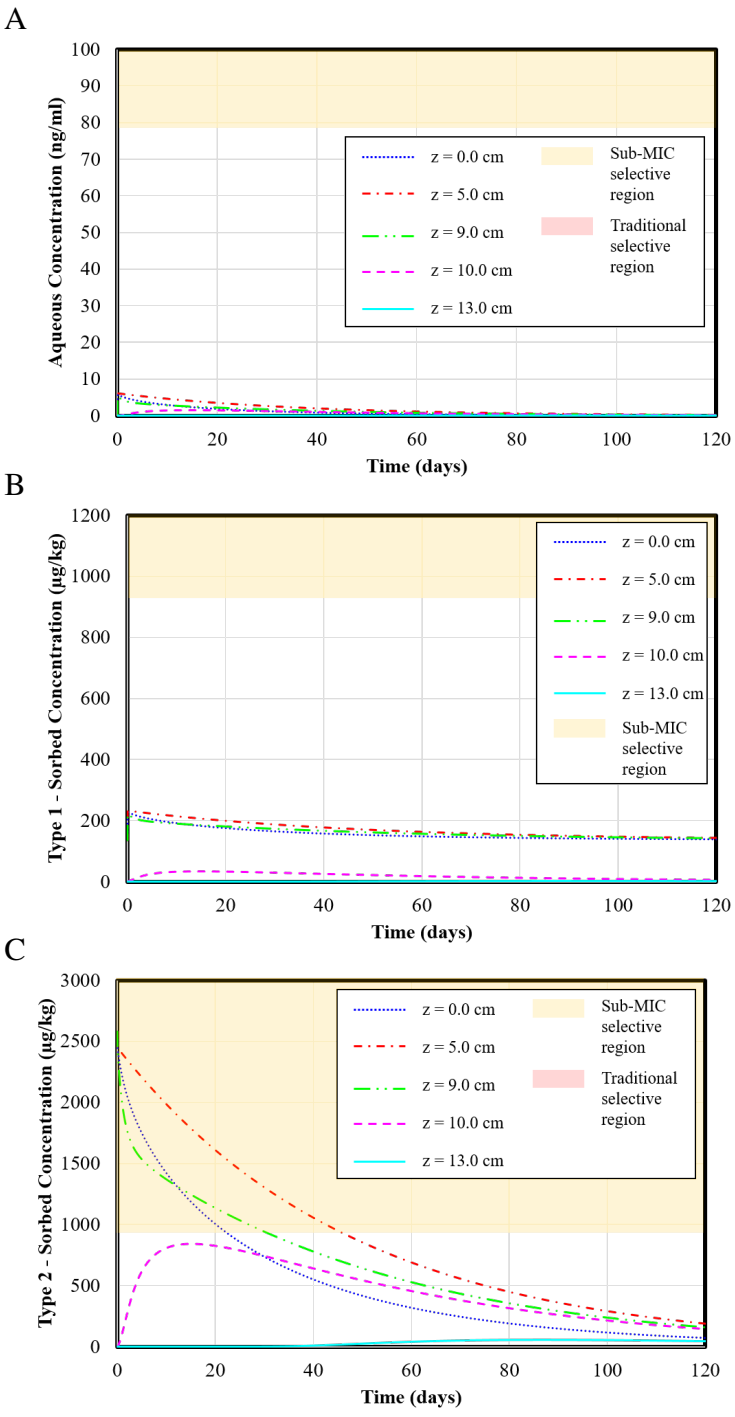

Figure 6.14: Predicted time dependent aqueous concentration (A), equilibrium sorption site (Type 1) concentration (B), and kinetic sorption site (Type 2) (C) concentration of OTC assuming surface application of manure with 10 cm incorporation, maximum OTC, f = 0.05, α = 0.12 1/hr, and $\mu_{s_1} = \mu_{s_2} = 0.00088$

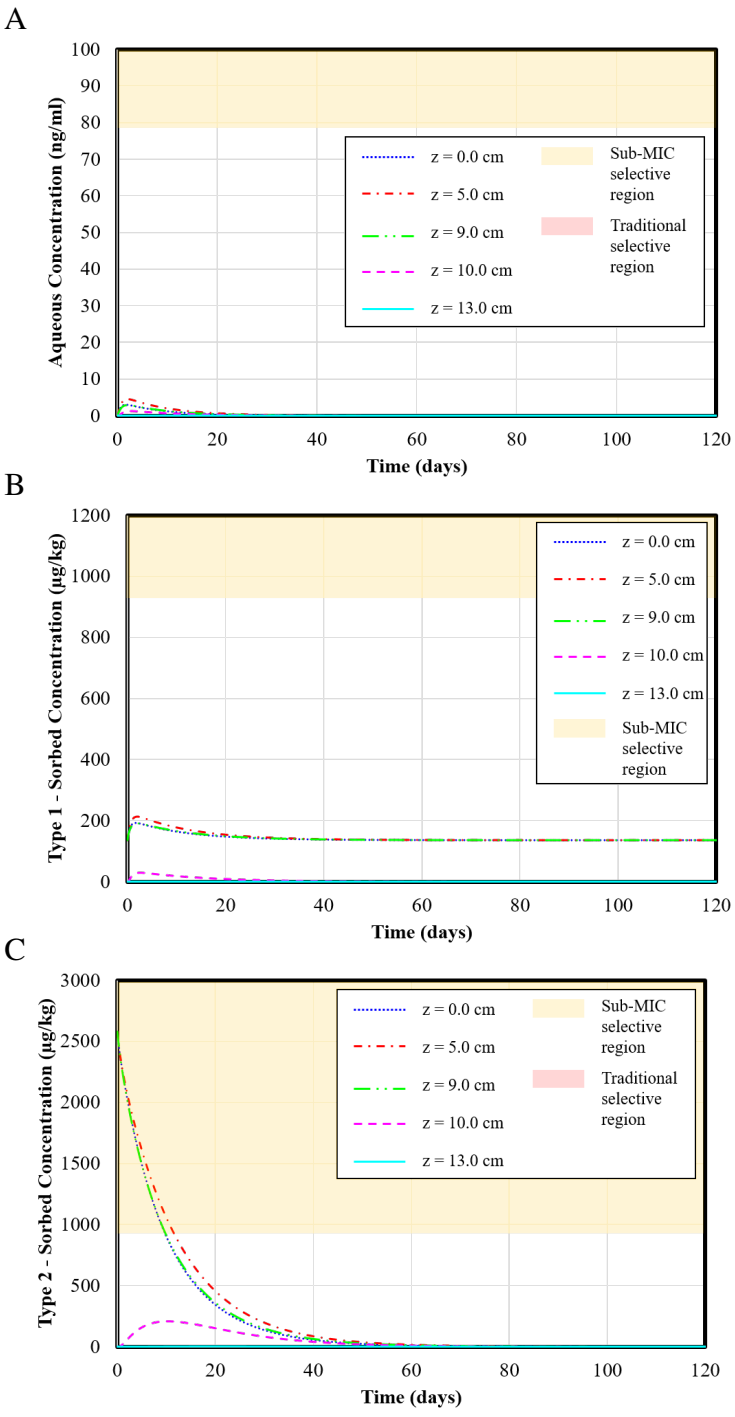

Figure 6.15: Predicted time dependent aqueous concentration (A), equilibrium sorption site (Type 1) concentration (B), and kinetic sorption site (Type 2) (C) concentration of OTC assuming surface application of manure with 10 cm incorporation, maximum OTC, f = 0.05, α = 0.003 1/hr, and $\mu_{s_1} = \mu_{s_2} = 0.0035$

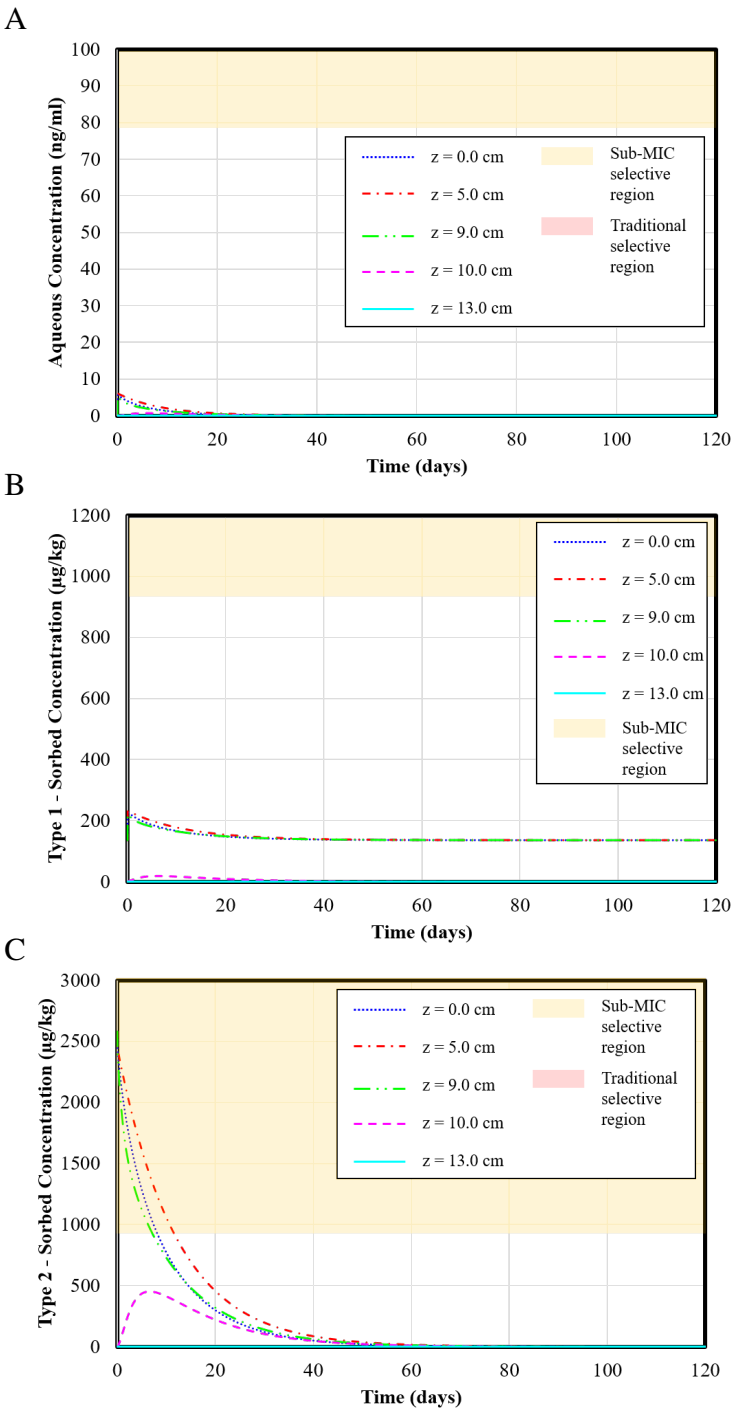

Figure 6.16: Predicted time dependent aqueous concentration (A), equilibrium sorption site (Type 1) concentration (B), and kinetic sorption site (Type 2) (C) concentration of OTC assuming surface application of manure with 10 cm incorporation, maximum OTC, f = 0.05, α = 0.12 1/hr, and $\mu_{s_1} = \mu_{s_2} = 0.0035$

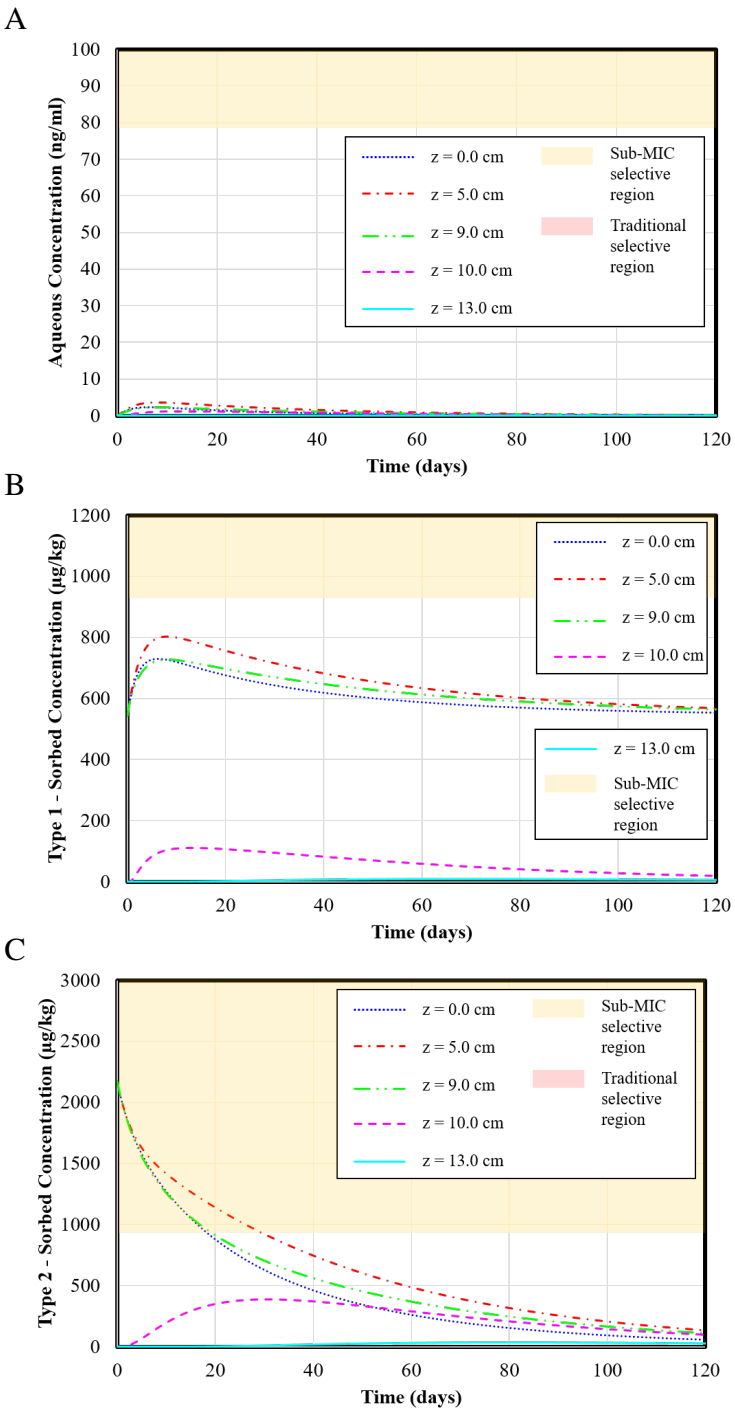

Figure 6.17: Predicted time dependent aqueous concentration (A), equilibrium sorption site (Type 1) concentration (B), and kinetic sorption site (Type 2) (C) concentration of OTC assuming surface application of manure with 10 cm incorporation, maximum OTC, f = 0.2, α = 0.003 1/hr, and $\mu_{s_1} = \mu_{s_2} = 0.00088$

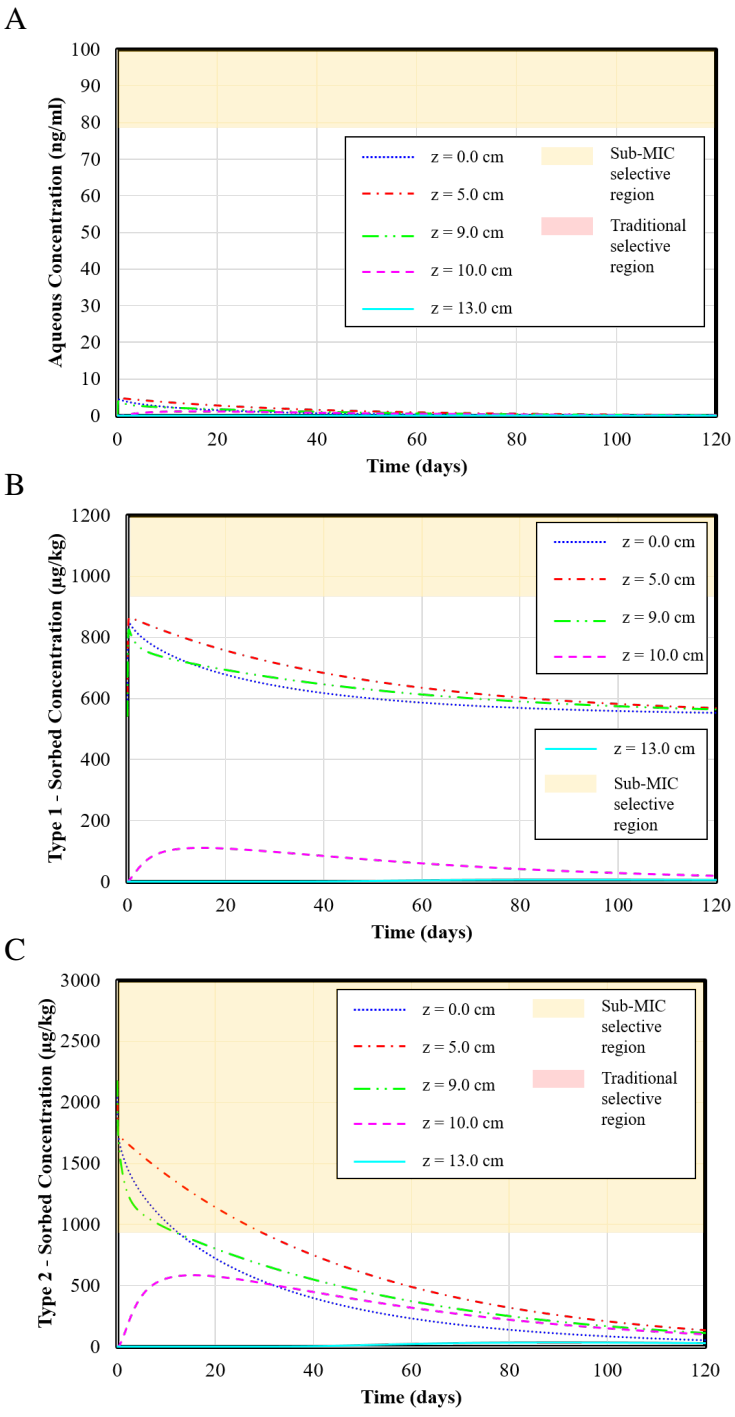

Figure 6.18: Predicted time dependent aqueous concentration (A), equilibrium sorption site (Type 1) concentration (B), and kinetic sorption site (Type 2) (C) concentration of OTC assuming surface application of manure with 10 cm incorporation, maximum OTC, f = 0.2, α = 0.12 1/hr, and $\mu_{s_1} = \mu_{s_2} = 0.00088$

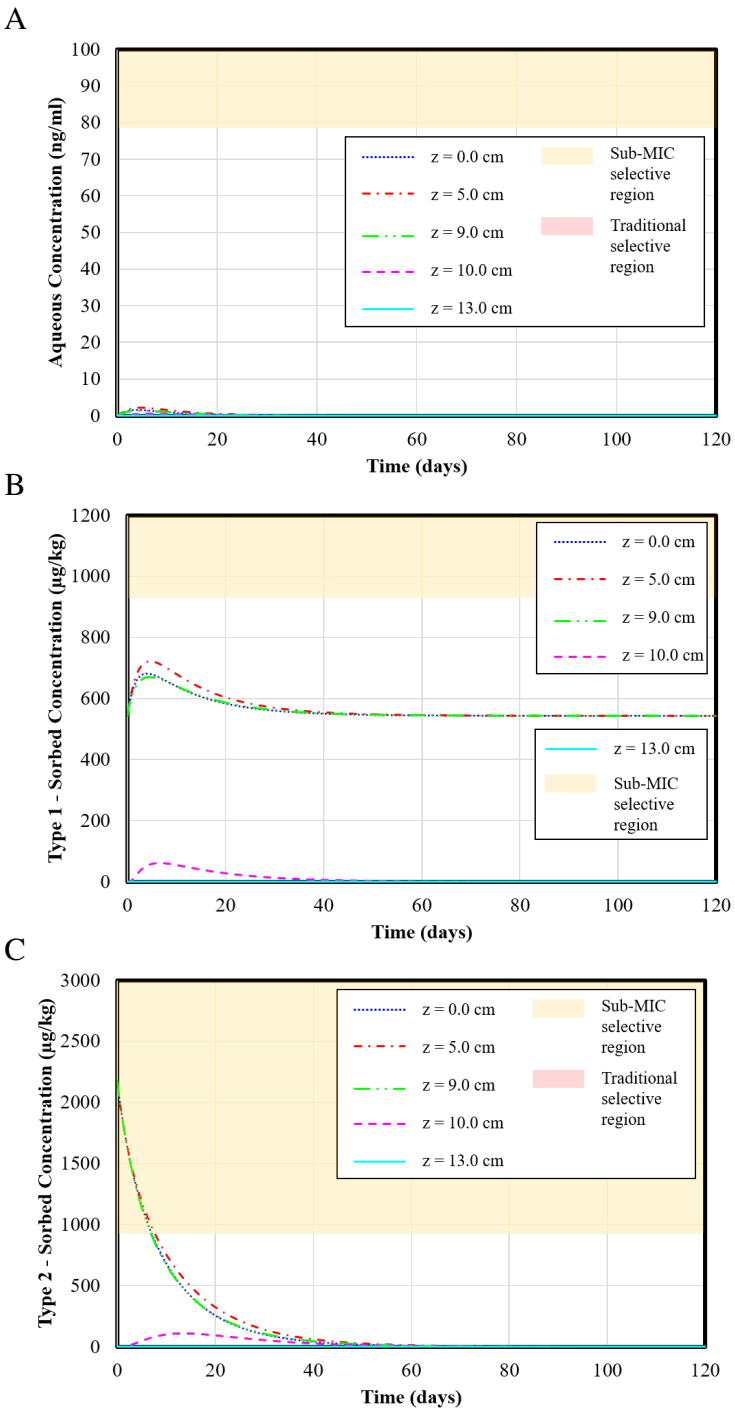

Figure 6.19: Predicted time dependent aqueous concentration (A), equilibrium sorption site (Type 1) concentration (B), and kinetic sorption site (Type 2) (C) concentration of OTC assuming surface application of manure with 10 cm incorporation, maximum OTC, f = 0.2, α = 0.003 1/hr, and $\mu_{s_1} = \mu_{s_2} = 0.0035$

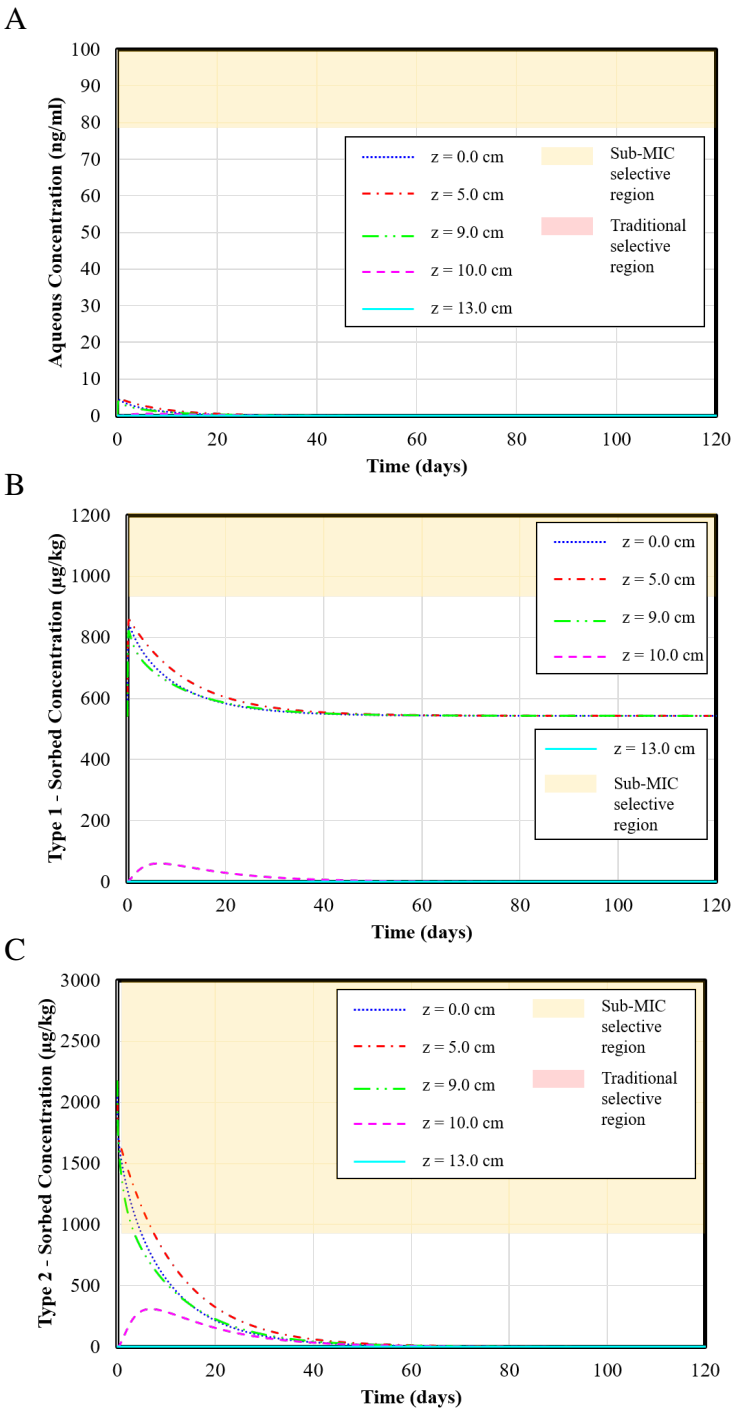

Figure 6.20: Predicted time dependent aqueous concentration (A), equilibrium sorption site (Type 1) concentration (B), and kinetic sorption site (Type 2) (C) concentration of OTC assuming surface application of manure with 10 cm incorporation, maximum OTC, f = 0.2, α = 0.12 1/hr, and $\mu_{s_1} = \mu_{s_2} = 0.0035$

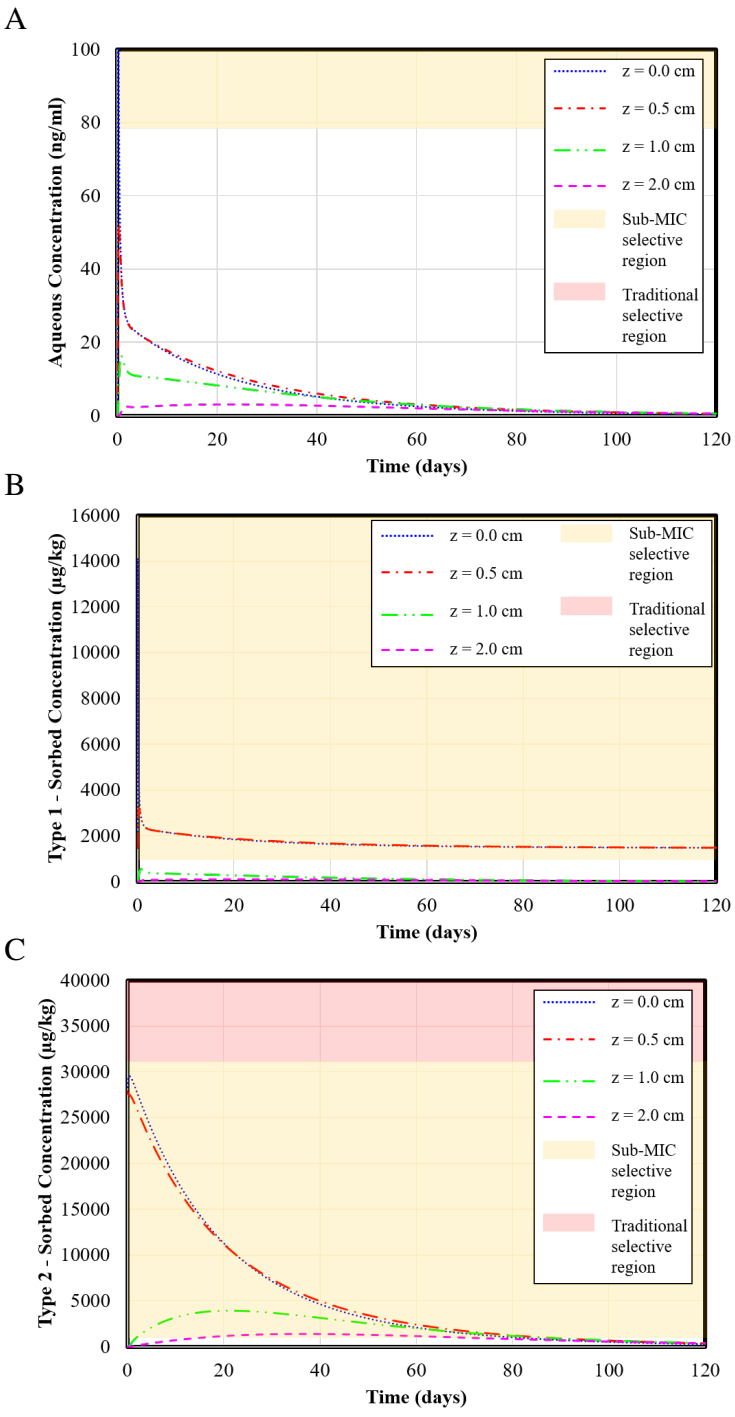

Figure 6.21: Predicted time dependent aqueous concentration (A), equilibrium sorption site (Type 1) concentration (B), and kinetic sorption site (Type 2) (C) concentration of OTC assuming liquid application of manure without incorporation, maximum OTC, f = 0.05, α = 0.003 1/hr, and $\mu_{s_1} = \mu_{s_2}$ = 0.00088

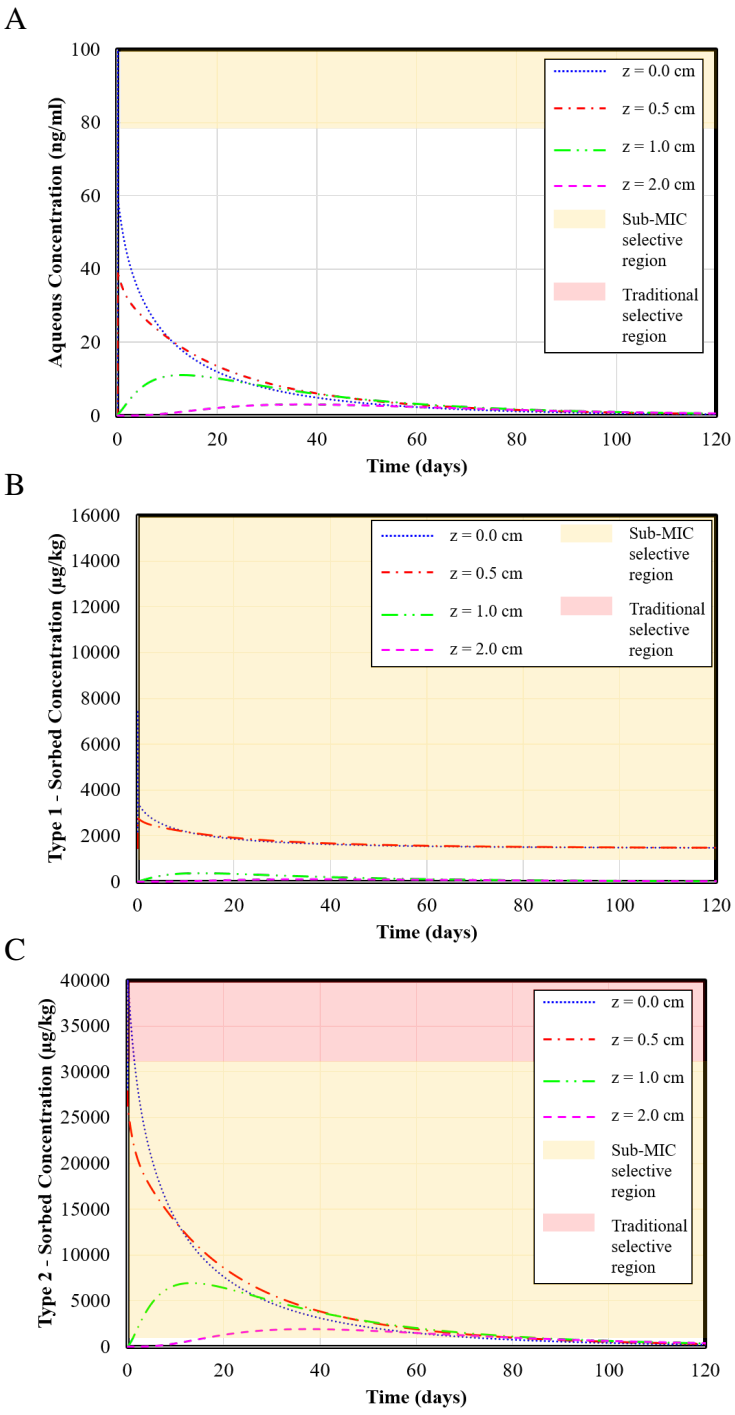

Figure 6.22: Predicted time dependent aqueous concentration (A), equilibrium sorption site (Type 1) concentration (B), and kinetic sorption site (Type 2) (C) concentration of OTC assuming liquid application of manure without incorporation, maximum OTC, f = 0.05, α = 0.12 1/hr, and $\mu_{s_1} = \mu_{s_2}$ = 0.00088

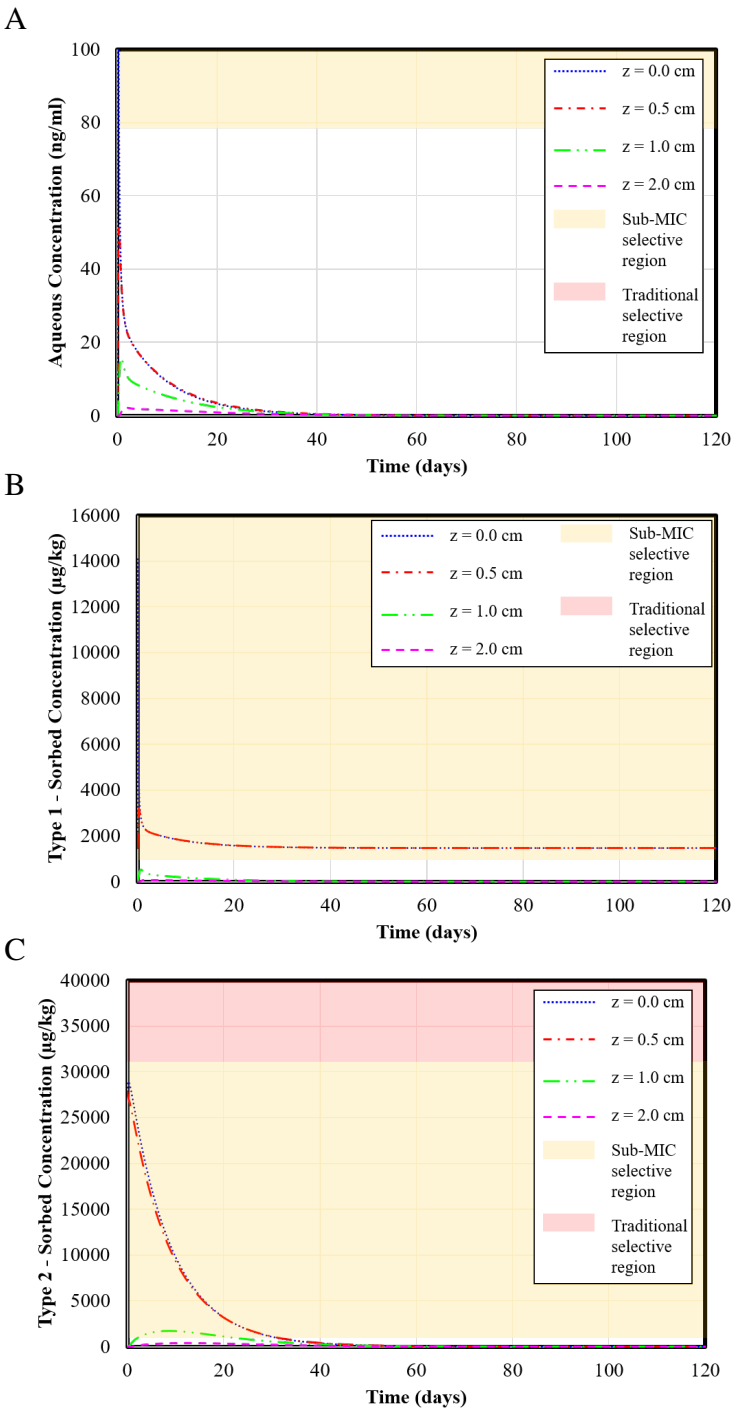

Figure 6.23: Predicted time dependent aqueous concentration (A), equilibrium sorption site (Type 1) concentration (B), and kinetic sorption site (Type 2) (C) concentration of OTC assuming liquid application of manure without incorporation, maximum OTC, f = 0.05, α = 0.003 1/hr, and $\mu_{s_1} = \mu_{s_2} = 0.0035$

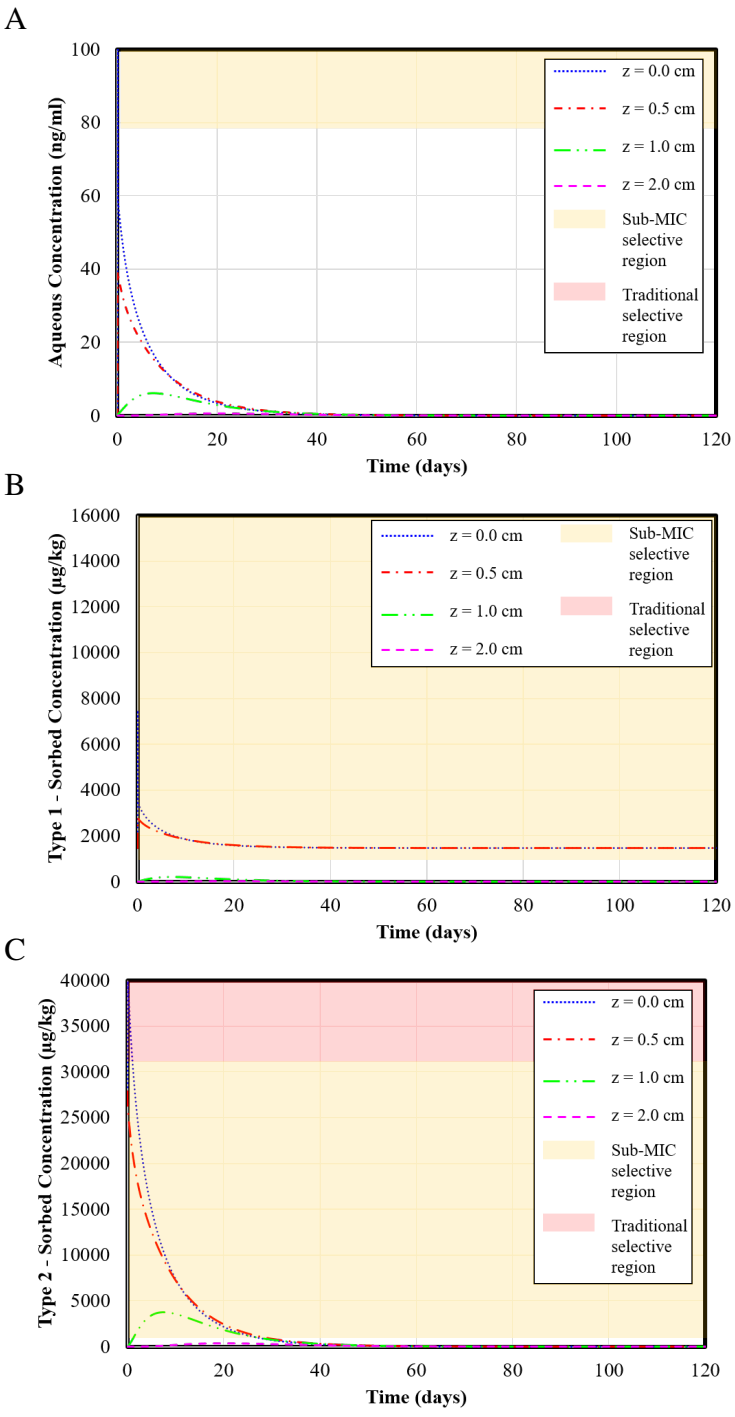

Figure 6.24: Predicted time dependent aqueous concentration (A), equilibrium sorption site (Type 1) concentration (B), and kinetic sorption site (Type 2) (C) concentration of OTC assuming liquid application of manure without incorporation, maximum OTC, f = 0.05, α = 0.12 1/hr, and $\mu_{s_1} = \mu_{s_2} = 0.0035$

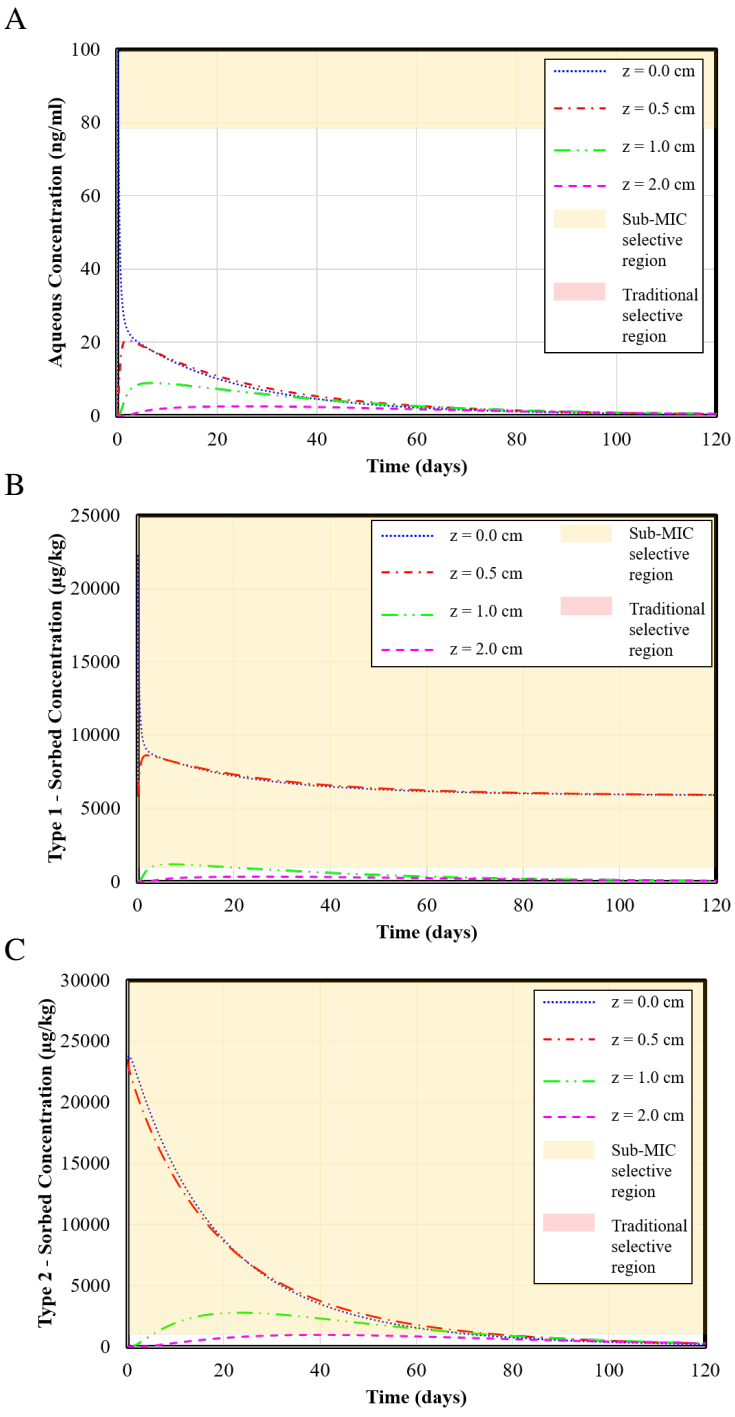

Figure 6.25: Predicted time dependent aqueous concentration (A), equilibrium sorption site (Type 1) concentration (B), and kinetic sorption site (Type 2) (C) concentration of OTC assuming liquid application of manure without incorporation, maximum OTC, f = 0.20, α = 0.003 1/hr, and $\mu_{s_1} = \mu_{s_2}$ = 0.00088

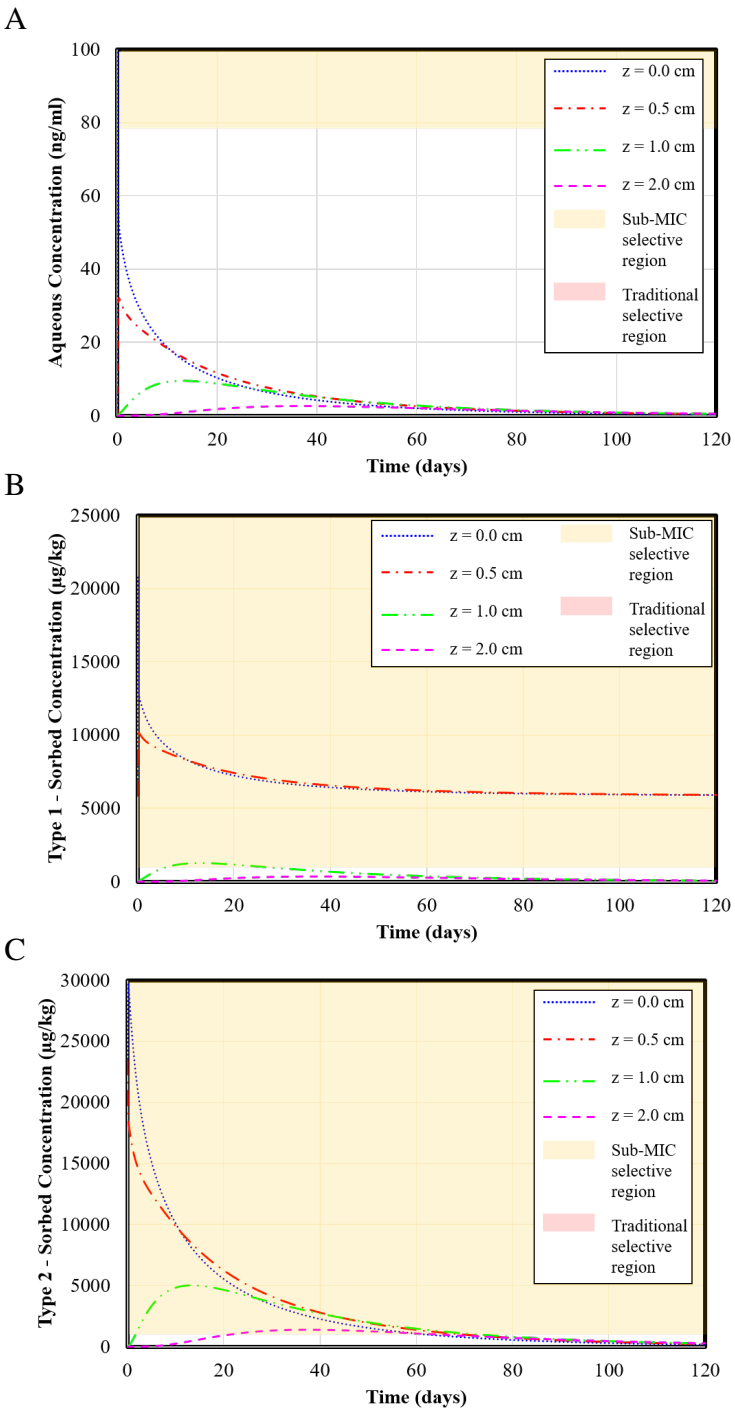

Figure 6.26: Predicted time dependent aqueous concentration (A), equilibrium sorption site (Type 1) concentration (B), and kinetic sorption site (Type 2) (C) concentration of OTC assuming liquid application of manure without incorporation, maximum OTC, f = 0.20, α = 0.12 1/hr, and $\mu_{s_1} = \mu_{s_2}$ = 0.00088

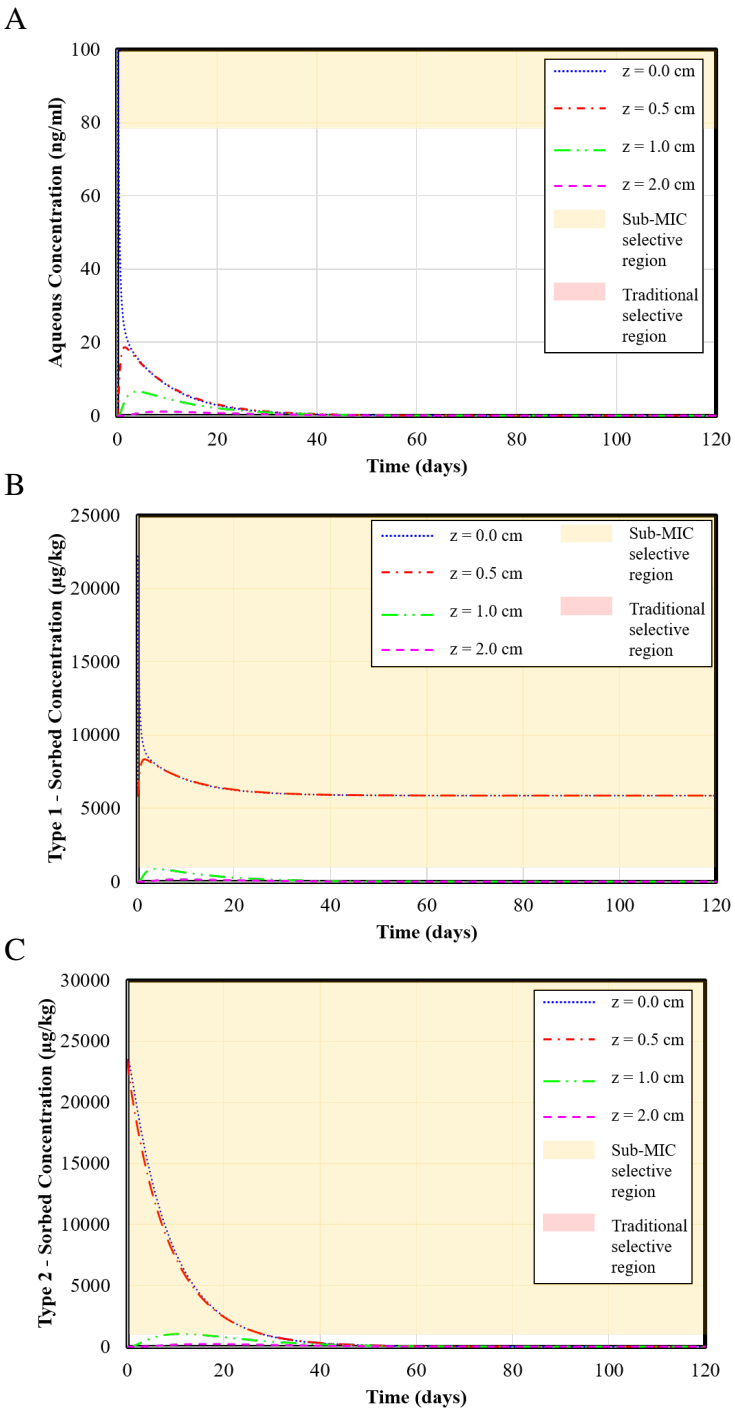

Figure 6.27: Predicted time dependent aqueous concentration (A), equilibrium sorption site (Type 1) concentration (B), and kinetic sorption site (Type 2) (C) concentration of OTC assuming liquid application of manure without incorporation, maximum OTC, f = 0.20, α = 0.003 1/hr, and $\mu_{s_1} = \mu_{s_2} = 0.0035$

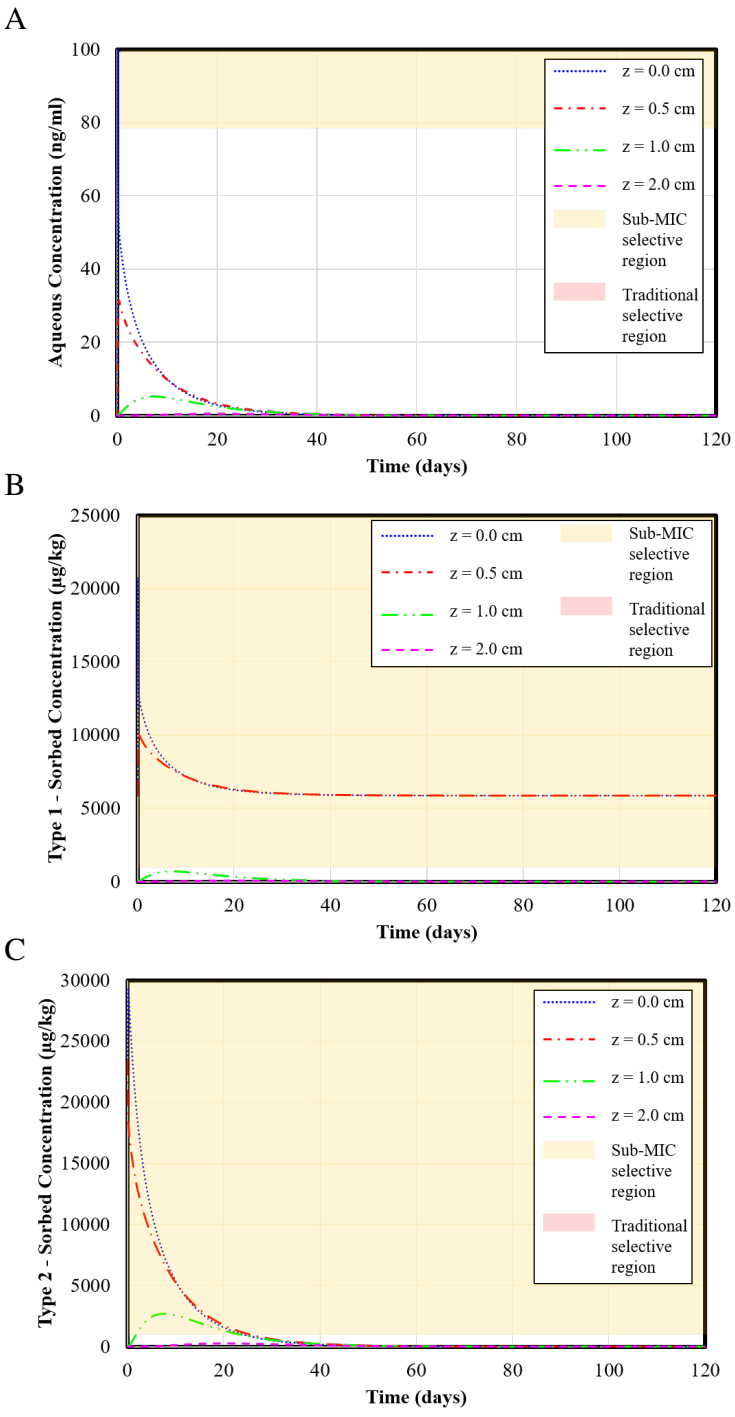

Figure 6.28: Predicted time dependent aqueous concentration (A), equilibrium sorption site (Type 1) concentration (B), and kinetic sorption site (Type 2) (C) concentration of OTC assuming liquid application of manure without incorporation, maximum OTC, f = 0.20, α = 0.12 1/hr, and $\mu_{s_1} = \mu_{s_2} = 0.0035$

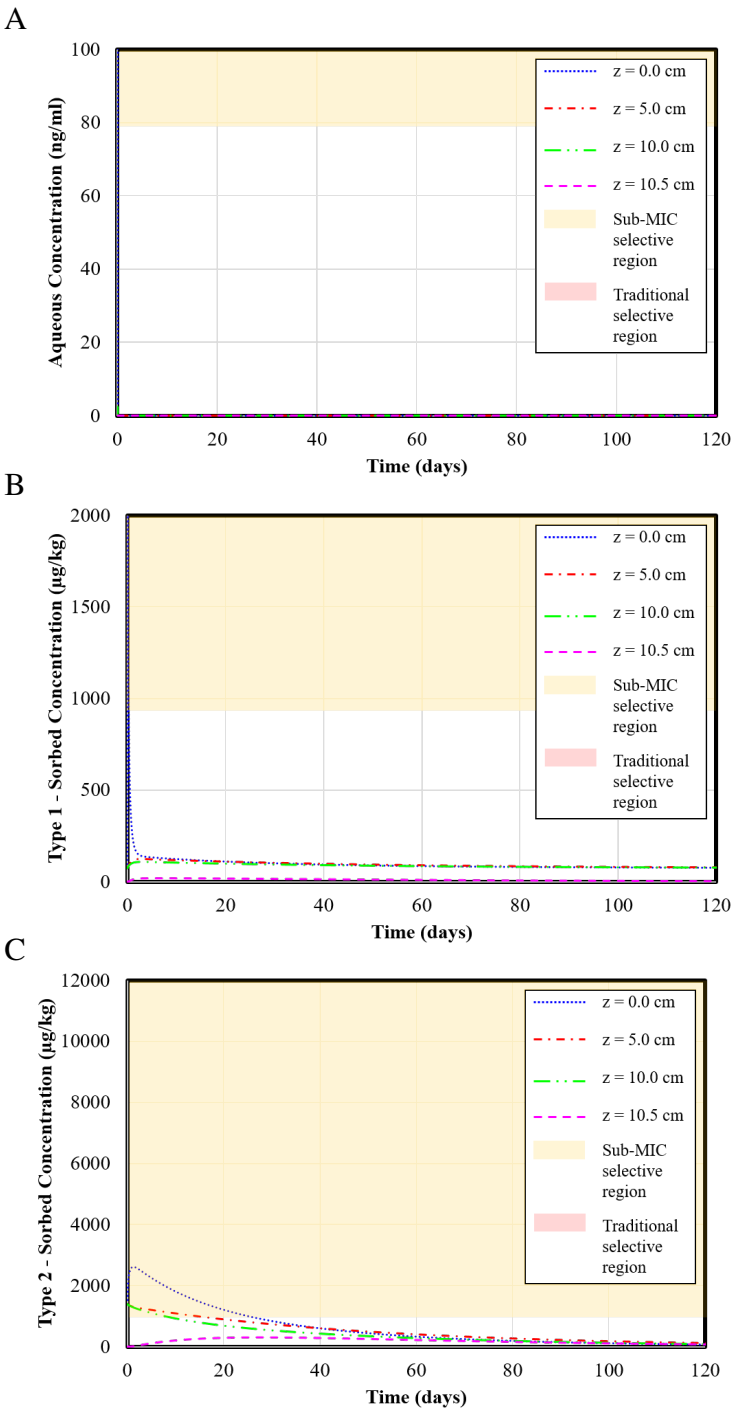

Figure 6.29: Predicted time dependent aqueous concentration (A), equilibrium sorption site (Type 1) concentration (B), and kinetic sorption site (Type 2) (C) concentration of OTC assuming liquid application of manure with 10 cm incorporation, maximum OTC, f = 0.05, α = 0.003 1/hr, and $\mu_{s_1} = \mu_{s_2}$ = 0.00088

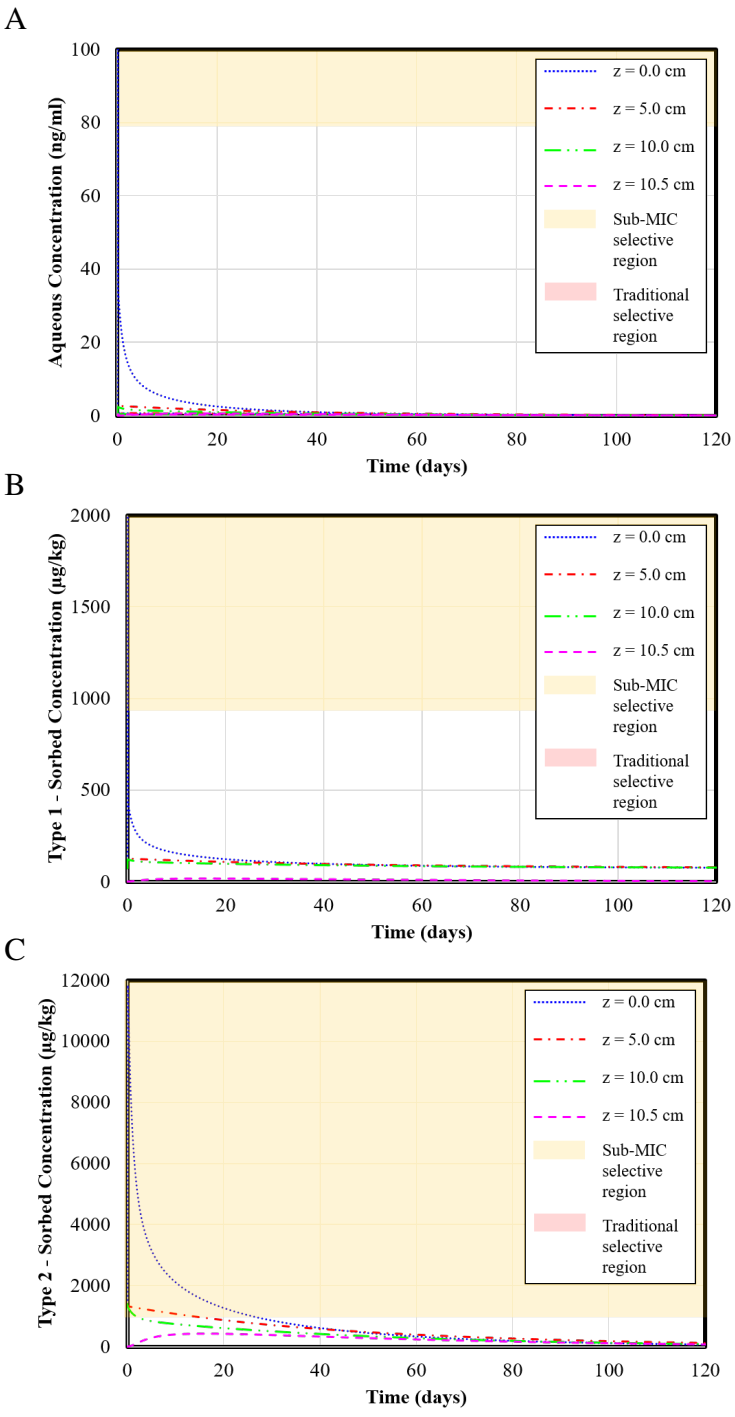

Figure 6.30: Predicted time dependent aqueous concentration (A), equilibrium sorption site (Type 1) concentration (B), and kinetic sorption site (Type 2) (C) concentration of OTC assuming liquid application of manure with 10 cm incorporation, maximum OTC, f = 0.05, α = 0.12 1/hr, and $\mu_{s_1} = \mu_{s_2} = 0.00088$

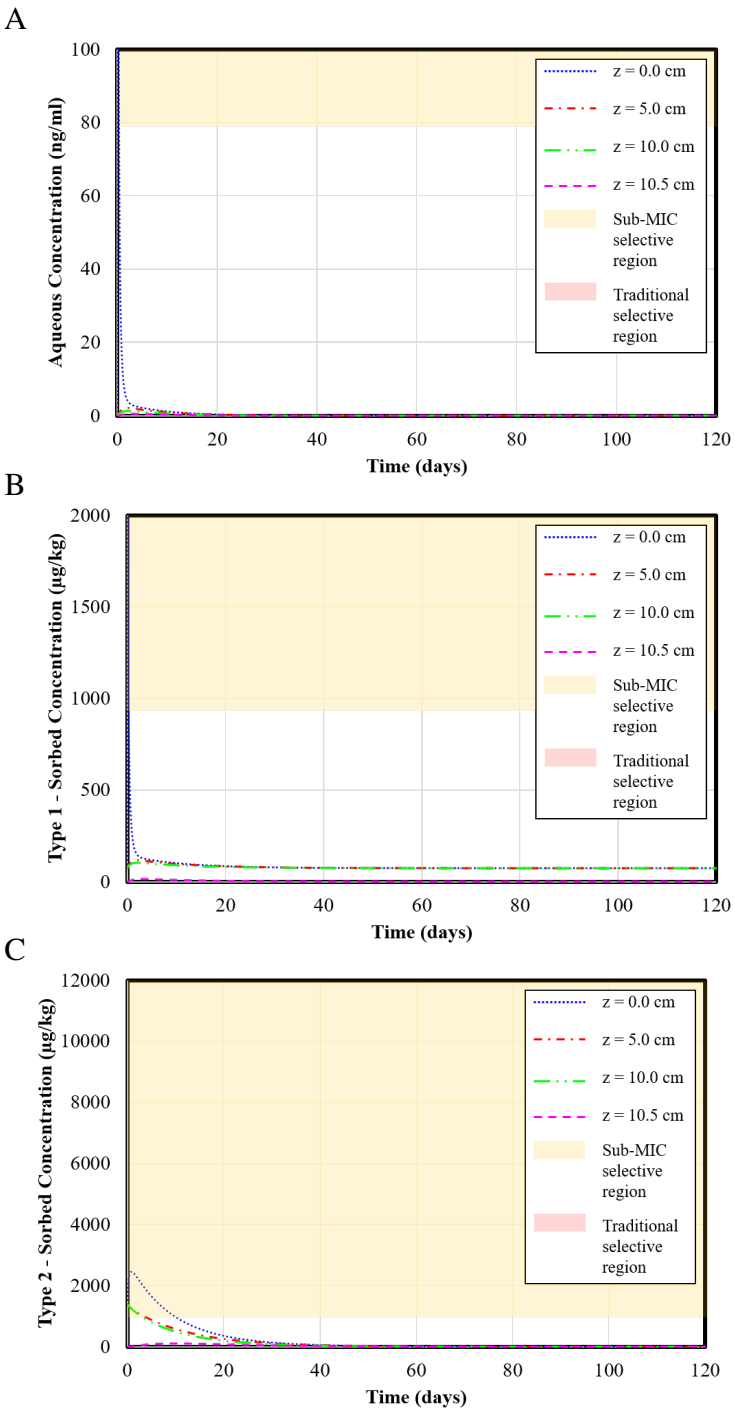

Figure 6.31: Predicted time dependent aqueous concentration (A), equilibrium sorption site (Type 1) concentration (B), and kinetic sorption site (Type 2) (C) concentration of OTC assuming liquid application of manure with 10 cm incorporation, maximum OTC, f = 0.05, α = 0.003 1/hr, and $\mu_{s_1} = \mu_{s_2} = 0.0035$

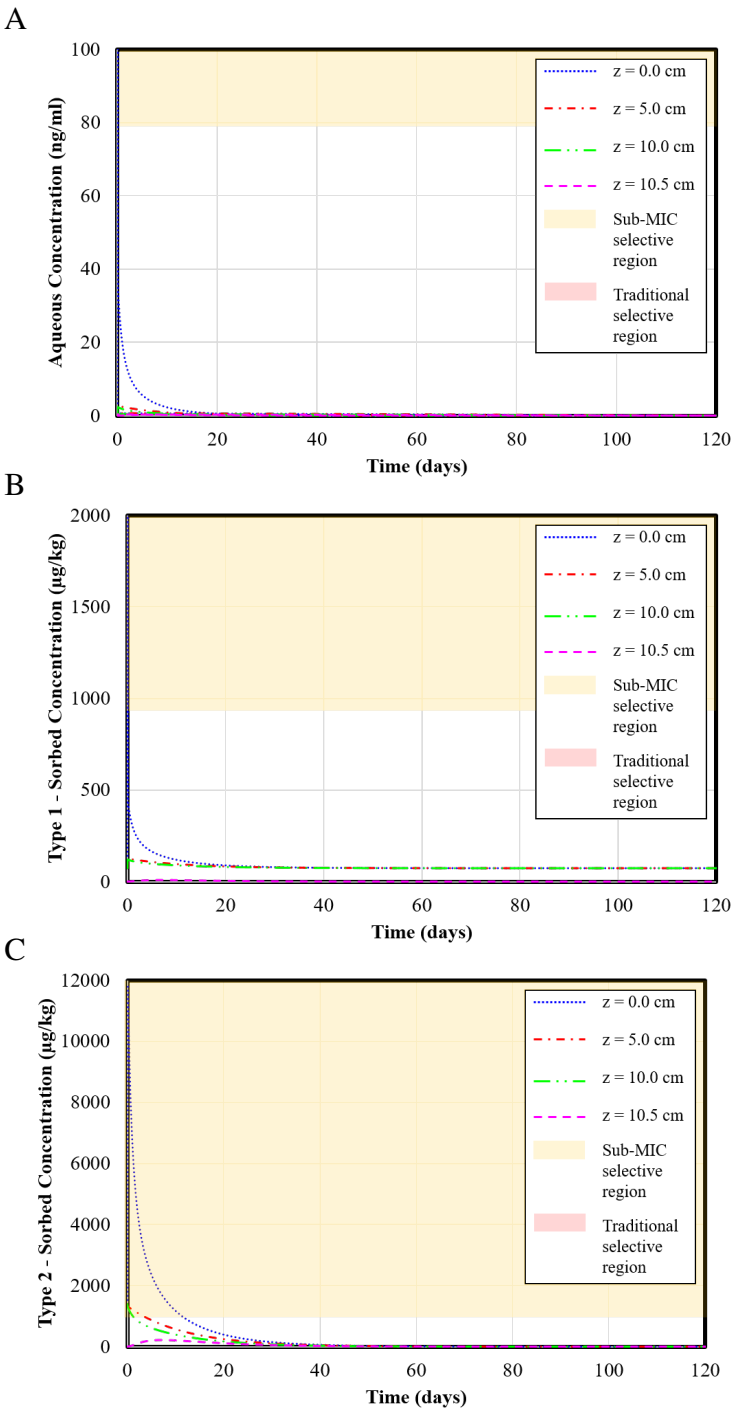

Figure 6.32: Predicted time dependent aqueous concentration (A), equilibrium sorption site (Type 1) concentration (B), and kinetic sorption site (Type 2) (C) concentration of OTC assuming liquid application of manure with 10 cm incorporation, maximum OTC, f = 0.05, α = 0.12 1/hr, and $\mu_{s_1} = \mu_{s_2} = 0.0035$

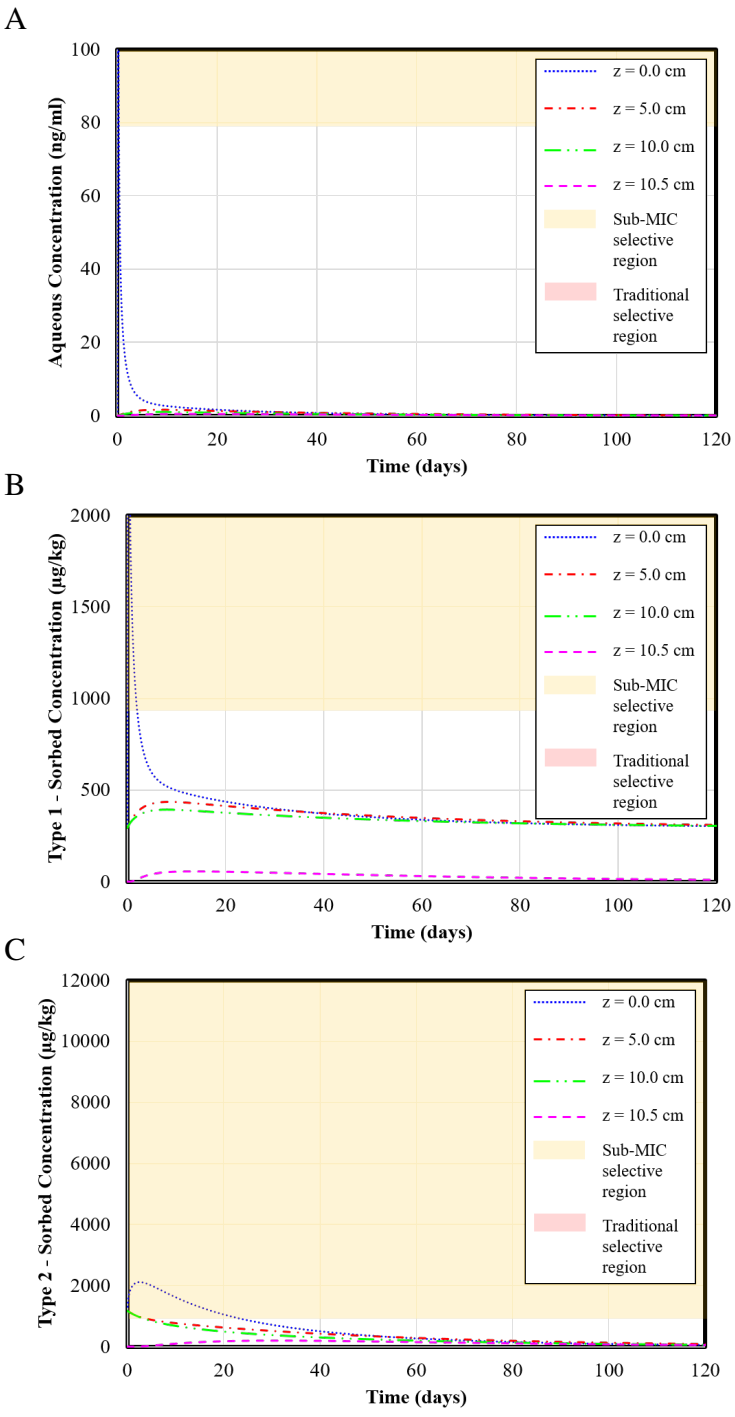

Figure 6.33: Predicted time dependent aqueous concentration (A), equilibrium sorption site (Type 1) concentration (B), and kinetic sorption site (Type 2) (C) concentration of OTC assuming liquid application of manure with 10 cm incorporation, maximum OTC, f = 0.20, α = 0.003 1/hr, and $\mu_{s_1} = \mu_{s_2}$ = 0.00088

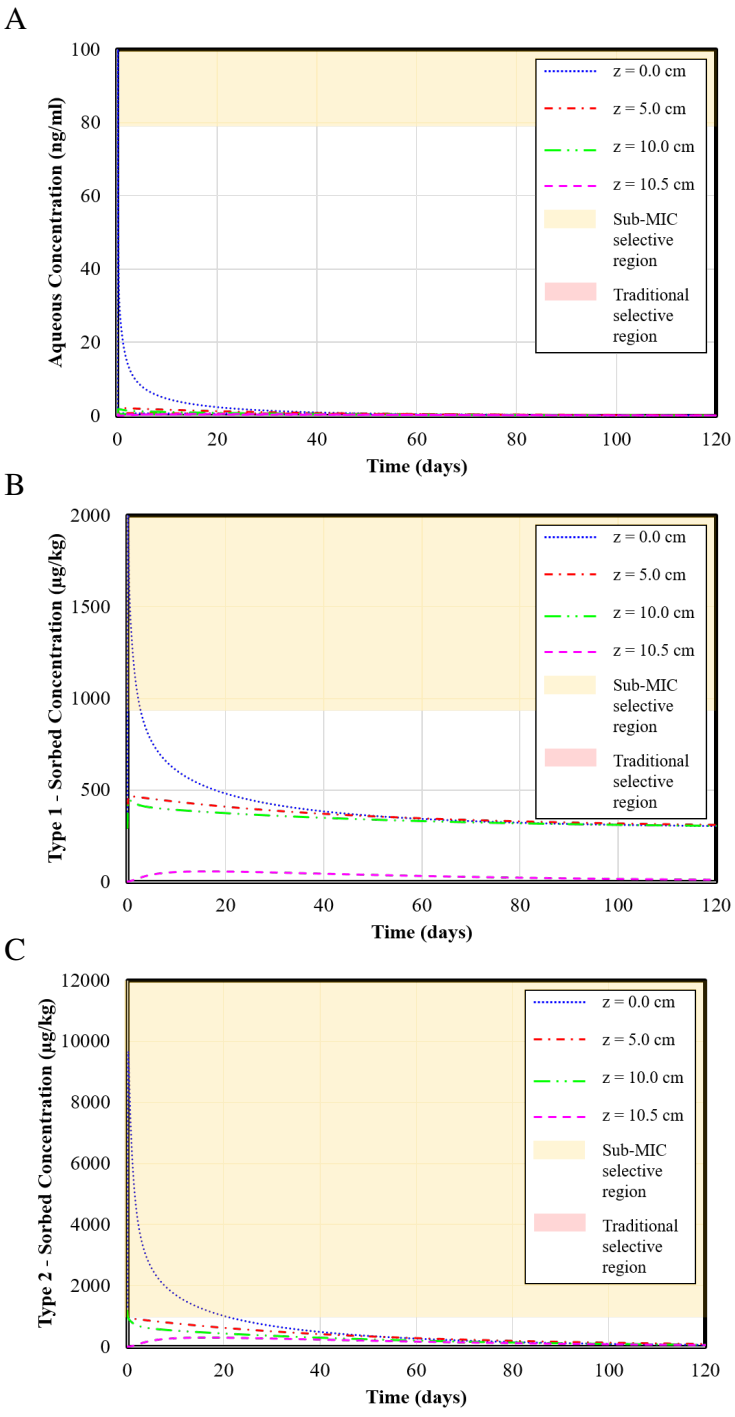

Figure 6.34: Predicted time dependent aqueous concentration (A), equilibrium sorption site (Type 1) concentration (B), and kinetic sorption site (Type 2) (C) concentration of OTC assuming liquid application of manure with 10 cm incorporation, maximum OTC, f = 0.20, α = 0.12 1/hr, and $\mu_{s_1} = \mu_{s_2} = 0.00088$

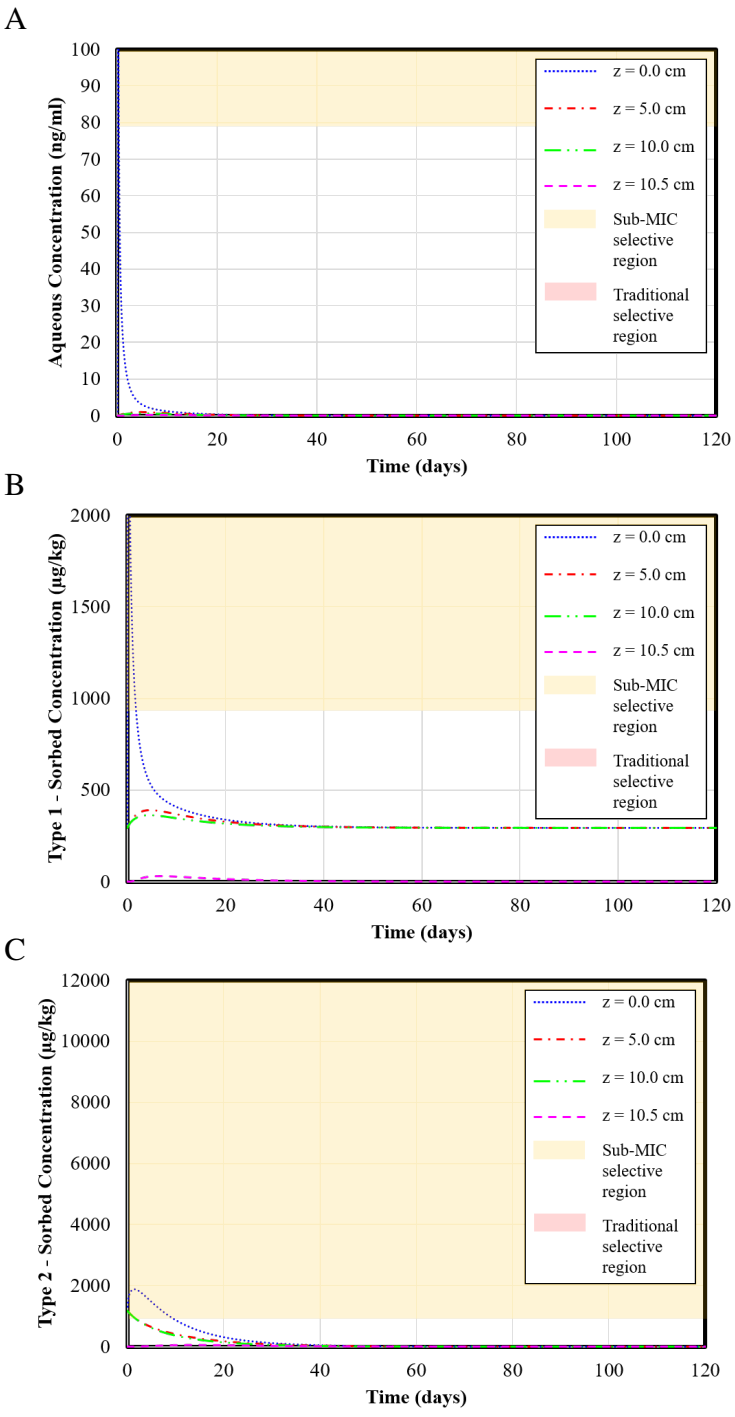

Figure 6.35: Predicted time dependent aqueous concentration (A), equilibrium sorption site (Type 1) concentration (B), and kinetic sorption site (Type 2) (C) concentration of OTC assuming liquid application of manure with 10 cm incorporation, maximum OTC, f = 0.20, α = 0.003 1/hr, and $\mu_{s_1} = \mu_{s_2}$ = 0.0035

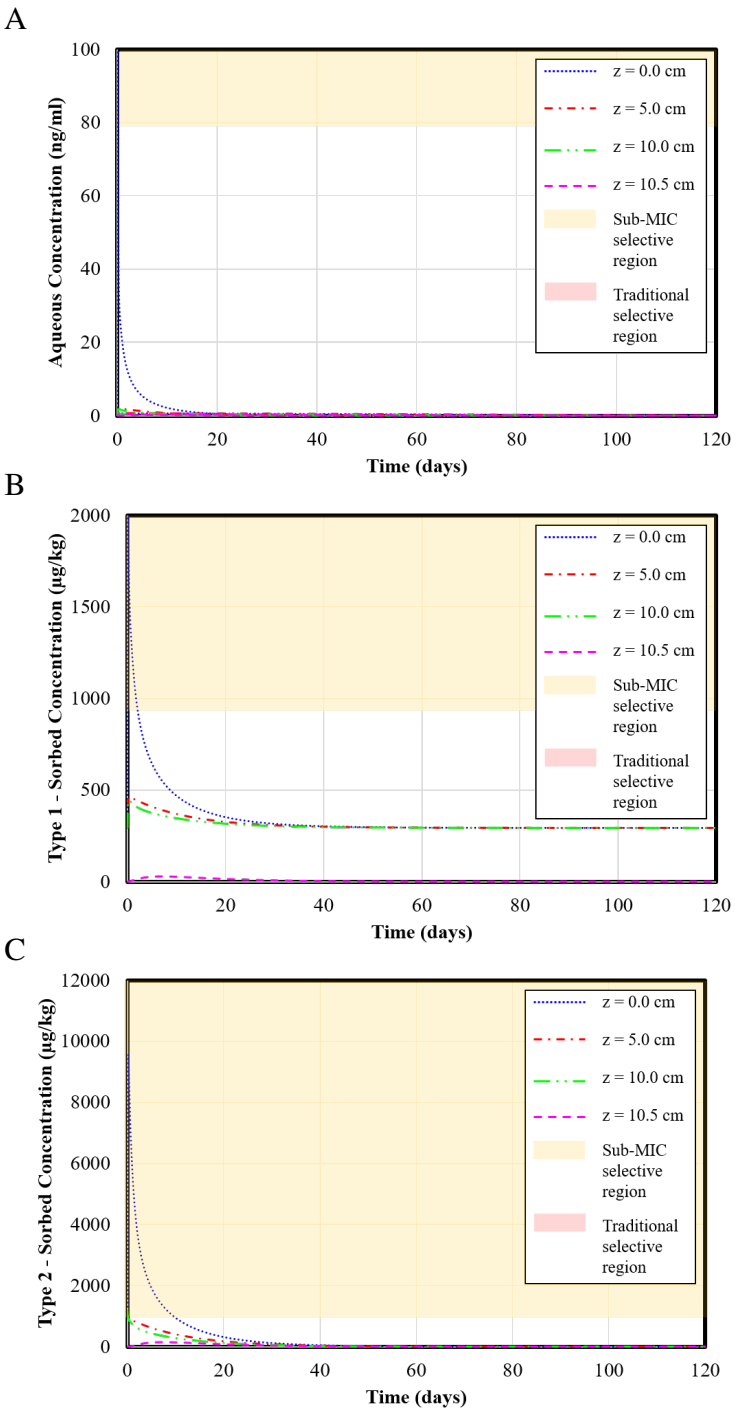

Figure 6.36: Predicted time dependent aqueous concentration (A), equilibrium sorption site (Type 1) concentration (B), and kinetic sorption site (Type 2) (C) concentration of OTC assuming liquid application of manure with 10 cm incorporation, maximum OTC, f = 0.20, α = 0.12 1/hr, and $\mu_{s_1} = \mu_{s_2} = 0.0035$

6.5 Environmental significance

The selection and spread of antibiotic resistance is a worldwide human health concern. The use of antibiotics in large scale livestock production operations, followed by land application of manure, is a common agricultural practice around the world which can be a direct route of entry of antibiotics, ARBs and ARGs to the ecosystem (Williams-Nguyen et al., 2016). Several of studies have addressed the fate and occurrence of antibiotics in the different environmental compartments (soil, surface water, groundwater, sediment); however studies that evaluate the potential to harbor resistance is limited. The human health risk posed by ARBs originating from land application of antibiotic-associated manure has not been proven, but is presumed to be an indirect exposure pathway.

This study demonstrated the effects of dilution due to the incorporation of manure in soil and a reduced OTC concentration in the land applied manure as important elements to minimize the potential selection for antibiotic resistance. Incorporation of manure reduces odor problems and conserves nitrogen by minimizing ammonia volatilization. However, incorporation of manure in soil is not always possible. Thus, implementing manure management practices (e.g. stockpiling, composting, etc.) to reduce OTC concentrations in manure, seems as a better option to minimize the potential selection of antibiotic resistance.

Biotic and abiotic (temperature, aeration, light) processes have been reported to reduce OTC concentrations in manure. Several authors have highlighted temperature as the most important factor to diminish OTC concentrations in manure (Ratasuk et al., 2012; Wang and Yates, 2008). Others have studied different treatment techniques for the removal of OTC in manure, including anaerobic digestion, stockpiling, composting and sun drying (Arikan et al., 2006; Storteboom et al., 2007; Arikan et al., 2009; Ratasuk et al., 2012; Amarakoon et al., 2016). Kinetic studies have demonstrated that OTC removal efficiencies

can range from 59% - 99% and half-lives from 0.4 to 56 days. Hence, proper storage and manure management treatments for OTC-associated manure can be critical in reducing OTC concentrations prior to manure land application and reduce the risk of antibiotic resistant bacteria developing due to land application of manure.

6.6 Conclusions

The model predicted soil bound OTC remained in the mixing zone over the period of simulation indicating minimal mobility. OTC remained within the incorporation region, suggesting reduced potential to reach groundwater sources. The scenarios of surface and liquid manure application assuming minimum OTC resulted in aqueous, equilibrium and kinetic site concentrations below the selection region throughout the entire simulation time.

Comparison of our work and results from the studies discussed, show OTC concentrations in soil at levels with the potential to exert a selective pressure. Ranges of OTC residual levels have been reported to cause selection, accumulation and promote horizontal gene transfer. Greater depth of manure incorporation reduced concentrations levels in aqueous and solid media. Liquid application of the slurry required addition of water to reduce the solids fraction in the waste which at the same time diluted OTC concentrations in the liquid waste.

At the moment, no experimental data is available for comparison of simulated soil conditions which highlights the need of research that investigate the fate, transport and dynamics of amended soils with OTC-contaminated manure. Research studies that assess the effect of soil-bound OTC at the sub-MIC and traditional level on soil microbial communities are also required to validate the antibiotic resistance selection assessment in this work.

7. SUMMARY AND CONCLUSIONS

The increased use and overuse of antibiotics in livestock production has resulted in the release of antibiotics, antibiotic resistant bacteria (ARBs) and antibiotic resistant genes (ARGs) into the environment and land application of animal waste is a significant source. Land application of animal manure is a worldwide common agricultural practice due to its value as a nutrient supply and as a low cost disposal method of animal waste. Consequently, the question is: ***Does OTC in manure and current animal waste management practices introduce OTC to the soil environment at concentrations that could potentially select for antibiotic resistance?***

An extensive literature review for the occurrence of Oxytetracycline (OTC) in various aqueous and solid media revealed that approximately 80% of the reported OTC concentrations were from solid media. The origins include: sediment, sludge, fresh and aged manure and soil. Soil medium had the highest number of observations followed by sediment from fish farms. Concentrations range from 10^{-1} $\mu g/kg$ to 10^{3} $\mu g/kg$ from soil and 10^{1} $\mu g/kg$ to 10^{5} $\mu g/kg$ from fish farms. Fresh and aged manure concentrations range from 10^{1} $\mu g/kg$ to 10^{5} $\mu g/kg$ and 10^{1} $\mu g/kg$ to 10^{4} $\mu g/kg$, respectively. These ranges reflect management of manure for different animals and agricultural practices for countries all over the world.

Manure associated-OTC concentrations indicate the potential for OTC to be introduced into soil medium from land application management practices. Land application of animal waste has been identified as a large areal scale means of antibiotic introduction (OTC in this case), antibiotic resistant bacteria (ARBs) and antibiotic resistant genes (ARGs) which could potentially facilitate the development of ARBs, accelerate the evolution of organisms, and mobilize and transfer ARGs to pathogens and other bacteria.

Experimental studies of antibiotic resistance selection have demonstrated Tetracycline (Gullberg et al., 2011; Quinlan et al., 2011; Liu et al., 2011; Lundström et al., 2016) and Oxytetracycline (Peng et al., 2014) resistance enrichment in aqueous media at concentration levels as low as $\mu g/L$. Even though OTC and other members of the Tetracycline family of antibiotics sorbs strongly to soils and retain antimicrobial activity (Peng et al., 2014), limited data is available on concentration levels of soil-bound OTC and their selection for antibiotic resistance.

OTC has been reported by several authors (Jones et al., 2005; Figueroa et al., 2004; Figueroa and MacKay, 2005; Aga et al., 2005; Chander et al., 2005; ter Laak et al., 2006b), to sorb strongly to soil components, such as aluminosilicates, organic matter and metal oxides, through multiple mechanisms and has been identified as persistent (half-life of 33 days in manure amended soil). Reported sorption mechanisms include: cation and anion exchange, cation bridging, surface complexation and hydrophobic partitioning. Partition coefficients (K_d) in soil samples range from 115 to 269,097 L/kg.

Given the strong sorption, high variability and complex interaction of OTC and soils components, a model to predict partition coefficients based on soil properties was developed (equation 3.1, chapter 3). The analysis process of the available data on OTC-soil sorption highlighted the importance of the electrolyte solution on the sorption process. $CaCl_2$ is typically used in sorption experiments as the aqueous solvent to improve centrifugation and minimize exchange of cations. However, in the case of OTC, calcium-OTC complexation and competition of sorption sites may occur altering quantification of the soil sorption partition coefficient (K_d). Even sorption studies, with the same soil samples, performed with buffer solutions 1,4-piperazinediethanesulfonic acid (PIPES) and 2-(N-morpholino)ethanesulfonic acid (MES) showed discrepancies in K_d (Figure 3.6). These observations highlight the importance of the methodology selected to evaluate OTC sorption on soils. Overall, additional sorption studies using PIPES as electrolyte solute are

required to test the applicability of the model developed for K_d predictions.

The developed model for K_d estimations was the result of a multiple stepwise regression (MSR) which identified cation exchange capacity (CEC), organic matter (OM) and free or crystalline aluminum and iron oxides extracted by dithionite citrate bicarbonate (DCB (Al+Fe)). These parameters were determined to dominate the behavior of OTC with soil. The data utilized for the MSR was that from Figueroa et al. (2010) which used PIPES as electrolyte solution for the sorption experiments. Equation 3.1 explained about 95% of the variation on measured K_d (Figure 3.3).

To date, the fate and transport of OTC in soils and resulting concentrations levels from land application of OTC-contaminated manure have not been modeled based on field data. Thus, one of the objectives of this dissertation was to assess the fate and transport of OTC in soil (spatially and temporarily) as a result of different management practices including: swine manure application as a liquid or slurry on a sandy loam soil considering 0, 10 and 25 cm of incorporation depth. To this end, another goal was to compare simulated aqueous and solid concentrations with reported OTC concentrations as potential selective levels for antibiotic resistance.

To address this issue, a two-site, one-rate, non-equilibrium model (equations 4.50, 4.51 and 4.54) was selected for simulating the mobility of OTC in a sandy loam soil. This model was chosen because: 1) it has repeatedly been proven to improve mobility modeling approximations for many pesticides in comparison with the classical advection-dispersion equation (ADE); 2) it includes a kinetic-mass transfer rate which can simulate a release of OTC-bound residues un soil, a behavior that has been previously reported for OTC and other Tetracyclines (Hamscher et al., 2002; Liu et al., 2015); and 3) it offers a higher degree of complexity without increasing the level of uncertainty for parameters included in the model that are difficult to quantify. The two-site, one-rate, non-equilibrium model does not have an exact solution, therefore the Finite Difference method (chapter 5) was used to

approximate a solution of the partial differential equations (PDEs) (equations 4.50, 4.51 and 4.54) that constitute the model.

By running a wide range of scenarios, the model predicted the conditions that would result in potentially generating antibiotic resistance due to OTC exposure. Simulation results predicted OTC concentration levels in soil within the sub-MIC selection window for the cases of slurry application considering maximum OTC in manure (29 mg/kg) and incorporations depths of 0 and 10 cm. Simulated results of liquid manure and surface application considering minimum OTC in manure (48 $\mu g/kg$) are not presented since concentrations in manure were significantly below the sub-MIC selective region. For the cases of liquid manure application considering maximum OTC in manure (29 mg/kg) and no incorporation, simulation results predict concentrations in soil within the sub-MIC selection window throughout the entire simulated time (120 days). For the cases of liquid manure application also considering maximum OTC in manure and 10 cm incorporation depth, simulation results predict concentrations in soil within the sub-MIC selection window for up to 30 days.

These observations demonstrate that concentrations of OTC in manure on the order of 29 mg/kg can result in soil-bound concentrations levels that could potentially select for antibiotic resistant bacteria, particularly, in cases where no incorporation is implemented. Regulatory policies for animal manure and wastewater are designed to control the level of nutrients and microorganisms that might impact surface water, groundwater and amended soils. However, such regulation policies do not provide controls for antibiotics, ARBs and ARGs introduced to the soil and surrounding environments that may exert a selective pressure and contribute to the development and dissemination of antibiotic resistance among bacterial populations. Currently, the European Union has regulatory limits for antibiotic concentrations in soil of 100 $\mu g/kg$. As is presented in this work, typical manure amendment rates and ranges of reported OTC concentration in manure show the potential for

harboring resistance.

Although controversy emerged in the scientific community over the use of antibiotics in animals for non-therapeutic purposes (as growth promoters) due to the potential of developing antibiotic resistant bacteria and exposure of humans, the debate still continues in the United States and other countries. The risk posed to humans by antibiotic resistant bacteria originating from agriculture practices has not been clearly established, but is likely an indirect pathway of exposure.

OTC concentrations in swine manure together with current waste management practices of land application of manure as fertilizer present the potential of selection for antibiotic resistance. There is a need of more research studies that assess the microbial activity of soil-bound OTC to compare OTC concentration levels in soil with antibiotic selectivity ranges. Future studies should take into account different soil samples to assess the sorption and microbial activity behavior various soil compositions.

REFERENCES

Aga, D., O'Connor, S., Ensley, S., Payero, J., Snow, D., and Tarkalson, D. (2005). "Determination of the persistence of tetracycline antibiotics and their degradates in manure-amended soil using enzyme-linked immunosorbent assay and liquid chromatography-mass spectrometry." *Journal of Agricultural and Food Chemistry*, 53(18), 7165–7171.

Aga, D. S., Goldfish, R., and Kulshrestha, P. (2003). "Application of elisa in determining the fate of tetracyclines in land-applied livestock wastes." *Analyst*, (6), 658–662.

Alavi, N., Babaei, A. A., Shirmardi, M., Naimabadi, A., and Goudarzi, G. (2015). "Assessment of oxytetracycline and tetracycline antibiotics in manure samples in different cities of khuzestan province, iran." *Environmental Science and Pollution Research*, 22.

Altfelder, S., Streck, T., Maraqa, M. A., and Voice, T. C. (2001). "Nonequilibrium sorption of dimethylphthalateŮcompatibility of batch and column techniques." *Soil Sci. Soc. Am. J.*, 65, 102–111.

Amarakoon, I. D., Zvomuya, F., Sura, S., Larney, F. J., Cessna, A. J., Xu, S., and McAllister, T. A. (2016). "Dissipation of antimicrobials in feedlot manure compost after oral administration versus fortification after excretion." *Journal of Environmental Quality*, 45, 503–510.

An, J., Chen, H., Wei, S., and Gu, J. (2015). "Antibiotic contamination in animal manure, soil, and sewage sludge in shenyang, northeast china." *Environ Earth Sci*, 74, 5077–5086.

Andreu, V., Vazquez-Roig, P., Blasco, C., and Picó, Y. (2009). "Determination of tetracycline residues in soil by pressurized liquid extraction and liquid chromatography tandem mass spectrometry." *Analytical and bioanalytical chemistry*, 394(5), 1329–1339.

Arikan, O., Mulbry, W., Ingram, D., and Millner, P. (2009). "Minimally managed com-

posting of beef manure at the pilot scale: Effect of manure pile construction on pile temperature profiles and on the fate of oxytetracycline and chlortetracycline." *Bioresource Technology*, 100, 4447–4453.

Arikan, O., Sikora, L., Mulbry, W., Khan, S., Rice, C., and Foster, G. (2006). "The fate and effect of oxytetracycline during the anaerobic digestion of manure from therapeutically treated calves." *Process Biochemistry*, 41, 1637–1643.

Aristilde, L., Marichal, C., Brendlé, J. M., Lanson, B., and Charlet, L. (2010). "Interactions of oxytetracycline with a smectite clay: A spectroscopic study with molecular simulations." *Environmental Science and Technology*, 44(20), 7839–7845.

Ashbolt, N. J., Amzquita, A., Backhaus, T., Borriello, P., Brandt, K. K., Collignon, P., Coors, A., Finley, R., Gaze, W. H., Heberer, T., Lawrence, J. R., Larsson, D. J., McEwen, S. A., Ryan, J. J., Schnfeld, J., Silley, P., Snape, J. R., den Eede, C. V., , and Topp, E. (2013). "Human health risk assessment (hhra) for environmental development and transfer of antibiotic resistance." *Environ. Health Perspect.*, 121 (9), 993–1001.

Awad, Y., Kim, S.-C., El-Azeem, S. A., Kim, K.-H., Kim, K.-R., Kim, K., Jean, C., Lee, S. S., and Ok, Y. S. (2013). "Veterinary antibiotics contamination in water, sediment, and soil near a swine manure composting facility." *Environ Earth Sci*, (June), 1–8.

Baguer, A., Jensen, J., and Krogh, P. H. (2000). "Effects of the antibiotics oxytetracycline and tylosin on soil fauna." *Chemosphere*, 40(7), 751–757.

Bao, Y. and Zhou, Q. (2015). "Temporal changes in horsebean bioavailability and accumulation after removing extractable oxytetracycline fractions in soils." *RSC Advances*, 5, 32572–32579.

Baquero, F., Martínez, J.-L., and Cantón, R. (2008). "Antibiotics and antibiotic resistance in water environments." *Current opinion in biotechnology*, 19(3), 260–265.

Barry, D. A. and Parker, J. C. (1987). "Approximations for solute transport through porous media with flow transverse to layering." *Transport in Porous Media*, 2 (1), 65–82.

Bear, J. and Verruijt, A. (1987). *Modeling groundwater flow and pollution*. D. Reidel Publishing Company.

Bengtsson-Palme, J. and Larsson, D. J. (2015). "Antibiotic resistance genes in the environment: prioritizing risks." *Nature Views - Microbiology*, 13 (6), 396.

Björklund, H., Bondestam, J., and Bylund, G. (1990). "Residues of oxytetracycline in wild fish and sediments from fish farms." *Aquaculture*, 86, 359–367.

Blackwell, P., Kay, P., and Boxall, A. (2007). "The dissipation and transport of veterinary antibiotics in a sandy loam soil." *Chemosphere*, 67(2), 292–299.

Boleas, S., Alonso, C., Pro, J., Fernandez, C., Carbonell, G., and Tarazona, J. (2005). "Toxicity of the antimicrobial oxytetracycline to soil organisms in a multi-species-soil system (msů3) and influence of manure co-addition." *Journal of Hazardous Materials*, 122, 233–241.

Box, A., Mevius, D. J., Schellen, P., Verhoef, J., and Fluit, A. C. (2005). "Integrons in escherichia coli from food-producing animals in the netherlands." *Microbial Drug Resistance*, 11(1), 53–57 Source type: scholarlyjournals; Object type: Article; Object type: Feature; CSAUnique: MD-0001116817; AccNum: 6263933; ISSN: 1076-6294; Peer Reviewed: true.

Boxall, A., Fogg, L. A., Baird, D., Lewis, C., Telfer, T., Kolpin, D., Gravell, A., Pemberton, E. J., and Boucard, T. (2006). "Targeted monitoring study for veterinary medicines in the environment." *Report No. SC030183/SR*, Environment Agency.

Brambilla, G., Patrizii, M., Filippis, S. P. D., Bonazzi, G., Mantovi, P., Barchi, D., and Migliore, L. (2007). "Oxytetracycline as environmental contaminant in arable lands." *Analytica Chimica Acta*, 586(12), 326–329.

Bronswijk, J. J. B., Hamminga, W., , and Oostindie, K. (1995). "Field-scale solute transport in a heavy clay soil." *Water Resources Research*, 31 (3), 517–526.

Brown, K. D., Kulis, J., Thomson, B., Chapman, T. H., and Mawhinney, D. B. (2006).

"Occurrence of antibiotics in hospital, residential, and dairy effluent, municipal wastewater, and the rio grande in new mexico." *Science of the Total Environment*, 366, 772–783.

Brusseau, M. (1998). *Physical nonequilibrium in soils: modeling and application*. Ann Arbor Press, INC, Chapter Multiprocess nonequilibrium and nonideal transport of solutes in porous media, 63–82.

Brusseau, M., Jessup, R., and Rao, P. (1989). "Modeling the transport of solute influence by multiprocess nonequilibrium." *Water Resources Research*, 25 (9), 1971–1988.

Brusseau, M., Jessup, R., and Rao, S. (1992). "Modeling solute transport influenced by multiprocess nonequilibrium and transformation reactions." *Water Resources Research*.

Buckley, D. L. (1985). "A spectral, voltammetric and chromatographic investigation of the complexation of oxytetracycline hydrochloride to metals of varying valency." M.S. thesis, School of Chemical Sciences, The National Institute for Higher Education, Dublin, School of Chemical Sciences, The National Institute for Higher Education, Dublin.

Capone, D. G., Weston, D. P., Miller, V., and Shoemaker, C. (1996). "Antibacterial residues in marine sediments and invertebrates following chemotherapy in aquaculture." *Aquaculture*, 145(14), 55–75.

Celia, M., Bouloutas, E., and Zarba, R. (1990). "A general mass-conservative numerical solution for the unsaturated flow equation." *Water Resources Research*, 26 (7), 1483–1496.

CFR (2017). *CFR-Title 21*. Chapter I, Subchapter E, Part 558, Subpart B, Section 558.450.

Chander, Y., Kumar, K., Goyal, S., and Gupta, S. (2005). "Antibacterial activity of soil-bound antibiotics." *Journal of environmental quality*, 34(6), 1952–1957.

Chee-Sanford, J., Mackie, R., Koike, S., Krapac, I., Lin, Y., Yannarell, A., Maxwell, S., and Aminov, R. (2009). "Fate and transport of antibiotic residues and antibiotic resistance genes following land application of manure waste." *Journal of environmental quality*, 38(3), 1086–1108.

Chen, G., He, W., Wang, Y., Zou, Y., Liang, J., Liao, X., and Wu, Y. (2014). "Effect of different oxytetracycline addition methods on its degradation behavior in soil." *Science of the Total Environment*.

Chen, Y. S., Zhang, H. B., Luo, Y. M., and Song, J. (2012). "Occurrence and assessment of veterinary antibiotics in swine manures: A case study in east china." *Chinese Science Bulletin*, 57(6), 606–614.

Chen, Z., Zhang, Y., Gao, Y., Boyd, S., Zhu, D., and Li, H. (2015). "Influence of dissolved organic matter on tetracycline bioavailability to an antibiotic-resistant bacterium." *Environmental Science and Technology*, 49, 10903–10910.

Chessa, L., Jechalke, S., Ding, G., Pusino, A., Mangia, N. P., and Smalla, K. (2016). "The presence of tetracycline in cow manure changes the impact of repeated manure application on soil bacterial communities." *Biology and fertility of soils*, 52(8), 1121–1134.

Chopra, I. and Roberts, M. (2001). "Tetracycline antibiotics: Mode of action, applications, molecular biology, and epidemiology of bacterial resistance." *Microbiology and Molecular Biology Reviews*, 65(2), 232–260.

Chu, B. (2011). "Sorption and transport of veterinary antibiotics in agroforestry buffer, grass buffer and cropland soils." Ph.D. thesis, University of Missouri-Columbi, University of Missouri-Columbi.

Coats, K. and Smith, B. (1964). "Dead-end pore volume and dispersion in porous media." *Soc. Petrol. Eng. J.*, 4, 73–84.

Collaizzi, J. L. and Klink, P. R. (1969). "ph-partition behavior of tetracyclines." *Journal of Pharmaceutical Science*, 58(10), 1184–1189.

Craig, J. (2004). "Reactive contaminant transport modeling using analytica element flow solutions." Ph.D. thesis, State University of New York at Buffalo, State University of New York at Buffalo.

Davidson, J. and Chang, R. (1972). "Transport of picloram in relation to soil physical conditions and pore-water velocity." *Soil Sci. Soc. Amer. Proc.*, 36, 257–261.

Davidson, J. and McDougal, J. (1973). "Experimental and predicted movement of three herbicides in a water saturated soil." *J. En*, 2(4), 428–433.

Davies, J. (1997). *Origins, acquisition and dissemination of antibiotic resistance determinants*. Antibiotic Resistance: Origins, Evolution, Selection and Spread, John Wiley and Sons, West Sussex, Englanf, 15–35.

Davis, J. G., Truman, C. C., Kim, S. C., Ascough, J. C. I., and Carlson, K. (2006). "Antibiotic transport via runoff and soil loss.." *Journal of environmental quality*, 35(6), 2250–2260.

Davison, H., Low, J. C., and Woolhouse, M. (2000). "What is antibiotic resistance and how can we measure it?." *Trends in Microbiology*, 8(12), 554–559.

D'Costa, V. M., McGrann, K. M., Hughes, D. W., and D.Wright, G. (2006). "Sampling the antibiotic resistome." *Science*, 113 (5759), 374–377.

de Cazes, M., Abejón, R., Belleville, M.-P., and Sanchez-Marcano, J. (2014). "Membrane bioprocesses for pharmaceutical micropollutant removal from waters." *Membranes*, 4, 692–729.

de Liguoro, M., Cibin, V., Capolongo, F., Sørensen, B. H., and Montesissa, C. (2003). "Use of oxytetracycline and tylosin in intensive calf farming: evaluation of transfer to manure and soil.." *Chemosphere*, 52(1), 203.

Drlica, K. (2003). "The mutant selection window and antimicrobial resistance." *Journal of Antimicrobial Chemotherapy*, 52(1), 11–17.

Drlica, K. and Zhao, X. (2007). "Mutant selection window hypothesis updated." *Clinical Infectious Diseases*, 44(5), 681–688.

EPA (2012). "Npdes permit writers' manual for concentrated animal feeding operations." *Report No. EPA 833-F-12-001*, U.S. Environmental Protection Agency.

Essington, M. (2015). *Soil and Water Chemistry*. CRC PRESS.

Essington, M. E., Lee, J., and Seo, Y. (2010). "Adsorption of antibiotics by montmorillonite and kaolinite." *Soil Sci. Soc. Am. J.*, 74(5), 1577–1588.

Fedler, C. and Borreli, J. (2001). "Re-evaluating surface application rates for texas ossf systems." *Report no.*, Texas Tech University.

Fey, P. D., Safranek, T. J., Rupp, M. E., Dunne, E. F., Ribot, E., Iwen, P. C., Bradford, P. A., Angulo, F. J., and Hinrichs, S. H. (2000). "Ceftriaxone-resistant salmonella infection acquired by a child from cattle." *N Engl J Med*, 342(17), 1242–1249.

Feyen, J., Jacques, D., Timmerman, A., and Vanderborght, J. (1998). "Modelling water flow and solute transport in heterogeneous soils: A review of recent approaches." *J. agric. Engng Res.*, 70, 231–256.

Field, M. and Leij, F. (2014). "Combined physical and chemical nonequilibrium transport model for solution conduits." *Journal of Contaminant Hydrology*, 157, 37–46.

Figueroa, R. (2012). "Investigation of the sorption behavior of veterinary antibiotics to whole soils, organic matter and animal manure." Ph.D. thesis, University of Connecticut, University of Connecticut.

Figueroa, R., Leonard, A., and MacKay, A. (2004). "Modeling tetracycline antibiotic sorption to clays." *Environmental Science and Technology*, 38(2), 476–483.

Figueroa, R. and MacKay, A. (2005). "Sorption of oxytetracycline to iron oxides and iron oxide-rich soils." *Environmental Science and Technology*, 39(17), 6664–6671.

Figueroa, R., Vasudevan, D., and MacKay, A. (2010). "Trends in soil sorption coefficients within common antimicrobial families." *Chemosphere*, 79(8), 786–793.

Finley, R. L., Collignon, P., Larsson, D. G. J., McEwen, S. A., Li, X.-Z., Gaze, W. H., Reid-Smith, R., Timinouni, M., Graham, D. W., and Topp, E. (2013). "The scourge of antibiotic resistance: The important role of the environment." *Clinical Infectious Diseases*, 57 (5), 704–710.

Forsberg, K., Reyes, A., Bin, W., Selleck, E., Sommer, M. O. A., and Dantas, G. (2012). "The shared antibiotic resistome of soil bacteria and human pathogens.." *Science*, 337(6098), 1107–1111.

Gamerdinger, A., Wagenet, R., and van Genuchten, M. (1990). "Application two-site/two-region models for studyngi simultaneous nonequilibrium transport and degradation of pesticides." *Soil Sci. Soc. Am. J.*, 54, 957–963.

Gao, P., Munir, M., and Xagoraraki, I. (2012). "Correlation of tetracycline and sulfonamide antibiotics with corresponding resistance genes and resistant bacteria in a conventional municipal wastewater treatment plant." *Science of the Total Environment*, 421422(1), 173–183.

Ghosh, S. and LaPara, T. M. (2007). "The effects of subtherapeutic antibiotic use in farm animals on the proliferation and persistence of antibiotic resistance among soil bacteria." *The ISME Journal*, 1, 191–203.

Gong, W., Liu, X., He, H., Wang, L., and Dai, G. (2012). "Quantitatively modeling soilwater distribution coefficients of three antibiotics using soil physicochemical properties." *Chemosphere*, 89(7), 825–831.

Goode, D. and Konikow, L. (1989). "Modification of a method of characteristics solute transport model to incorporate decay and equilibrium-controlled sorption or ion exchange." *Water Resources Investigations Report 89-4030*, U.S. Geological Survey, Reston, Virginia.

Grzybowski, B. A. (2009). *Chemistry in motion: reaction-diffusion systems for micro and nano technology*. John WIley and Sons Ltd., Chapter Ch. 4: Putting it all together: Reaction-Diffusion Equations and the Methods of Solving them, 61–91.

Gullberg, E., Cao, S., Berg, O. G., Ilbäck, C., Sandegren, L., Hughes, D., and Andersson, D. I. (2011). "Selection of resistant bacteria at very low antibiotic concentrations." *PLoS Pathog*, 7(7), – e1002158.

Halling Sørensen, B., Lykkeberg, A., Ingerslev, F., Blackwel, P. A., and Tjørnelund, J. (2003). "Characterisation of the abiotic degradation pathways of oxytetracyclines in soil interstitial water using lcŰmsŰms." *Chemosphere*, 50, 1331–1342.

Halling-Sørensen, B., Sengeløv, G., and Tjørnelund, J. (2002). "Toxicity of tetracyclines and tetracycline degradation products to environmentally relevant bacteria, including selected tetracycline-resistant bacteria." *Archives of Environmental Contamination and Toxicology*, 42(3), 263–271.

Hamscher, G., Abu-Quare, A., Sczesny, S., Höper, H., and Nau, H. (2000). "Determination of tetracyclines and tylosin in soil and water samples from agricultural areas in lower saxony." *Euroresidue IV conference (8-10 May 2000)*, Veldhoven, Netherlands, National Institute of Public Health and the Environment (RIVM).

Hamscher, G., Pawelzick, H. T., Höper, H., and Nau, H. (2005). "Different behavior of tetracyclines and sulfonamides in sandy soils after repeated fertilization with liquid manure." *Environmental Toxicology and Chemistry*, 24(4), 861–868.

Hamscher, G., Sczesny, S., Hoper, H., and Nau, H. (2002). "Determination of persistent tetracycline residues in soil fertilized with liquid manure by high-performance liquid chromatography with electrospray ionization tandem mass spectrometry.." *Analytical Chemistry*, 74(7), 1509.

Hashimoto, I., Deshpande, K., and Thomas, H. (1964). "Peclet number and retardation factors for ion excjange columns." *Ind. Eng. Chem. Fundamen.*, 3(3), 213–218.

Hengnirun, S., Barrington, S., Prasher, S., and Lyew, D. (1999). "The development of models simulating nitrogen transport in soil and manure." *Canadian Agricultural Engineering*, 41(1), 35–45.

Heuer, H., Kopmann, C., Binh, C. T. T., Top, E. M., and Smalla, K. (2009). "Spreading antibiotic resistance through spread manure: characteristics of a novel plasmid type with low %g+c content." *Environmental Microbiology*, 11(4), 937–949.

Heuer, H., Schmitt, H., and Smalla, K. (2011). "Antibiotic resistance gene spread due to manure application on agricultural fields." *Current opinion in microbiology*, 14(3), 236–243.

Hirsch, R., Ternes, T., Haberer, K., and Kratz, K.-L. (1999). "Occurrence of antibiotics in the aquatic environment." *Science of the Total Environment*, 225(12), 109–118.

Hoffman, J. (2001). *Numerical Methods for Engineers and Scientists*. Marcel Dekker, Inc.

Hogarth, W., Noye, B., Stagnitti, J., Parlange, J., and G, B. (1990). "A comparative study of finite difference methods for solving the one-dimensional transport equation with an initial-boundary value discontinuity." *Computers Math. Applic.*, 20(11), 67–82.

Hu, X., Zhou, Q., and Luo, Y. (2010). "Occurrence and source analysis of typical veterinary antibiotics in manure, soil, vegetables and groundwater from organic vegetable bases, northern china." *Environmental Pollution*, 158(9), 2992–2998.

Huang, K., Mohanty, B., and Genuchten, M. V. (1996). "A new convergence criterion for the modified picard iteration method to solve the variably saturated flow equation." *Journal of hydrology*, 178, 69–91.

Huang, K., Mohanty, B., Leij, F., and van Genuchten, M. (1998). "Solution of the nonlinear transport equation using modified picard iteration." *Advances in Water Resources*, 21, 237–349.

Huang, K., Toride, N., and van Genuchten, M. T. (1995). "Experimental investigation of solute transport in large, homogeneous and heterogeneous saturated soils columns." *Transport in Porous Media*, 18, 283–302.

Huang, K., Šimůnek, J., and van Genuchten, M. (1997). "A third-order numerical scheme with upwind weighting for solving the solute transport equation." *International Journal for Numerical Methods in Engineering*, 40, 1623–1637.

Huang, M., dong Yang, Y., hui Chen, D., Chen, L., and dong Guo, H. (2012). "Removal mechanism of trace oxytetracycline by aerobic sludge." *Process Safety and Environ-*

mental Protection, 90 (2), 141–146.

Huang, X., Liu, C., Li, K., Liu, F., Liao, D., Liu, L., Zhu, G., and Liao, J. (2013). "Occurrence and distribution of veterinary antibiotics and tetracyline resistance genes in farland soils around swine feedlots in fujian, province, china." *Environmental Science and Pollution Research*, 1–9.

Hunter, J. E. B., Bennett, M., Hart, C. A., Shelley, J. C., and Walton, J. R. (1994). "Apramycin-resistant escherichia coli isolated from pigs and a stockman." *Epidemiology and infection*, 112(3), 473–480.

Huyakorn, P. and Pinder, G. (1983). *Computational Methods in Subsurface Flow*. Academic Press, INC.

Igboekwe, M. and Amos-Uhegbu, C. (2011). *Earth and Environmental Sciences*. InTech, Chapter Fundamental Approach in Groundwater Flow and Solute Transport Modelling Using the Finite Difference Method, 301–328.

Ingebritsen, S. and Sanford, W. (1998). *Groundwater in geologic processes*. Cambridge University Press.

Jacobsen, A. M. and Halling-Sørensen, B. (2006). "Multi-component analysis of tetracyclines, sulfonamides and tylosin in swine manure by liquid chromatographytandem mass spectrometry." *Analytical and bioanalytical chemistry*, 384(5), 1164–1174.

Jacobsen, P. and Berglind, L. (1988). "Persistence of oxytetracycline in sediments from fish farms." *Aquaculture*, 70(4), 365–370.

Jechalke, S., Heuer, H., Siemens, J., Amelung, W., and Smalla, K. (2014). "Fate and effects of veterinary antibioitcs in soil." *Trends in Microbiology*, 22 (9), 536–545.

Jia, A., Xiao, Y., Hu, J., Asami, M., and Kunikane, S. (2009). "Simultaneous determination of tetracyclines and their degradation products in environmental waters by liquid chromatographyelectrospray tandem mass spectrometry." *Journal of Chromatography A*, 1216(22), 4655–4662.

Jones, A. D., Bruland, G. L., Agrawal, S. G., and Vasudevan, D. (2005). "Factors influencing the sorption of oxytetracycline to soils." *Environmental Toxicology and Chemistry*, 24(4), 761–770.

Jury, W. and Flühler, H. (1992). "Transport of chemicals through soil: mechanism, models, and field applications." *Advances in Agronomy*, 47, 141–201.

Jury, W. A., Gardner, W. R., and Gardner, W. H. (1991). *Soil physics*. Wiley.

Kamra, S., Lennartz, B., Genuchten, M. V., and Widmoser, P. (2001). "Evaluating non-equilibrium solute transport in small soil columns." *Journal of Contaminant Hydrology*, 48, 189–212.

Karci, A. and Balcioǵlu, I. A. (2009). "Investigation of the tetracycline, sulfonamide, and fluoroquinolone antimicrobial compounds in animal manure and agricultural soils in turkey." *Science of the Total Environment*, 407(16), 4652–4664.

Kay, P., Blackwell, P., and Boxall, A. (2004). "Fate of veterinary antibiotics in a macroporous tile drained clay soil." *Environmental Toxicology and chemistry*, 23(5), 1136–1144.

Kay, P., Blackwell, P., and Boxall, A. (2005a). "Column studies to investigate the fate of veterinary antibiotics in clay soils following slurry application to agricultural land." *Chemosphere*, 60(4), 497–507.

Kay, P., Blackwell, P., and Boxall, A. (2005b). "A lysimeter experiment to investigate the leaching of veterinary antibiotics through a clay soil and comparison with field data." *Environmental pollution*, 134(2), 333–341.

Kay, P., Blackwell, P., and Boxall, A. (2005c). "Transport of veterinary antibiotics in overland flow following the application of slurry to arable land." *Chemosphere*, 59(7), 951–959.

Kennedy, A. C. and Smith, K. L. (1995). "Soil microbial diversity and the sustainability of agricultural soils." *Plant and soil*, 170(1), 75–86.

Kerry, J., Coyne, R., Gilroy, D., Hiney, M., and Smith, P. (1996). "Spatial distribution of oxytetracycline and elevated frequencies of oxytetracycline resistance in sediments beneath a marine salmon farm following oxytetracycline therapy." *Aquaculture*, 145(14), 31–39.

Key, N., McBride, W. D., Ribaudo, M., and Sneeringer, S. (2011). "Trends and developments in hog manure management: 1998-2009." *Economic Information Bulletin 81*, United States Department of Agriculture (September 2011).

Kilonzo-Nthenge, A., Rotich, E., and Nahashon, S. N. (2013). "Evaluation of drug-resistant enterobacteriaceae in retail poultry and beef." *Poultry science*, 92(4), 1098–1107.

Kim, S., Eichhorn, P., Jensen, J., Weber, A. S., and Aga, D. (2005). "Removal of antibiotics in wastewater: Effect of hydraulic and solid retention times on the fate of tetracycline in the activated sludge process." *Environmental Science and Technology*, 39, 5816–5823.

Kim, S., Jensen, J., Aga, D., and Weber, A. (2007). "Fate of tetracycline resistant bacteria as a function of activated sludge process organic loading and growth rate." *Water science and technology*, 55(1-2), 291–297.

Kim, S.-C. and Carlson, K. (2007). "Temporal and spatial trends in the occurrence of human and veterinary antibiotics in aqueous and river sediment matrices." *Environmental Science and Technology*, 41, 50–57.

Kim, S.-C., Yang, J. E., Ok, Y.-S., and Carlson, K. (2010). "Dissolved and colloidal fraction transport of aantibioitcs in soil under biotic and abiotic conditions." *Water Quality Research Journal of Canada*, 45(3), 275–285.

Knapp, C., Angemann, C., Hanson, M., Keen, P., Hall, K., and Graham, D. (2008). "Indirect evidence of transposon-mediated selection of antibiotic resistance genes in aquatic systems at low-level oxytetracycline exposures." *Environmental Science and Technology*, 42(14), 5348–5353.

Kohanski, M., DePristo, M., and Collins, J. (2010). "Sublethal antibiotic treatment leads to multidrug resistance via radical-induced mutagenesis." *Mollecular Cell*, 37, 311–320.

Kolpin, D., Furlong, E., Meyer, M., Thurman, M., Zaugg, S., Barber, L., and Buxton, H. (2002). "Pharmaceuticals, hormones, and other organic wastewater contaminants in u.s. streams, 19992000: a national reconnaissance." *Environ.Sci.Technol.*, 36(6), 1202–1211.

Kong, W., Li, C., Dolhi, J. M., Li, S., He, J., and Qiao, M. (2012). "Characteristics of oxytetracycline sorption and potential bioavailability in soils with various physical-chemical properties." *Chemosphere*, 87(5), 542–548.

Konikow, L. (2011). "The secret to successful solute transport." *Ground Water*, 49(2), 144–159.

Konikow, L., Reilley, T., Barlow, P., and Voss, C. (2007). *The Handbook of Groundwater Engineering*. CR, Chapter Groundwater modeling, 23.1–23.60.

Kulshrestha, P. (2007). "Fate and transport of persistent tetracycline residues in the environment." Ph.D. thesis, University at Buffalo, University at Buffalo.

Kulshrestha, P., Giese, R., and Aga, D. (2004). "Investigating the molecular interactions of oxytetracycline in clay and organic matter: insights on factors affecting its mobility in soil." *Environmental Science and Technology*, 38(15), 4097–4105.

Kumar, K., Gupta, S. C., and Baidoo, S. K. (2005). "Antibiotic uptake by plants from soil fertilized with animal manure." *Journal of environmental quality*, 34(6), 2082–2085 M3: Article.

Kuzmin, D. (2010). *A guide to numerical methods for transport equations*. University Erlangen-Nuremberg.

Kyselková, M., Jirout, J., Chroňáková, A., Vrchotová, N., Bradley, R., Schmitt, K., and Elhottová, D. (2013). "Cow excrements enhance the occurrence of tetracycline resistance genes in soil regardless of their oxytetracycline content." *Chemosphere*, 93, 2413–2418.

Ladha, N. (1999). "Modleing solute transport in soils from ataratiri." M.S. thesis, University of Toronto, University of Toronto.

Lamb, J., Rosen, C., Bongard, P., Kaiser, D., Fernandez, F., and Barber, B. (2015). "Fertilizing corn grown on irrigated sandy soils." *Report No. AG-NM-1501 (2015)*, University of Minnesota.

Lapidus, L. and Amundson, N. (1952). "Mathematics of adsorption in beds. vi. the effect of longitudinal diffusion in ion exchange and chromatographic columns." *J. Phys. Chem.*, 56 (8), 984–988.

Lapidus, L. and Pinder, G. (1999). *Numerical Solution of Partial DifDifferent Equations in Science and Engineering*. John WIley and Sons Inc.

Lee, J., Seo, Y., and Essington, M. (2014). "Sorption and transport of veterinary pharmaceuticals in soil - a laboratory study." *Soil Sci. Soc. Am. J.*, 78, 1531–1543.

Leij, F. and Bradford, S. (2009). "Combined physical and chemical nonequilibrium transport model: Analytical solution, moments, and application to colloids." *Journal of Contaminant Hydrology*, 110, 87–99.

Leij, F. and Toride, N. (1998). *Physical nonequilibrium in soils: modeling and application*. Ann Arbor Press, INC, Chapter Analytical solutions for nonequilibrium transport models, 117–156.

Leij, F. and van Genuchten, M. (2000). *Handbook of soil science*. CRC PRESS, Chapter Solute transport, A183 – A227.

Leij, F. and van Genuchten, M. T. (1995). "Approximate analytical solution for solute transport in two-layer porous media." *Transport in porous media*, 18, 65–85.

Levy, S. B., Fitzgerald, G. B., and Macone, A. B. (1976). "Changes in intestinal flora of farm personnel after introduction of a tetracycline-supplemented feed on a farm." *New England Journal of Medicine*, 295(11), 583–588.

Li, D., Yang, M., Hu, J., Ren, L., and Zhang, Y. (2008). "Determination and fate of

oxytetracycline and related compounds in oxytetracycline production wastewater and receiving river." *Environmental Toxicology and Chemistry*, 27 (1), 80–86.

Li, G. (2004). "Laboratory simulation of solute transport and retention in a karst aquifer." Ph.D. thesis, Florida State University, Florida State University.

Li, L.-L., Huang, L.-D., Chung, R.-S., Fok, K.-H., and Zhang, Y.-S. (2010). "Sorption and dissipation of tetracyclines in soils and compost." *Pedosphere*, 20(6), 807–816.

Li, S.-G., Ruan, F., and McLaughlin, D. (1992). "A space-time accurate method for solving solute transport problems." *Water Resources Research*, 28 (9), 2297–2306.

Li, Y., Zhang, X., Li, W., Lu, X., Liu, B., and Wang, J. (2013). "The residues and environmental risks of multiple veterinary antibiotics in animal faeces." *Environ. Monit. Assess.*, 185, 2211–2220.

Liu, A., Fong, A., Becket, E., Yuan, J., Tamae, C., Medrano, L., Maiz, M., Wahba, C., Lee, C., Lee, K., Tran, K. P., Yang, H., Hoffman, R. M., Salih, A., and Miller, J. H. (2011). "Selective advantage of resistant strains at trace levels of antibiotics: a simple and ultrasensitive color test for detection of antibiotics and genotoxic agents." *Antimicrobial Agents and Chemotherapy*, 55 (3), 1204–1210.

Liu, Y., Bao, Y., Cai, Z., Zhang, Z., Cao, P., Li, X., and Zhou, Q. (2015). "The effect of aging on sequestration and bioaccessibility of oxytetracycline in soils." *Environmental Science and Pollution Research*, 22, 10425–10433.

Loftin, K., Adams, C., Meyer, M., and Surampalli, R. (2008). "Eff ects of ionic strength, temperature, and ph on degradation of selected antibiotics." *Journal of Environmental Quality*.

Logan, J. D. (2001). *Transport Modeling in Hydrogeochemical Systems*. Springer.

Loke, M.-L., Tjørnelund, J., and Halling-Sørensen, B. (2002). "Determination of the distribution coefficient (logkd) of oxytetracycline, tylosin a, olaquindox and metronidazole in manure." *Chemosphere*, 48(3), 351–361.

Lorimor, J., Powers, W., and Sutton, A. (2004). "Manure management system series - manure characteristics." *Report No. MWPS-18 Section 1 Seconf Edition*, Midwest Plan Services - Iowa State University.

Lundström, S. V., Östmanb, M., Bengtsson-Palme, J., Rutgersson, C., Thoudal, M., Sircar, T., Blanck, H., Eriksson, K., Tysklind, M., , Flach, C.-F., and Larsson, D. J. (2016). "Minimal selective concentrations of tetracycline in complex aquatic bacterial biofilms." *Science of the Total Environment*, 553, 587–595.

Ma, L. and Selim, H. (1998). *Physical nonequilibrium in soils: modeling and application*. Ann Arbor Press, INC, Chapter Coupling of retention aprroaches to physical nonequilibrium models, 83–116.

MacKay, A. and Canterbury, B. (2005). "Oxytetracycline sorption to organic matter by metal-bridging." *Journal of Environmental Quality*, 34, 1964–1971.

MacKay, A. A. and Vasudevan, D. (2012). "Polyfunctional ionogenic compound sorption: Challenges and new approaches to advance predictive models." *Environmental Science and Technology*, 46, 9209–9223.

Mackie, R. I., Koike, S., Krapac, I., Chee-Sanford, J., Maxwell, S., and Aminov, R. (2006). "Tetracycline residues and tetracycline resistance genes in groundwater imimpact by swine production facilities." *Animal Biotechnology*, 17, 157–176.

Magga, Z., Tzovoluo, D., Theodoropoulou, M., and Tsakiroglou, C. (2012). "Combining experimental techniques with non-linear numerical models to assess the sorption of pesticides on soils." *Journal of Contaminant Hydrology*, 129-130, 62–69.

Mao, M. and Ren, L. (2004). "Simulating nonequilibrium transport of atrazine through saturated soil." *Ground Water*, 42(4), 500–508.

Martin, S. (1979). "Equilibrium and kinetic studies on the interaction of tetracyclines with calcium and magnesium." *Biophysical Chemistry*, 10, 319–326.

Martínez, J. L. (2008). "Antibiotics and antibiotic resistance genes in natural environ-

ments." *Science*, 321(5887), 365–367.

Martínez, J. L. (2009). "Environmental pollution by antibiotics and by antibiotic resistance determinants." *Environmental Pollution*, 157(11), 2893–2902.

Martínez-Carballo, E., González-Barreiro, C., Scharf, S., and Gans, O. (2007). "Environmental monitoring study of selected veterinary antibiotics in animal manure and soils in austria." *Environmental Pollution*, 148, 570–579.

Mathew, A., Cissell, R., and Liamthong, S. (2007). "Antibiotic resistance in bacteria associated with food animals: a united states perspective of livestock production." *Foodborne Pathogens and disease*, 4(2), 115–133.

McManus, P., Stockwell, V., Sundin, G., and Jones, A. (2002). "Antibiotic use in plant agriculture.." *Annual Review of Phytopathology*, 40(1), 443.

Mehl, S. (2006). "Use of picard and newton iteration for solving nonlinear ground water flow equations." *Ground Water*, 44 (4), 583–594.

Merck and Co. (2002). *Merck veterinary manual*. Merck and Co., Whitehouse, N.J., <https://libcat.tamu.edu/vwebv/holdingsInfo?bibId=2090753> Title from home page (viewed Aug. 9, 2002).

Mikkelsen, R. and Hartz, T. (2008). "Nitrogen sources for organic crop production." *Better Crops*, 92(4), 16–19.

Miranda, C. D. and Zemelman, R. (2002). "Bacterial resistance to oxytetracycline in chilean salmon farming." *Aquaculture*, 212(14), 31–47.

Muñoz, M., Autenrieth, R., and Mendoza-Sanchez, I. (2017). "Environmental occurrence of oxytetracycline and the potential selection of antibiotic resistance in bacteria." *XVI World Water Congress - Cancun, Mexico*, International Water Resources Association (IWRA), 1–15 (May 29 - June 3).

Nkedi-Kizza, P. (1983). "Modeling tritium and chloride-36 transport through an aggregated oxisol." *Water Resources Research*, 19(3), 691–700.

NRCS (2008). "Soil quality indicators - bulk density." *Report no.*, National Resources Conservation Services.

OECD (2000). "Oecd guideline for the testest of chemicals guideline 106 - january 2000.

Orem, W., Lerch, H., and Rawlik, P. (1997). "Geochemistry of surface and pore water at usgs site in wetlands of south florida: 1994 and 1995." *Open-File Report 97-454*, USGS.

Palmer, A., Angelino, E., and Kishony, R. (2010). "Chemical decay of an antibiotic inverts selection for resistance." *Nature Chemical Biology*, 6, 105–107.

Park, J.-H., Feng, Y., Ji, P., Voice, T. C., and Boyd, S. A. (2003). "Assessment of bioavailability of soil-sorbed atrazine." *Appl Environ Microbiol.*, 69(6), 3288–3298.

Parlange, J., Steenhuis, T., Haverkamp, R., Barry, D., Culligan, P., Hogarth, W., Parlange, M., Ross, P., and Stagnitti, F. (1999). *Vadose zone hydrology : cutting across disciplines*. Oxford University Press Inc., Chapter Soil properties and water movement, 99–129.

Patten, D., Kunkle, D. W. W., and Douglass, L. (1980). "Effect of antibiotics in beef cattle feces on nitrogen and carbon mineralization in soil and on plant growth and composition." *Journal of Environmental Quality*, 9 (1), 167–172.

Peak, N., Knapp, C., Yang, R., Hanfelt, M., Smith, M., Aga, D., and Graham, D. (2007). "Abundance of six tetracycline resistance genes in wastewater lagoons at cattle feedlots with different antibiotic use strategies." *Environmental microbiology*, 9(1), 143–151.

Peng, F.-J., Zhou, L.-J., Ying, G.-G., Liu, Y.-S., and Zhao, J.-L. (2014). "Antibacterial activity of soil-bound antimicrobials oxytetracycline and ofloxacin." *Environmental Toxicology and Chemistry*, 33 (4), 776–783.

Pils, J. R. V. and Laird, D. (2005). "The role of soil clays and clay-humic complexes in processes contcontrol colloidal stability and the sorption and degradation of tetracyclines." Ph.D. thesis, Iowa State University, Iowa State University.

Popova, I. E., Bair, D. A., Tate, K. W., and Parikh, S. J. (2013). "Sorption, leaching,

and surface runoff of beef cattle veterinary pharmaceuticals under simulated irrigated pasture conditions." *J. Environ. Qual.*, 42, 1167–1175.

Popova, I. E., Josue, R., Deng, S., and Hattey, J. A. (2017). "Tetracycline resistance in semi-arid agricultural soils under long-term swine effluent application." *Journal of Environmental Scienece and Health, Part B*.

Popowska, M., Miernik, A., Rzeczycka, M., and Lopaciuk, A. (2010). "The impact of environmental contamination with antibiotics on levels of resistance in soil bacteria." *Journal of Environmental Quality*, 39, 1679–1687.

Pornsukarom, S. and Thakur, S. (2016). "Assessing the impact of manure application in commercial swine farms on the transmission of antimicrobial resistant salmonella in the environment." *PLOS One*, 1–17.

Pruden, A., Larsson, D. J., Amzquita, A., Collignon, P., Brandt, K. K., Graham, D. W., Lazorchak, J. M., Suzuki, S., Silley, P., Snape, J. R., Topp, E., Zhang, T., , and Zhu, Y.-G. (2013). "Management options for reducing the release of antibiotics and antibiotic resistance genes to the environment." *Environmental Health Perspectives*, 121 (8), 878–885.

Pruden, A., Pei, R., Storteboom, H., and Carlson, K. (2006). "Antibiotic resistance genes as emerging contaminants: Studies in northern colorado." *Environmental Science and Technology*, 40(23), 7445–7450.

Quinlan, E. L., Nietch, C. T., Blocksom, K., Lazorchak, J. M., Batt, A. L., Griffiths, R., and Klemm, D. J. (2011). "Temporal dynamics of periphyton exposed to tetracycline in stream mesocosms." *Environmental Science and Technology*, 45, 10684–10690.

Rabølle, M. and Spliid, N. H. (2000). "Sorption and mobility of metronidazole, olaquindox, oxytetracycline and tylosin in soil." *Chemosphere*, 40(7), 715–722.

Rao, S. (2002a). *Applied Numerical Methods for Engineers and Scientists*. Prentice Hall, Chapter Numerical Differentiation, 500–559.

Rao, S. (2002b). *Applied Numerical Methods for Engineers and Scientists*. Prentice Hall, Chapter Partial Differential Equations, 794–884.

Rao, S. (2002c). *Applied Numerical Methods for Engineers and Scientists*. Prentice Hall, Chapter Solutionof simultaneous linear algebraic equations, 141–269.

Ratasuk, N., Boonsaner, M., and Hawker, D. W. (2012). "Effect of temperature, ph and illumination on abiotic degradation of oxytetracycline in sterilized swine manure." *Journal of Environmental Science and Health, Part A*, 47((11)), 1687–1694.

Recktenwald, G. W. (2011). "Finite-difference approximations to the heat equation.

Reddy, J. (2015). *An Introduction to Nonlinear Finite Element Analysis - with applications to heat transfer, fuid mechanics, and Solid mechanics*. Oxford University Press Inc., second edition edition.

Rees, T., Bright, D., Fay, R., Christensen, A., Anders, R., Anders, B., Baharie, B., and Land, M. (1995). "Geohydrology, water quality, and nitrogen geochemistry in the saturated and saturated zones beneath various land uses, riveside and san bernardino counties, califronia, 1991-93." *Water-Resources Investigations Report 94-4127*, USGS.

Riffaldi, R., Levi-Minzi, R., and Saviozzi, A. (1983). "Humic fractions of organic wastes." *Agriculture, Ecosystems and Environment*, 10, 353–359.

Rose, P. and Pedersen, J. (2005). "Fate of oxytetracycline in streams receiving aquaculture discharges: Model simulations." *Environmental Toxicology and Chemistry*, 24(1), 40–50.

Samuelsen, O. B. (1989). "Degradation of oxytetracycline in seawater at two different temperatures and light intensities, and the persistence of oxytetracycline in the sediment from a fish farm." *Aquaculture*, 83(12), 7–16.

Samuelsen, O. B., Torsvik, V., and Ervik, A. (1992). "Long-range changes in oxytetracycline concentration and bacterial resistance towards oxytetracycline in a fish farm sediment after medication." *Science of the Total Environment*, 114(0), 25–36.

Sanderson, H., Ingerslev, F., Brain, R., Sørensen, B. H., Bestari, J., Wilson, C., Johnson, D., and Solomon, K. (2005). "Dissipation of oxytetracycline, chlortetracycline, tetracycline and doxycycline using hplc-uv and lc/ms/ms under aquatic semi-field microcosm conditions." *Chemosphere*, 60, 619–629.

Sarmah, A., Meyer, M., and Boxall, A. (2006). "A global perspective on the use, sales, exposure pathways, occurrence, fate and effects of veterinary antibiotics (vas) in the environment." *Chemosphere*, 65(5), 725–759.

Sassman, S. and Lee, L. (2005). "Sorption of three tetracyclines by several soils: Assessing the role of ph and cation exchange." *Environmental Science and Technology*, 39(19), 7452–7459.

Schmitt, H., Stoob, K., Hamscher, G., Smit, E., and Seinen, W. (2006). "Tetracyclines and tetracycline resistance in agricultural soils: Microcosm and field studies.." *Microbial ecology*, 51(3), 267–276.

Schwaiger, K., Harms, K., Hoölzel, C., Meyer, K., Karl, M., and Bauer, J. (2009). "Tetracycline in liquid manure selects for co-occurrence of the resistance genes tet(m) and tet(l) in enterococcus faecalis." *Veterinary Microbiology*, 139, 386–392.

Selim, H. (2015). *Transport and fate of chemicals in soils: Principles and Applications*. CR, Chapter Transport, 63–102.

Selim, H. M., Davidson, J., and Rao, P. (1977). "Transport reactive ssolute through multilayered soils." *Soil Sci*, 41, 3–10.

Selim, H. M., J.M., D., and Mansell, R. (1976). "Evaluation of a two-site adsorption-desorption model for describing solute transport in soils.." *In Proc. Summer Computer Simulation conference*, Washington, DC.

Selim, H. M. and Ma, L. (1998). *Physical nonequilibrium in soils: modeling and application*. Ann Arbor Press, INC.

Sengeløv, G., Agerso, Y., Sørensen, B. H., Baloda, S. B., Andersen, J. S., and Jensen, L. B.

(2003). “Bacterial antibiotic resistance levels in danish farmland as a result of treatment with pig manure slurry.” *Environment International*, 28(7), 587–595.

Serrano, S. (2001). “Solute transport under non-linear sorption and decay.” *Water Resources*, 35(6), 1525–1533.

Shao, B., Chen, D., Zhang, J., Wu, Y., and Sun, C. (2009). “Determination of 76 pharmaceutical drugs by liquid chromatographytandem mass spectrometry in slaughterhouse wastewater.” *Journal of Chromatography A*, 1216(47), 8312–8318.

Shentu, J., Zhang, K., Shen, D., Wang, M., and Feng, H. (2015). “Effect from low-level exposure of oxytetracycline on abundance of tetracycline resistance genes in arable soils.” *Environmental Science and Pollution Research*, 22, 13102–13110.

Sim, W.-J., Lee, J.-W., Lee, E.-S., Shin, S.-K., Hwang, S.-R., and Oh, J.-E. (2011). “Occurrence and distribution of pharmaceuticals in wastewater from households, livestock farms, hospitals and pharmaceutical manufactures.” *Chemosphere*, 82(2), 179–186.

Simon, N. S. (2005). “Loosely bound oxytetracycline in riverine sediments from two tributaries of the chesapeake bay.” *Environmental Science and Technology*, 39(10), 3480–3487.

Singh, G., van Genuchten, M., Spender, W., Cliath, M., and Yates, S. (1996). “Measured and predicted transport of two s-triazine herbicides through soil columns.” *Water, air and soil pollution*, 86, 137–149.

Sithole, B. B. and Guy, R. D. (1987a). “Models for tetracycline in aquatic environments 2, interation whit humic substances.” *Water, air and soil pollution*, 32(3-4), 315–321.

Sithole, B. B. and Guy, R. D. (1987b). “Models for tetracycline in aquatic environments. i. interaction with bentonite clay systems.” *Water, air and soil pollution*, 32(3-4), 303–314.

Smith, D. L., Harris, A. D., Johnson, J. A., Silbergeld, E. K., and Morris, J. G. (2002). “Animal antibiotic use has an early but important impact on the emergence of antibi-

otic resistance in human commensal bacteria." *Proceedings of the National Academy of Sciences*, 99(9), 6434–6439.

Socolofsky, S. A. and Jirka, G. H. (2005). *Special Topics in Mixing and Transport Processes in the Environment, 5th edition*. Chapter Advective Diffusion Equation, 29–50.

Spika, J. S., Waterman, S. H., Hoo, G. W. S., Louis, M. E. S., Pacer, R. E., James, S. M., Bissett, M. L., Mayer, L. W., Chiu, J. Y., Hall, B., Greene, K., Potter, M. E., Cohen, M. L., and Blake, P. A. (1987). "Chloramphenicol-resistant salmonella newport traced through hamburger to dairy farms." *N Engl J Med*, 316(10), 565–570.

Sposito, G. (2008). *The Chemistry of Soils*. Oxford University Press Inc.

G. Sposito and R. Reginato, eds. (1992). *Oportunities in Basic Soil Science Research*. Soil Science Society of America, Inc.

Spurlock, F., Juang, K., and van Genuchten, M. (1995). "Isothern nonnonlinear and nonequilibrium sorption effects on transport of fenuron and monuron in soil columns." *Environ. Sci. Technol*, 29, 1000–1007.

Stagnitti, F., Villiers, N., andT. S. Steenhuis, J.-Y. P., de Rooij, G. H., Li, L., Barry, D. A., Xiong, X., and Li, P. (2003). "Solute and contamiant transport in heterogeneous soils." *Bull. Environ. Contam. Toxicol.*, 71, 737–745.

Stichler, C. and McFarland, M. (1997). "Crop nutrient need in South and Southwest Texas." *Report No. B-6053*, Texas A&M University - AgriLIFE Extension.

Stone, J., Dresi, E., Lupo, C., and Clay, S. (2011). "Land application of tylosin and chlortetracycline swine manure: Impacts to soil nutrients and soil microbial community structure." *Journal of Environmental Science and Health, Part B.*, 46, 752–762.

Storteboom, H., Kim, S.-C., Doesken, K., Carlson, K., Davis, J., and Pruden, A. (2007). "Response of antibiotics and resistance genes to high-intensity and low-intensity manure management." *Journal of Environmental Quality*, 36, 1695–1703.

Swanson, R. and Dutt, G. (1973). "Chemical and physical processes that affect atrazine

and distribution in soil systems." *Soil Sci. Soc. Am. J.*, 37(6), 872–876.

Tacker, P., Vories, E., and Huitink, G. (2008). *Corn Production Handbook*. Number MP437, Cooperative extension service - University of Arkansas, Chapter Drainage and Irrigation, 13–22.

Teixido, M., Granados, M., Prat, M., and Beltran, J. (2012). "Sorption of tetracyclines onto natural soils: data analysis and prediction." *Environmental Science and Pollution Research*, 19(8), 3087–3095.

ter Laak, T., Gebbink, W., and Tolls, J. (2006a). "The effect of ph and ionic strenght on the sorption of sulfachloropyridazine, tylosin and oxytetracycline to soil.." *Environmental Toxicology and Chemistry*, 25(4), 22–22.

ter Laak, T. L., Gebbink, W. A., and Tolls, J. (2006b). "Estimation of soil sorption coefficients of veterinary pharmaceuticals from soil properties." *Environmental Toxicology and Chemistry*, 25(4), 933–941.

Thiele-Bruhn, S. (2005). "Microbial inhibition by pharmaceutical antibiotics in different soils-dose response relations determined with the iron(iii) reduction test." *Environmental Toxicology and Chemistry*, 24(4), 869–876.

Thiele-Bruhn, S. and Beck, I.-C. (2005). "Effects of sulfonamide and tetracycline antibiotics on soil microbial activity and microbial biomass." *Chemosphere*, 59(4), 457–465.

Thomas, J. (1995a). *Numerical Partial Differential Equations - Finite Difference Methods*. Springer, Chapter Chapter 5: Hyperbolic Equations, 205–259.

Thomas, J. (1995b). *Numerical Partial Differential Equations - Finite Difference Methods*. Springer, Chapter Chapter 2: Some Theoretical Considerations, 41–96.

Thomas, J. (1995c). *Numerical Partial Differential Equations - Finite Difference Methods*. Springer, Chapter Chapter 3: Stability, 97–145.

Tolls, J. (2001). "Sorption of veterinary pharmaceuticals in soils: A review." *Environmental Science and Technology*, 35(17), 3397–3406.

Toride, N., Leij, F., and van Genuchten, M. (1993). "A comprehensive set of analytical solutions for non-equilibrium solute transport with first order daecay and zero order production." *Water Resources Research*, 29(7), 2167–2182.

Travis, C. (1978). "Mathematical description of adsorption and transport of reactive ssolute in soil: a review of selected literature." *Report No. ORNL-5403*, Oak Ridge National Laboratory.

USDA (2009a). *Agricultural Waste Management Field Handbook*, Vol. Part 651. USDA NRCS, Chapter Agricultural Waste Characteristics, 4–1 – 4–26.

USDA (2009b). *Agricultural Waste Management Field Handbook*, Vol. Part 651. USDA NRCS, Chapter Waste Utilization, 11–1 – 11–36.

van der Zee, S. and Leijnse, A. (2013). *Soil processes and current trands in quality assessment*. Intech, Chapter Solute transport in soil, 33–86.

van Genuchten, M. A. T. (1981). "Non-equilibrium transport parameters from miscible displacement experiments." *Report No. 119*, United States Department of Agriculture - Science and Education Administration - U.S. Salinity Laboratory - Riverside, California.

van Genuchten, M. A. T., J.M., D., and Wierenga, P. J. (1974). "An evaluation of kinetic and equilibrium equations for the prediction of pesticide movement through porous media." *Soil Sci. Soc. Am. Proc.*, 38, 29–35.

van Genuchten, M. A. T. and Wagenet, R. (1989). "Two-site/two-region models for pestcide transport and degradation: theoretical development and analytical solutions." *Soil Sci. Soc. Am. J.*, 53(5), 1303–1310.

van Genuchten, M. A. T. and Wierenga, P. J. (1976). "Mass transfer studies in sorbing porous media I. Analytical solutions." *Soil Science Society of America Journal*.

van Genuchten, M. T. and Alves, W. (1982). "Analytical solutions of the one-dimensional convective dispersive solute transport equation." *Technical Bulletin Number 1661*,

USDA (June).

van Genuchten, M. T., Leij, F. J., Skaggs, T. H., Toride, N., Bradford, S. A., and Pontedeiro, E. M. (2013). "Exact analytical solutions for contaminant transport in rivers 1. the equilibrium advection-dispersion equation." *J. Hydro. Hydromech.*, 61(2), 146–160.

van Genuchten, M. T. and Wierenga, P. (1986). *Methods of Soil Analysis. Part 1. Physical and Mineralogical Methods*. American Society of Agronomy-Soil Science Society of America, Chapter Solute dispersion coefficients and retardation factors, 1025–1054.

van Genuchten, M. T., Wierenga, P., and O'Connor, G. (1977a). "Mass transfer studies in sorbing porous media: II. Experimental evaluation with tritium (^3H_2O)." *Soil Sci. Soc. Am. J.*, 41, 272–278.

van Genuchten, M. T., Wierenga, P., and O'Connor, G. (1977b). "Mass transfer studies in sorbing porous media: III. Experimental evaluation with 2,4,5-T." *Soil Sci. Soc. Am. J.*, 41, 278–285.

Šimůnek, J. (2005). *Encyclopedia of hydrological sciences*. John Wiley and Sons Ltd, Chapter Models of water flow and solute transport in the unsaturated zone, 1171–1180.

Šimůnek, J. and van Genuchten, M. (2007). *The Handbook of Groundwater Engineering*. CRC PRESS, Chapter Contaminant Transport in the Unsaturated Zone: Theory and Modeling, 22.1–22.46.

Wang, Q. and Yates, S. (2008). "Laboratory study of oxytetracycline degradation kinetics in animal manure and soil." *Journal of Agricultural and Food Chemistry*, 56(5), 1683–1688.

Watanabe, N., Bergamaschi, B., Loftin, K., Meyer, M., and Harter, T. (2010). "Use and environmental occurrence of antibiotics in freestall dairy farms with manured forage fields." *Environmental Science and Technology*, 44(17), 6591–6600.

Watkinson, A. J., Murby, E. J., and Costanzo, S. D. (2007). "Removal of antibiotics in conventional and advanced wastewater treatment: Implications for environmental

discharge and wastewater recycling." *Water Research*, 41(18), 4164–4176.

Wegst-Uhrich, S. R., Navarro, D. A., Zimmerman, L., and Aga, D. (2014). "Assessing antibiotic sorption in soil: a literature review and new case studies on sulfonamides and macrolides." *Chemistry Central Journal*, 8(5), 1–12.

Wehrhan, A. (2006). *Fate of veterinary pharmaceuticals in soil: An experimental and numerical study on the mobility, sorption and transformation of sulfadiazine*. Forschungszentrum Jlich GmbH.

WHO (2009). "Critically important antimicrobials for human medicine: 2nd revision." *Report no.*, Department of Food Safety, Zoonoses and Foodborne Dieseases.

Williams-Nguyen, J., Sallach, J. B., Bartelt-Hunt, S., Boxall, A. B., Durso, L. M., McLain, J. E., Singer, R. S., Snow, D. D., and Zilles, J. L. (2016). "Antibiotics and antibioti resistance in agroecosystems: State of science." *Journal of Environmental Quality*, 45, 394–406.

Winckler, C., Engels, H., Hund-Rinke, K., Luckow, T., Simon, M., and Steffens, G. (2004). "Behaviour of tetracycline and other veterinary antibiotics in organic fertilizers and soil working title: Effects of tetracyclines and other veterinary pharmaceuticals on soil (verhalten von tetracyclinen und anderen veterinärantibiotika in wirtschaftsdünger und boden - arbeitstitel: Wirkung von tetrazyklinen und anderen tierarzneimitteln auf die bodenfunktion)." *Report No. UFOPLAN 200-73-248*, Umweltbundesamtes.

Witte, W. (1998). "Medical consequences of antibiotic use in agriculture." *Science*, 279(5353), 996–997.

Wright, G. D. (2010). "Antibiotic resistance in the environment: a link to the clinic?." *Current Opinion in Microbiology*, 13, 589–594.

Wu, L., Pan, X., Chen, L., Huan, Y., Teng, Y., Luo, Y., and Christie, P. (2013). "Occurrence and distribution of heavy metals and tetracyclines in agricultural soils after typical land use change in east china." *Environmental Science and Pollution Research*, 20(12), 8342–

8354.

Yang, Q., Zhang, J., Zhu, K., and Zhang, H. (2009). "Influence of oxytetracycline on the structure and activity of microbial community in wheat rhizosphere soil." *Journal of Environmental Science*, 21, 954–959.

Yang, S. and Carlson, K. (2003). "Evolution of antibiotic occurrence in a river through pristine, urban andagricultural landscapes." *Water Research*, 37, 4645–4656.

Yin, C., Luo, Y., Teng, Y., Zhang, H., Chen, Y., and Zhao, Y. (2012). "Pollution characteristics and accumulation of antibiotics in typical protected vegetable soils." *Huan Jing Ke Xue*, 33(8), 2810–2816.

Yue, D. (2011). "Lecture notes - marine hydrolecture (lecture 2 - basic concepts). http://web.mit.edu/2.20/www/lectures/lec02/lecture2.pdf.

Zarba, R. (1988). "A numerical investigation of unsaturated flow." M.S. thesis, Massachusetts Institute of Technology, Massachusetts Institute of Technology.

Zhang, H., Luo, Y., Wu, L., Huang, Y., and Christie, P. (2015). "Residues and potential ecological risks of veterinary antibiotics in manures and composts associated with protected vegetable farming." *Environ Sci Pollut Res*, 22, 5908–5918.

Zhang, Y., Zhang, C., Parker, D. B., Snow, D. D., Zhou, Z., and Li, X. (2013). "Occurrence of antimicrobials and antimicrobial resistance genes in beef cattle storage ponds and swine treatment lagoons." *Science of the Total Environment*, 463-464, 631–638.

Zhao, L., Dong, Y. H., and Wang, H. (2010). "Residues of veterinary antibiotics in manures from feedlot livestock in eight provinces of china." *Science of the Total Environment*, 408, 1069–1075.

Zheng, C. and Bennett, G. (2002a). *Applied Contaminant Transport Modeling*. John WIley and Sons Inc, Chapter Ch-10. Building a Contaminant Transport Model, 271–315.

Zheng, C. and Bennett, G. (2002b). *Applied Contaminant Transport Modeling*. John WIley and Sons Inc, Chapter Ch-4. Transport with chemical reactions, 78–106.

Zheng, C. and Bennett, G. (2002c). *Applied Contaminant Transport Modeling*. John WIley and Sons Inc, Chapter Ch-7. Simulation of Advective-Dispersive Transport, 171–234.

Zheng, C. and Bennett, G. (2002d). *Applied Contaminant Transport Modeling*. John WIley and Sons Inc, Chapter Ch-5. Mathematical model and analytical solutions, 107–122.

Zheng, C. and Bennett, G. (2002e). *Applied Contaminant Transport Modeling*. John WIley and Sons Inc, Chapter Ch-12. Model Calibration and Sensitivity Analysis, 316–348.

Zhou, L. (2002). "Solute transport in layered and heterogeneous soils." Ph.D. thesis, Louisiana State University and Agricultural and Mechanical College, Louisiana State University and Agricultural and Mechanical College.

Zhou, L.-J., Ying, G.-G., Liu, S., Zhang, R.-Q., Lai, H.-J., Chen, Z.-F., and Pan, C.-G. (2013). "Excretion masses and environmental occurrence of antibiotics in typical swine and dairy cattle farms in china." *Science of the Total Environment*, 444, 183–195.

Zilles, J., Shimada, T., Jindal, A., Robert, M., and Raskin, L. (2005). "Presence of macrolide-lincosamide-streptogramin b and tetracycline antimicrobials in swine waste treatment processes and amended soil." *Water Environment Research*, 77(1), 57–62.

Zou, Y. and Zheng, W. (2013). "Modeling manure colloid-facilitated transport of the weakly hydrophobic antibiotic florfenicol in saturated soil columns." *Environ. Sci. Technol*, 47, 5185–5192.

Zwonitzer, M. R., Soupir, M. L., Jarboe, L. R., and Smith, D. R. (2016). "Quantifying attachment and antibiotic resistance of escherichia coli from conventional and organic swine manure." *Journal of Environmental Quality*, 45, 609–617.

APPENDIX A

OTC CONCENTRATIONS IN AQUEOUS MEDIA

Table A.1: OTC Concentrations in aqueous media

Source	Media	Concentration (ng/ml)	Location	Reference
Ag	Surface water	0.05 0.32	Korea	Awad et al. (2013)
		4.49	UK	Boxall et al. (2006)
		0.01 0.01 0.01 0.01 0.01 0.01 0.01 1.78 0.83 1.12 0.48 0.38 0.25	USA	Kim et al. (2007)
		0.015 0.018 0.024 0.021 0.016 0.019 0.312 0.204 0.072 0.02 0.021 0.019	China	Shao et al. (2009)
		0.07	USA	Yang and Carlson (2003)

Table A.1: Continued

Source	Media	Concentration (ng/ml)	Location	Reference
Ag	Surface water	0.15	USA	Yang and Carlson (2003)
	WWTP influent	0.163 1.481 0.095 0.928 0.367 1.19 0.26 2.942	China	Shao et al. (2009)
	WWTP effluent	0.081 0.916 0.011 0.113 0.082 0.526 0.011 0.1	China	Shao et al. (2009)
	Runoff	0.9	UK	Blackwell et al. (2007)
		32 71.7	UK	Kay et al. (2005c)
		0.26 0.11	USA	Popova et al. (2013)
	Groundwater	0.15 0.19	Germany	Hamscher et al. (2000)
		0.08 0.13	USA	Mackie et al. (2006)
	WW lagoon	0.093 0.31 0.66 0.19 0.1 0.18	USA	Watanabe et al. (2010)
		1.471 2.138 0.01 0.394 0.125	USA	Zhang et al. (2013)
		1.41 0.586	China	Zhou et al. (2013)

Table A.1: Continued

Source	Media	Concentration (ng/ml)	Location	Reference
Ag	Anaerobic Digestor	9800 6800 6600 6900 4000	USA	Arikan et al. (2006)
Urban	Surface water	0.0022	China	Jia et al. (2009)
		0.01 0.01 0.01 0.01 0.01 0.01 0.01 0.02 0.02	USA	Kim and Carlson (2007)
		0.34	USA	Kolpin et al. (2002)
	WWTP influent	0.0226	USA	Gao et al. (2012)
		0.0725	China	Jia et al. (2009)
		8.66	China	Sim et al. (2011)
		0.64	USA	Yang and Carlson (2003)
	WWTP effluent	0.021	USA	Gao et al. (2012)
		0.0038	China	Jia et al. (2009)
		3.38	China	Sim et al. (2011)
		0.66	USA	Yang and Carlson (2003)
Industrial	Surface water	712 689 523 612 531 371 484 411 235	China	Li et al. (2008)
	WWTP influent	920000	China	Li et al. (2008)
	WWTP effluent	19500	China	Li et al. (2008)

APPENDIX B

OTC CONCENTRATIONS IN SOLID MEDIA

Table B.1: OTC Concentrations in solid media

Source	Media	Concentration (μg/kg)	Location	Reference
Ag	Sediment	1160 1900 650 930 940 1100 3280 2710 700 1340	USA	Simon (2005)
		6.2 7.1 8 6.8 7.4 13 13.2 13.9 18.1 19.7 18.9 5.6 5.9 6.1 23.7 23.1 24.1 10.5 8.7	USA	Kim and Carlson (2007)

Table B.1: Continued

Source	Media	Concentration (μg/kg)	Location	Reference
Ag	Sediment	8.7 35.7 35.4 35.2	USA	Kim and Carlson (2007)
		0.47 1.43	Korea	Awad et al. (2013)
		813	UK	Boxall et al. (2006)
Fish farm	Sediment	130 4900 1200 3600 2400 1000 460	Norway	Jacobsen and Berglind (1988)
		60 100 290 10 50 200 50 200 300 500 10 60 100 200 10 100 10400 900 4100 4700 1500 9300 6300 2100 4400	Finland	Björklund et al. (1990)

Table B.1: Continued

Source	Media	Concentration (μg/kg)	Location	Reference
Fish farm	Sediment	6700 2600 4200 1600 800 3600 2200 1200 3700 2500 1300 3700 1700 5600 2700 4400 1800 500 5700 2300 4400 1300 900	Finland	Björklund et al. (1990)
		26200 15800 30500 20600 39000 9800 4100 1700 283300 287000 139000 107000 71000 41600 20400 190600	Norway	Samuelsen et al. (1992)

Table B.1: Continued

Source	Media	Concentration (μg/kg)	Location	Reference
Fish farm	Sediment	103500 100000 66700 35100 18300 7800 4600	Norway	Samuelsen et al. (1992)
		900 200 500 1200 800 3400 1400 1100 1000 1600 1100 800 500 300 900 600 800 700	USA	Capone et al. (1996)
		1300 3800 4500 4500 4200	Ireland	Kerry et al. (1996)
		26000 285000	Norway	Samuelsen et al. (1992)
Urban	Sediment	5.1 5.8 5.9 2.6 1.8 2.8 19.5	USA	Kim and Carlson (2007)

Table B.1: Continued

Source	Media	Concentration (μg/kg)	Location	Reference
Urban	Sediment	18.8 19.1 7.3 7.6 8.4 8.2 7.5 9.3 6.8 7.5 7.6 9.4 10.4 9.9 56.2 56 56.2	USA	Kim and Carlson (2007)
Industrial	Sediment	236000 262000 171000 197000 240000 166000 212000 201000 139000	China	Li et al. (2008)
Urban	Sludge	174.21 1553.5 7369.67	China	An et al. (2015)
Industrial	Sludge	3.76E+06	China	Li et al. (2008)
Cattle	Sludge	109	USA	Watanabe et al. (2010)
		4.6 2.6 13.4 24.6 4.6 9.5 1.9 2.9	USA	Zhang et al. (2013)

Table B.1: Continued

Source	Media	Concentration (μg/kg)	Location	Reference
Swine	Sludge	65.6 16 32.6 14.6 7.7 8.4	USA	Zhang et al. (2013)
		0.35 0.41 4.26	USA	Mackie et al. (2006)
		178 127	China	Zhou et al. (2013)
Cattle	Fresh	11300	USA	Patten et al. (1980)
		871700	Italy	de Liguoro et al. (2003)
		130 1940	China	Zhang et al. (2015)
		210 10370	China	Li et al. (2013)
		320 59590	China	Zhao et al. (2010)
		70 620 100 450	Iran	Alavi et al. (2015)
		18000	USA	Arikan et al. (2009)
		62000	USA	Arikan et al. (2006)
Swine	Fresh	210 29000	Austria	Martínez-Carballo et al. (2007)
		1600 136000	Germany	Winckler et al. (2004)
		21.5 43429	China	Zhang et al. (2015)
		150 59060	China	Zhao et al. (2010)
		730 56810	China	Li et al. (2013)
		371 799 1700 558	China	Zhou et al. (2013)

Table B.1: Continued

Source	Media	Concentration (μg/kg)	Location	Reference
Swine	Fresh	371 235 661	China	Zhou et al. (2013)
Poultry	Fresh	19 416750	China	Zhang et al. (2015)
		960 13390	China	Li et al. (2013)
		340 5870 80 490 540 550 47 170 340 13770	Iran	Alavi et al. (2015)
		270 10560	China	Zhao et al. (2010)
Cattle	Aged	60	Turkey	Karci and Balcioǵlu (2009)
		19000 8780 7930 11910 6360 2110 820	Italy	de Liguoro et al. (2003)
		12000 8200 5900 2500 12900 2300 2700 1500 2100 7700 1600 300	USA	Arikan et al. (2009)

Table B.1: Continued

Source	Media	Concentration (μg/kg)	Location	Reference
Cattle	Aged	300 400 4600	USA	Arikan et al. (2009)
Swine	Aged	1400 1600 37 60 880 990	Denmark	Jacobsen and Halling-Sørensen (2006)
		18000 25000 27000 29000 24000 22000 1000	Italy	Brambilla et al. (2007)
		1000 2000 3000 6000 5000 5000 8000	Italy	Brambilla et al. (2007)
		19000	China	Zhou et al. (2013)
Poultry	Aged	330 260 230 470	Turkey	Karci and Balcioǵlu (2009)

Table B.2: OTC Concentrations in soil

Media	Concentration (μg/kg)	Location	Reference
Soil	1410 52.3 8.59	China	Zhou et al. (2013)
	0.9 8.6	Germany	Hamscher et al. (2000)
	526 399 370 180 64 91 63 148 101 47 67 25 28 24	UK	Blackwell et al. (2007)
	270.05 0.55 51.89 0.67 0.77 0.52 2.67 64.98 0.81 0.9 22.08 1.1 3.6 1.02	USA	Aga et al. (2005)
	17.62 608.82 1398.47	China	An et al. (2015)
	25 32.1 22.4	Spain	Andreu et al. (2009)

Table B.2: Continued

Media	Concentration (μg/kg)	Location	Reference
Soil	34.2 29.6 52.2 45.7 32.2 15.7 32.3 105.4 95.8 34.5 45.2 52.2 22.7 25.4 67.6 34.5 28.5 92.9	Spain	Andreu et al. (2009)
	10 20 30 110 130 140 140 230 500	Turkey	Karci and Balcioǵlu (2009)
	309 349 922 1073 62 131 168 1541 274 158 322 135	UK	Kay et al. (2004)

Table B.2: Continued

Media	Concentration (μg/kg)	Location	Reference
Soil	194 104 258 51 213 182	UK	Kay et al. (2004)
	11.3 79.5 7.2 613.2 8.3 23.1 44.7 219.1 7.2 613.2 192 82.65 17.15 14.57 23.34 11.72 6.61 7.4 7.1 6.61 13.21 6.05 5.66	China	Huang et al. (2013)
	0.09 0.52 0.31 0.71	Korea	Awad et al. (2013)
	0.48 1.54 6.72 2.92 0.91 1.58	China	Wu et al. (2013)

Table B.2: Continued

Media	Concentration (μg/kg)	Location	Reference
Soil	0.91 0.99 0.3 1.17 1.67 0.71 0.87 0.91 1.03 0.48	China	Wu et al. (2013)
	6.06 332.02	China	Yin et al. (2012)
	130 216 206 157 188 127	Italy	Brambilla et al. (2007)
	6 7	Italy	de Liguoro et al. (2003)
	124 2683	China	Hu et al. (2010)
	305	UK	Boxall et al. (2006)
	500	USA	Zilles et al. (2005)

APPENDIX C

THOMAS ALGORITHM

C.1 Thomas Algorithm programed for Matlab

```
function M = Thomas_al(nodes, a, b, c, RHS )

    C_t(1) = c(1)/b(1);
    rhs_tt(1) = RHS(1)/b(1);

    for j = 2:nodes-1
        B_t(j) = b(j) - a(j)*C_t(j-1);
        rhs_t(j) = RHS(j) - a(j)*rhs_tt(j-1);
        C_t(j) = c(j)/B_t(j);
        rhs_tt(j) = rhs_t(j)/B_t(j);
    end

        B_t(nodes) = b(nodes)-a(nodes)*C_t(nodes-1);
        rhs_t(nodes) = RHS(nodes) - a(nodes)*rhs_tt(nodes-1);
        M(nodes) = rhs_t(nodes)/B_t(nodes);

        for jj = nodes-1:-1:1
            M(jj) = rhs_tt(jj) - C_t(jj)*M(jj+1);
        end
end
```

APPENDIX D

FINITE DIFFERENCE METHOD

$$\frac{\partial c}{\partial t}+\frac{\rho_b}{\theta}\frac{\partial s_1}{\partial t}+\frac{\rho_b}{\theta}\frac{\partial s_2}{\partial t}=D\frac{\partial^2 c}{\partial x^2}-v\frac{\partial c}{\partial x}-\mu_L c-\frac{\rho_b}{\theta}\mu_{s1}s_1-\frac{\rho_b}{\theta}\mu_{s2}s_2 \tag{D.1}$$

$$s_1=f(c)=fK_f c^N \tag{D.2}$$

$$\frac{\partial c}{\partial t}+\frac{\rho_b}{\theta}\frac{\partial fK_f c^N}{\partial t}+\frac{\rho_b}{\theta}\frac{\partial s_2}{\partial t}=D\frac{\partial^2 c}{\partial x^2}-v\frac{\partial c}{\partial x}-\mu_l c-\frac{\rho_b}{\theta}\mu_{s1}fK_f c^N-\frac{\rho_b}{\theta}\mu_{s2}s_2 \tag{D.3}$$

$$\frac{\partial\left(1+\frac{\rho_b fK_f c^{N-1}}{\theta}\right)c}{\partial t}+\frac{\rho_b}{\theta}\frac{\partial s_2}{\partial t}=D\frac{\partial^2 c}{\partial x^2}-v\frac{\partial c}{\partial x}-\mu_l c-\frac{\rho_b}{\theta}\mu_{s1}fK_f c^N-\frac{\rho_b}{\theta}\mu_{s2}s_2 \tag{D.4}$$

$$\frac{\partial\theta\left(1+\frac{\rho_b fK_f c^{N-1}}{\theta}\right)c}{\partial t}+\rho_b\frac{\partial s_2}{\partial t}=\theta D\frac{\partial^2 c}{\partial x^2}-\theta v\frac{\partial c}{\partial x}-\theta\mu_l c-\rho_b\mu_{s1}fK_f c^N-\rho_b\mu_{s2}s_2 \tag{D.5}$$

$$M=\theta Rc=\theta\left(1+\frac{\rho_b fK_f c^{N-1}}{\theta}\right)c=\theta c+\rho_b K_f c^N \tag{D.6}$$

$$\frac{\partial M}{\partial c}=\frac{\partial(\theta c+\rho_b fK_d c^N)}{\partial c}=\theta+\rho_b K_d N c^{N-1} \tag{D.7}$$

$$\frac{\partial M}{\partial c}\frac{\partial c}{\partial t} = \frac{\partial M}{\partial t} = \frac{\partial \left(\theta + \rho_b f K_d N c^{N-1}\right) c}{\partial t} \tag{D.8}$$

$$\frac{\partial M}{\partial t} + \rho_b \frac{\partial s_2}{\partial t} = \theta D \frac{\partial^2 c}{\partial x^2} - \theta v \frac{\partial c}{\partial x} - \theta \mu_l c - \rho_b \mu_{s1} f K_f c^N - \rho_b \mu_{s2} s_2 \tag{D.9}$$

Full discretization

$$\begin{aligned} \frac{M_i^{n+1} - M_i^n}{\Delta t} + \rho_b \frac{s_{2_i}^{n+1} - s_{2_i}^n}{\Delta t} &= \theta D \left(\frac{c_{i+1}^{n+\frac{1}{2}} - 2c_i^{n+\frac{1}{2}} + c_{i-1}^{n+\frac{1}{2}}}{\Delta x^2} \right) \\ &- \theta v \left(\frac{c_{i+1}^{n+\frac{1}{2}} - c_{i-1}^{n+\frac{1}{2}}}{2\Delta x} \right) \\ &- \theta \mu_l c_i^{n+\frac{1}{2}} - \rho_b \mu_{s1} f K_f {c_i}^{n+\frac{1}{2}N} \\ &- \rho_b \mu_{s2} s_{2_i}^{n+\frac{1}{2}} \end{aligned} \tag{D.10}$$

Adding w_1 and w_2 as the temporal weighting factors for the concentration from the dispersion and advection term respectively.

$$
\begin{aligned}
\frac{M_i^{n+1} - M_i^n}{\Delta t} + \rho_b \frac{s_{2_i}^{n+1} - s_{2_i}^n}{\Delta t} &= w_1 \theta D \left(\frac{c_{i+1}^{n+1} - 2c_i^{n+1} + c_{i-1}^{n+1}}{\Delta x^2} \right) \\
&- w_2 \theta v \left(\frac{c_{i+1}^{n+1} - c_{i-1}^{n+1}}{2\Delta x} \right) \\
&- w_4 \theta \mu_l c_i^{n+1} \\
&- w_4 \rho_b \mu_{s1} f K_f {c_i}^{n+1^N} \\
&- w_4 \rho_b \mu_{s2} s_{2_i}^{n+1} \\
&+ (1 - w_1) \theta D \left(\frac{c_{i+1}^n - 2c_i^n + c_{i-1}^n}{\Delta x^2} \right) \\
&- (1 - w_2) \theta v \left(\frac{c_{i+1}^n - c_{i-1}^n}{2\Delta x} \right) \\
&- (1 - w_4) \theta \mu_l c_i^n \\
&- (1 - w_4) \rho_b \mu_{s1} f K_f {c_i}^{n^N} \\
&- (1 - w_4) \rho_b \mu_{s2} s_{2_i}^n
\end{aligned}
\tag{D.11}
$$

Moving all $n+1$ term to the left hand side

$$\begin{aligned}
\frac{M_i^{n+1}-M_i^n}{\Delta t} &+ \rho_b \frac{s_{2_i}^{n+1}-s_{2_i}^n}{\Delta t} \\
&- w_1\theta D\left(\frac{c_{i+1}^{n+1}-2c_i^{n+1}+c_{i-1}^{n+1}}{\Delta x^2}\right) \\
&+ w_2\theta v\left(\frac{c_{i+1}^{n+1}-c_{i-1}^{n+1}}{2\Delta x}\right) \\
&+ w_4\theta\mu_l c_i^{n+1} \\
&+ w_4\rho_b\mu_{s1} f K_f {c_i}^{n+1^N} + w_4\rho_b\mu_{s2}s_{2_i}^{n+1} \\
&= (1-w_1)\theta D\left(\frac{c_{i+1}^{n}-2c_i^{n}+c_{i-1}^{n}}{\Delta x^2}\right) \\
&- (1-w_2)\theta v\left(\frac{c_{i+1}^{n}-c_{i-1}^{n}}{2\Delta x}\right) \\
&- (1-w_4)\theta\mu_l c_i^n \\
&- (1-w_4)\rho_b\mu_{s1} f K_f {c_i}^{n^N} - (1-w_4)\rho_b\mu_{s2}s_{2_i}^n
\end{aligned} \tag{D.12}$$

Individualizing each term and multiplying times Δt

$$\begin{aligned}
& M_i^{n+1} - M_i^n + \rho_b s_{2_i}^{n+1} - \rho_b s_{2_i}^n \\
- & \frac{w_1\theta D\Delta t}{\Delta x^2}c_{i+1}^{n+1} + \frac{2w_1\theta D\Delta t}{\Delta x^2}c_i^{n+1} - \frac{w_1\theta D\Delta t}{\Delta x^2}c_{i-1}^{n+1} \\
+ & \frac{w_2\theta v\Delta t}{2\Delta x}c_{i+1}^{n+1} - \frac{w_2\theta v\Delta t}{2\Delta x}c_{i-1}^{n+1} + w_4\theta\mu_l\Delta t c_i^{n+1} \\
+ & w_4\Delta t\rho_b\mu_{s1} f K_f {c_i}^{n+1^N} + w_4\Delta t\rho_b\mu_{s2}s_{2_i}^{n+1} \\
= & \frac{(1-w_1)\theta D\Delta t}{\Delta x^2}c_{i+1}^{n} - \frac{2(1-w_1)\theta D\Delta t}{\Delta x^2}c_i^{n} + \frac{(1-w_1)\theta D\Delta t}{\Delta x^2}c_{i-1}^{n} \\
- & \frac{(1-w_2)\theta v\Delta t}{2\Delta x}c_{i+1}^{n} + \frac{(1-w_2)\theta v\Delta t}{2\Delta x}c_{i-1}^{n} - (1-w_4)\theta\mu_l\Delta t c_i^n \\
- & (1-w_4)\Delta t\rho_b\mu_{s1} f K_f {c_i}^{n^N} - (1-w_4)\Delta t\rho_b\mu_{s2}s_{2_i}^n
\end{aligned} \tag{D.13}$$

Grouping common terms c_{i-1}^{n+1}, c_i^{n+1} and c_{i+1}^{n+1}

$$
\begin{aligned}
& M_i^{n+1} - M_i^n + \rho_b s_{2_i}^{n+1} - \rho_b s_{2_i}^n \\
+ & \left[-\frac{w_1 \theta D \Delta t}{\Delta x^2} - \frac{w_2 \theta v \Delta t}{2 \Delta x} \right] c_{i-1}^{n+1} \\
+ & \left[\frac{2 w_1 \theta D \Delta t}{\Delta x^2} + w_4 \theta \mu_l \Delta t \right] c_i^{n+1} \\
+ & \left[-\frac{w_1 \theta D \Delta t}{\Delta x^2} + \frac{w_2 \theta v \Delta t}{2 \Delta x} \right] c_{i+1}^{n+1} \\
+ & \left[w_4 \Delta t \rho_b \mu_{s1} f K_f \right] {c_i}^{n+1^N} \\
+ & \left[w_4 \Delta t \rho_b \mu_{s2} \right] s_{2_i}^{n+1} \\
= & \left[\frac{(1-w_1) \theta D \Delta t}{\Delta x^2} + \frac{(1-w_2) \theta v \Delta t}{2 \Delta x} \right] c_{i-1}^n \\
+ & \left[-\frac{2(1-w_1) \theta D \Delta t}{\Delta x^2} - (1-w_4) \theta \mu_l \Delta t \right] c_i^n \\
+ & \left[\frac{(1-w_1) \theta D \Delta t}{\Delta x^2} - \frac{(1-w_2) \theta v \Delta t}{2 \Delta x} \right] c_{i+1}^n \\
- & \left[(1-w_4) \Delta t \rho_b \mu_{s1} f K_f \right] {c_i}^{nN} \\
- & \left[(1-w_4) \Delta t \rho_b \mu_{s2} \right] s_{2_i}^n
\end{aligned}
\tag{D.14}
$$

Discretizing s_2

$$
\frac{\partial s_2}{\partial t} = \alpha \left[(1-f) K_f c^N - s_2 \right] - \mu_{s2} s_2 \tag{D.15}
$$

$$
\begin{aligned}
\frac{s_{2_i}^{n+1} - s_{2_i}^n}{\Delta t} = & \; w_3 \alpha (1-f) K_f {c_i^{n+1}}^N + (1-w_3) \alpha (1-f) K_f {c_i^n}^N \\
& - w_3 \alpha s_{2_i}^{n+1} - (1-w_3) \alpha s_{2_i}^n - w_3 \mu_{s2} s_{2_i}^{n+1} - (1-w_3) \mu_{s2} s_{2_i}^n
\end{aligned}
\tag{D.16}
$$

$$
\begin{aligned}
s_{2_i}^{n+1} - s_{2_i}^{n} &= \Delta t w_3 \alpha (1-f) K_f {c_i^{n+1}}^N + \Delta t (1-w_3) \alpha (1-f) K_f {c_i^n}^N \\
&\quad - \Delta t w_3 \alpha s_{2_i}^{n+1} - \Delta t (1-w_3) \alpha s_{2_i}^{n} \\
&\quad - \Delta t w_3 \mu_{s2} s_{2_i}^{n+1} - \Delta t (1-w_3) \mu_{s2} s_{2_i}^{n} \qquad \text{(D.17)}
\end{aligned}
$$

$$
\begin{aligned}
s_{2_i}^{n+1} + \Delta t w_3 \alpha s_{2_i}^{n+1} + \Delta t w_3 \mu_{s2} s_{2_i}^{n+1} &= \Delta t w_3 \alpha (1-f) K_f {c_i^{n+1}}^N \\
&\quad + \Delta t (1-w_3) \alpha (1-f) K_f {c_i^n}^N \\
&\quad + s_{2_i}^{n} - \Delta t (1-w_3) \alpha s_{2_i}^{n} \\
&\quad - \Delta t (1-w_3) \mu_{s2} s_{2_i}^{n} \qquad \text{(D.18)}
\end{aligned}
$$

$$
\begin{aligned}
(1 + \Delta t w_3 (\alpha + \mu_{s2})) s_{2_i}^{n+1} &= \Delta t w_3 \alpha (1-f) K_f {c_i^{n+1}}^N \\
&\quad + \Delta t (1-w_3) \alpha (1-f) K_f {c_i^n}^N \\
&\quad + (1 - \Delta t (1-w_3)(\alpha + \mu_{s2})) s_{2_i}^{n} \qquad \text{(D.19)}
\end{aligned}
$$

$$
\begin{aligned}
s_{2_i}^{n+1} &= \frac{\Delta t w_3 \alpha (1-f) K_f}{(1 + \Delta t w_3 (\alpha + \mu_{s2}))} {c_i^{n+1}}^N \\
&\quad + \frac{\Delta t (1-w_3) \alpha (1-f) K_f}{(1 + \Delta t w_3 (\alpha + \mu_{s2}))} {c_i^n}^N \\
&\quad + \frac{(1 - \Delta t (1-w_3)(\alpha + \mu_{s2}))}{(1 + \Delta t w_3 (\alpha + \mu_{s2}))} s_{2_i}^{n} \qquad \text{(D.20)}
\end{aligned}
$$

Replacing $S_{2_i}^{n+1}$

$$
\begin{aligned}
& M_i^{n+1} - M_i^n \\
+ \quad & (\rho_b + w_4 \Delta t \rho_b \mu_{s2}) \left[\frac{\Delta t w_3 \alpha (1-f) K_f}{(1 + \Delta t w_3 (\alpha + \mu_{s2}))} {c_i^{n+1}}^N \right. \\
& \qquad + \frac{\Delta t (1-w_3) \alpha (1-f) K_f}{(1 + \Delta t w_3 (\alpha + \mu_{s2}))} {c_i^n}^N \\
& \qquad \left. + \frac{(1 - \Delta t (1-w_3)(\alpha + \mu_{s2}))}{(1 + \Delta t w_3 (\alpha + \mu_{s2}))} s_{2_i}^n \right] \\
- \quad & \rho_b s_{2_i}^n \\
+ \quad & \left[-\frac{w_1 \theta D \Delta t}{\Delta x^2} - \frac{w_2 \theta v \Delta t}{2 \Delta x} \right] c_{i-1}^{n+1} \\
+ \quad & \left[\frac{2 w_1 \theta D \Delta t}{\Delta x^2} + w_4 \theta \mu_l \Delta t \right] c_i^{n+1} \\
+ \quad & \left[-\frac{w_1 \theta D \Delta t}{\Delta x^2} + \frac{w_2 \theta v \Delta t}{2 \Delta x} \right] c_{i+1}^{n+1} \\
+ \quad & \left[w_4 \Delta t \rho_b \mu_{s1} f K_f \right] {c_i}^{n+1^N} \\
= \quad & \left[\frac{(1-w_1) \theta D \Delta t}{\Delta x^2} + \frac{(1-w_2) \theta v \Delta t}{2 \Delta x} \right] c_{i-1}^n \\
+ \quad & \left[-\frac{2(1-w_1) \theta D \Delta t}{\Delta x^2} - (1-w_4) \theta \mu_l \Delta t \right] c_i^n \\
+ \quad & \left[\frac{(1-w_1) \theta D \Delta t}{\Delta x^2} - \frac{(1-w_2) \theta v \Delta t}{2 \Delta x} \right] c_{i+1}^n \\
- \quad & \left[(1-w_4) \Delta t \rho_b \mu_{s1} f K_f \right] {c_i}^{n N} \\
- \quad & \left[(1-w_4) \Delta t \rho_b \mu_{s2} \right] s_{2_i}^n
\end{aligned}
\tag{D.21}
$$

$$
\begin{aligned}
& M_i^{n+1} - M_i^n \\
+ \quad & \left[(\rho_b + w_4 \Delta t \rho_b \mu_{s2}) \frac{\Delta t w_3 \alpha (1-f) K_f}{(1 + \Delta t w_3 (\alpha + \mu_{s2}))} \right] {c_i^{n+1}}^N \\
+ \quad & \left[(\rho_b + w_4 \Delta t \rho_b \mu_{s2}) \frac{\Delta t (1-w_3) \alpha (1-f) K_f}{(1 + \Delta t w_3 (\alpha + \mu_{s2}))} \right] {c_i^n}^N \\
+ \quad & \left[(\rho_b + w_4 \Delta t \rho_b \mu_{s2}) \frac{(1 - \Delta t (1-w_3)(\alpha + \mu_{s2}))}{(1 + \Delta t w_3 (\alpha + \mu_{s2}))} \right] s_{2_i}^n \\
- \quad & [\rho_b] \, s_{2_i}^n \\
+ \quad & \left[-\frac{w_1 \theta D \Delta t}{\Delta x^2} - \frac{w_2 \theta v \Delta t}{2 \Delta x} \right] c_{i-1}^{n+1} \\
+ \quad & \left[\frac{2 w_1 \theta D \Delta t}{\Delta x^2} + w_4 \theta \mu_l \Delta t \right] c_i^{n+1} \\
+ \quad & \left[-\frac{w_1 \theta D \Delta t}{\Delta x^2} + \frac{w_2 \theta v \Delta t}{2 \Delta x} \right] c_{i+1}^{n+1} \\
+ \quad & [w_4 \Delta t \rho_b \mu_{s1} f K_f] \, {c_i}^{n+1^N} \\
= \quad & \left[\frac{(1-w_1) \theta D \Delta t}{\Delta x^2} + \frac{(1-w_2) \theta v \Delta t}{2 \Delta x} \right] c_{i-1}^n \\
+ \quad & \left[-\frac{2(1-w_1) \theta D \Delta t}{\Delta x^2} - (1-w_4) \theta \mu_l \Delta t \right] c_i^n \\
+ \quad & \left[\frac{(1-w_1) \theta D \Delta t}{\Delta x^2} - \frac{(1-w_2) \theta v \Delta t}{2 \Delta x} \right] c_{i+1}^n \\
- \quad & [(1-w_4) \Delta t \rho_b \mu_{s1} f K_f] \, {c_i}^{nN} \\
- \quad & [(1-w_4) \Delta t \rho_b \mu_{s2}] \, s_{2_i}^n
\end{aligned}
\tag{D.22}
$$

Taking care of the term $\left[(\rho_b + w_4\Delta t\rho_b\mu_{s2})\,\frac{\Delta t w_3\alpha(1-f)K_f}{(1+\Delta t w_3(\alpha+\mu_{s2}))}\right] c_i^{n+1^N}$ which is now going to be called E_i^{n+1} and $\left[(\rho_b + w_4\Delta t\rho_b\mu_{s2})\,\frac{\Delta t(1-w_3)\alpha(1-f)K_f}{(1+\Delta t w_3(\alpha+\mu_{s2}))}\right] c_i^{n^N}$ which is now going to be called E_i^n. Taking care of the term $[w_4\Delta t\rho_b\mu_{s1}fK_f]\,c_i^{n+1^N}$ which is now going to be called H_i^{n+1} and $[(1-w_4)\Delta t\rho_b\mu_{s1}fK_f]\,c_i^{n^N}$ which is now going to be called H_i^n.

$$
\begin{aligned}
& M_i^{n+1} - M_i^n + E_i^{n+1} + E_i^n + H_i^{n+1} + H_i^n \\
+ & \left[-\frac{w_1\theta D\Delta t}{\Delta x^2} - \frac{w_2\theta v\Delta t}{2\Delta x}\right] c_{i-1}^{n+1} \\
+ & \left[\frac{2w_1\theta D\Delta t}{\Delta x^2} + w_4\theta\mu_l\Delta t\right] c_i^{n+1} \\
+ & \left[-\frac{w_1\theta D\Delta t}{\Delta x^2} + \frac{w_2\theta v\Delta t}{2\Delta x}\right] c_{i+1}^{n+1} \\
= & \left[\frac{(1-w_1)\theta D\Delta t}{\Delta x^2} + \frac{(1-w_2)\theta v\Delta t}{2\Delta x}\right] c_{i-1}^{n} \\
+ & \left[-\frac{2(1-w_1)\theta D\Delta t}{\Delta x^2} - (1-w_4)\theta\mu_l\Delta t\right] c_i^{n} \\
+ & \left[\frac{(1-w_1)\theta D\Delta t}{\Delta x^2} - \frac{(1-w_2)\theta v\Delta t}{2\Delta x}\right] c_{i+1}^{n} \\
- & \left[(1-w_4)\Delta t\rho_b\mu_{s2}\right] s_{2_i}^n \\
- & \left[(\rho_b + w_4\Delta t\rho_b\mu_{s2})\,\frac{(1-\Delta t(1-w_3)(\alpha+\mu_{s2}))}{(1+\Delta t w_3(\alpha+\mu_{s2}))}\right] s_{2_i}^n + [\rho_b]\, s_{2_i}^n
\end{aligned}
\tag{D.23}
$$

Writing the iterative term $m+1$

$$
\begin{aligned}
& M_i^{n+1,m+1} - M_i^n + E_i^{n+1,m+1} + E_i^n + H_i^{n+1,m+1} + H_i^n \\
+ & \left[-\frac{w_1 \theta D \Delta t}{\Delta x^2} - \frac{w_2 \theta v \Delta t}{2\Delta x} \right] c_{i-1}^{n+1,m+1} \\
+ & \left[\frac{2w_1 \theta D \Delta t}{\Delta x^2} + w_4 \theta \mu_l \Delta t \right] c_i^{n+1,m+1} \\
+ & \left[-\frac{w_1 \theta D \Delta t}{\Delta x^2} + \frac{w_2 \theta v \Delta t}{2\Delta x} \right] c_{i+1}^{n+1,m+1} \\
= & \left[\frac{(1-w_1) \theta D \Delta t}{\Delta x^2} + \frac{(1-w_2) \theta v \Delta t}{2\Delta x} \right] c_{i-1}^{n} \\
+ & \left[-\frac{2(1-w_1) \theta D \Delta t}{\Delta x^2} - (1-w_4) \theta \mu_l \Delta t \right] c_i^{n} \\
+ & \left[\frac{(1-w_1) \theta D \Delta t}{\Delta x^2} - \frac{(1-w_2) \theta v \Delta t}{2\Delta x} \right] c_{i+1}^{n} \\
- & \left[(1-w_4) \Delta t \rho_b \mu_{s2} \right] s_{2_i}^n \\
- & \left[(\rho_b + w_4 \Delta t \rho_b \mu_{s2}) \frac{(1 - \Delta t (1-w_3)(\alpha + \mu_{s2}))}{(1 + \Delta t w_3 (\alpha + \mu_{s2}))} \right] s_{2_i}^n + \left[\rho_b \right] s_{2_i}^n
\end{aligned}
\tag{D.24}
$$

Aplying Taylor series expansion following the Modified Picard philosophy for $M^{n+1,m+1}$ with respect to c at $c^{n+1,m}$ (Celia et al., 1990; Huang et al., 1998)

$$M_i^{n+1,m+1} = M_i^{n+1,m} + \left(\frac{\partial M_i}{\partial c_i}\right)^{n+1,m} (c_i^{n+1,m+1} - c_i^{n+1,m}) \tag{D.25}$$

$$M_i^{n+1,m+1} = \theta c_i^{n+1,m+1} + \rho_b K_f {c_i^{n+1,m+1}}^N \tag{D.26}$$

$$M_i^{n+1,m} = \theta c_i^{n+1,m} + \rho_b K_f {c_i^{n+1,m}}^N \tag{D.27}$$

$$M_i^n = \theta c_i^n + \rho_b K_f {c_i^n}^N \tag{D.28}$$

$$B_i^{n+1,m} = \left(\frac{\partial M_i}{\partial c_i}\right)^{n+1,m} = \theta + \rho_b K_f N {c_i^{n+1,m}}^{N-1} \tag{D.29}$$

Aplying Taylor series expansion following the Modified Picard philosophy for $E^{n+1,m+1}$ with respect to c at $c^{n+1,m}$

$$E_i^{n+1,m+1} = E_i^{n+1,m} + \left(\frac{\partial E_i}{\partial c_i}\right)^{n+1,m} (c_i^{n+1,m+1} - c_i^{n+1,m}) \tag{D.30}$$

$$E_i^{n+1,m+1} = (\rho_b + w_4 \Delta t \rho_b \mu_{s2}) \frac{\Delta t w_3 \alpha (1-f) K_f}{(1 + \Delta t w_3 (\alpha + \mu_{s2}))} {c_i^{n+1,m+1}}^N \tag{D.31}$$

$$E_i^{n+1,m} = (\rho_b + w_4 \Delta t \rho_b \mu_{s2}) \frac{\Delta t w_3 \alpha (1-f) K_f}{(1 + \Delta t w_3 (\alpha + \mu_{s2}))} {c_i^{n+1,m}}^N \tag{D.32}$$

$$E_i^n = (\rho_b + w_4 \Delta t \rho_b \mu_{s2}) \frac{\Delta t (1 - w_3) \alpha (1 - f) K_f}{(1 + \Delta t w_3 (\alpha + \mu_{s2}))} c_i^{n^N} \tag{D.33}$$

$$F_i^{n+1,m} = \left(\frac{\partial E_i}{\partial c_i} \right)^{n+1,m} = (\rho_b + w_4 \Delta t \rho_b \mu_{s2}) \frac{\Delta t w_3 \alpha (1 - f) K_f}{(1 + \Delta t w_3 (\alpha + \mu_{s2}))} N c_i^{n+1,m^{N-1}} \tag{D.34}$$

Aplying Taylor series expansion following the Modified Picard philosophy for $H^{n+1,m+1}$ with respect to c at $c^{n+1,m}$

$$H_i^{n+1,m+1} = H_i^{n+1,m} + \left(\frac{\partial H_i}{\partial c_i} \right)^{n+1,m} (c_i^{n+1,m+1} - c_i^{n+1,m}) \tag{D.35}$$

$$H_i^{n+1,m+1} = w_4 \Delta t \rho_b \mu_{s1} f K_f c_i^{n+1,m+1^N} \tag{D.36}$$

$$H_i^{n+1,m} = w_4 \Delta t \rho_b \mu_{s1} f K_f c_i^{n+1,m^N} \tag{D.37}$$

$$H_i^n = (1 - w_4) \Delta t \rho_b \mu_{s1} f K_f c_i^{n^N} \tag{D.38}$$

$$I_i^{n+1,m} = \left(\frac{\partial H_i}{\partial c_i} \right)^{n+1,m} = w_4 \Delta t \rho_b \mu_{s1} f K_f N c_i^{n+1,m^{N-1}} \tag{D.39}$$

Replacing $M_i^{n+1,m+1}$ and $E_i^{n+1,m+1}$

$$
\begin{aligned}
& M_i^{n+1,m} + B_i^{n+1,m}(c_i^{n+1,m+1} - c_i^{n+1,m}) - M_i^n \\
+ \quad & E_i^{n+1,m} + F_i^{n+1,m}(c_i^{n+1,m+1} - c_i^{n+1,m}) + E_i^n \\
+ \quad & H_i^{n+1,m} + I_i^{n+1,m}(c_i^{n+1,m+1} - c_i^{n+1,m}) + H_i^n \\
+ \quad & \left[-\frac{w_1 \theta D \Delta t}{\Delta x^2} - \frac{w_2 \theta v \Delta t}{2\Delta x} \right] c_{i-1}^{n+1,m+1} \\
+ \quad & \left[\frac{2w_1 \theta D \Delta t}{\Delta x^2} + w_4 \theta \mu_l \Delta t \right] c_i^{n+1,m+1} \\
+ \quad & \left[-\frac{w_1 \theta D \Delta t}{\Delta x^2} + \frac{w_2 \theta v \Delta t}{2\Delta x} \right] c_{i+1}^{n+1,m+1} \\
= \quad & \left[\frac{(1-w_1) \theta D \Delta t}{\Delta x^2} + \frac{(1-w_2) \theta v \Delta t}{2\Delta x} \right] c_{i-1}^{n} \\
+ \quad & \left[-\frac{2(1-w_1) \theta D \Delta t}{\Delta x^2} - (1-w_4) \theta \mu_l \Delta t \right] c_i^{n} \\
+ \quad & \left[\frac{(1-w_1) \theta D \Delta t}{\Delta x^2} - \frac{(1-w_2) \theta v \Delta t}{2\Delta x} \right] c_{i+1}^{n} \\
- \quad & \left[(1-w_4) \Delta t \rho_b \mu_{s2} \right] s_{2_i}^n \\
- \quad & \left[(\rho_b + w_4 \Delta t \rho_b \mu_{s2}) \frac{(1 - \Delta t (1-w_3)(\alpha + \mu_{s2}))}{(1 + \Delta t w_3 (\alpha + \mu_{s2}))} \right] s_{2_i}^n + \left[\rho_b \right] s_{2_i}^n
\end{aligned}
\tag{D.40}
$$

Substracting the iterative term $c_{i-1}^{n+1,m}$, $c_i^{n+1,m}$ and $c_{i+1}^{n+1,m}$ on the left and on the right hand side to maintain balance

$$
\begin{aligned}
& M_i^{n+1,m} + B_i^{n+1,m}(c_i^{n+1,m+1} - c_i^{n+1,m}) - M_i^n \\
+ \;& E_i^{n+1,m} + F_i^{n+1,m}(c_i^{n+1,m+1} - c_i^{n+1,m}) + E_i^n \\
+ \;& H_i^{n+1,m} + I_i^{n+1,m}(c_i^{n+1,m+1} - c_i^{n+1,m}) + H_i^n \\
+ \;& \left[-\frac{w_1\theta D\Delta t}{\Delta x^2} - \frac{w_2\theta v\Delta t}{2\Delta x}\right]\left(c_{i-1}^{n+1,m+1} - c_{i-1}^{n+1,m}\right) \\
+ \;& \left[\frac{2w_1\theta D\Delta t}{\Delta x^2} + w_4\theta\mu_l\Delta t\right]\left(c_i^{n+1,m+1} - c_i^{n+1,m}\right) \\
+ \;& \left[-\frac{w_1\theta D\Delta t}{\Delta x^2} + \frac{w_2\theta v\Delta t}{2\Delta x}\right]\left(c_{i+1}^{n+1,m+1} - c_{i+1}^{n+1,m}\right) \\
= \;& \left[\frac{(1-w_1)\theta D\Delta t}{\Delta x^2} + \frac{(1-w_2)\theta v\Delta t}{2\Delta x}\right] c_{i-1}^n \\
+ \;& \left[-\frac{2(1-w_1)\theta D\Delta t}{\Delta x^2} - (1-w_4)\theta\mu_l\Delta t\right] c_i^n \\
+ \;& \left[\frac{(1-w_1)\theta D\Delta t}{\Delta x^2} - \frac{(1-w_2)\theta v\Delta t}{2\Delta x}\right] c_{i+1}^n \\
- \;& \left[(1-w_4)\Delta t\rho_b\mu_{s2}\right] s_{2_i}^n \\
- \;& \left[(\rho_b + w_4\Delta t\rho_b\mu_{s2})\,\frac{(1-\Delta t(1-w_3)(\alpha+\mu_{s2}))}{(1+\Delta t w_3(\alpha+\mu_{s2}))}\right] s_{2_i}^n + \left[\rho_b\right] s_{2_i}^n \\
- \;& \left[-\frac{w_1\theta D\Delta t}{\Delta x^2} - \frac{w_2\theta v\Delta t}{2\Delta x}\right] c_{i-1}^{n+1,m} \\
- \;& \left[\frac{2w_1\theta D\Delta t}{\Delta x^2} + w_4\theta\mu_l\Delta t\right] c_i^{n+1,m} \\
- \;& \left[-\frac{w_1\theta D\Delta t}{\Delta x^2} + \frac{w_2\theta v\Delta t}{2\Delta x}\right] c_{i+1}^{n+1,m}
\end{aligned}
\tag{D.41}
$$

Grouping similar terms

$$
\begin{aligned}
&+ \left[-\frac{w_1\theta D\Delta t}{\Delta x^2} - \frac{w_2\theta v\Delta t}{2\Delta x}\right]\left(c_{i-1}^{n+1,m+1} - c_{i-1}^{n+1,m}\right) \\
&+ \left[\frac{2w_1\theta D\Delta t}{\Delta x^2} + w_4\theta\mu_l\Delta t\right. \\
&\qquad \left. + B_i^{n+1,m} + F_i^{n+1,m} + I_i^{n+1,m}\right]\left(c_i^{n+1,m+1} - c_i^{n+1,m}\right) \\
&+ \left[-\frac{w_1\theta D\Delta t}{\Delta x^2} + \frac{w_2\theta v\Delta t}{2\Delta x}\right]\left(c_{i+1}^{n+1,m+1} - c_{i+1}^{n+1,m}\right) \\
&= M_i^n - M_i^{n+1,m} - E_i^{n+1,m} - E_i^n - H_i^{n+1,m} - H_i^n \\
&+ \left[\frac{(1-w_1)\theta D\Delta t}{\Delta x^2} + \frac{(1-w_2)\theta v\Delta t}{2\Delta x}\right] c_{i-1}^n \\
&+ \left[-\frac{2(1-w_1)\theta D\Delta t}{\Delta x^2} - (1-w_4)\theta\mu_l\Delta t\right] c_i^n \\
&+ \left[\frac{(1-w_1)\theta D\Delta t}{\Delta x^2} - \frac{(1-w_2)\theta v\Delta t}{2\Delta x}\right] c_{i+1}^n \\
&- \left[(1-w_4)\Delta t\rho_b\mu_{s2}\right] s_{2_i}^n \\
&- \left[\left(\rho_b + w_4\Delta t\rho_b\mu_{s2}\right)\frac{(1-\Delta t(1-w_3)(\alpha+\mu_{s2}))}{(1+\Delta t w_3(\alpha+\mu_{s2}))}\right] s_{2_i}^n \\
&+ \left[\rho_b\right] s_{2_i}^n \\
&- \left[-\frac{w_1\theta D\Delta t}{\Delta x^2} - \frac{w_2\theta v\Delta t}{2\Delta x}\right] c_{i-1}^{n+1,m} \\
&- \left[\frac{2w_1\theta D\Delta t}{\Delta x^2} + w_4\theta\mu_l\Delta t\right] c_i^{n+1,m} \\
&- \left[-\frac{w_1\theta D\Delta t}{\Delta x^2} + \frac{w_2\theta v\Delta t}{2\Delta x}\right] c_{i+1}^{n+1,m}
\end{aligned}
\tag{D.42}
$$

Defining r and Cr

$$r = \frac{D\Delta t}{\Delta x^2} \tag{D.43}$$

$$Cr = \frac{v\Delta t}{\Delta x} \tag{D.44}$$

Replacing r and Cr

$$
\begin{aligned}
&+ \quad \left[-w_1\theta r - w_2\theta\frac{Cr}{2}\right]\left(c_{i-1}^{n+1,m+1} - c_{i-1}^{n+1,m}\right) \\
&+ \quad [2w_1\theta r + w_4\theta\mu_l\Delta t \\
&\qquad\qquad +B_i^{n+1,m} + F_i^{n+1,m} + I_i^{n+1,m}]\left(c_i^{n+1,m+1} - c_i^{n+1,m}\right) \\
&+ \quad \left[-w_1\theta r + w_2\theta\frac{Cr}{2}\right]\left(c_{i+1}^{n+1,m+1} - c_{i+1}^{n+1,m}\right) \\
&= \quad M_i^n - M_i^{n+1,m} - E_i^{n+1,m} - E_i^n - H_i^{n+1,m} - H_i^n \\
&+ \quad \left[(1-w_1)\theta r + (1-w_2)\theta\frac{Cr}{2}\right] c_{i-1}^n \\
&+ \quad [-2(1-w_1)\theta r - (1-w_4)\theta\mu_l\Delta t]\, c_i^n \\
&+ \quad \left[(1-w_1)\theta r - (1-w_2)\theta\frac{Cr}{2}\right] c_{i+1}^n \\
&- \quad [(1-w_4)\Delta t\rho_b\mu_{s2}]\, s_{2_i}^n \\
&- \quad \left[(\rho_b + w_4\Delta t\rho_b\mu_{s2})\,\frac{(1-\Delta t(1-w_3)(\alpha+\mu_{s2}))}{(1+\Delta t w_3(\alpha+\mu_{s2}))}\right] s_{2_i}^n \\
&+ \quad [\rho_b]\, s_{2_i}^n \\
&- \quad \left[-w_1\theta r - w_2\theta\frac{Cr}{2}\right] c_{i-1}^{n+1,m} \\
&- \quad [2w_1\theta r + w_4\theta\mu_l\Delta t]\, c_i^{n+1,m} \\
&- \quad \left[-w_1\theta r + w_2\theta\frac{Cr}{2}\right] c_{i+1}^{n+1,m}
\end{aligned}
\tag{D.45}
$$

Discretizing a pulse boundary condition

$$
vc - D\frac{\partial c}{\partial x} = vg \tag{D.46}
$$

$$
vc_i - D\frac{c_{i+1} - c_{i-1}}{2\Delta x} = vg \tag{D.47}
$$

$$2\Delta xvc_i - D(c_{i+1} - c_{i-1}) = 2\Delta xvg \tag{D.48}$$

$$\frac{2\Delta xv}{D}c_i - c_{i+1} + c_{i-1} = \frac{2\Delta xv}{D}g \tag{D.49}$$

$$c_{i-1} = c_{i+1} - \frac{2\Delta xv}{D}c_i + \frac{2\Delta xv}{D}g \tag{D.50}$$

Replacing the term $c_{i-1}^{n+1,m+1}$, $c_{i-1}^{n+1,m}$ and c_{i-1}^{n} with the boundary condition

$$\begin{aligned}
&+ \left[-w_1\theta r - w_2\theta\frac{Cr}{2}\right]\left(c_{i+1}^{n+1,m+1} - \frac{2\Delta xv}{D}c_i^{n+1,m+1} + \frac{2\Delta xv}{D}g\right)\\
&+ \left[2w_1\theta r + w_4\theta\mu_l\Delta t + B_i^{n+1,m} + F_i^{n+1,m} + I_i^{n+1,m}\right]\left(c_i^{n+1,m+1} - c_i^{n+1,m}\right)\\
&+ \left[-w_1\theta r + w_2\theta\frac{Cr}{2}\right]\left(c_{i+1}^{n+1,m+1} - c_{i+1}^{n+1,m}\right)\\
&= M_i^n - M_i^{n+1,m} - E_i^{n+1,m} - E_i^n - H_i^{n+1,m} - H_i^n\\
&+ \left[(1-w_1)\theta r + (1-w_2)\theta\frac{Cr}{2}\right]\left(c_{i+1}^n - \frac{2\Delta xv}{D}c_i^n + \frac{2\Delta xv}{D}g\right)\\
&+ \left[-2(1-w_1)\theta r - (1-w_4)\theta\mu_l\Delta t\right]c_i^n\\
&+ \left[(1-w_1)\theta r - (1-w_2)\theta\frac{Cr}{2}\right]c_{i+1}^n\\
&- \left[(1-w_4)\Delta t\rho_b\mu_{s2}\right]s_{2_i}^n\\
&- \left[\left(\rho_b + w_4\Delta t\rho_b\mu_{s2}\right)\frac{(1-\Delta t(1-w_3)(\alpha+\mu_{s2}))}{(1+\Delta tw_3(\alpha+\mu_{s2}))}\right]s_{2_i}^n + \left[\rho_b\right]s_{2_i}^n\\
&- \left[-w_1\theta r - w_2\theta\frac{Cr}{2}\right]\left(c_{i+1}^{n+1,m} - \frac{2\Delta xv}{D}c_i^{n+1,m} + \frac{2\Delta xv}{D}g\right)\\
&- \left[2w_1\theta r + w_4\theta\mu_l\Delta t\right]c_i^{n+1,m}\\
&- \left[-w_1\theta r + w_2\theta\frac{Cr}{2}\right]c_{i+1}^{n+1,m}
\end{aligned} \tag{D.51}$$

$$
\begin{aligned}
&+ \quad \left[-w_1\theta r - w_2\theta\frac{Cr}{2}\right]\left(c_{i+1}^{n+1,m+1} - c_{i+1}^{n+1,m}\right) \\
&- \quad \left[-w_1\theta r - w_2\theta\frac{Cr}{2}\right]\left(\frac{2\Delta xv}{D}c_i^{n+1,m+1} - \frac{2\Delta xv}{D}c_i^{n+1,m}\right) \\
&+ \quad \left[-w_1\theta r - w_2\theta\frac{Cr}{2}\right]\left(\frac{2\Delta xv}{D}g - \frac{2\Delta xv}{D}g\right) \\
&+ \quad \left[2w_1\theta r + w_4\theta\mu_l\Delta t + B_i^{n+1,m} + F_i^{n+1,m} + I_i^{n+1,m}\right]\left(c_i^{n+1,m+1} - c_i^{n+1,m}\right) \\
&+ \quad \left[-w_1\theta r + w_2\theta\frac{Cr}{2}\right]\left(c_{i+1}^{n+1,m+1} - c_{i+1}^{n+1,m}\right) \\
&= \quad M_i^n - M_i^{n+1,m} - E_i^{n+1,m} - E_i^n - H_i^{n+1,m} - H_i^n \\
&+ \quad \left[(1-w_1)\theta r + (1-w_2)\theta\frac{Cr}{2}\right]\left(c_{i+1}^n - \frac{2\Delta xv}{D}c_i^n + \frac{2\Delta xv}{D}g\right) \\
&+ \quad \left[-2(1-w_1)\theta r - (1-w_4)\theta\mu_l\Delta t\right]c_i^n \\
&+ \quad \left[(1-w_1)\theta r - (1-w_2)\theta\frac{Cr}{2}\right]c_{i+1}^n \\
&- \quad \left[(1-w_4)\Delta t\rho_b\mu_{s2}\right]s_{2_i}^n \\
&- \quad \left[\left(\rho_b + w_4\Delta t\rho_b\mu_{s2}\right)\frac{(1-\Delta t(1-w_3)(\alpha+\mu_{s2}))}{(1+\Delta t w_3(\alpha+\mu_{s2}))}\right]s_{2_i}^n + \left[\rho_b\right]s_{2_i}^n \\
&- \quad \left[-w_1\theta r - w_2\theta\frac{Cr}{2}\right]\left(c_{i+1}^{n+1,m} - \frac{2\Delta xv}{D}c_i^{n+1,m} + \frac{2\Delta xv}{D}g\right) \\
&- \quad \left[2w_1\theta r + w_4\theta\mu_l\Delta t\right]c_i^{n+1,m} \\
&- \quad \left[-w_1\theta r + w_2\theta\frac{Cr}{2}\right]c_{i+1}^{n+1,m}
\end{aligned}
\tag{D.52}
$$

$$
\begin{aligned}
&+ \quad \Big[2w_1\theta r + w_4\theta\mu_l\Delta t + B_i^{n+1,m} + F_i^{n+1,m} + I_i^{n+1,m} \\
&\qquad\qquad - \left(-w_1\theta r - w_2\theta\frac{Cr}{2}\right)\left(\frac{2\Delta xv}{D}\right)\Big]\left(c_i^{n+1,m+1} - c_i^{n+1,m}\right) \\
&+ \quad \left[-w_1\theta r + w_2\theta\frac{Cr}{2} - w_1\theta r - w_2\theta\frac{Cr}{2}\right]\left(c_{i+1}^{n+1,m+1} - c_{i+1}^{n+1,m}\right) \\
&= \quad M_i^n - M_i^{n+1,m} - E_i^{n+1,m} - E_i^n - H_i^{n+1,m} - H_i^n \\
&+ \quad \left[(1-w_1)\theta r + (1-w_2)\theta\frac{Cr}{2}\right]\left(c_{i+1}^n - \frac{2\Delta xv}{D}c_i^n + \frac{2\Delta xv}{D}g\right) \\
&+ \quad \left[-2(1-w_1)\theta r - (1-w_4)\theta\mu_l\Delta t\right]c_i^n \\
&+ \quad \left[(1-w_1)\theta r - (1-w_2)\theta\frac{Cr}{2}\right]c_{i+1}^n \\
&- \quad \left[(1-w_4)\Delta t\rho_b\mu_{s2}\right]s_{2_i}^n \\
&- \quad \left[\left(\rho_b + w_4\Delta t\rho_b\mu_{s2}\right)\frac{(1-\Delta t(1-w_3)(\alpha+\mu_{s2}))}{(1+\Delta tw_3(\alpha+\mu_{s2}))}\right]s_{2_i}^n + \left[\rho_b\right]s_{2_i}^n \\
&- \quad \left[-w_1\theta r - w_2\theta\frac{Cr}{2}\right]\left(c_{i+1}^{n+1,m} - \frac{2\Delta xv}{D}c_i^{n+1,m} + \frac{2\Delta xv}{D}g\right) \\
&- \quad \left[2w_1\theta r + w_4\theta\mu_l\Delta t\right]c_i^{n+1,m} \\
&- \quad \left[-w_1\theta r + w_2\theta\frac{Cr}{2}\right]c_{i+1}^{n+1,m}
\end{aligned}
\tag{D.53}
$$

APPENDIX E

OTC LOADING RATE ESTIMATES FOR TRANSPORT SIMULATIONS

Table E.1: Summary of values utilized for simulations

Description	Value	Units	Reference
Crop	Corn		
Crop yield	150	bushel/acre	Stichler and McFarland (1997)
Crop nitrogen (N) demand	240	lb N/acre	Stichler and McFarland (1997)
% of inorganic N denitrified	20	%	Table 11-8 of USDA (2009b)
% of N loss through leaching	10	%	Table 11-7 of USDA (2009b)
% application losses	5	%	Table 11-6 of USDA (2009b)

E.1 Nitrogen demand:

- N plant requirement considering denitrification:

$$\frac{\text{Crop nitrogen (N) demand}}{\%\text{ of N retained after denitrification}} = \frac{240\frac{lb\,\text{N}}{acre}}{1-0.2} = 300\frac{lb\,\text{N}}{acre} \tag{E.1}$$

- N plant requirement considering leaching losses:

$$\frac{\text{N plant requirement considering denitrification}}{\%\text{ retained after leaching losses}} = \frac{300\frac{lb\,\text{N}}{acre}}{1-0.1} = 333\frac{lb\,\text{N}}{acre} \tag{E.2}$$

- N to apply:

$$\frac{\text{N plant requirement considering leaching losses}}{\%\text{ retained after application losses}} = \frac{333\frac{lb\,\text{N}}{acre}}{1-0.05} = 351\frac{lb\,\text{N}}{acre} \quad \text{(E.3)}$$

E.2 Slurry application calculations:

- Slurry loading:

$$\frac{\text{N to apply}}{\text{Manure N content}} = \frac{351\frac{lb\,\text{N}}{acre}\cdot\frac{acre}{4046.8\text{m}^2}}{6\frac{lb\,\text{N}}{\text{ton}_{manure}}\cdot\frac{\text{ton}}{907.2\text{Kg}}} = 13.11\frac{\text{Kg}_{slurry}}{\text{m}^2} \quad \text{(E.4)}$$

- OTC loading:

$$\frac{\text{Slurry loading}\ \cdot \text{OTC in manure}}{z\cdot\rho_b} =$$

$$\frac{13.11\frac{\text{Kg}_{slurry}}{\text{m}^2}\cdot 29000\frac{\mu\text{g}_{OTC}}{\text{Kg}_{slurry}}}{0.005\text{m}\cdot 1.4\frac{Kg_{soil}}{L}\cdot 1000\frac{\text{L}}{\text{m}^3}} = 54,330.9\frac{\mu\text{g}_{OTC}}{\text{Kg}_{soil}} \quad \text{(E.5)}$$

$$\frac{13.11\frac{\text{Kg}_{slurry}}{\text{m}^2}\cdot 29000\frac{\mu\text{g}_{OTC}}{\text{Kg}_{slurry}}}{0.10\text{m}\cdot 1.4\frac{Kg_{soil}}{L}\cdot 1000\frac{\text{L}}{\text{m}^3}} = 2,716.5\frac{\mu\text{g}_{OTC}}{\text{Kg}_{soil}} \quad \text{(E.6)}$$

$$\frac{13.11\frac{\text{Kg}_{slurry}}{\text{m}^2}\cdot 29000\frac{\mu\text{g}_{OTC}}{\text{Kg}_{slurry}}}{0.25\text{m}\cdot 1.4\frac{Kg_{soil}}{L}\cdot 1000\frac{\text{L}}{\text{m}^3}} = 1,086.6\frac{\mu\text{g}_{OTC}}{\text{Kg}_{soil}} \quad \text{(E.7)}$$

E.3 Diluted slurry application calculations:

- Volume of slurry applied per area:

$$\frac{\text{Slurry loading}}{\rho_{\text{manure}}} = \frac{13.11\frac{\text{Kg}_{slurry}}{\text{m}^2}}{0.99\frac{\text{Kg}_{slurry}}{\text{L}_{slurry}}} = 13.2\frac{\text{L}_{slurry}}{\text{m}^2} \quad \text{(E.8)}$$

- Volume of diluted slurry applied per area: Assuming slurry has a 10% of solids in manure. Solids content needs to be reduced to 3%. According to Table 11-2 in

(USDA, 2009b), 15 $\frac{gal_{H_2O}}{ft^3}$ of manure need to be added to reduced the solids content from 10% to 3%.

$$\begin{aligned} V_{ds} &= \text{Volume of slurry} + \text{Volume of water} \\ &= 13.2\frac{\text{L}_{slurry}}{\text{m}^2} + \left(13.2\frac{\text{L}_{slurry}}{\text{m}^2} \cdot 15\frac{\text{gal}_{water}}{\text{ft}^3_{slurry}} \cdot 0.134\frac{\text{ft}_{water}}{\text{gal}_{water}}\right) \\ &= 39.9\frac{\text{L}_{ds}}{\text{m}^2} \end{aligned} \tag{E.9}$$

- OTC in diluted slurry:

$$\begin{aligned} &\frac{\text{Slurry loading} \cdot \text{OTC in manure}}{V_{ds}} \\ = &\frac{13.11\frac{\text{Kg}_{slurry}}{\text{m}^2} \cdot 29000\frac{\mu\text{g}_{OTC}}{\text{Kg}_{slurry}}}{39.9\frac{\text{L}_{ds}}{\text{m}^2}} = 9538.21\frac{\mu\text{g}_{OTC}}{\text{L}_{ds}} \end{aligned} \tag{E.10}$$

- Volume of solids:

$$\begin{aligned} V_{solids} &= V_{ds} \cdot \frac{\%TS}{100} \\ &= 39.9\frac{L_{ds}}{\text{m}^2} \cdot 0.03 = 1.2\frac{L_{solids}}{\text{m}^2} \end{aligned} \tag{E.11}$$

- Mass of solids:

$$\begin{aligned} Mass_{solids} &= V_{solids} \cdot \rho_{ds} \\ &= 1.2\frac{L_{solids}}{\text{m}^2} \cdot 1\frac{Kg}{L} = 1.2\frac{Kg_{solids}}{\text{m}^2} \end{aligned} \tag{E.12}$$

- Volume of liquid:

$$
\begin{aligned}
V_{liquid} &= V_{ds} - V_{solids} \\
&= 39.9\frac{L_{ds}}{\mathrm{m}^2} - 1.2\frac{L_{solids}}{\mathrm{m}^2} = 38.7\frac{L_{Ls}}{\mathrm{m}^2}
\end{aligned} \tag{E.13}
$$

- Mass Balance:

$$
\begin{aligned}
V_{liquid} \cdot OTC_{liquid} + Mass_{solid} \cdot OTC_{solids} &= V_{ds} \cdot OTC_{ds} \\
V_{liquid} \cdot OTC_{liquid} + Mass_{solid} \cdot (K_d \cdot OTC_{liquid}) &= V_{ds} \cdot OTC_{ds} \\
38.7\tfrac{L_{Ls}}{\mathrm{m}^2} \cdot OTC_{liquid} + 1.2\tfrac{Kg_{solids}}{\mathrm{m}^2} \cdot 38\tfrac{L}{Kg} \cdot OTC_{liquid} &= 39.9\frac{\mathrm{L}_{ds}}{\mathrm{m}^2} \cdot 9538.21\frac{\mu\mathrm{g}_{OTC}}{\mathrm{L}_{ds}}
\end{aligned}
$$

$$
OTC_{liquid} = 4514.5\frac{\mu\mathrm{g}_{OTC}}{\mathrm{L}_{ds}} \tag{E.14}
$$

$$
\begin{aligned}
OTC_{solid} &= K_d \cdot OTC_{liquid} \\
&= 38\frac{L}{Kg} \cdot 4514.5\frac{\mu\mathrm{g}_{OTC}}{\mathrm{L}_{ds}} = 171,552\frac{\mu\mathrm{g}_{OTC}}{\mathrm{Kg}_{solid}}
\end{aligned} \tag{E.15}
$$

- OTC loading:

$$\frac{OTC_{solid} \cdot Mass_{solid}}{z \cdot \rho_b}$$

$$= \frac{171,552 \frac{\mu g_{OTC}}{\text{Kg}_{solid}} \cdot 1.2 \frac{Kg_{solids}}{\text{m}^2}}{0.005m \cdot 1.4 \frac{Kg_{soil}}{L} \cdot 1000 \frac{\text{L}}{\text{m}^3}} = 29,409.9 \frac{\mu \text{g}_{OTC}}{\text{Kg}_{soil}} \quad \text{(E.16)}$$

$$= \frac{171,552 \frac{\mu g_{OTC}}{\text{Kg}_{solid}} \cdot 1.2 \frac{Kg_{solids}}{\text{m}^2}}{0.10m \cdot 1.4 \frac{Kg_{soil}}{L} \cdot 1000 \frac{\text{L}}{\text{m}^3}} = 1,470.4 \frac{\mu \text{g}_{OTC}}{\text{Kg}_{soil}} \quad \text{(E.17)}$$

$$= \frac{171,552 \frac{\mu g_{OTC}}{\text{Kg}_{solid}} \cdot 1.2 \frac{Kg_{solids}}{\text{m}^2}}{0.25m \cdot 1.4 \frac{Kg_{soil}}{L} \cdot 1000 \frac{\text{L}}{\text{m}^3}} = 588.2 \frac{\mu \text{g}_{OTC}}{\text{Kg}_{soil}} \quad \text{(E.18)}$$

APPENDIX F

SENSITIVITY ANALYSIS

Table F.1: Aqueous and solid media concentrations estimated for the sensitivity analysis of the two-site, one rate, non-equilibrium model

Variable	Tested values	Aqueous concentration	Sorption sites at equilibrium (type 1)	Time dependent sorption sites (type 2)
ρ_b	1.2	4.83	4.15	3.64
	1.4	422.8	362.8	317.9
	1.6	4254.9	3649.4	3195.4
K_d	565	4.87	4.15	3.62
	665	365.4	362.8	363.3
	765	3647.0	3649.4	3652.0
N	0.8	6.05	4.15	3.27
	1.0	337.0	362.8	390.1
	1.2	3652.9	3649.4	3650.3
f	0.01	4.40	4.15	3.65
	0.05	74.2	362.8	623.0
	0.09	3916.0	3649.4	3411.6
α	0.001	3.15	4.15	4.26
	0.003	329.4	362.8	366.5
	0.005	3825.4	3649.4	3533.2
DT_{50S}	23	4.04	4.15	4.21
	33	359.2	362.8	364.8
	43	3552.8	3649.4	3702.1
OTC in manure	38	3.29	4.15	5.02
	48	287.2	362.8	438.4
	58	2889.1	3649.4	4409.7
θ	0.1	4.28	4.15	4.13
	0.2	366.9	362.8	362.2
	0.3	3666.4	3649.4	3644.5

Note: concentration values are evaluated at z = 10 cm and t = 2.94 days. Values of each parameter represent $a_k - \Delta a_k$, a_k, and $a_k + \Delta a_k$, where a_k is the base case. For example, for the parameter ρ_b: $a_k - \Delta a_k$ = 1.2 L/kg, a_k = 1.4 L/kg and $a_k + \Delta a_k$ = 1.6 L/kg.

Table F.1: Continued

Variable	Tested values	Aqueous concentration	Sorption sites at equilibrium (type 1)	Time dependent sorption sites (type 2)
v	1.13	4.26	4.15	4.14
	2.13	366.4	362.8	362.3
	3.13	3664.3	3649.4	3644.9
D	2.11	4.38	4.15	4.01
	3.11	370.4	362.8	358.1
	4.11	3671.4	3649.4	3635.3
DT_{50L}	23	4.15	4.15	4.15
	33	362.8	362.8	362.8
	43	3649.4	3649.4	3649.4

Note: concentration values are evaluated at z = 10 cm and t = 2.94 days. Values of each parameter represent $a_k - \Delta a_k$, a_k, and $a_k + \Delta a_k$, where a_k is the base case. For example, for the parameter ρ_b: $a_k - \Delta a_k$ = 1.2 L/kg, a_k = 1.4 L/kg and $a_k + \Delta a_k$ = 1.6 L/kg.

Table F.2: Sensitivity coefficient for aqueous, Sorption sites at equilibrium and analysis result comparisons

Variable	Tested values	Aqueous concentration	Sorption sites at equilibrium (type 1)	Time dependent sorption sites (type 2)
ρ_b	1.2	4.8	420	4238.5
	1.6	4.1	359.2	3632.0
K_d	565	4.8	17.3	16.0
	765	4.1	3.8	19.9
N	0.8	9.5	129.0	17.5
	1.2	5.3	163.8	5.4
f	0.01	0.3	360.8	333.3
	0.09	1.1	5855	535.1
α	0.001	1.5	50.1	264
	0.005	0.3	9.3	290
DT_{50S}	23	0.4	11.9	318.8
	43	0.3	8.6	226.6
OTC in manure	38	4.1	362.9	3649.4
	58	5.0	438.5	4409.7
θ	0.1	0.3	8.2	34.0
	0.3	0.1	1.8	14.7
v	1.13	0.2	7.7	36.2
	3.13	0.0	1.6	14.1
D	2.11	0.7	23.6	68.4
	4.11	0.6	19.3	58.0
DT_{50L}	23	0.0	0.0	0.0
	43	0.0	0.0	0.0

Note: concentration values are evaluated at z = 10 cm and t = 2.94 days.

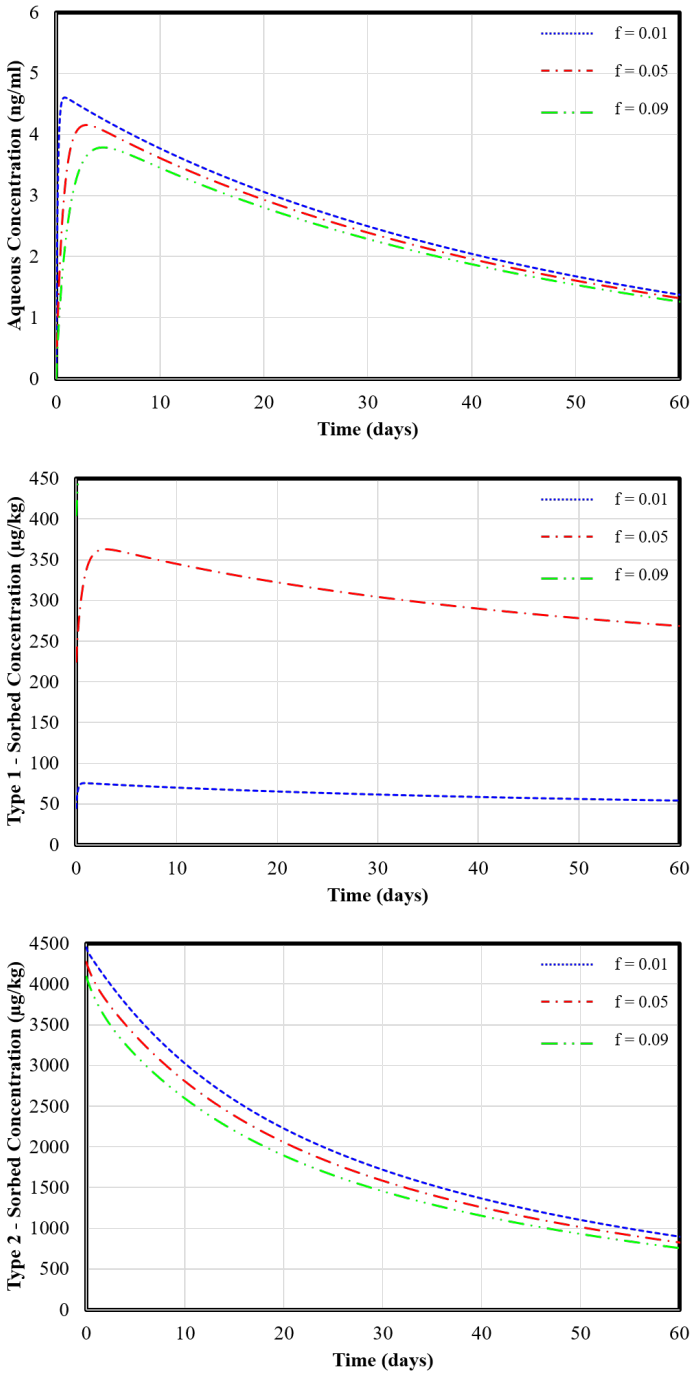

Figure F.1: Sensitivity analysis results for the fraction of available exchange sites at equilibrium (f). Predicted time dependent aqueous concentration (A), equilibrium sorption site (Type 1) concentration (B), and kinetic sorption site (Type 2) (C) concentration of OTC assuming surface application of manure with 10 cm incorporation depth.

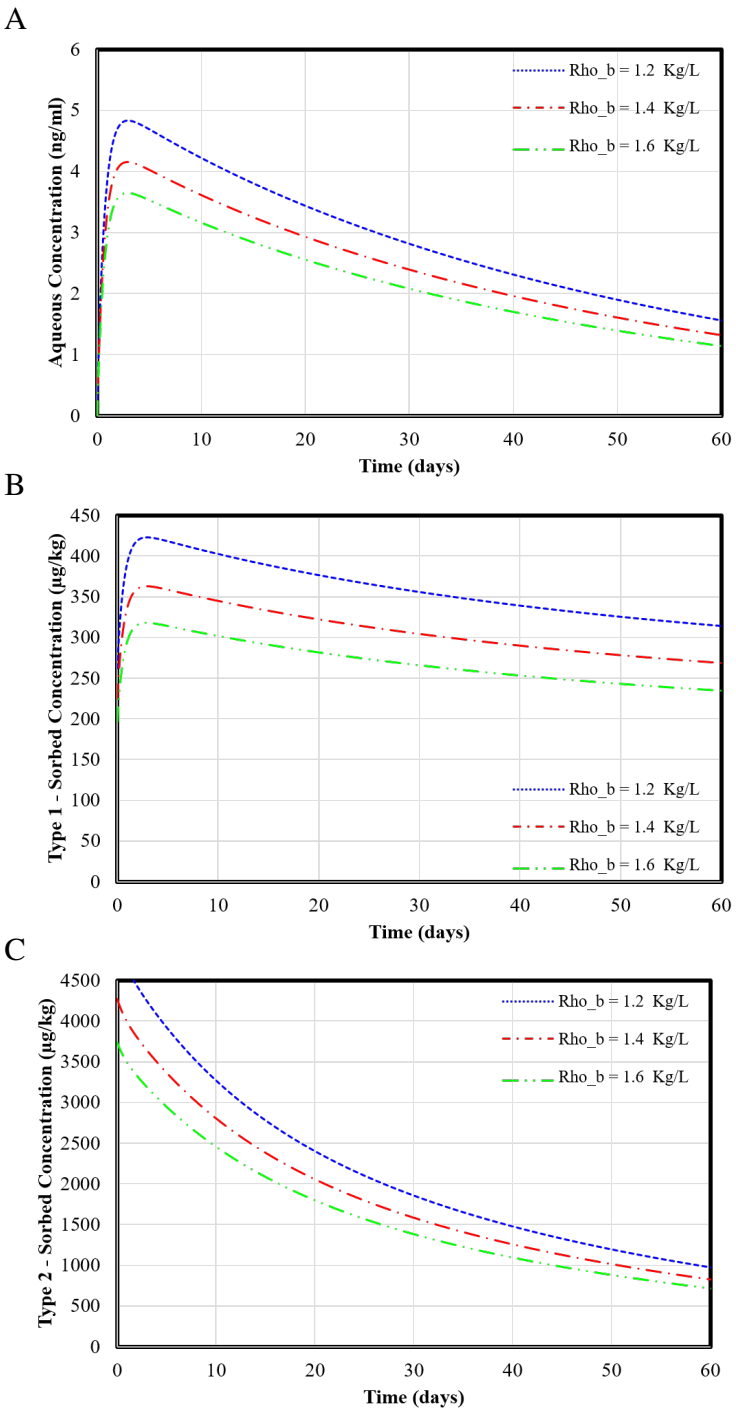

Figure F.2: Sensitivity analysis results for soil bulk density (ρ_b). Predicted time dependent aqueous concentration (A), equilibrium sorption site (Type 1) concentration (B), and kinetic sorption site (Type 2) (C) concentration of OTC assuming surface application of manure with 10 cm incorporation depth.

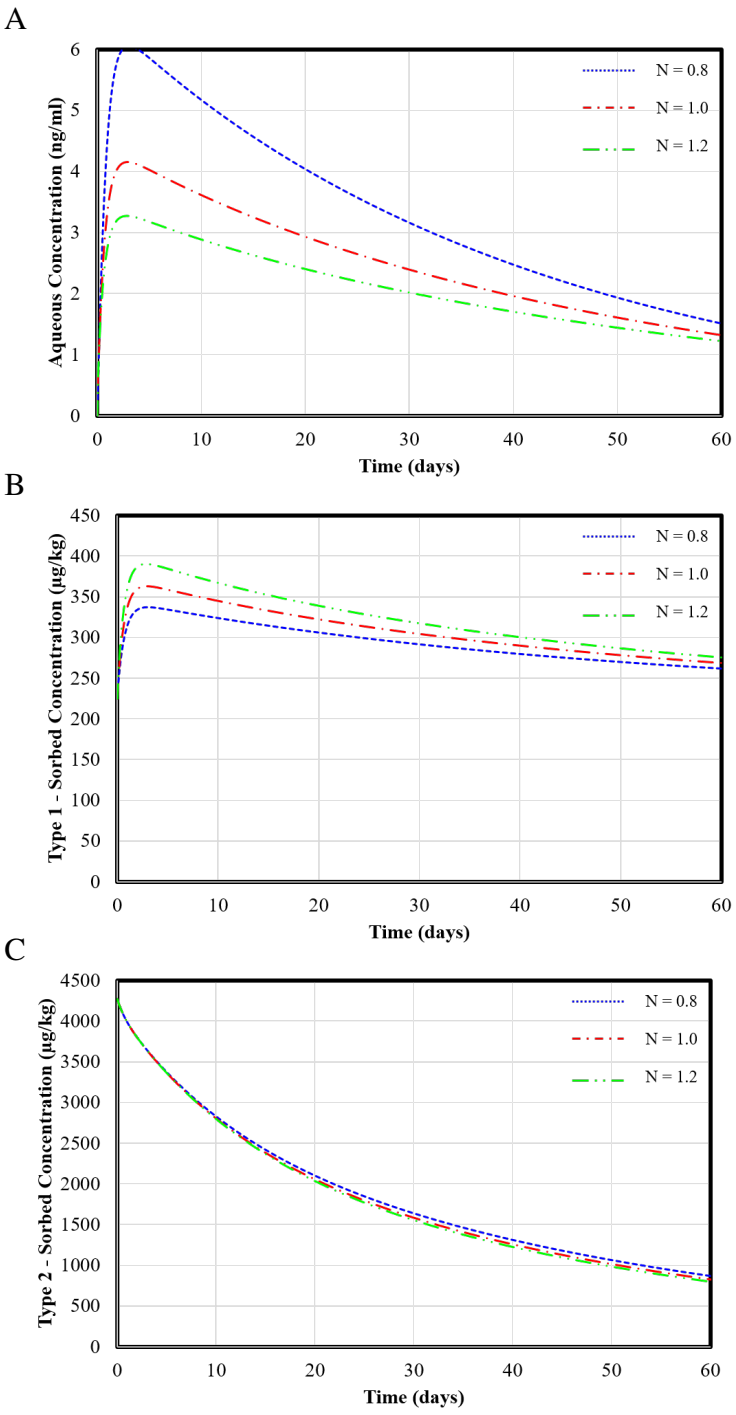

Figure F.3: Sensitivity analysis results for Freundlich sorption isotherm exponent (N). Predicted time dependent aqueous concentration (A), equilibrium sorption site (Type 1) concentration (B), and kinetic sorption site (Type 2) (C) concentration of OTC assuming surface application of manure with 10 cm incorporation depth.

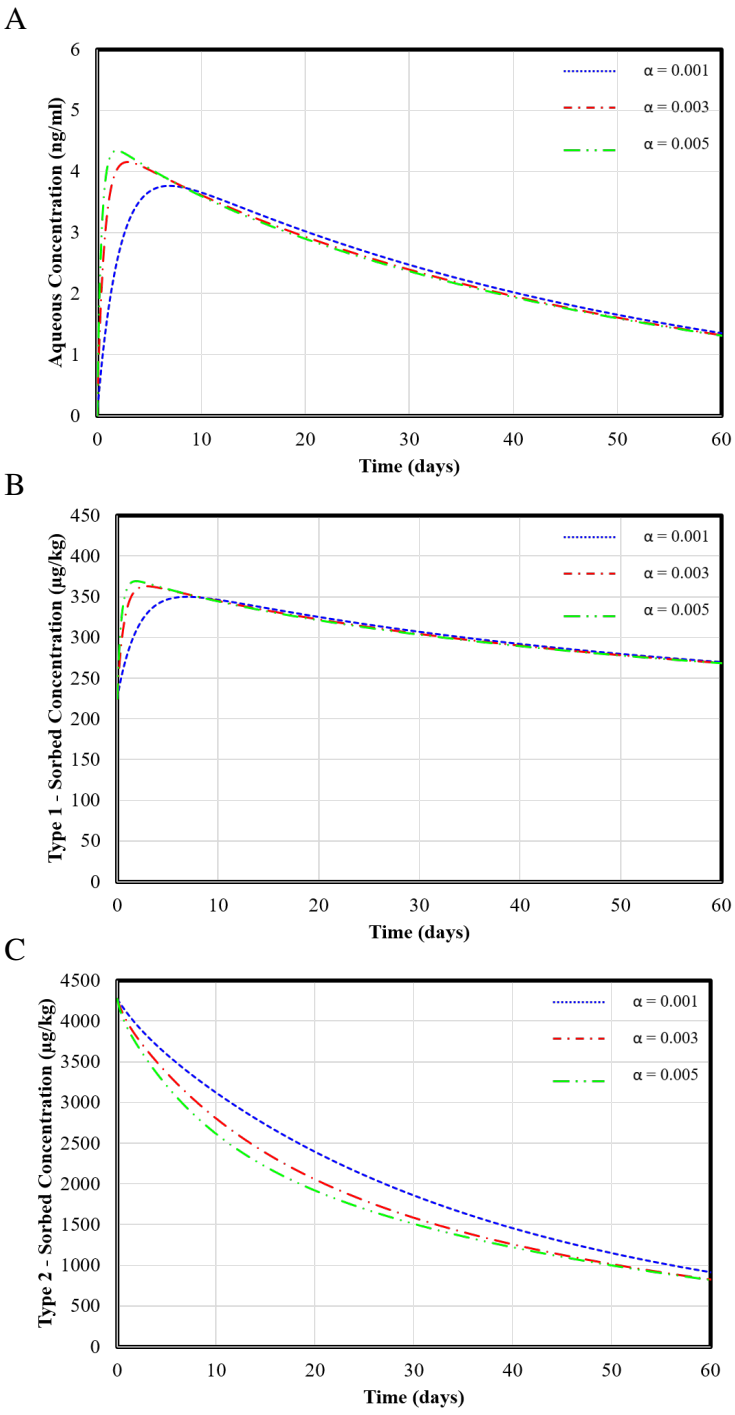

Figure F.4: Sensitivity analysis results for the first order kinetic rate coefficient (α). Predicted time dependent aqueous concentration (A), equilibrium sorption site (Type 1) concentration (B), and kinetic sorption site (Type 2) (C) concentration of OTC assuming surface application of manure with 10 cm incorporation depth.

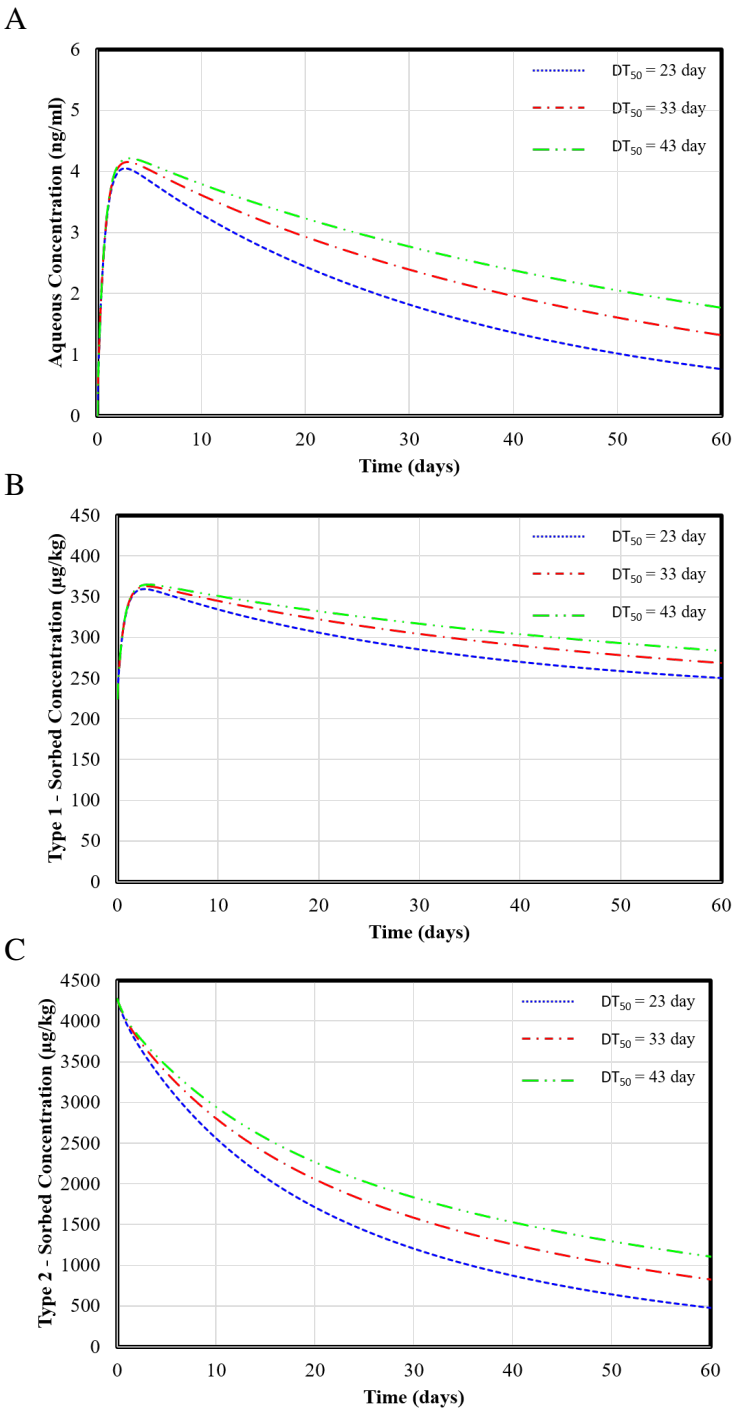

Figure F.5: Sensitivity analysis results for the degradation rate in solid media (μ_s). Predicted time dependent aqueous concentration (A), equilibrium sorption site (Type 1) concentration (B), and kinetic sorption site (Type 2) (C) concentration of OTC assuming surface application of manure with 10 cm incorporation depth.

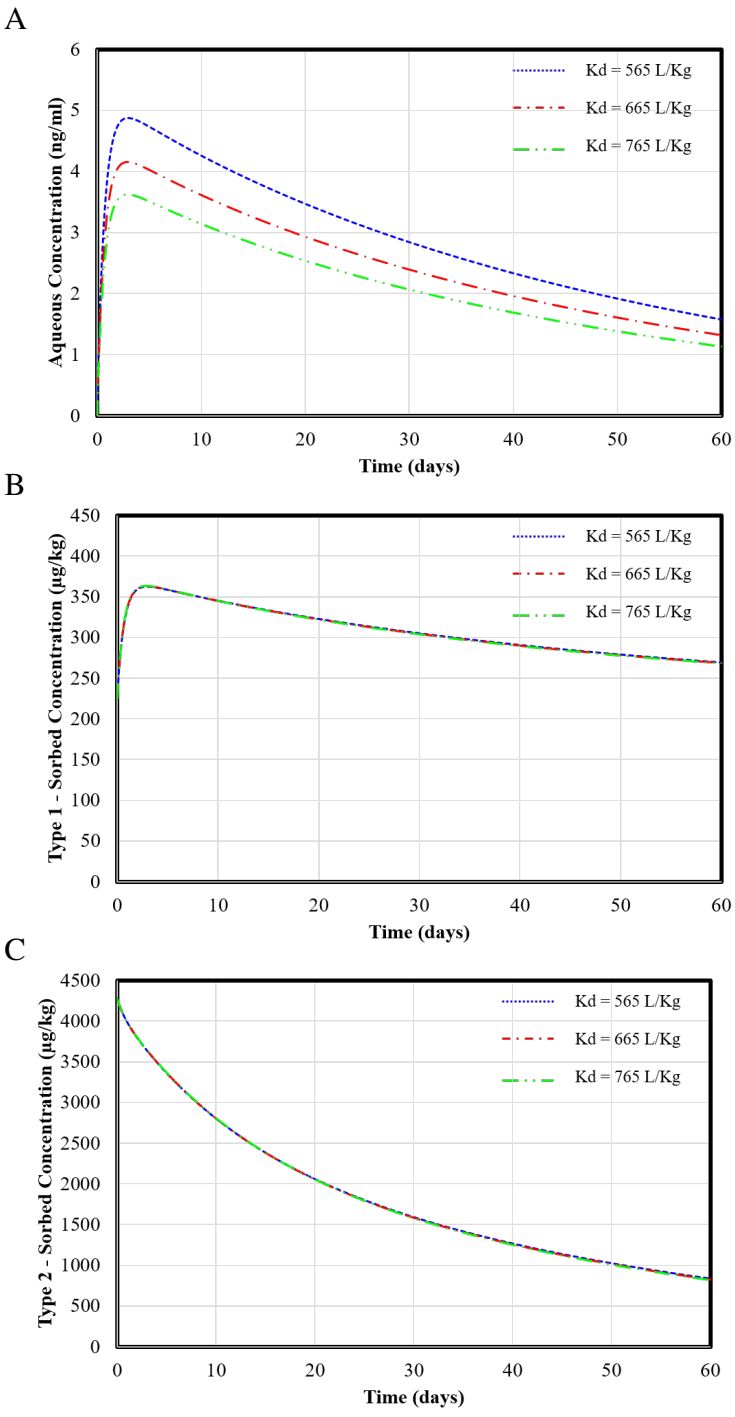

Figure F.6: Sensitivity analysis results for the partition coefficient (K_d). Predicted time dependent aqueous concentration (A), equilibrium sorption site (Type 1) concentration (B), and kinetic sorption site (Type 2) (C) concentration of OTC assuming surface application of manure with 10 cm incorporation depth.

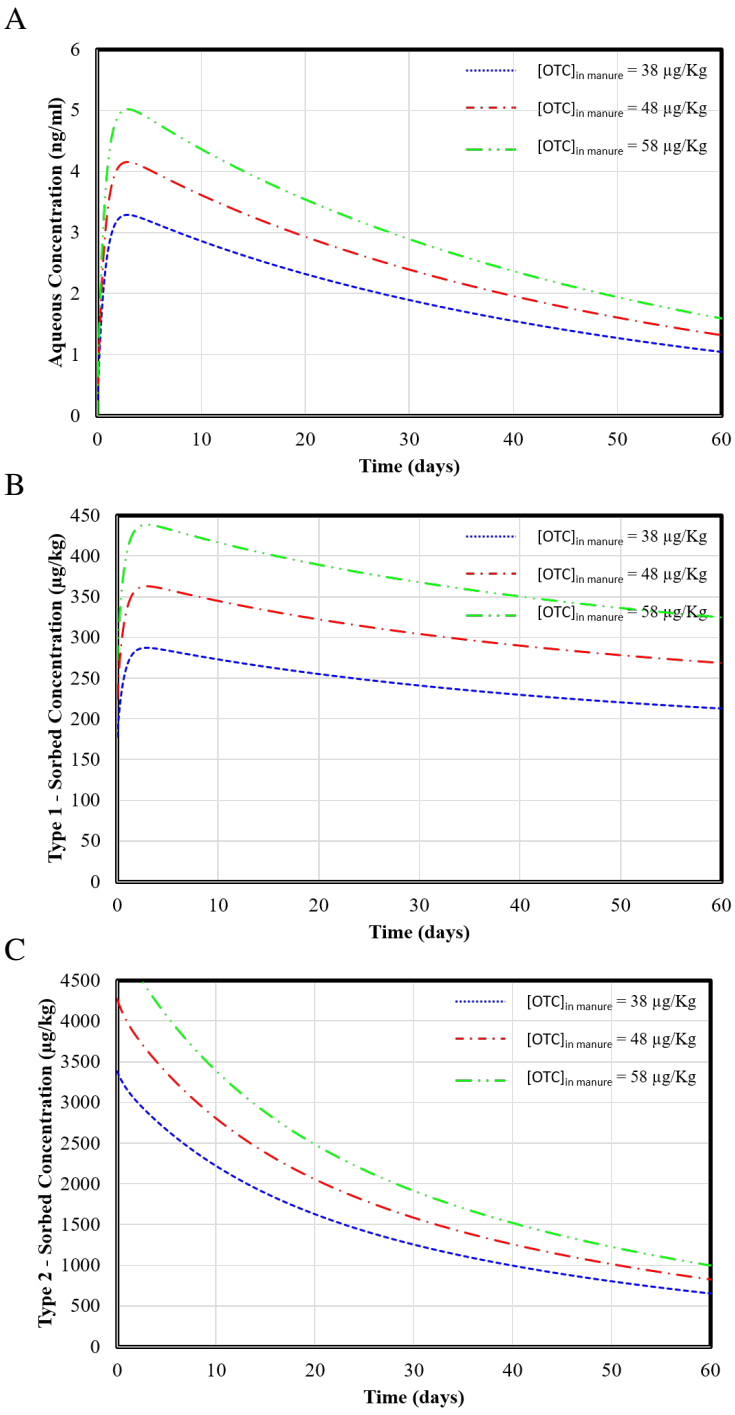

Figure F.7: Sensitivity analysis results for the concentration of OTC in manure. Predicted time dependent aqueous concentration (A), equilibrium sorption site (Type 1) concentration (B), and kinetic sorption site (Type 2) (C) concentration of OTC assuming surface application of manure with 10 cm incorporation depth.

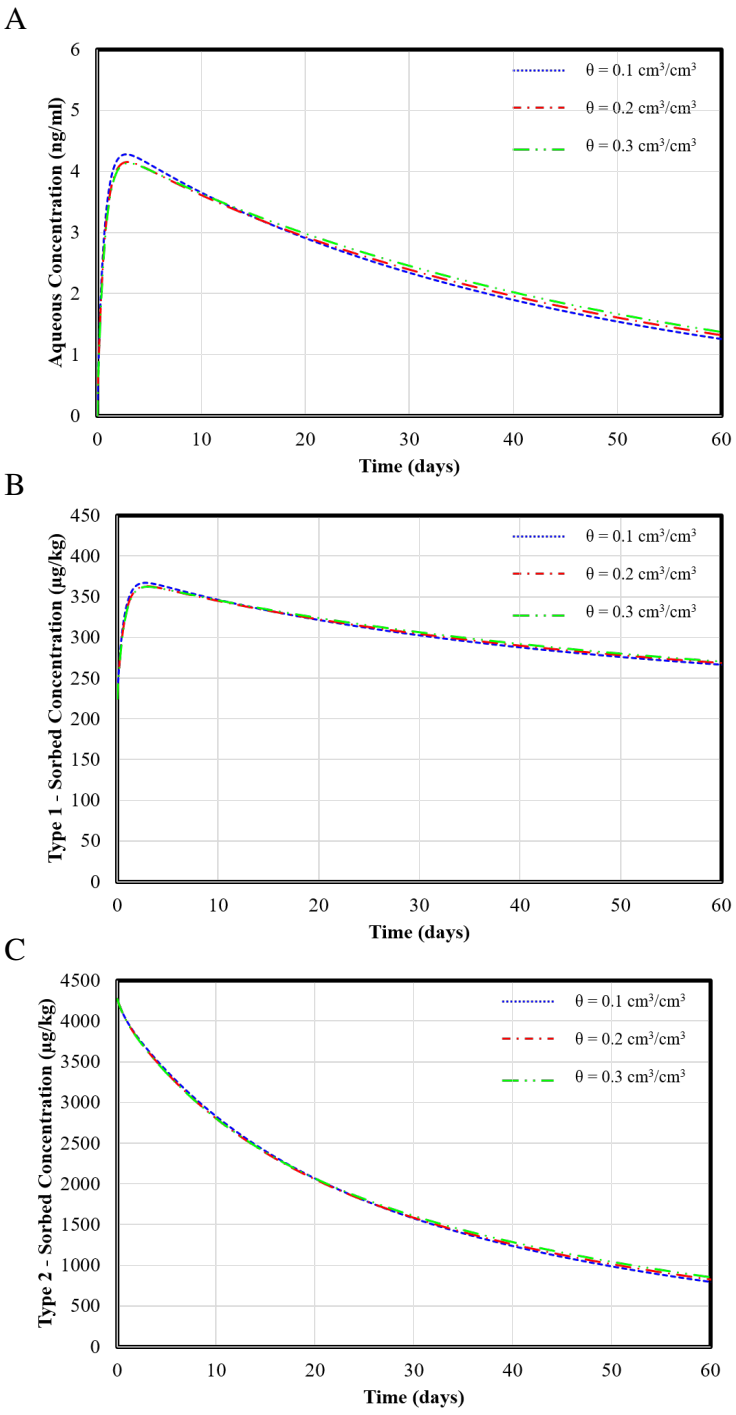

Figure F.8: Sensitivity analysis results for the moisture content (θ). Predicted time dependent aqueous concentration (A), equilibrium sorption site (Type 1) concentration (B), and kinetic sorption site (Type 2) (C) concentration of OTC assuming surface application of manure with 10 cm incorporation depth.

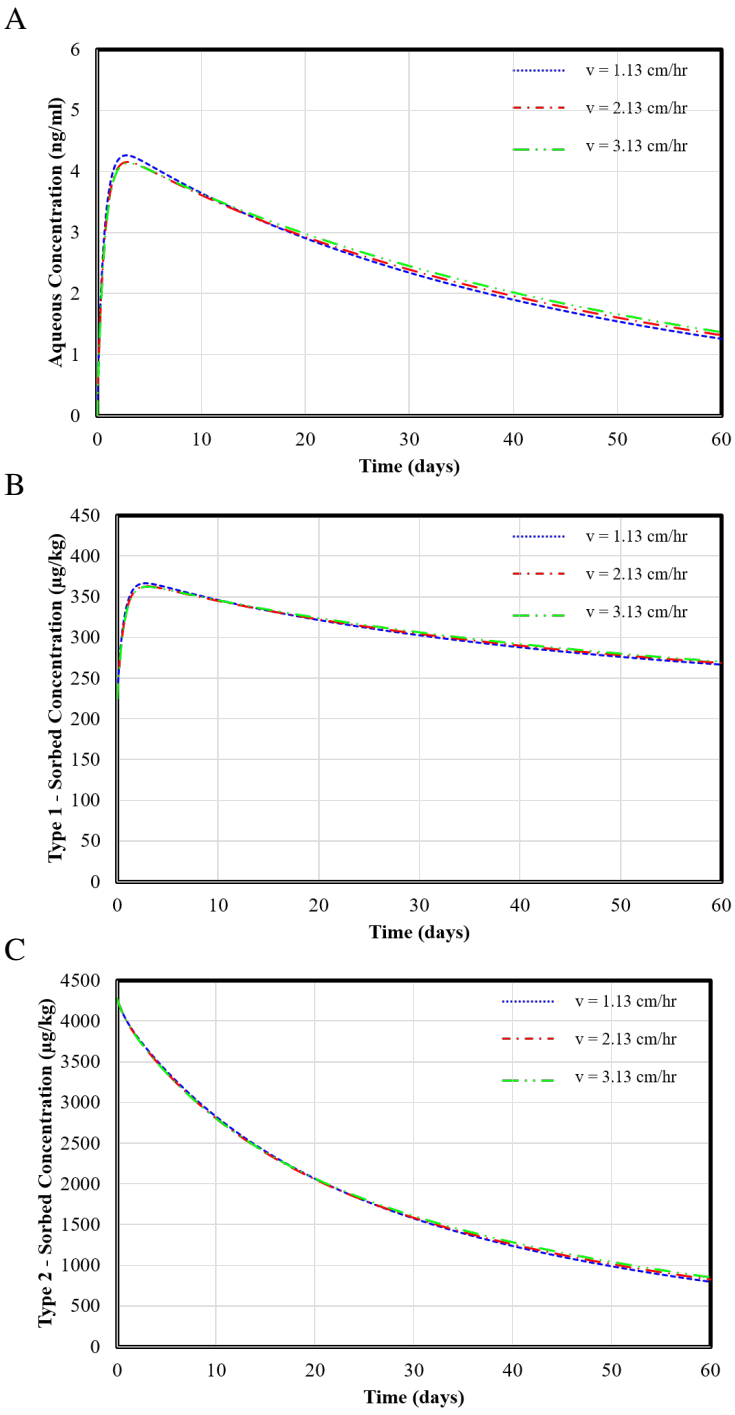

Figure F.9: Sensitivity analysis results for the pore water velocity (v). Predicted time dependent aqueous concentration (A), equilibrium sorption site (Type 1) concentration (B), and kinetic sorption site (Type 2) (C) concentration of OTC assuming surface application of manure with 10 cm incorporation depth.

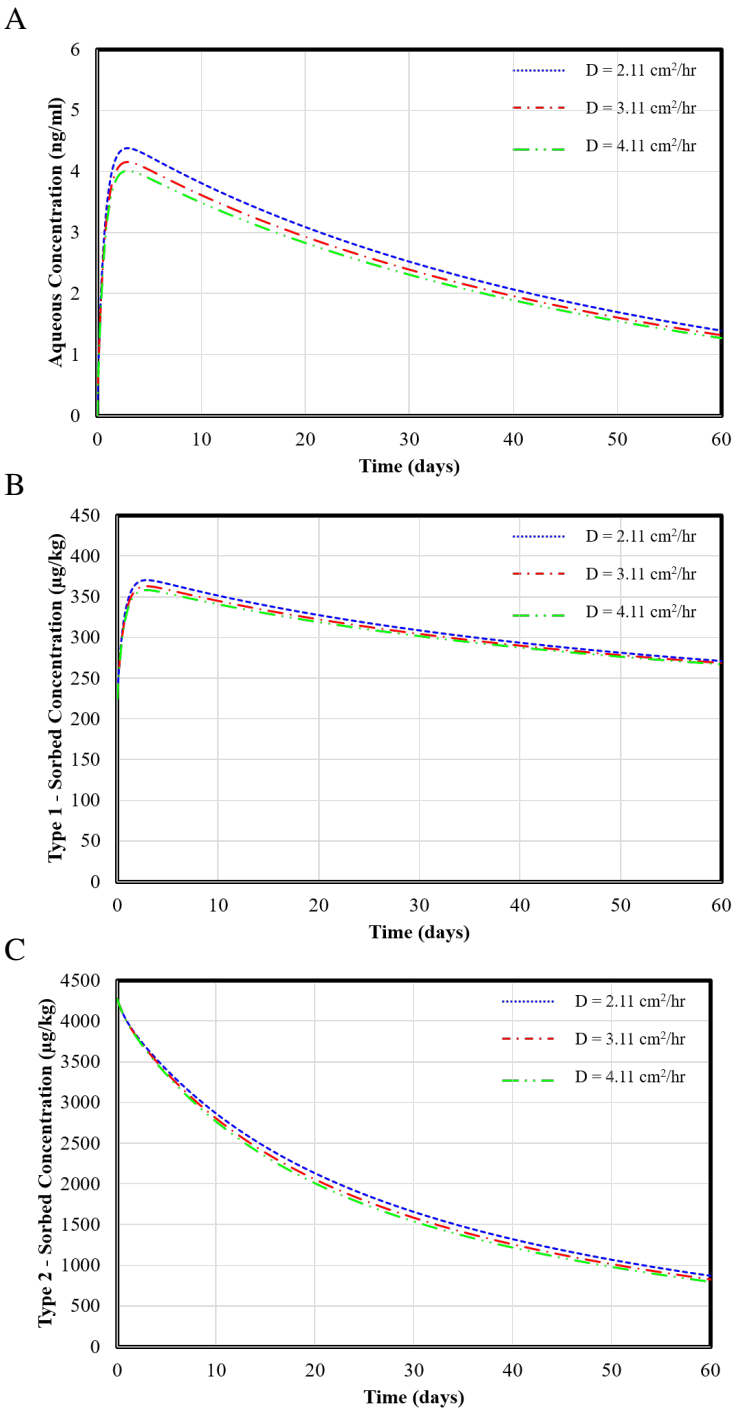

Figure F.10: Sensitivity analysis results for dispersion coefficient (D). Predicted time dependent aqueous concentration (A), equilibrium sorption site (Type 1) concentration (B), and kinetic sorption site (Type 2) (C) concentration of OTC assuming surface application of manure with 10 cm incorporation depth.

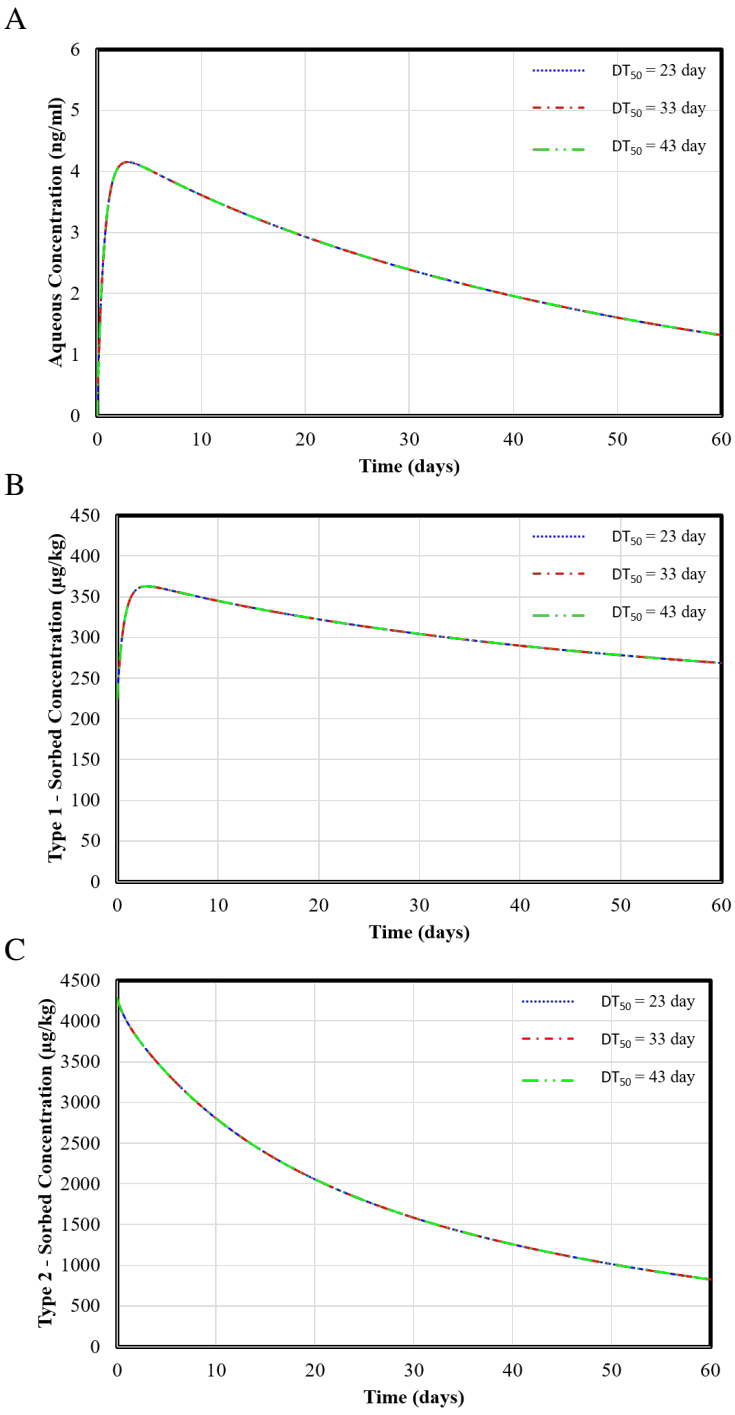

Figure F.11: Sensitivity analysis results for the degradation rate in aqueous media (μ_L). Predicted time dependent aqueous concentration (A), equilibrium sorption site (Type 1) concentration (B), and kinetic sorption site (Type 2) (C) concentration of OTC assuming surface application of manure with 10 cm incorporation depth.